Faculteit Farmaceutische, Biomedische en Diergeneeskundige Wetenschappen

Departement Farmaceutische Wetenschappen

Understanding the role of the gastrointestinal tract and the gut microbiome on the biotransformation, absorption and bioavailability of xenobiotics: chlorogenic acid as model compound

Inzicht in de rol van het gastro-intestinaal stelsel en het darmmicrobioom op de biotransformatie, absorptie en biologische beschikbaarheid van xenobiotica: chlorogeenzuur als modelverbinding

Proefschrift voorgelegd tot het behalen van de graad van doctor in de farmaceutische wetenschappen aan de Universiteit Antwerpen

te verdedigen door

Olivier MORTELE

Promotoren: prof. dr. Nina Hermans & prof. dr. Alexander L.N. van Nuijs

Antwerpen, 2021

Members of the jury

Promotors

    Prof. dr. Nina Hermans

    University of Antwerp, Dpt. of Pharmaceutical Sciences

    Natural Products and Food – Research & Analysis (NatuRA)

    Antwerpen, Belgium

    Prof. dr. Alexander L.N. van Nuijs

    University of Antwerp, Dpt. of Pharmaceutical Sciences

    Toxicological Centre

    Antwerpen, Belgium

Internal jury members

    Prof. dr. Paul Cos

    University of Antwerp, Dpt. of Pharmaceutical Sciences

    Laboratory of Microbiology, Parasitology and Hygiene (LMPH)

    Antwerpen, Belgium

    Prof. dr. Philippe Jorens

    University of Antwerp/Antwerp University Hospital, Dpt. of Critical Care Medicine

    Clinical pharmacotherapy and toxicology

    Edegem, Belgium

External jury members

    Dr. Lubertus Bijlsma

    University Jaume I

    Q-AMS - Public Health and Environmental Analytical Chemistry

    Castellon de la Plana, Spain

    Prof. dr. Cláudia Nunes dos Santos

    University of Lisbon, NOVA Medical School

    Molecular Nutrition and Health Lab

    Lisbon, Portugal

LIST OF ABBREVIATIONS

3-CQA	3-caffeoylquinic acid
4-CQA	4-caffeoylquinic acid
4-NP	4-nitrophenol
4-NP-Gluc	4-nitrophenol-glucuronide
4-NP-Sulf	4-nitrophenol-sulfate
5-CQA	5-caffeoylquinic acid
ABC	ATP binding cassette
ACE	Agiotensin-converting enzyme
ACN	Acetonitrile
API	Active pharmaceutical ingredient
BCRP	Breast cancer resistance protein
BMI	Body Mass Index
CFU/g	Colony forming units per gram
CYP450	Cytochrome P450 enzymes
DMEM	Dulbecco's modified eagle medium
DMSO	Dimethyl sulfoxide
EMA	European Medicines Agency
ESI	Electrospray ionisation
FCS	Foetal calf serum
FDA	Food and Drug Administration

GIDM-Colon	Gastrointestinal dialysis model with colon phase
Gluc-direct	Glucuronidation replicate without previous phase I incubation
HBSS	Hank's balanced salt solution
HCl	Hydrochloric acid
HICYT	Human intestinal cytosol
HIM	Human intestinal microsomes
LC-MS/MS	Liquid chromatography coupled to triple quadrupole mass spectrometry
LC-Q-TOF-MS	Liquid chromatography coupled to quadrupole time-of-flight mass spectrometry
LEfSe	Linear discriminant analysis effect size
LLOQ	Lower limit of quantification
MEM	Eagle's minimum essential medium
MeOH	Methanol
MilliQ	Deionized water
MPP	MassProfiler Professional
MRP2	Multidrug resistance-associated protein 2
MS/MS	Tandem mass spectrometry
m/z	Mass over charge

NADPH	Nicotinamide adenine dinucleotide phosphate
NaN$_3$	Sodiumazide
NaOH	Sodium hydroxide
P$_{app}$	Apparent permeability coefficient
PAPs	Adenosine-3'-phosphate 5'-phosphosulfate
PCoA	Principal coordinates analysis
PCR	Polymerase chain reaction
P-gp	P-glycoprotein
PenStrep	10 000 U/mL Penicillin and 10 000 µg/mL streptomycin mix
PMSF	Phenylmethylsulfonyl-fluoride
PPARγ	Peroxisome proliferators'-activated receptor γ
Ppm	Parts per million
QC	Quality control
QCH	Quality control high
QCL	Quality control low
QCM	Quality control mid
Rcf	Relative centrifugal force
ROS	Reactive oxygen species
Rpm	Rotations per minute
RSD	Relative standard deviation
SCFA	Short-chain fatty acids

SD	Standard deviation
SHIME	The simulation of the human intestinal microbial ecosystem
Sulf-direct	Sulfation replicate without previous phase I incubation
SULTs	Sulfotransferases
T2D	Type 2 diabetes
TEER	Trans-epithelial resistance
TIM-1	TNO computer-controlled, dynamic *in vitro* gastrointestinal model of the stomach and small intestine
TIM-2	TNO computer-controlled, dynamic *in vitro* gastrointestinal model of the Colon
UDPGA	Uridinediphosphate glucuronic acid
UGTs	Uridine 5'-diphospho(UDP)-glucuronosyltransferases
WCB	Wilkin-Chalgren Anaerobe Broth

TABLE OF CONTENTS

CHAPTER 1: GENERAL INTRODUCTION
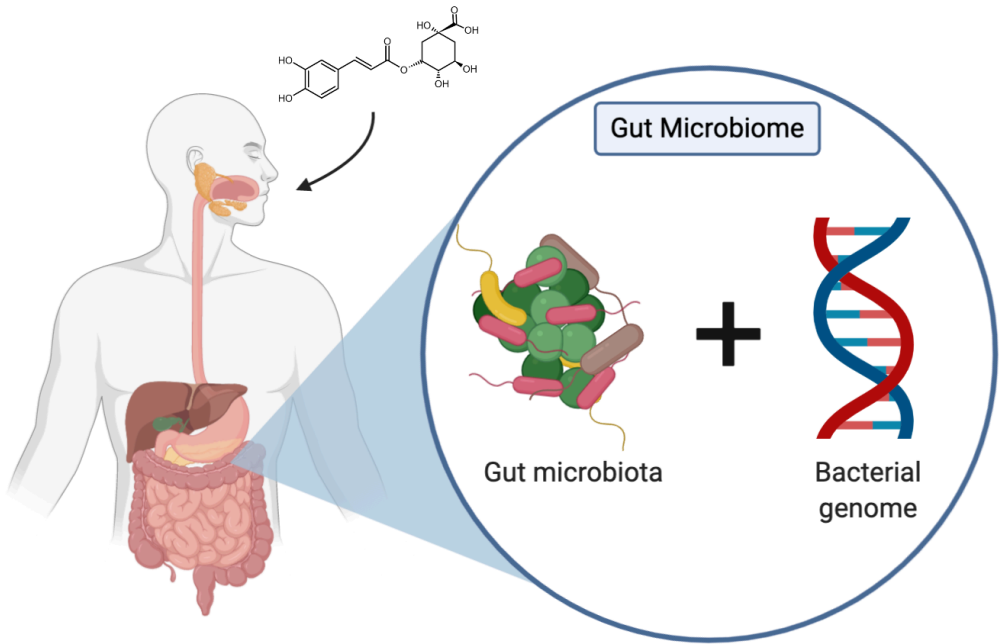
CHAPTER 1

1.1 Impact of the gastrointestinal tract on the bioavailability and activity of orally ingested xenobiotics

1.1.1 Introduction

During the past decade, researchers have shown an increased interest in the fate of orally ingested exogenous compounds, such as food components/supplements and pharmaceuticals in the gastrointestinal system (Dupont et al. 2019). Data of the Food and Drug Administration (FDA) confirms that oral administration is still the most common route of drug delivery. The FDA approved 59 and 48 new pharmaceutical drugs in 2018 and 2019 respectively, of which 33 (55%) and 26 (54%) were new oral drug formulations (FDA 2019, FDA 2020). The systemic absorption of an orally ingested xenobiotic from the gastrointestinal tract depends on the dissolution and stability of the drug formulation and xenobiotic (e.g. active pharmaceutical ingredient (API)) and absorption across the intestinal epithelium. These processes are determined by the interplay between formulation-characteristics of the xenobiotic, physicochemical properties of the xenobiotic and the physiology of the gastrointestinal tract (Vertzoni et al. 2019). The gastrointestinal tract contains diverse compartments with varying physiological properties such as pH, oxygen level, peristaltic movements resulting in differences in residence times, enzymatic activity, intestinal microflora, which could influence the bioavailability, activity and/or toxicity of these compounds (Mudie et al. 2010, Abuhelwa et al. 2017). A thorough knowledge of the impact of these anatomical and physiological variables on the bioavailability, activity and/or toxicity of xenobiotics is essential further research on formulation and dosing strategies. In the field op drug-development, an in-depth understanding of the gastrointestinal behavior of the API can lead to a more evidence-based approach rather than a trial-and-error approach resulting in a cost- and time-reduced procedure (Van Den Abeele et al. 2017). Application of relevant *in vitro* or *in silico* gastrointestinal models can aid in the development of this research field (Hens et al. 2017).

1.1.2   Anatomy and physiology of the gastrointestinal tract

The gastrointestinal tract can be seen as a series of connected muscular tubes passing throughout the body from mouth to anus (Figure 1-1).
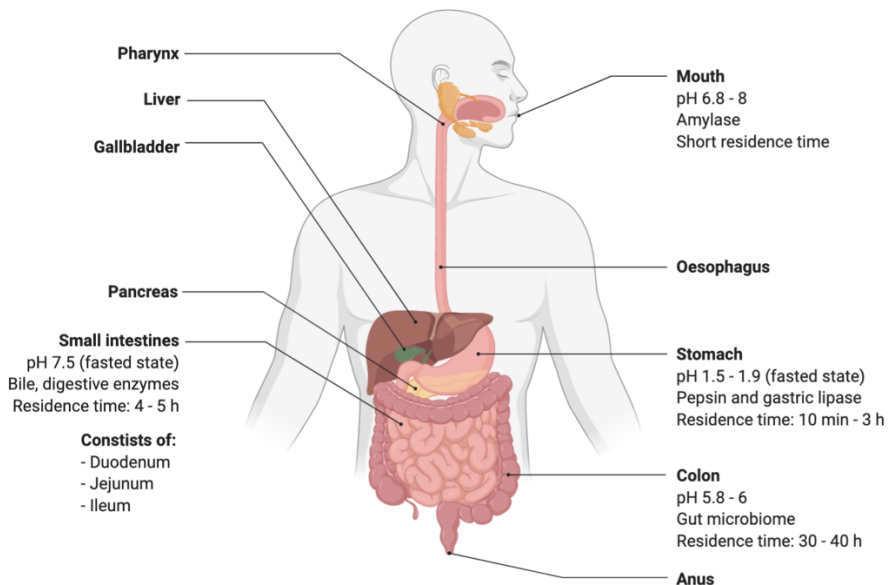
Figure 1-1: The human gastrointestinal tract and the liver, gallbladder and pancreas*.*

1.1.2.1   The mouth

Ingested materials are mixed with saliva and physically broken down by chewing (mastication) in the mouth. Saliva, at a pH of 6.8 – 8, contains the enzyme amylase which is responsible for the initial breakdown of polysaccharides and will lubricate the ingested material to improve the swallowing-process (deglutition) where the ingested material is transported through oesophagus to the stomach. Residence time of ingested materials in the mouth will differ dependent of the matrix. Most food-materials will require mastication, and thus increasing the exposure time to the saliva, while the residence time of most pharmaceuticals or food supplements will be extremely short as they are swallowed immediately (DeSesso and Jacobson 2001, Vertzoni et al. 2019).

1.1.2.2   The stomach

The gastric fluid is composed of multiple components (i) derived from the stomach such as gastric acid, enzymes and mucus, (ii) ingested or (iii) derived from the duodenum through reflux. The gastric environment is mostly described as an acidic environment, with reported pH values of 1.5-1.9 in a fasted state. However, in a fed state, gastric fluid pH will rise, postprandial pH values of 4.9 have been reported, dependent of the meal volume and composition which could influence the formulation disintegration and solubility of the xenobiotic (Simonian et al. 2005, Vertzoni et al. 2019). While the upper half of the stomach will store food entering from the oesophagus, the lower half is responsible for digestion by mechanically contractions and mixing the ingested material with acid, pepsin and gastric lipase resulting in a semi-solid mixture called chyme (Silverthorn 2010). Parietal cells of the gastric glands will produce gastric acid (HCl) which can denature proteins, but also has a protective function as few bacteria or other ingested microorganisms can survive in the acidic environment (pH 1.5-3.5) (Dieterich et al. 2018). Furthermore, the low pH will inactivate the salivary amylase.

The two main enzymes present in the gastric fluid are pepsin and gastric lipase. Chief cells of the gastric glands will produce pepsinogen, which is activated to pepsin in the stomach lumen by a proton (H$^+$), and gastric lipase. Pepsin will be responsible for the digestion of proteins in the stomach and has a maximal activity at pH 2, while no activity has been described at pH 5.5 or more (Vertzoni et al. 2019). Gastric lipase is reported to be active between the pH range of 3-5.5. The importance of gastric lipase is limited as only 10% of the lipid digestion occurs in the stomach (Silverthorn 2010). The muscular contractions will push the chyme against the closed sphincter. Particles with a diameter of 2-5 mm will pass to the duodenum. Gastric emptying time can vary between 10 min for a glass of water in the fasted state and 3 h or more for a standardized FDA high-caloric breakfast, meaning the intake of food can have a pronounced effect on the gastric residence time of the xenobiotic (Pal et al. 2007,

Koziolek et al. 2014, Mudie et al. 2014, Vertzoni et al. 2019). Absorption of xenobiotics in the stomach is limited due to the small epithelial surface (DeSesso and Jacobson 2001).

1.1.2.3 The small intestine

The small intestine is responsible for the majority of digestion and absorption. The small intestine consists out of the duodenum, jejunum and ileum (Figure 1-1). Pancreatic and intestinal fluids including bile, bicarbonate and digestive enzymes are secreted into the small intestinal lumen during the digestive state. The intestinal fluid will be slightly alkalic (pH of approximately 7.5) in the fasted state due to the presence of bicarbonate ions, resulting in an optimal environment for intestinal and pancreatic enzymes. However, high variability in small intestinal lumen pH during the first hour after consumption of a glass of water has been reported. The consumption of a meal led to decreased pH values 3 h postprandial, ranging from pH 4.8 to 6.5 (Kalantzi et al. 2006, Riethorst et al. 2016, Vertzoni et al. 2019). The intestinal epithelium and the pancreas will produce digestive enzymes. Peptidases, disaccharidases and enteropeptidases are examples of brush border enzymes that are anchored to the luminal side of the enterocytes. The secreted pancreatic enzymes include amylases, proteolytic enzymes, lipases and phospholipases (Silverthorn 2010). The small intestine has a total length varying between 3 and 8 m with typical structural properties of the intestinal cell wall, including villi and microvilli, resulting in a large surface area for absorption of food nutrients, pharmaceuticals and other compounds (Figure 1-2). Absorption occurs mainly in the duodenum and proximal part of the jejunum (DeSesso and Jacobson 2001, Teitelbaum et al. 2013, Vertzoni et al. 2019). The small intestinal transit time is relatively stable with reported mean intervals between 4 – 5 h (Sarosiek et al. 2010, Stillhart et al. 2020).
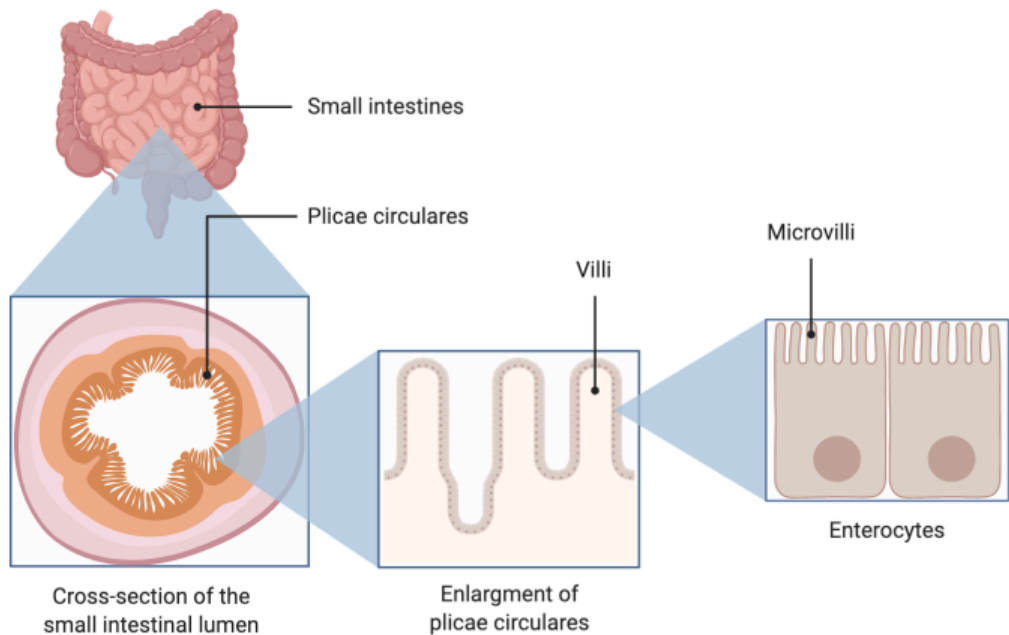
Figure 1-2: Detailed overview of the small intestinal mucosa.

1.1.2.4   The large intestine

The large intestine is composed of the appendix, cecum, ascending, transverse, descending and sigmoid colon, rectum and the anus (Figure 1-3). The main functions of the large intestine are (i) processing unabsorbed and undigested chyme, (ii) absorption of the remaining water, electrolytes and vitamins and (iii) formation and directing of feces to the rectum for elimination (Silverthorn 2010, Azzouz and Sharma 2020). Absorption of electrolytes such as sodium, chloride and potassium by passive or active pathways will result in an osmotic gradient responsible for the water absorption (Kiela and Ghishan 2016, Azzouz and Sharma 2020). Traditionally, it was believed that no significant digestion took place in the large intestine. However, the past decades multiple studies have shown that the bacteria residing in the colon are responsible for fermentation of indigestible carbohydrates into short-chain fatty acids (SCFA) (Silverthorn 2010). Pyruvate, produced by the colonic bacteria as result of glycolysis of the non-digested carbohydrates, is the precursor for SCFA acetate,

propionate and butyrate production through various metabolic pathways. Acetate and butyrate are both derived from acetyl-CoA resulting from pyruvate, while propionate may derive from succinate, propanediol and/or acrylate (Zhao et al. 2019). The pH of the colon environment in a fasted state is reported to be about 7.8, while the pH will drop in the fed state to approximately 5.8-6 due to enhanced bacterial fermentation, and thus SCFA formation, of indigested fibers in the consumed meal (Koziolek et al. 2015).

Transverse colon

Ascending colon

Cecum

Appendix

Anus

Descending colon

Sigmoid colon

Rectum
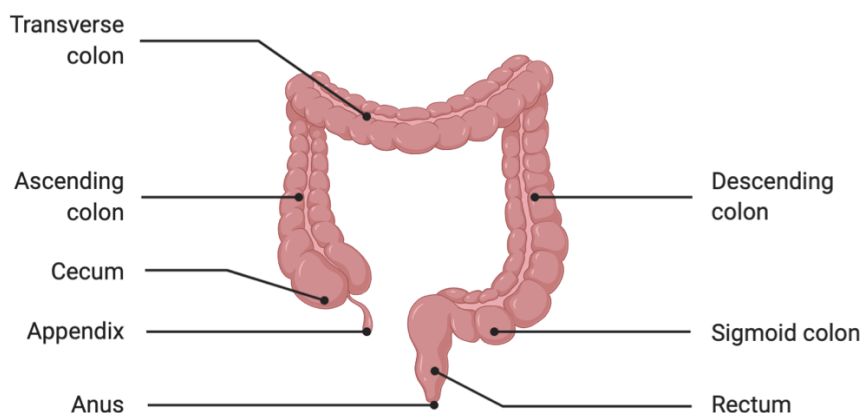
Figure 1-3: The different regions of the large intestine.

The physicochemical properties of the colon remained underinvestigated in comparison to the upper gastrointestinal tract, as it was believed that absorption of orally administered xenobiotics occurred mainly in the small intestine. However, xenobiotics with a low permeability and/or solubility in the upper gastrointestinal tract, drugs targeting the colon or included in an extended release formulation will be exposed to the colonic environment (Vertzoni et al. 2019). Only recently, the importance of the bacteria residing in the colon on the activity, bioavailability and/or toxicity of xenobiotics reaching the colon has been acknowledged.

1.2 The gut microbiome

1.2.1 Introduction

Every human being can be seen as an ecosystem on its own. Our body houses 10 times more bacterial cells than human cells, and to a lesser extent viruses, fungi, archaea, and protozoans (Stojancevic et al. 2014). The gastrointestinal tract accommodates between 10^{12}-10^{13} microorganisms with species diversity increasing longitudinally from mouth to colon, the latter harboring the most bacteria of the whole gastrointestinal tract also known as the gut microbiota (Figure 1-4).
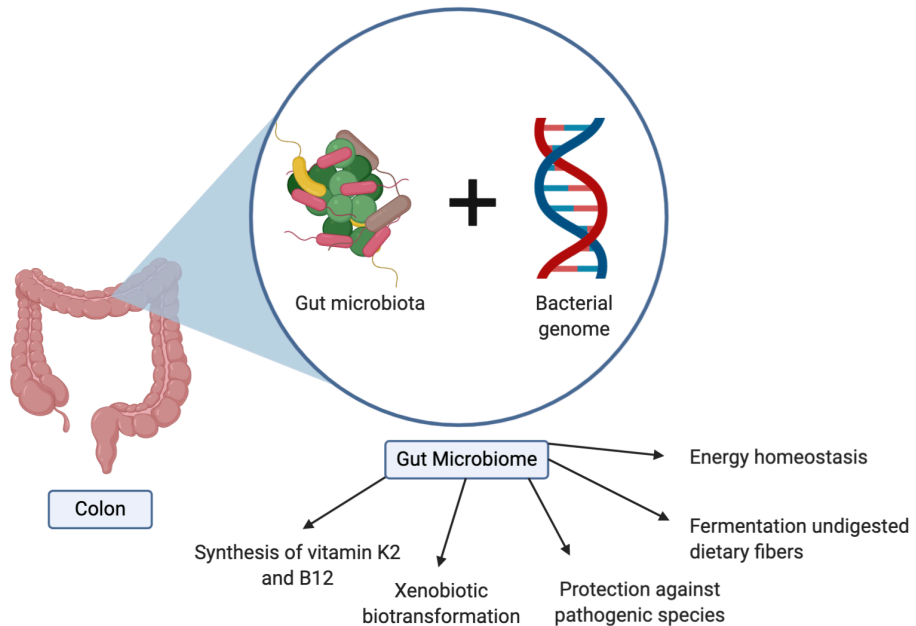
Figure 1-4: The gut microbiome is composed of the microorganisms living in the colon (gut microbiota) and their collective genome. The gut microbiome executes various important functions influencing the hosts' physiology.

The human gastrointestinal tract houses eight phyla, Firmicutes, Bacteroidetes, Proteobacteria, Fusobacteria, Verrucomicrobia, Cyanobacteria, Spirochaeates and Actinobacteria, with the first two accounting for 90% of the gut diversity. The gut microbiome, the gut microbiota living in the colon and their collective genomic

content, is estimated to contain 100 to 300-fold more genes than the human genome (Figure 1-4) (Borody et al. 2013, Stojancevic et al. 2014, Jandhyala et al. 2015). These insights have led to the understanding that the gut microbiome is responsible for immunological and gut-protective functions influencing the hosts' physiology and that it can be considered as an additional metabolizing organ (O'Hara and Shanahan 2006, Borody et al. 2013). The gut microbiome executes various important functions, including some that the host himself is unable to perform: synthesis of vitamins K2 and B12, development and regulation of the immune and nervous system, protection against pathogenic species, maintaining a barrier function, regulation of host fat storage and energy homeostasis, and stimulation of intestinal angiogenesis (Krajmalnik-Brown et al. 2012, Jandhyala et al. 2015).

1.2.2 Variables influencing the composition of the human gut microbiome

The composition of the gut microbiota depends on multiple factors including age, health status, immune system, drug use, lifestyle, the genetic background of the host, hygiene and type of diet leading to interindividual variation (Krajmalnik-Brown et al. 2012).

1.2.2.1 Age

The first gut microbiota profile in infants is mainly dependent of the mode of delivery. In vaginally born infants, *Lactobacillus* and *Prevotella,* microorganisms of the maternal vagina will mainly colonize the intestines of the child. The intestines of infants born by cesarean section, is mainly colonized by microorganisms of the maternal skin flora (*Streptococcus, Propionibacterium* and *Corynebacterium*). However, these differences are no longer reflected in adult gut microbiota composition (Dominguez-Bello et al. 2010, Falony et al. 2016). An adult-like phylogenetic composition of the gut microbiota is developed by the age of 3 years, however bacterial diversity keeps increasing with age (Yatsunenko et al. 2012). The gut microbiota profile remains constant during

adulthood, although differences resulting from diet-type, drug-use etc. have been described (Krajmalnik-Brown et al. 2012). Reduced bacterial diversity and metabolic capacity of the gut microbiome has been described in the elderly population (Nagpal et al. 2018).

1.2.2.2 Diet

Research have pointed out that dietary habits are considered to be one of the most important factors influencing the gut microbiota composition. Vegan and vegetarian diets have been linked with a greater abundance of the Bacteroidetes phylum while individuals consuming a Western diet (a diet high in in fats and sugars, and low in dietary fibers) are characterized by an enrichment of Firmicutes (De Filippo et al. 2010, Glick-Bauer and Yeh 2014, Jain et al. 2018).

1.2.2.3 Drug use

One of the major pharmaceutical drugs affecting the gut microbiota are antibiotics. They will affect both the pathogenic and beneficial bacteria and can lead to alterations of the gut microbiota over a longer period of time. Ciprofloxacin has shown to result in a loss of diversity and shifts in gut microbiota-composition within 4 days after start of the therapy. Microbiota composition began to return to the initial state 1 week after the end of the antibiotic-treatment, however, even within a period of 10 months, the return was incomplete (Dethlefsen and Relman 2011). Even four years post-treatment, differences in gut microbiota composition due to clarithromycin and metronidazole treatment could still be observed (Jakobsson et al. 2010).

Apart from antibiotics, other pharmaceutical drugs, such as proton pump inhibitors, laxatives, statins, angiotensin-converting enzyme (ACE) inhibitors and beta-blockers have been associated with dysbiosis of the gut microbiota (Weersma et al. 2020). As an example, multiple studies have reported reduced abundances of *Clostridium* and

Intestinibacter and increased abundances of *Escherichia/Shigella* after metformin intake (Forslund et al. 2015, Bryrup et al. 2019).

1.2.2.4   *Genetics*

Goodrich et al. (2014) reported higher similarities in gut microbiome composition for monozygotic twins when compared to dizygotic twins suggesting the presence of a heritable component in shaping the gut microbiome. Members of the phylum Bacteroidetes are reported to be not heritable, while taxa from the phyla Firmicutes and Actinobacteria did show a heritable component (Goodrich et al. 2014, Goodrich et al. 2016).

1.2.3   Metabolic capacity of the gut microbiome

One of the main metabolic functions of the gut microbiome is the fermentation of non-digestible polysaccharides to monosaccharides and subsequently to bacterial fermentation products such as acetate, propionate and butyrate. These SCFA represent the primary source of energy for the colonocytes and maintenance and proliferation of the intestinal flora (Donohoe et al. 2011, Pascale et al. 2018). Microbial fermentation primarily occurs in the cecum and ascending colon due to high substrate availability and rapid microbial growth resulting in a more acidic environment (pH 5-6). Substrate availability declines significantly towards the distal colon leading to a decreased fermentation activity of the gut microbiota (Pascale et al. 2018). 95% of the produced SCFA is absorbed by the colonocytes and provides approximately 10% of the daily caloric requirements (den Besten et al. 2013).

1.2.3.1   *Microbiotic biotransformation of xenobiotics*

The gut microbiome can directly and indirectly influence the bioavailability, activity and possible toxicity of ingested compounds (Figure 1-5-a) (Koppel et al. 2017, Wilson and Nicholson 2017). Examples of direct interferences are the conversion of the

prodrug sulfasalazine to the active compound 5-aminosalicylic acid (5-ASA) by azoreductase (Figure 1-6-A). The cardiac glycoside digoxin is an example of inactivation by the gut microbiome (Figure 1-6-B) (Koppel et al. 2017). Another example of a direct interaction is the direct binding of xenobiotics or dietary components to the bacteria (Carmody and Turnbaugh 2014, Spanogiannopoulos et al. 2016). Examples of indirect interferences are the alteration of host genes expression (e.g. lower expression of CYP450 enzymes), competition and/or inhibition of host enzymes by microbial biotransformation products and reactivation of drugs by deconjugation of phase II biotransformation products after enterohepatic circulation (Carmody and Turnbaugh 2014, Spanogiannopoulos et al. 2016).
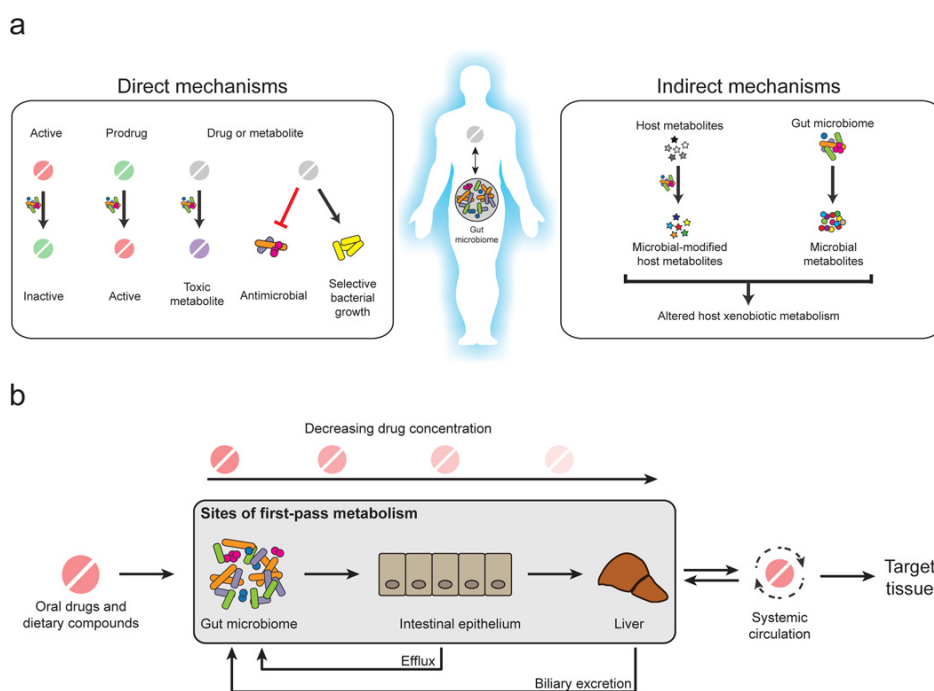
Figure 1-5: a) Overview of the direct and indirect mechanisms linking the gut microbiome and xenobiotic biotransformation. Biotransformation of xenobiotics by the gut microbiome may result in activation or inactivation of the compounds or formation of toxic biotransformation products. Examples of indirect influences are activation of xenobiotics during enterohepatic cycling, altered host xenobiotic biotransformation due to competition of microbial biotransformation products or metabolites for enzyme binding sites. **b)** The gut microbiome can be seen as a site of

first-pass biotransformation as the gut microbiome may alter xenobiotics prior to absorption. Figure from Spanogiannopoulos et al. (2016).
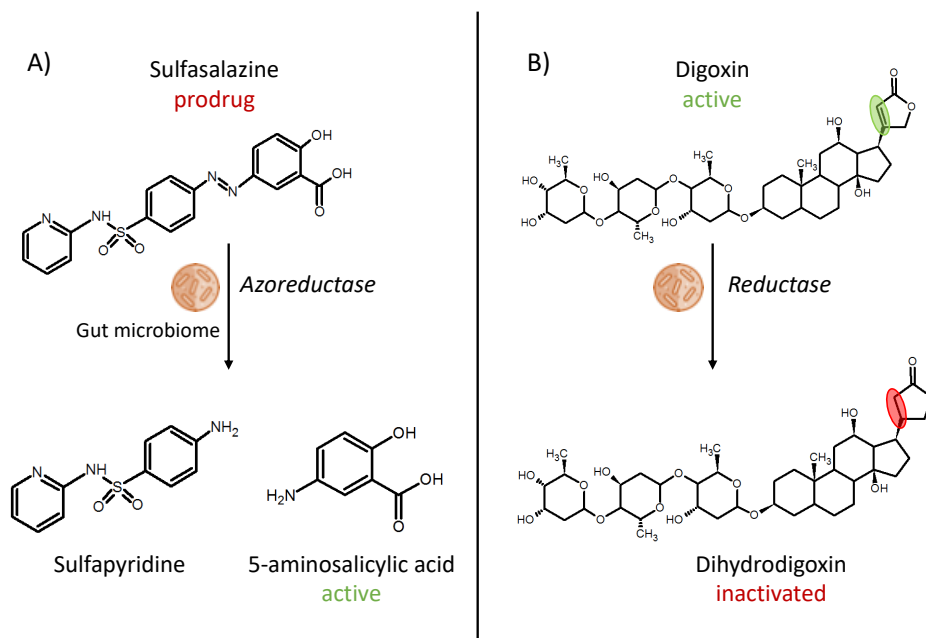
Figure 1-6: Examples of direct interactions of the gut microbiome on the activity of xenobiotics. (A) Prodrug sulfasalazine is biotransformed to active compound 5-aminosalicylic acid by the gut microbiome. (B) Digoxin is inactivated by reduction of the double bond with formation of dihydrodigoxin..

Important differences between hepatic and bacterial metabolism have been observed. Liver metabolic pathways consist mostly out of oxidative phase I reactions, by the cytochrome P450 enzymes (CYP450), and conjugation phase II reactions, by involvement of uridine 5'-diphospho(UDP)-glucuronosyltransferases (UGTs), sulfotransferases (SULTs), etc., typically leading to the conversion of lipophilic compounds into more hydrophilic compounds to enhance excretion. The major biotransformation reactions by the gut microbiome are reductive, due to the high reduction potential of anaerobic bacteria, and hydrolytic reactions. In addition, the gut microbiome is responsible for processing glutathione conjugates of xenobiotics excreted in the bile, deacylation, demethylation, decarboxylation, dehydroxylation, dealkylation, dehalogenation, deamination, acetylation, and

oxidation/dehydrogenation (Venema and van den Abbeele 2013, Stojancevic et al. 2014, Wilson and Nicholson 2017). These chemical differences between human and microbial biotransformation reactions result from an increased diversity of enzymes and from a difference in biotransformation purpose. While the goal of human biotransformation evolved to facilitate excretion of xenobiotcs from the human body, the microbiotic biotransformation aims to promote microbial growth through production of bacterial fermentation products (Koppel et al. 2017). Besides oral and rectal administrated drugs, other administration routes (e.g. intravenous) can result in the presence of the drug in the colon by secretion or diffusion from the systemic circulation or by enteric and hepatic secretion into the intestinal lumen (Figure 1-5-b) (Stojancevic et al. 2014). Most new pharmaceutical drug candidates experience biopharmaceutical problems like low solubility and/or low permeability leading to longer contact with the gut microbiome. Furthermore, there is currently a lack of knowledge on how the microbiotic biotransformation varies between individuals and different disease-states. This shows the need for more biotransformation studies including the role of the gut microbiome (Sousa et al. 2008).

1.2.4   The gut microbiome in health and disease

Perturbations in composition and function of the gut microbiome has been associated with a wide range of human diseases including obesity (Ley et al. 2005, Ley et al. 2006, Turnbaugh et al. 2008, Turnbaugh et al. 2009), type 2 diabetes (T2D) (Larsen et al. 2010, Qin et al. 2012, Sedighi et al. 2017), cardiovascular diseases (Brown and Hazen 2015, Yang et al. 2015, Yan et al. 2017), inflammatory bowel disease (Machiels et al. 2014, Schirmer et al. 2018), colorectal cancer (Wang et al. 2012, Wu et al. 2013) and neurological disorders (Adams et al. 2011, Li et al. 2017, Strati et al. 2017) (Table 1-1).Deviating results are reported for some diseases stressing the importance for further research. Both increased as decreased abundances of phylum Bacteroidetes

have been associated with autism spectrum disorder (Strati et al. 2017). Distinguishing if the observed dysbiosis is due to causality or effect remains a challenge as various mechanisms, such as dietary habits, bowel function and medication, can lead to changes in gut microbiota (Shreiner et al. 2015). Furthermore, little is known on the effect of disease-associated dysbiosis on microbial biotransformation of xenobiotics and potential inter-individual differences between disease-states.

Table 1-1: Examples of human diseases associated with gut microbiome-dysbiosis.

Disease	Associated dysbiosis	References
Obesity	• Increase in Firmicutes/Bacteroidetes ratio • Decrease in microbiota diversity	Ley et al. (2005, 2006), Turnbaugh et al. (2008, 2009)
Type 2 diabetes (T2D)	• Decrease in phyla Firmicutes and class Clostridia • Increase in *Lactobacillus* • Decrease in *Bifidobacterium*	Larsen et al. (2010), Qin et al. 2012), Sedighi et al. (2017)
Hypertension	• Decrease in butyrate producing bacteria (*Faecalibacterium* and *Roseburia*) • Increase in Firmicutes/Bacteroidetes ratio • Decrease in microbiota diversity	Yang et al. (2015), Yan et al. (2017)
Inflammatory bowel disease	• Decrease in butyrate-producing Firmicutes (e.g. *Faecalibacterium prausnitzii)* • Increase in taxa from family *Enterobacteriaceae* • Increase in mucolytic *Ruminococcus* sp.	Machiels et al. (2014), Schirmer et al. (2018)
Colorectal cancer	• Decrease in butyrate producing bacteria (*Faecalibacterium* and *Roseburia*) • Increase in *Bacteroides fragilis* (enterotoxigenic)	Wang et al. (2012), Wu et al. (2013)
Autism spectrum disorder	• Increase in Firmicutes/Bacteroidetes ratio due to decrease of relative abundance of Bacteroidetes • Increase in Bacteroidetes and *Lactobacillus* sp. • Decrease in microbiota diversity	Adams et al. (2011), LI et al. (2017), Strati et al. (2017)

1.2.5 *In vitro* versus *in vivo* biotransformation studies

In vivo animal or clinical studies to investigate the colonic biotransformation of xenobiotics experience some limitations and disadvantages. First of all, these studies are time-consuming, labor-intensive and expensive (Verhoeckx et al. 2015). During *in vivo* studies, access to the gut is difficult to accomplish as it would require a long catheter trough the throat or nose, or a tube stuck up the rectum. Furthermore, animal studies mostly lead to the sacrifice of the animals to be able to sample the different compartments of the gut (Venema and van den Abbeele 2013, Venema 2015). Based on the 3R principle, replacement, reduction and refinement of animal studies, *in vitro* gastrointestinal models offer an alternative approach to study the colonic metabolism. In general, *in vitro* models of the gastrointestinal tract contain multiple compartments to mimic the different parts of the digestive system (mouth, stomach, small and large intestine) (Verhoeckx et al. 2015). Easy access to the different compartments allows dynamic and multiple sampling over time which can help in the understanding of the different steps of the gut fermentation (Verhoeckx et al. 2015). The disadvantage of *in vitro* models is that they are not fully representative for the *in vivo* conditions. Therefore, it is important to create conditions that closely mimic the *in vivo* situation to obtain a high level of physiological significance (Venema and van den Abbeele 2013, Verhoeckx et al. 2015).

1.2.5.1 In vitro models of the gut microbiome

In *in vitro* gut microbiome models, a distinction can be made between static short-term batch incubations (i.e. test-tube containing fecal suspension and substrate), single stage reactors or semi-continuous systems (i.e. comprising a static bioreactor to which needed enzymes are added manually and stirred) and multi-compartmental continuous models (i.e. emphasize dynamic changes in the digestive tract: changes in temperature, pH and digestive secretions, direct connection between compartments, peristalsis) among the wide range of available *in vitro* gastrointestinal tract and

fermentation models (Venema and van den Abbeele 2013, Verhoeckx et al. 2015). Static batch incubations are frequently used but are not able to provide accurate results since they tend to over-simplify the *in vivo* situation. A better representation of the *in vivo* situation can be acquired with semi-continuous (e.g. gastrointestinal dialysis model with colon phase (GIDM-Colon)) or multi-compartmental continuous models (e.g. SHIME®, TIM-2.) (Venema 2015).
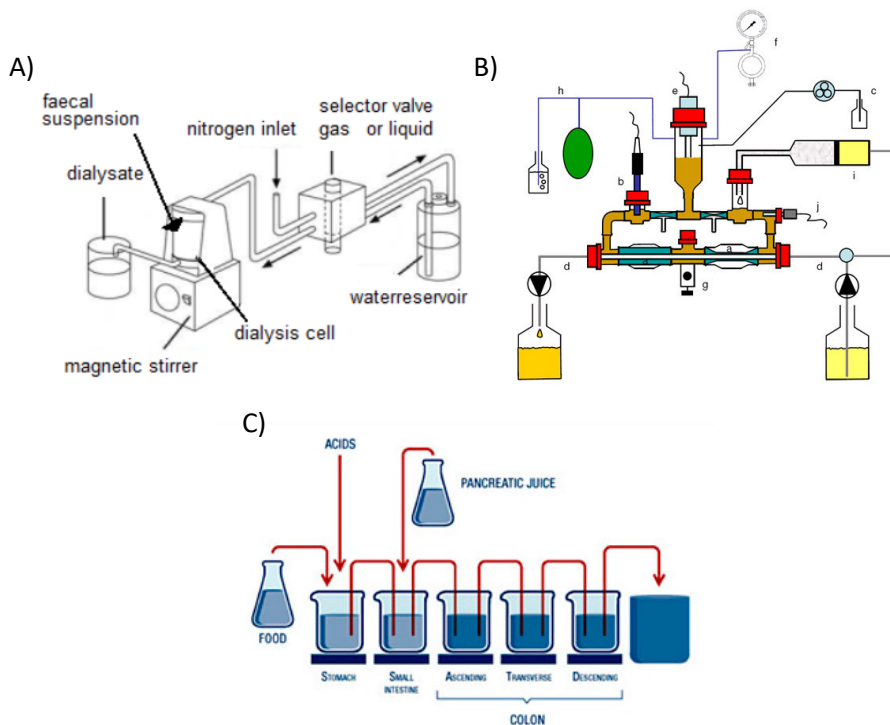
Figure 1-7: Overview of available in vitro gastrointestinal models including the gut microbiome. A) The gastrointestinal dialysis model with colon phase (GIDM-Colon), B) The TNO computer-controlled in vitro gastrointestinal model of the Colon (TIM-2), C) The Simulation of the Human Intestinal Microbial Ecosystem (SHIME). From (Breynaert et al. 2015, Van de Wiele et al. 2015, Venema 2015).

1.2.5.1.1   GIDM-Colon

The GIDM-Colon (Figure 1-7-A) was developed at the Laboratory of Natural Products and Food – Research and Analysis (NatuRA) of the University of Antwerp (Belgium).

This semi-continuous model is able to simulate the gastric, small intestinal and colonic physiological conditions including the presence of digestive enzymes, bile and the colonic gut microbiota. The model uses continuously stirred dialysis cells, which enable dialysis during the small intestinal and colonic stage. The use of separate dialysis cells allows the inclusion of multiple replicates, blank and negative control samples in one experimental run. Dialysis cells are inoculated with the microbiota from individual or pooled fecal samples after a 17 h incubation step in Wilkin-Chalgren Anaerobe Broth (WCB). The anaerobic environment during the colonic stage is guaranteed as dialysis cells are placed in an anaerobic glove box (5% CO_2, 5% H_2, 90% N_2) (Breynaert et al. 2015).

Table 1-2: Overview of the differences in features between the GIDM-Colon, TIM-1 and TIM-2 and the SHIME.

Features	GIDM-Colon	TIM-1 and TIM-2	SHIME
Multiple colon compartments?	No	Yes	Yes
Transfer of content?	Manual	Automatic	Automatic
Stabilization period?	17 h	17 h	2 weeks
Dialysis?	Yes	Yes	No

1.2.5.1.2   TIM-1 and TIM-2

The TNO computer-controlled, dynamic *in vitro* gastrointestinal model of the Colon (TIM-2, Figure 1-7-B) was developed around the year 2000 and is based on the gastric and small intestinal gastrointestinal model (TIM-1). TIM-1 consists out of 4 glass chambers simulating the stomach, duodenum, jejunum and ileum while TIM-2 simulates the ascending, transverse and descending colon. Both TIM-1 and TIM-2 use glass chambers with flexible internal walls. Water between the glass and the flexible membranes is responsible for maintaining the body temperature (37 °C). Furthermore,

peristaltic movements can be simulated by application of pressure in specific sequences on the water resulting in contraction of the flexible membranes and mixing of the luminal content. The model enables dialysis to prevent accumulation of microbial metabolites, which could lead to inhibition of bacterial activity or bacterial death. A 17 h stabilization period is applied after inoculation of the colonic glass chambers with gut microbiota. The model is flushed with N_2 to ensure the anaerobic environment (Venema 2015).

1.2.5.1.3 SHIME

The Simulation of the Human Intestinal Microbial Ecosystem (SHIME) model has been previously developed at Ghent University (Belgium). The model is composed out of 5 stages including the stomach, the small intestine, the ascending, transverse and descending colon (Figure 1-7-C). The content is automatically transferred between the different compartments by pumps at specified intervals. A nutritional medium and a pancreatic-bile solution are added to the gastric and small intestine compartment respectively three times a day. The colon compartments are filled with nutritional medium and inoculated with fecal sample from one individual followed by a two week stabilization period. The colon stages are continuously stirred with a continuous pH and volume control. pH is set at 5.6-5.9 for the ascending colon, 6.1-6.4 for the transverse colon and 6.6-6.9 for the descending colon. The headspace compartments of the colon stages are daily flushed with N_2 to ensure an anerobic environment. In comparison to the GIDM-Colon and TIM-2, no dialysis is performed in this model (Van de Wiele et al. 2015).

1.3 Chlorogenic acid

1.3.1 Introduction

The term chlorogenic acids is the collective of naturally occurring phenolic compounds composed of an ester of quinic acid with one or more hydroxycinnamic acids such as caffeic acid and ferulic acid (Wianowska and Gil 2018). The predominant species in the human diet is 5-caffeoylquinic acid (5-CQA), referred to as chlorogenic acid throughout the thesis, composed of the ester of caffeic acid and quinic acid (Figure 1-8). It is the major polyphenolic compound found in coffee and is also present in tea, fruits and vegetables (Konishi and Kobayashi 2004, dos Santos et al. 2006, Naveed et al. 2018).

Chlorogenic acid

Caffeic acid   Quinic acid
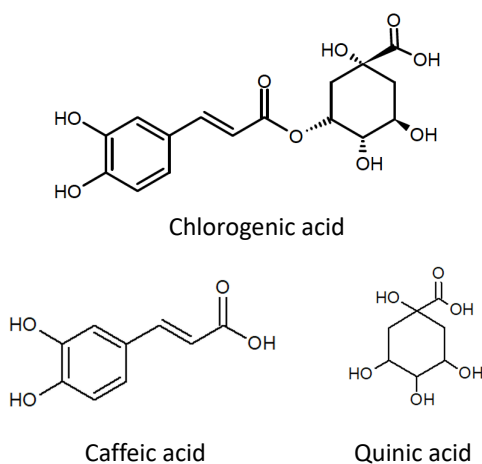
Figure 1-8: Overview of the chemical structures of chlorogenic acid, caffeic acid and quinic acid.

Chlorogenic acid has been associated with multiple health-promoting properties such as antidiabetic (Hunyadi et al. 2012), anti-inflammatory (dos Santos et al. 2006, Liang and Kitts 2018), antioxidative (Agudelo-Ochoa et al. 2016), and antihypertensive effects (Mubarak et al. 2012, Santana-Galvez et al. 2017). A meta-analysis including 25 case-control and 16 cohort studies (Li et al. 2013) and epidemiological data (Schmit et al. 2016) suggest an inverse association between coffee consumption and colorectal

cancer incidence, but prevention of coronary heart disease and some cancers were described (Dupas et al. 2006, Schmit et al. 2016). In-depth knowledge on the gastrointestinal behavior of chlorogenic acid can aid in a better understanding of the biological properties of chlorogenic acid.

1.3.2 Microbiotic biotransformation of chlorogenic acid

Stalmach et al. (2010) reported a recovery of 70% of the initial chlorogenic acids intake after coffee consumption in the ileal fluid of ileostomy patients, suggesting that this fraction will reach the colon and will be exposed to the gut microbiota. Accordingly, Stalmach et al. (2009, 2010) reported a higher recovery of microbial biotransformation products (Figure 1-9) of chlorogenic acids in the urine of healthy human volunteers with an intact colon in comparison to the ileostomy patients, substantiating an important role for the gut microbiota in the biotransformation of chlorogenic acids and the colon on absorption of its microbial metabolites (Stalmach et al. 2009, Stalmach et al. 2010). Multiple studies have studied and confirmed the biotransformation of chlorogenic acid by the gut microbiome in rats, humans and *in vitro* models (Gonthier MP 2003, Olthof et al. 2003, Konishi and Kobayashi 2004, Rechner et al. 2004, Gonthier et al. 2006, Del Rio et al. 2010, Tomas-Barberan et al. 2014, Breynaert et al. 2015, Pinta et al. 2018).

1.3.3 *In vivo* bioavailability of chlorogenic acid

Multiple studies have reported an influence of the microbiotic biotransformation of chlorogenic acid on the *in vivo* bioavailability. The *in vivo* bioavailability of chlorogenic acid(s) was studied in humans and rats after coffee consumption (Dupas et al. 2006, Stalmach et al. 2009, Stalmach et al. 2010), oral ingestion of a green coffee extract (Farah et al. 2008) or a chlorogenic acid supplemented diet (Gonthier et al. 2003, Li et al. 2020). Farah et al. (2008) and Gonthier et al. (2003) studied the bioavailability of chlorogenic acid in humans and rats respectively, including the microbial biotransformation products in the formula of the apparent bioavailability. Farah et al.

(2008) reported an apparent bioavailability of 33% ± 27% for chlorogenic acid after oral ingestion of a green coffee extract. Gonthier and colleagues (2003) stated that the bioavailability of chlorogenic acid is highly dependent on its microbial biotransformation as 57% (mol/mol) of the orally ingested dose of chlorogenic acid was recovered as microbial biotransformation products in the plasma. These studies, however, do not allow to make statements on the absorption of chlorogenic acid and its microbial biotransformation products across the intestinal cell wall which remains an opportunity for further research.
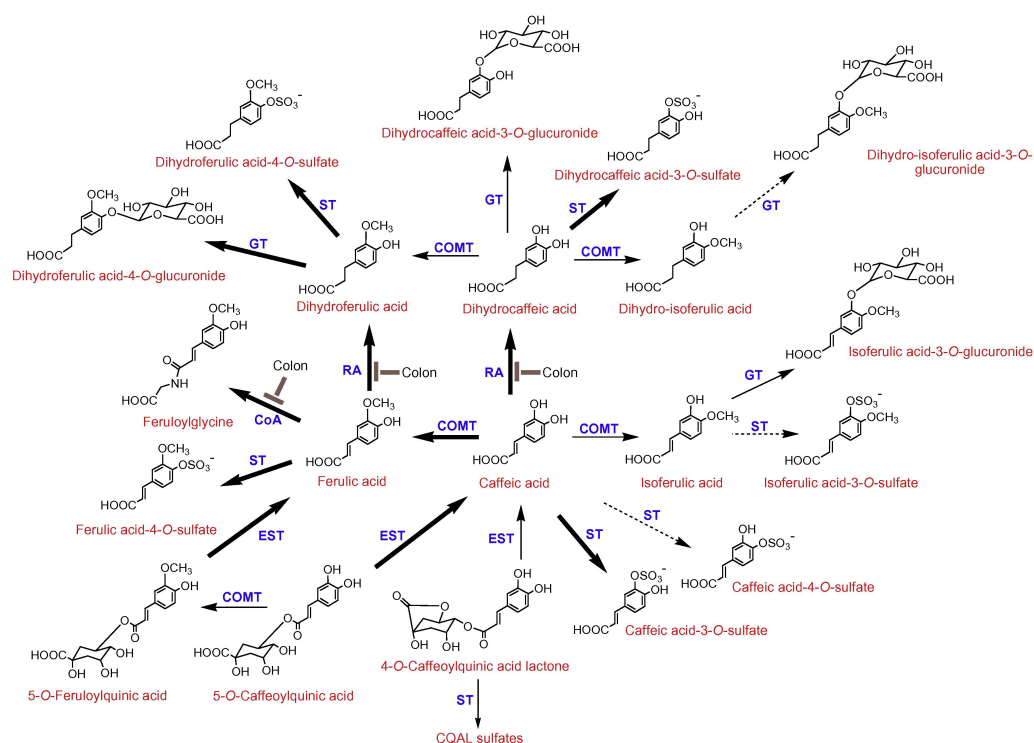
Figure 1-9: Proposed biotransformation pathway of chlorogenic acids after coffee-consumption by Stalmach et al. (2010). Biotransformation steps absent in individuals without colon are indicated. Bold and dotted arrows indicate major and minor biotransformation steps respectively. COMT: catechol-O-methyltransferase, ET: esterase, RA: reductase, GT: UDP-glucuronyltransferase, ST: sulfuryl-O-transerase, Co-A: co-enzyme A. Figure from (Stalmach et al. 2010).

1.4   Objectives and outline of the thesis

The gut microbiome has been neglected during drug development, formulation and dosing strategies since little is known about the effect of this newly proposed metabolic organ on the activity, possible toxicity and bioavailability of orally administered xenobiotics. The main objective of this PhD is to gain more insights in the role of the gut microbiome on the gastrointestinal fate of orally ingested xenobiotics as well as investigating inter-population differences between lean and obese volunteers. Consequently, the objectives of this PhD project were to:

1. Optimize a ready-to-use *in vitro* platform including the GIDM-Colon and bioanalytical strategies to investigate the gastrointestinal biotransformation of xenobiotics.

2. Application of the *in vitro* platform to investigate interindividual differences in microbiotic biotransformation of xenobiotics between a lean and obese population.

3. Expand the *in vitro* gastrointestinal platform with an *in vitro* permeability and an *in vitro* intestinal first-pass assay using a Caco-2 cell-line and human intestinal microsomes (HIM)/cytosol (HICYT) preparations respectively. These assays can be applied to study the *in vitro* intestinal absorption and *in vitro* intestinal first-pass biotransformation of xenobiotics and their microbial biotransformation products.

Chapter 2 discusses the optimization of a ready-to-use gut microbiome biotransformation platform using an *in vitro* gastrointestinal dialysis-model with colon phase together with an instrumental platform using liquid chromatography coupled to high resolution mass spectrometry (LC-Q-TOF-MS). Both pre-analytical phase and data-analysis workflows are optimized. The second part of this chapter discusses the

compatibility of parallel GIDM-Colon experiments covering different sampling timepoints and dialysis timings.

The optimized gut microbiome biotransformation platform is applied in **Chapter 3** to study interindividual differences in microbiotic biotransformation of chlorogenic acid between a lean and obese population. Differences in biotransformation rate and number of identified biotransformation products are discussed.

The aim of **Chapter 4** is to investigate the *in vitro* intestinal absorption of chlorogenic acid and quinic acid, one of its most prominent microbial biotransformation products, using a bidirectional Caco-2 permeability assay.

The intestinal first-pass biotransformation of chlorogenic acid and two of its microbial biotransformation products, caffeic acid and quinic acid, is investigated. The intestinal phase I and phase II biotransformation products are investigated using an *in vitro* biotransformation assay including human intestinal microsomes and human intestinal cytosol preparations. Results are discussed in **Chapter 5.**

Chapter 6 concludes the PhD thesis with a critical discussion of the presented results followed by some insights in necessary future research.

References

Abuhelwa AY, Williams DB, Upton RN and Foster DJR. Food, gastrointestinal pH, and models of oral drug absorption. *European Journal of Pharmaceutics and Biopharmaceutics* 2017, 112: 234-248.

Adams JB, Johansen LJ, Powell LD, Quig D and Rubin RA. Gastrointestinal flora and gastrointestinal status in children with autism--comparisons to typical children and correlation with autism severity. *BMC Gastroenterology* 2011, 11: 22.

Agudelo-Ochoa GM, Pulgarín-Zapata IC, Velásquez-Rodriguez CM, Duque-Ramírez M, Naranjo-Cano M, Quintero-Ortiz MM, Lara-Guzmán OJ and Muñoz-Durango K. Coffee Consumption Increases the Antioxidant Capacity of Plasma and Has No Effect on the Lipid Profile or Vascular Function in Healthy Adults in a Randomized Controlled Trial. *The Journal of Nutrition* 2016, 146(3): 524-531.

Azzouz LL and Sharma S (2020). Physiology, Large Intestine. *StatPearls*. Treasure Island (FL), StatPearls Publishing.

Borody TJ, Paramsothy S and Agrawal G. Fecal microbiota transplantation: indications, methods, evidence, and future directions. *Current gastroenterology reports* 2013, 15(8): 337-337.

Breynaert A, Bosscher D, Kahnt A, Claeys M, Cos P, Pieters L and Hermans N. Development and Validation of an in vitro Experimental GastroIntestinal Dialysis Model with Colon Phase to Study the Availability and Colonic Metabolisation of Polyphenolic Compounds. *Planta Medica* 2015, 81(12-13): 1075-1083.

Brown JM and Hazen SL. The gut microbial endocrine organ: bacterially derived signals driving cardiometabolic diseases. *Annual Review of Medicine* 2015, 66: 343-359.

Bryrup T, Thomsen CW, Kern T, Allin KH, Brandslund I, Jørgensen NR, Vestergaard H, Hansen T, Hansen TH, Pedersen O and Nielsen T. Metformin-induced changes of the gut microbiota in healthy young men: results of a non-blinded, one-armed intervention study. *Diabetologia* 2019, 62(6): 1024-1035.

Carmody RN and Turnbaugh PJ. Host-microbial interactions in the metabolism of therapeutic and diet-derived xenobiotics. *Journal of Clinical Investigation* 2014, 124(10): 4173-4181.

De Filippo C, Cavalieri D, Di Paola M, Ramazzotti M, Poullet JB, Massart S, Collini S, Pieraccini G and Lionetti P. Impact of diet in shaping gut microbiota revealed by a comparative study in children from Europe and rural Africa. *Proceedings of the National Academy of Sciences of the United States of America 2010*, 107(33): 14691-14696.

Del Rio D, Stalmach A, Calani L and Crozier A. Bioavailability of Coffee Chlorogenic Acids and Green Tea Flavan-3-ols. *Nutrients* 2010, 2(8): 820-833.

den Besten G, van Eunen K, Groen AK, Venema K, Reijngoud D-J and Bakker BM. The role of short-chain fatty acids in the interplay between diet, gut microbiota, and host energy metabolism. *Journal of lipid research* 2013, 54(9): 2325-2340.

DeSesso JM and Jacobson CF. Anatomical and physiological parameters affecting gastrointestinal absorption in humans and rats. *Food and Chemical Toxicology* 2001, 39(3): 209-228.

Dethlefsen L and Relman DA. Incomplete recovery and individualized responses of the human distal gut microbiota to repeated antibiotic perturbation. *Proceedings of the National Academy of Sciences of the United States of America* 2011, 108 Suppl 1(Suppl 1): 4554-4561.

Dieterich W, Schink M and Zopf Y. Microbiota in the Gastrointestinal Tract. *Medical sciences (Basel, Switzerland)* 2018, 6(4): 116.

Dominguez-Bello MG, Costello EK, Contreras M, Magris M, Hidalgo G, Fierer N and Knight R. Delivery mode shapes the acquisition and structure of the initial microbiota across multiple body habitats in newborns. *Proceedings of the National Academy of Sciences of the United States of America* 2010, 107(26): 11971.

Donohoe DR, Garge N, Zhang X, Sun W, O'Connell TM, Bunger MK and Bultman SJ. The microbiome and butyrate regulate energy metabolism and autophagy in the mammalian colon. *Cell metabolism* 2011, 13(5): 517-526.

dos Santos MD, Almeida MC, Lopes NP, de Souza G, oacute, ria E, iacute and lia P. Evaluation of the Anti-inflammatory, Analgesic and Antipyretic Activities of the Natural Polyphenol Chlorogenic Acid. *Biological and Pharmaceutical Bulletin* 2006, 29(11): 2236-2240.

Dupas C, Marsset Baglieri A, Ordonaud C, Tome D and Maillard MN. Chlorogenic acid is poorly absorbed, independently of the food matrix: A Caco-2 cells and rat chronic absorption study. *Molecular Nutrition & Food Research* 2006, 50(11): 1053-1060.

Dupont D, Alric M, Blanquet-Diot S, Bornhorst G, Cueva C, Deglaire A, Denis S, Ferrua M, Havenaar R, Lelieveld J, Mackie AR, Marzorati M, Menard O, Minekus M, Miralles B, Recio I and Van den Abbeele P. Can dynamic in vitro digestion systems mimic the physiological reality? *Critical Reviews in Food Science and Nutrition* 2019, 59(10): 1546-1562.

Falony G, Joossens M, Vieira-Silva S, Wang J, Darzi Y, Faust K, Kurilshikov A, Bonder MJ, Valles-Colomer M, Vandeputte D, Tito RY, Chaffron S, Rymenans L, Verspecht C, De Sutter L, Lima-Mendez G, D'Hoe K, Jonckheere K, Homola D, Garcia R, Tigchelaar EF, Eeckhaudt L, Fu J, Henckaerts L, Zhernakova A, Wijmenga C and Raes J. Population-level analysis of gut microbiome variation. *Science* 2016, 352(6285): 560-564.

Farah A, Monteiro M, Donangelo CM and Lafay S. Chlorogenic Acids from Green Coffee Extract are Highly Bioavailable in Humans. *The Journal of Nutrition* 2008, 138(12): 2309-2315.

FDA. (2019). "Novel Drug Approvals for 2018." 2020, from https://www.fda.gov/drugs/new-drugs-fda-cders-new-molecular-entities-and-new-therapeutic-biological-products/novel-drug-approvals-2018.

FDA. (2020). "Novel Drug Approvals for 2019." 2020, from https://www.fda.gov/drugs/new-drugs-fda-cders-new-molecular-entities-and-new-therapeutic-biological-products/novel-drug-approvals-2019.

Forslund K, Hildebrand F, Nielsen T, Falony G, Le Chatelier E, Sunagawa S, Prifti E, Vieira-Silva S, Gudmundsdottir V, Pedersen HK, Arumugam M, Kristiansen K, Voigt AY, Vestergaard H, Hercog R, Costea PI, Kultima JR, Li J, Jorgensen T, Levenez F, Dore J, Meta HITc, Nielsen HB, Brunak S, Raes J, Hansen T, Wang J, Ehrlich SD, Bork P and Pedersen O. Disentangling type 2 diabetes and metformin treatment signatures in the human gut microbiota. *Nature* 2015, 528(7581): 262-266.

Glick-Bauer M and Yeh M-C. The health advantage of a vegan diet: Exploring the gut microbiota connection. *Nutrients* 2014, 6(11): 4822-4838.

Gonthier MP, Remesy C, Scalbert A, Cheynier V, Souquet JM, Poutanen K and Aura AM. Microbial metabolism of caffeic acid and its esters chlorogenic and caftaric acids by human faecal microbiota in vitro. *Biomedicine & Pharmacotherapy* 2006, 60(9): 536-540.

Gonthier MP, Verny MA, Besson C, Rémésy C and Scalbert A. Chlorogenic Acid Bioavailability Largely Depends on Its Metabolism by the Gut Microflora in Rats. *The Journal of Nutrition* 2003, 133(6): 1853-1859.

Gonthier MP VM, Besson C, Rémésy C, Scalbert A. Chlorogenic acid bioavailability largely depends on its metabolism by the gut microflora in rats. *The Journal of Nutrition* 2003, 133(6): 1853-1859.

Goodrich JK, Davenport ER, Beaumont M, Jackson MA, Knight R, Ober C, Spector TD, Bell JT, Clark AG and Ley RE. Genetic Determinants of the Gut Microbiome in UK Twins. *Cell host & microbe* 2016, 19(5): 731-743.

Goodrich JK, Waters JL, Poole AC, Sutter JL, Koren O, Blekhman R, Beaumont M, Van Treuren W, Knight R, Bell JT, Spector TD, Clark AG and Ley RE. Human genetics shape the gut microbiome. *Cell* 2014, 159(4): 789-799.

Hens B, Corsetti M, Spiller R, Marciani L, Vanuytsel T, Tack J, Talattof A, Amidon GL, Koziolek M, Weitschies W, Wilson CG, Bennink RJ, Brouwers J and Augustijns P. Exploring gastrointestinal variables affecting drug and formulation behavior: Methodologies, challenges and opportunities. *International Journal of Pharmaceutics* 2017, 519(1-2): 79-97.

Hunyadi A, Martins A, Hsieh T-J, Seres A and Zupkó I. Chlorogenic Acid and Rutin Play a Major Role in the In Vivo Anti-Diabetic Activity of Morus alba Leaf Extract on Type II Diabetic Rats. *PLoS One* 2012, 7(11): e50619.

Jain A, Li XH and Chen WN. Similarities and differences in gut microbiome composition correlate with dietary patterns of Indian and Chinese adults. *AMB Express* 2018, 8(1): 104.

Jakobsson HE, Jernberg C, Andersson AF, Sjölund-Karlsson M, Jansson JK and Engstrand L. Short-term antibiotic treatment has differing long-term impacts on the human throat and gut microbiome. *PLoS One* 2010, 5(3): e9836.

Jandhyala SM, Talukdar R, Subramanyam C, Vuyyuru H, Sasikala M and Nageshwar Reddy D. Role of the normal gut microbiota. *World Journal of Gastroenterology* 2015, 21(29): 8787-8803.

Kalantzi L, Goumas K Fau - Kalioras V, Kalioras V Fau - Abrahamsson B, Abrahamsson B Fau - Dressman JB, Dressman Jb Fau - Reppas C and Reppas C. Characterization of the human upper gastrointestinal contents under conditions simulating bioavailability/bioequivalence studies. *Pharmaceutical research* 2006, 23(0724-8741 (Print)): 165-176.

Kiela PR and Ghishan FK. Physiology of intestinal absorption and secretion. *Best Practice & Research in Clinical Gastroenterology* 2016, 30(2): 145-159.

Konishi Y and Kobayashi S. Transepithelial Transport of Chlorogenic Acid, Caffeic Acid, and Their Colonic Metabolites in Intestinal Caco-2 Cell Monolayers. *Journal of Agricultural and Food Chemistry* 2004, 52(9): 2518-2526.

Koppel N, Maini Rekdal V and Balskus EP. Chemical transformation of xenobiotics by the human gut microbiota. *Science* 2017, 356(6344).

Koziolek M, Grimm M, Garbacz G, Kühn J-P and Weitschies W. Intragastric Volume Changes after Intake of a High-Caloric, High-Fat Standard Breakfast in Healthy Human Subjects Investigated by MRI. *Molecular Pharmaceutics* 2014, 11(5): 1632-1639.

Koziolek M, Schneider F, Grimm M, Modeβ C, Seekamp A, Roustom T, Siegmund W and Weitschies W. Intragastric pH and pressure profiles after intake of the high-caloric, high-fat meal as used for food effect studies. *Journal of Controlled Release* 2015, 220: 71-78.

Krajmalnik-Brown R, Ilhan ZE, Kang DW and DiBaise JK. Effects of gut microbes on nutrient absorption and energy regulation. *Nutrition in Clinical Practice* 2012, 27(2): 201-214.

Larsen N, Vogensen FK, van den Berg FW, Nielsen DS, Andreasen AS, Pedersen BK, Al-Soud WA, Sorensen SJ, Hansen LH and Jakobsen M. Gut microbiota in human adults with type 2 diabetes differs from non-diabetic adults. *PLoS One* 2010, 5(2): e9085.

Ley RE, Bäckhed F, Turnbaugh P, Lozupone CA, Knight RD and Gordon JI. Obesity alters gut microbial ecology. *Proceedings of the National Academy of Sciences of the United States of America* 2005, 102(31): 11070.

Ley RE, Turnbaugh PJ, Klein S and Gordon JI. Human gut microbes associated with obesity. *Nature* 2006, 444(7122): 1022-1023.

Li G, Ma D, Zhang Y, Zheng W and Wang P. Coffee consumption and risk of colorectal cancer: a meta-analysis of observational studies. *Public Health Nutrition* 2013, 16(2): 346-357.

Li L, Su C, Chen X, Wang Q, Jiao W, Luo H, Tang J, Wang W, Li S and Guo S. Chlorogenic Acids in Cardiovascular Disease: A Review of Dietary Consumption, Pharmacology, and Pharmacokinetics. *Journal of Agricultural and Food Chemistry* 2020, 68(24): 6464-6484.

Li Q, Han Y, Dy ABC and Hagerman RJ. The Gut Microbiota and Autism Spectrum Disorders. *Frontiers in Cellular Neuroscience* 2017, 11: 120.

Liang N and Kitts DD. Amelioration of Oxidative Stress in Caco-2 Cells Treated with Pro-inflammatory Proteins by Chlorogenic Acid Isomers via Activation of the Nrf2–Keap1–ARE-Signaling Pathway. *Journal of Agricultural and Food Chemistry* 2018, 66(42): 11008-11017.

Machiels K, Joossens M, Sabino J, De Preter V, Arijs I, Eeckhaut V, Ballet V, Claes K, Van Immerseel F, Verbeke K, Ferrante M, Verhaegen J, Rutgeerts P and Vermeire S. A decrease of the butyrate-producing species Roseburia hominis and Faecalibacterium prausnitzii defines dysbiosis in patients with ulcerative colitis. *Gut* 2014, 63(8): 1275-1283.

Mubarak A, Bondonno CP, Liu AH, Considine MJ, Rich L, Mas E, Croft KD and Hodgson JM. Acute Effects of Chlorogenic Acid on Nitric Oxide Status, Endothelial Function, and Blood Pressure in Healthy Volunteers: A Randomized Trial. *Journal of Agricultural and Food Chemistry* 2012, 60(36): 9130-9136.

Mudie DM, Amidon GL and Amidon GE. Physiological Parameters for Oral Delivery and in Vitro Testing. *Molecular Pharmaceutics* 2010, 7(5): 1388-1405.

Mudie DM, Murray K, Hoad CL, Pritchard SE, Garnett MC, Amidon GL, Gowland PA, Spiller RC, Amidon GE and Marciani L. Quantification of Gastrointestinal Liquid Volumes and Distribution Following a 240 mL Dose of Water in the Fasted State. *Molecular Pharmaceutics* 2014, 11(9): 3039-3047.

Nagpal R, Mainali R, Ahmadi S, Wang S, Singh R, Kavanagh K, Kitzman DW, Kushugulova A, Marotta F and Yadav H. Gut microbiome and aging: Physiological and mechanistic insights. *Nutrition and healthy aging* 2018, 4(4): 267-285.

Naveed M, Hejazi V, Abbas M, Kamboh AA, Khan GJ, Shumzaid M, Ahmad F, Babazadeh D, FangFang X, Modarresi-Ghazani F, WenHua L and XiaoHui Z. Chlorogenic acid (CGA): A pharmacological review and call for further research. *Biomedicine & Pharmacotherapy* 2018, 97: 67-74.

O'Hara AM and Shanahan F. The gut flora as a forgotten organ. *EMBO reports* 2006, 7(7): 688-693.

Olthof MR, Hollman PCH, Buijsman M, van Amelsvoort JMM and Katan MB. Chlorogenic acid, quercetin-3-rutinoside and black tea phenols are extensively metabolized in humans (vol 133, pg 1806, 2003). *Journal of Nutrition* 2003, 133(8): 2692-2692.

Pal A, Brasseur JG and Abrahamsson B. A stomach road or "Magenstrasse" for gastric emptying. *Journal of Biomechanics* 2007, 40(6): 1202-1210.

Pascale A, Marchesi N, Marelli C, Coppola A, Luzi L, Govoni S, Giustina A and Gazzaruso C. Microbiota and metabolic diseases. *Endocrine* 2018, 61(3): 357-371.

Pinta MN, Montoliu I, Aura AM, Seppanen-Laakso T, Barron D and Moco S. In Vitro Gut Metabolism of U-C-13 -Quinic Acid, The Other Hydrolysis Product of Chlorogenic Acid. *Molecular Nutrition & Food Research* 2018, 62(22): 7.

Qin J, Li Y, Cai Z, Li S, Zhu J, Zhang F, Liang S, Zhang W, Guan Y, Shen D, Peng Y, Zhang D, Jie Z, Wu W, Qin Y, Xue W, Li J, Han L, Lu D, Wu P, Dai Y, Sun X, Li Z, Tang A, Zhong S, Li X, Chen W, Xu R, Wang M, Feng Q, Gong M, Yu J, Zhang Y, Zhang M, Hansen T, Sanchez G, Raes J, Falony G, Okuda S, Almeida M, LeChatelier E, Renault P, Pons N, Batto JM, Zhang Z, Chen H, Yang R, Zheng W, Li S, Yang H, Wang J, Ehrlich SD, Nielsen R, Pedersen O, Kristiansen K and Wang J. A metagenome-wide association study of gut microbiota in type 2 diabetes. *Nature* 2012, 490(7418): 55-60.

Rechner AR, Smith MA, Kuhnle G, Gibson GR, Debnam ES, Srai SKS, Moore KP and Rice-Evans CA. Colonic metabolism of dietary polyphenols: Influence of structure on microbial fermentation products. *Free Radical Biology and Medicine* 2004, 36(2): 212-225.

Riethorst D, Mols R, Duchateau G, Tack J, Brouwers J and Augustijns P. Characterization of Human Duodenal Fluids in Fasted and Fed State Conditions. *Journal of Pharmaceutical Sciences* 2016, 105(1520-6017 (Electronic)): 673-681.

Santana-Galvez J, Cisneros-Zevallos L and Jacobo-Velazquez DA. Chlorogenic Acid: Recent Advances on Its Dual Role as a Food Additive and a Nutraceutical against Metabolic Syndrome. *Molecules* 2017, 22(3).

Sarosiek I, Selover KH, Katz LA, Semler JR, Wilding GE, Lackner JM, Sitrin MD, Kuo B, Chey WD, Hasler WL, Koch KL, Parkman HP, Sarosiek J and McCallum RW. The assessment of regional gut transit times in healthy controls and patients with gastroparesis using wireless motility technology. *Alimentary Pharmacology and Therapeutics* 2010, 31(2): 313-322.

Schirmer M, Franzosa EA, Lloyd-Price J, McIver LJ, Schwager R, Poon TW, Ananthakrishnan AN, Andrews E, Barron G, Lake K, Prasad M, Sauk J, Stevens B, Wilson RG, Braun J, Denson LA, Kugathasan S, McGovern DPB, Vlamakis H, Xavier RJ and Huttenhower C. Dynamics of metatranscription in the inflammatory bowel disease gut microbiome. *Nature Microbiology* 2018, 3(3): 337-346.

Schmit SL, Rennert HS, Rennert G and Gruber SB. Coffee Consumption and the Risk of Colorectal Cancer. *Cancer epidemiology, biomarkers & prevention : a publication of the American Association for Cancer Research, cosponsored by the American Society of Preventive Oncology* 2016, 25(4): 634-639.

Sedighi M, Razavi S, Navab-Moghadam F, Khamseh ME, Alaei-Shahmiri F, Mehrtash A and Amirmozafari N. Comparison of gut microbiota in adult patients with type 2 diabetes and healthy individuals. *Microbial Pathogenis* 2017, 111: 362-369.

Shreiner AB, Kao JY and Young VB. The gut microbiome in health and in disease. *Currunt Opinion in Gastroenterology* 2015, 31(1): 69-75.

Silverthorn DU. Human Physiology: un integrated approach. *Pearson international* San Francisco, USA, 2010.

Simonian HP, Vo L, Doma S, Fisher RS and Parkman HP. Regional postprandial differences in pH within the stomach and gastroesophageal junction. *Digestive Diseases and Sciences* 2005, 50(12): 2276-2285.

Sousa T, Paterson R, Moore V, Carlsson A, Abrahamsson B and Basit AW. The gastrointestinal microbiota as a site for the biotransformation of drugs. *Internation Journal of Pharmaceutics* 2008, 363(1-2): 1-25.

Spanogiannopoulos P, Bess EN, Carmody RN and Turnbaugh PJ. The microbial pharmacists within us: a metagenomic view of xenobiotic metabolism. *Nature Reviews Microbiology* 2016, 14(5): 273-287.

Stalmach A, Mullen W, Barron D, Uchida K, Yokota T, Cavin C, Steiling H, Williamson G and Crozier A. Metabolite profiling of hydroxycinnamate derivatives in plasma and urine after the ingestion of coffee by humans: identification of biomarkers of coffee consumption. *Drug Metabolism and Disposition* 2009, 37(8): 1749-1758.

Stalmach A, Steiling H, Williamson G and Crozier A. Bioavailability of chlorogenic acids following acute ingestion of coffee by humans with an ileostomy. *Archives of Biochemistry and Biophysics* 2010, 501(1): 98-105.

Stillhart C, Vučićević K, Augustijns P, Basit AW, Batchelor H, Flanagan TR, Gesquiere I, Greupink R, Keszthelyi D, Koskinen M, Madla CM, Matthys C, Miljuš G, Mooij MG, Parrott N, Ungell A-L, de Wildt SN, Orlu M, Klein S and Müllertz A. Impact of gastrointestinal physiology on drug absorption in special populations—An UNGAP review. *European Journal of Pharmaceutical Sciences* 2020, 147: 105280.

Stojancevic M, Bojic G, Al Salami H and Mikov M. The Influence of Intestinal Tract and Probiotics on the Fate of Orally Administered Drugs. *Current Issues in Molecular Biology* 2014, 16: 55-67.

Strati F, Cavalieri D, Albanese D, De Felice C, Donati C, Hayek J, Jousson O, Leoncini S, Renzi D, Calabrò A and De Filippo C. New evidences on the altered gut microbiota in autism spectrum disorders. *Microbiome* 2017, 5(1): 24.

Teitelbaum EN, Vaziri K, Zettervall S, Amdur RL and Orkin BA. Intraoperative small bowel length measurements and analysis of demographic predictors of increased length. *Clinical Anatomy* 2013, 26(7): 827-832.

Tomas-Barberan F, Garcia-Villalba R, Quartieri A, Raimondi S, Amaretti A, Leonardi A and Rossi M. In vitro transformation of chlorogenic acid by human gut microbiota. *Molecular Nutrition & Food Research* 2014, 58(5): 1122-1131.

Turnbaugh PJ, Backhed F, Fulton L and Gordon JI. Diet-induced obesity is linked to marked but reversible alterations in the mouse distal gut microbiome. *Cell Host Microbe* 2008, 3(4): 213-223.

Turnbaugh PJ, Hamady M, Yatsunenko T, Cantarel BL, Duncan A, Ley RE, Sogin ML, Jones WJ, Roe BA, Affourtit JP, Egholm M, Henrissat B, Heath AC, Knight R and Gordon JI. A core gut microbiome in obese and lean twins. *Nature* 2009, 457(7228): 480-484.

Van de Wiele T, Van den Abbeele P, Ossieur W, Possemiers S and Marzorati M (2015). The Simulator of the Human Intestinal Microbial Ecosystem (SHIME((R))). *The Impact of Food Bioactives on Health: in vitro and ex vivo models*. K. Verhoeckx, P. Cotter, I. Lopez-Exposito et al. Cham (CH)**:** 305-317.

Van Den Abeele J, Rubbens J, Brouwers J and Augustijns P. The dynamic gastric environment and its impact on drug and formulation behaviour. 2017, 96: 207-231.

Venema K (2015). The TNO In Vitro Model of the Colon (TIM-2). *The Impact of Food Bioactives on Health: in vitro and ex vivo models*. K. Verhoeckx, P. Cotter, I. López-Expósito et al. Cham, Springer International Publishing**:** 293-304.

Venema K and van den Abbeele P. Experimental models of the gut microbiome. *Best Practice & Research in Clinical Gastroenterology* 2013, 27(1): 115-126.

Verhoeckx K, Cotter P, Lopez-Exposito I, Kleiveland C, Lea T, Mackie A, Requena T, Swiatecka D and Wichers H. The Impact of Food Bioactives on Health: in vitro and ex vivo models. *Springer* Cham (CH), 2015: 338.

Vertzoni M, Augustijns P, Grimm M, Koziolek M, Lemmens G, Parrott N, Pentafragka C, Reppas C, Rubbens J, Van Den Alphabeele J, Vanuytsel T, Weitschies W and Wilson CG. Impact of regional differences along the gastrointestinal tract of healthy adults on oral drug absorption: An UNGAP review. *European Journal of Pharmaceutical Sciences* 2019, 134: 153-175.

Wang T, Cai G, Qiu Y, Fei N, Zhang M, Pang X, Jia W, Cai S and Zhao L. Structural segregation of gut microbiota between colorectal cancer patients and healthy volunteers. *ISME Journal* 2012, 6(2): 320-329.

Weersma RK, Zhernakova A and Fu J. Interaction between drugs and the gut microbiome. *Gut* 2020, 69(8): 1510.

Wianowska D and Gil M. Recent advances in extraction and analysis procedures of natural chlorogenic acids. *Phytochemistry Reviews* 2018, 18(1): 273-302.

Wilson ID and Nicholson JK. Gut microbiome interactions with drug metabolism, efficacy, and toxicity. *Translational Research* 2017, 179: 204-222.

Wu N, Yang X, Zhang R, Li J, Xiao X, Hu Y, Chen Y, Yang F, Lu N, Wang Z, Luan C, Liu Y, Wang B, Xiang C, Wang Y, Zhao F, Gao GF, Wang S, Li L, Zhang H and Zhu B. Dysbiosis signature of fecal microbiota in colorectal cancer patients. *Microbial Ecology* 2013, 66(2): 462-470.

Yan Q, Gu Y, Li X, Yang W, Jia L, Chen C, Han X, Huang Y, Zhao L, Li P, Fang Z, Zhou J, Guan X, Ding Y, Wang S, Khan M, Xin Y, Li S and Ma Y. Alterations of the Gut Microbiome in Hypertension. *Frontiers in cellular and infection microbiology* 2017, 7: 381-381.

Yang T, Santisteban MM, Rodriguez V, Li E, Ahmari N, Carvajal JM, Zadeh M, Gong M, Qi Y, Zubcevic J, Sahay B, Pepine CJ, Raizada MK and Mohamadzadeh M. Gut dysbiosis is linked to hypertension. *Hypertension* 2015, 65(6): 1331-1340.

Yatsunenko T, Rey FE, Manary MJ, Trehan I, Dominguez-Bello MG, Contreras M, Magris M, Hidalgo G, Baldassano RN, Anokhin AP, Heath AC, Warner B, Reeder J, Kuczynski J, Caporaso JG, Lozupone CA, Lauber C, Clemente JC, Knights D, Knight R and Gordon JI. Human gut microbiome viewed across age and geography. *Nature* 2012, 486(7402): 222-227.

Zhao C, Dong H, Zhang Y and Li Y. Discovery of potential genes contributing to the biosynthesis of short-chain fatty acids and lactate in gut microbiota from systematic investigation in E. coli. *npj Biofilms and Microbiomes* 2019, 5(1): 19.

CHAPTER 2: OPTIMIZATION OF AN *IN VITRO* GUT MICROBIOME BIOTRANSFORMATION PLATFORM
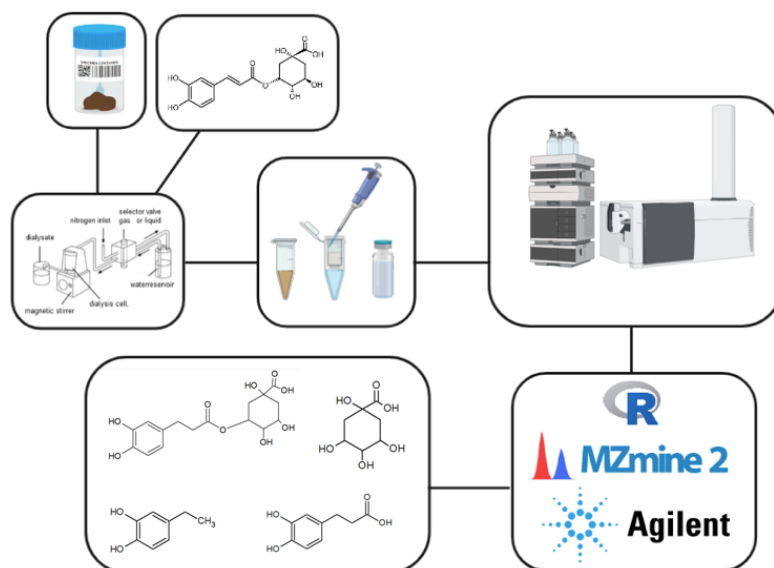
<u>Based on following papers:</u>

Mortelé O, Iturrospe E, Breynaert A, Verdickt E, Xavier B B, Lammens C, Malhotra-Kumar S, Jorens P G, Pieters L, van Nuijs A L N and Hermans N. Optimization of an in vitro gut microbiome biotransformation platform with chlorogenic acid as model compound: From fecal sample to biotransformation product identification. *Journal of Pharmaceutical and Biomedical Analysis* 2019, 175: 112768.

Mortelé O*, Vervliet P, Gys C, Degreef M, Cuykx M, Maudens K, Covaci A, van Nuijs A L N and Lai F Y. In vitro Phase I and Phase II metabolism of the new designer benzodiazepine cloniprazepam using liquid chromatography coupled to quadrupole time-of-flight mass spectrometry. *Journal of Pharmaceutical and Biomedical Analysis* 2018, 153: 158-167.

Vervliet P, **Mortelé O***, Gys C, Degreef M, Lanckmans K, Maudens K, Covaci A, van Nuijs A L N and Lai F Y. Suspect and non-target screening workflows to investigate the in vitro and in vivo metabolism of the synthetic cannabinoid 5Cl-THJ-018*. Drug Testing and Analysis* 2018, 11(3): 479-491.

*Joint first author

CHAPTER 2

CHAPTER 2

2.1 Introduction

As compared to the human genome, the cumulative genome content of the gut microbiota, also known as the gut microbiome, is estimated to contain 100 to 300-fold more genes than the human genome and contains 3.3-10 million nonredundant genes (Borody et al. 2013, Stojancevic et al. 2014, Jandhyala et al. 2015). It is therefore not surprising that the gut microbiome is able to influence the physiology of the host and that it is considered as an additional metabolizing organ (O'Hara and Shanahan 2006, Borody et al. 2013). Important differences between hepatic and bacterial metabolism have been observed. Liver metabolic pathways consist mostly out of oxidative phase I reactions through cytochrome P450 enzymes (CYP450), and conjugation phase II reactions through uridine 5'-diphospho(UDP)-glucuronosyltransferases (UGTs), sulfotransferases (SULTs), etc., typically leading to the conversion of lipophilic compounds into more hydrophilic compounds to enhance excretion. The majority of the biotransformation reactions by the gut microbiome are reductive, due to the high reduction potential of anaerobic bacteria, and hydrolytic (Venema and van den Abbeele 2013, Stojancevic et al. 2014, Wilson and Nicholson 2017).

These insights have led to the understanding that the gut microbiome can directly and indirectly influence the activity and toxicity of pharmaceuticals and other xenobiotics (Wilson and Nicholson 2017). Examples of direct interferences are the conversion of a prodrug to the active compound, inactivation, detoxification, change of efficacy and direct binding to xenobiotics or dietary components (Carmody and Turnbaugh 2014, Spanogiannopoulos et al. 2016). Examples of indirect interferences are the alteration of host genes expression (e.g. lower expression of CYP450 enzymes), competition and/or inhibition of host enzymes by microbial biotransformation products and reactivation of drugs by deconjugation of phase II biotransformation products after enterohepatic circulation (Carmody and Turnbaugh 2014, Spanogiannopoulos et al. 2016). Most new pharmaceutical drug candidates present biopharmaceutical problems like low solubility and/or low permeability leading to longer contact with the

gut microbiome. This shows the need for more biotransformation studies including the role of the gut microbiome (Sousa et al. 2008).

In vivo animal or clinical studies to investigate the colonic biotransformation of xenobiotics experience some disadvantages. First of all these studies are time-consuming, labor-intensive and expensive (Verhoeckx et al. 2015). Furthermore, animal studies mostly lead to the sacrifice of the animals to be able to sample the different compartments of the gut (Venema and van den Abbeele 2013, Venema 2015). *In vitro* gastrointestinal tract models offer an alternative approach to study the colonic metabolism. In general, *in vitro* models of the gastrointestinal tract contain multiple compartments to mimic the different parts of the digestive system (mouth, stomach, small and large intestine) by adjusting temperature, pH, enzymes and peristalsis (Verhoeckx et al. 2015). Easy access to the different compartments allows dynamic and multiple sampling over time which can help in the understanding of the different steps of the gut fermentation (Verhoeckx et al. 2015). The disadvantage of *in vitro* models is that they are not fully representative for the *in vivo* conditions. Therefore, it is important to create conditions that closely mimic the *in vivo* situation to obtain a high level of physiological significance (Venema and van den Abbeele 2013, Verhoeckx et al. 2015). Static batch incubations are frequently used but they tend to oversimplify the *in vivo* situation. A better representation of the *in vivo* situation can be acquired with semi-continuous models, e.g. the gastrointestinal dialysis model with colon phase (GIDM-Colon) (Breynaert et al. 2015) used during this project or multi-compartmental continuous models (e.g. SHIME®, TIM-2) (Venema 2015).

2.2   **Aims and preface**

The aim of this study was to optimize a complete and ready-to-use setup to investigate the gastrointestinal biotransformation of xenobiotics. First, the incubation medium and time of incubation of fecal slurry samples in the medium, before use in the GIDM-Colon during the colonic stage, were optimized in order to preserve the *in vivo* bacterial composition. Secondly, four different sample preparation methods were evaluated to obtain extracts compatible with the instrumental detection based on liquid chromatography coupled to high-resolution accurate-mass mass spectrometry. Thirdly, data analysis strategies for the elucidation of biotransformation pathways were optimized using complementary suspect and non-targeted screening workflows Chlorogenic acid was chosen as target compound for the optimization of the platform for two reasons. Firstly, this compound was previously used by Breynaert et al. during the development and validation of the GIDM-Colon (Breynaert et al. 2015). Secondly, the gastrointestinal metabolism of chlorogenic acid has been previously investigated in humans and rats by multiple studies which made it a suitable model compound (Gonthier MP 2003, Olthof et al. 2003, Konishi and Kobayashi 2004, Rechner et al. 2004, Gonthier et al. 2006, Del Rio et al. 2010, Tomas-Barberan et al. 2014, Breynaert et al. 2015, Pinta et al. 2018). In the second part of this chapter the compatibility of parallel GIDM-Colon experiments covering different sampling timepoints was evaluated.

2.3   Optimization of an *in vitro* gut microbiome biotransformation platform

2.3.1   Materials and methods

2.3.1.1   Chemicals and reagents

Sodium phosphate dibasic (Na_2HPO_4, ≥99%), sodium phosphatemonobasic dihydrate ($NaH_2PO_4 \cdot 2H_2O$, ≥99%), thioglycollate broth, pepsin from porcine gastric mucosa, bile extract porcine, pancreatin from porcine pancreas, theophylline (≥99%, anhydrous), quinic acid (98%), chlorogenic acid (≥95%), caffeic acid (≥98%), and dihydrocaffeic acid (98%) were acquired from Sigma-Aldrich (St Louis, MO, USA). Deionized water (milliQ) and sodium bicarbonate ($NaHCO_3$, >99.7%, ACS grade) were obtained from respectively Millipore (Burlington, Massachusetts, USA) and Acros Organics (Pittsburgh, Pennsylvania, USA). Hydrochloric acid (HCl, 32 wt.% for analysis), formic acid (98–100%, Suprapur) and sodium hydroxide pellets (NaOH) were acquired from Merck (Darmstadt, Germany). Acetonitrile (ACN) and methanol (MeOH, ≥99.9%, LC–MS grade) were obtained from Fisher Scientific (Hampton, New Hampshire, USA). Ultrapure water (Purelab flex apparatus) was acquired from ELGA Veolia (UK). Nitrogen gas (N_2, AZOTE N28) and a gas mixture of hydrogen, carbon dioxide and nitrogen (5% H_2, 5% CO_2 and 90% N_2, Alphagaz Mix) were obtained from Air Liquide Belge (Liege, Belgium).

2.3.1.2   Materials

Stirred ultrafiltration cells (model 8200, 200 mL, 63.5 mm diameter), the related controller (controller MF2 and reservoir RC800) and ultrafiltration discs (Ultracel, MWCO 1000 Da, 63.5 mm diameter) were acquired from Amicon Ltd (USA). A shaking warm water bath from VWR (Radnor, Pennsylvania, USA) was used during the gastric

stage of the GIDM-Colon model. Dialysis tubing (MWCO 12-14 kDa, Visking size 6 Inf Dia 27/32 – 21.5 mm: 30 M) and an immersion circulator (model 1122S) were acquired respectively from Medicell Ltd. (London, UK) and VWR, for use during the small intestinal stage. A Jacomex glove box T3 from TCPS (Belgium) was used to create an anaerobic environment during the colonic stage.

A Branson 5510DHT ultrasonic cleaner (40 kHz), a vortex mixer (100-2500 rpm) and a FreeZone 1 Liter Benchtop Freeze Dry System (model 7740030) were acquired from respectively Branson Ultrasonics (Danburry, USA), VWR and Labconco (Missouri, USA). A Sigma 1-15PK centrifuge and centrifugal filters (modified nylon membrane, 0.2 µm, 500 µL sample capacity) were obtained respectively from Sigma Laborzentrifugen GmbH (Germany) and VWR.

2.3.1.3   Fecal samples

2.3.1.3.1   Collection, processing and characterization of the fecal samples

Nine fecal samples were collected from human donors that met the following inclusion criteria: women, 25-45 years old, not pregnant, non-smoking, body mass index (BMI) < 25, no risk factors for metabolic diseases, non-vegetarian, normal defecation, no history of gastrointestinal disease, no intake of antibiotics six months, or pre- or probiotics supplements three months prior to fecal donation and no history of immunosuppressive or chemotherapeutic treatment. Fasting glycaemia and glycaemia after oral glucose tolerance test below 126 mg/dL and 200 mg/dL glucose respectively were mandatory. A complete list of all inclusion criteria can be found in supplementary information (Table SI-2.1, Table SI-2.2). Ethical approval for the project was acquired from the Ethical Committee of the Antwerp University Hospital (reference number: 16/43/442).

Donors collected the feces using Protocult collection containers (Ability Building Center, Rochester, USA). An overview of the fecal sample treatment before use in the GIDM-Colon is shown in Figure 2-1. After collection, fecal samples were held at room temperature together with an anaerocult bag from Merck and treated within 3 h before storage at -80 °C. The fecal slurry of 10% (w/v) feces in sterile phosphate buffer (0.1 M, pH 7.0, 0.58% w/v Na_2HPO_4, 1.03% w/v $NaH_2PO_4.2H_2O$, 3.45% thioglycolate broth) was prepared in an anaerobic glove box. Homogenization and elimination of solid particles was performed using a Stomacher® lab blender (VWR, Leuven, Belgium) for three minutes. Aliquots of 2 mL fecal slurry were stored at -80 °C. Characterization of the fecal samples was performed by the lab of Medical Microbiology (LMM, Prof. Malhotra-Kumar, University of Antwerp).

2.3.1.3.2   DNA quantification and 16S rDNA sequencing

DNA was isolated from fecal samples using QIAamp DNA Stool Mini Kit (Qiagen). The concentration of all isolated DNA was determined using a Qubit 2.0 Fluorometer (ThermoFisher Scientific) with the dsDNA HS Assay Kit. Presence of bacterial DNA was confirmed by 16S rDNA-targeting PCR which was visualized on a 2.0% agarose gel to confirm amplification of fragments with an appropriate length.

2.3.1.3.3   16S rDNA amplification of V3 and V4 regions

Amplification of the V3-V4 region of the 16S rDNA was performed in triplicate with 2x KAPA HiFi HotStart Ready Mix (Kapa Biosystems) with the following cycling profile: 95 °C for 3 min, [95 °C for 30 sec, 62 °C for 30 sec, and 72 °C for 50 sec]x25, 72 °C for 10 min.
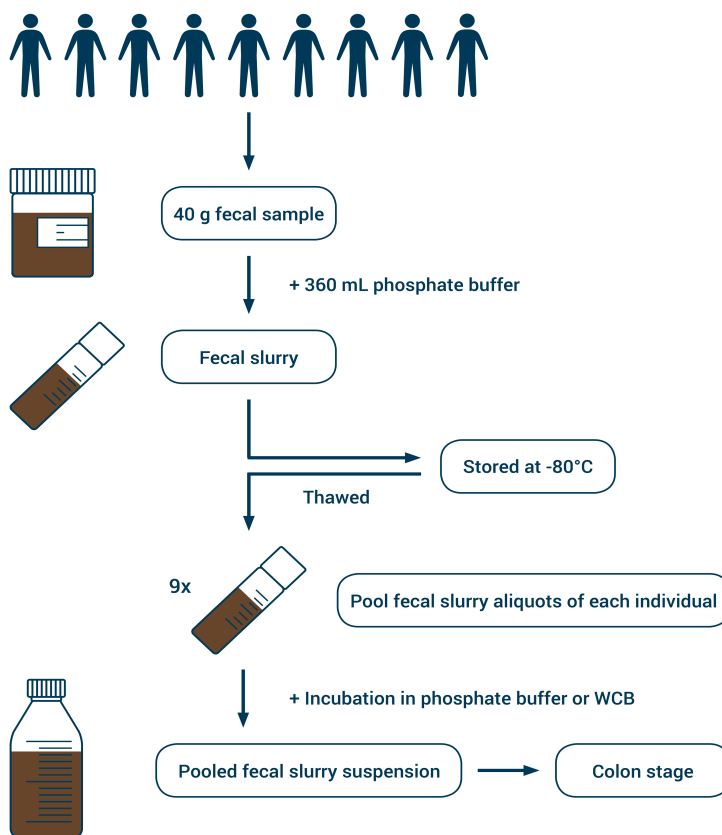
Figure 2-1: Overview of the fecal sample treatment before use in the gastrointestinal dialysis model with colon-stage (GIDM-Colon).

2.3.1.3.4 Library preparation

An index polymerase chain reaction (PCR) was performed with the Nextera XT Index Kit with dual indices. The concentration of each individual library was measured, mixed with a denatured PhiX control library, and diluted to a final concentration of 4 pM. This library was loaded onto a MiSeq V2 500 cycle cartridge and sequenced (2 x 250 bp) with the MiSeq (Illumina.Inc., USA).

Raw sequence reads were quality assessed using fastqc and data analysis was done using microbial genomics module inbuilt in CLC Genomics workbench v9.5.3 (clcbio,

Qiagen). Briefly, contigs were created by heuristically merging paired-end reads based on the Phred quality score of both reads. Contigs were aligned to the SILVA 16S database v.132 (Pruesse et al. 2007) and binned based on the sequence similarity. Taxonomic classification was performed binned contigs with the SILVA v.132 database.

2.3.1.3.5   *Evaluation of storage time on gut microbiome composition*

In order to assess the impact of the storage conditions on the microbial composition, fecal samples from three volunteers were collected. Fecal samples were processed as described in 2.3.1.3.1. For each individual, equal amounts of fecal material were collected in separate tubes and stored at -80 °C. The fecal material was thawed after 1, 3, 6, 12, 18 and 24 month(s) for DNA isolation and 16S rDNA sequencing.

2.3.1.3.6   *Incubation of fecal slurry suspension*

Before use in the GIDM-Colon, 2 mL fecal slurry aliquots of all donors were pooled and a suitable medium was added before incubation leading to a 10% (v/v) pooled fecal slurry suspension (Figure 2-1). Two different incubation mediums for the pooled fecal slurry suspension were tested. The use of the first medium, Wilkins-Chalgren Anaerobe Broth (WCB) was based on the protocol described by Breynaert et al. (Breynaert et al. 2015). A sterile phosphate buffer (0.1 M, pH 7) was tested as a second incubation medium. The pooled fecal suspensions were incubated (continuously stirred) for 17 h in the anaerobic glove box and samples of both pools were taken before and after 17 h incubation and characterized by 16S rDNA gene sequencing as described above.

To optimize the incubation time, a pooled fecal slurry suspension was incubated for 24 h in phosphate buffer, and aliquoted every 2 h, to determine the anaerobic colony forming units per gram (CFU/g). The same experiment was carried out with WCB, with a sample after 17 h of incubation (cf. the original protocol).

Serial dilutions (from 10^{-1} to 10^{-8}) of the samples were prepared with brain heart infusion (BHI) broth (BD Biosciences, Franklin Lakes, NJ, USA), plated on an anaerobic agar OXOID0972 (Oxoid, Basingstoke, UK) and incubated for 72 h at 37 °C in a bug box anaerobic workstation (Ruskinn Technology Ltd, Bridgend, UK). The colonies were counted after 72 h with spiral plater (EddyJet).

2.3.1.4   *Protocol GIDM-Colon*

To study the colonic biotransformation of the model compound chlorogenic acid, a validated *in vitro* continuous flow dialysis-model with colon phase (GIDM-Colon, Figure 2-2) was used as described by Breynaert et al. (2015). Gastric and small intestinal conditions were in agreement with the consensus paper of the COST Infogest network (Minekus et al. 2014). Ultrafiltration cells of the intestinal stage were equipped with a semi-permeable dialysis membrane (detailed figure in supplementary information Figure SI-2-1) to simulate one-way absorption through passive diffusion from intestinal lumen to mucosa. One blank sample (containing no chlorogenic acid), one negative control sample (containing no fecal slurry suspension) and two replicate samples were used (Figure 2-2)). The inclusion of a negative control sample will allow us to differentiate microbial biotransformation products from chlorogenic acid degradation products resulting from thermal instability (Dawidowicz and Typek 2010).

2.3.1.4.1   *Gastric stage*

During the gastric stage, 78 mg of chlorogenic acid was dissolved in 1 mL 16% (w/v) pepsin (19.6% protein, 622 U/mg protein) together with 49 mL 0.1 M HCl solution and set at a pH of 2 using 6 M HCl. Samples were incubated for 1 h in a shaking water bath at 37 °C (120 strokes/min). After the gastric stage, 1 mL of sample was collected and stored at –80 °C for further analysis.

2.3.1.4.2   Small intestinal stage

The content of the gastric stage was immediately transferred manually to ultrafiltration cells to simulate the small intestinal stage and 50 mL of ultrapure water was added. Dialysis bags containing 1 M $NaHCO_3$ were used to alter the pH from 2 till 7.5 in 30 min. The volume of 1 M $NaHCO_3$ needed to alter the pH was determined based on the blank sample. Ultrafiltration cells were placed in a water bath (35-37 °C), continuously stirred and connected with a water tank and a N_2 gas input using push bottom control switches (supplementary information Fig.SI-2-1). N_2 gas puts pressure on the cells (2 bar) to enable dialysis. After 30 min of dialysis, 15 mL of a pancreatin-bile solution was added to each cell. This solution was prepared dissolving 0.4% (w/v) of pancreatin (32 000 FIP-U lipase, 143 600 FIP-U amylase, 16 400 FIP-U protease) and 0.766% (w/v) of bile in 0.1 M $NaHCO_3$. Dialysis was performed for an extra 2 h. After the small intestinal stage, 1 mL samples were collected from the retentate and dialysate fraction and stored at –80 °C for further analysis.

2.3.1.4.3   Colonic stage

In order to simulate the colonic stage, the pH of the retentate samples was adjusted to 5.8-6.0 using 1 M HCl and ultrafiltration cells were transferred to an anaerobic glove box (0.5% oxygen, 35-37 °C). 50 mL of 10% (v/v) fecal slurry suspension was added to each ultrafiltration cell with exception of the negative control sample. Instead, 50 mL of sterile phosphate buffer solution was added to the negative control sample. Ultrafiltration cells were continuously stirred and pressure was introduced on top of the ultrafiltration cells (0.8 bar N_2) to obtain dialysis. To prevent an excessive loss of dialysis cell fluid overnight, no pressure was introduced on the dialysis cells between 6 h and 24 h of colonic dialysis. Samples (1 mL) were taken after 0, 2, 4, 6 and 24 h and stored at –80 °C.
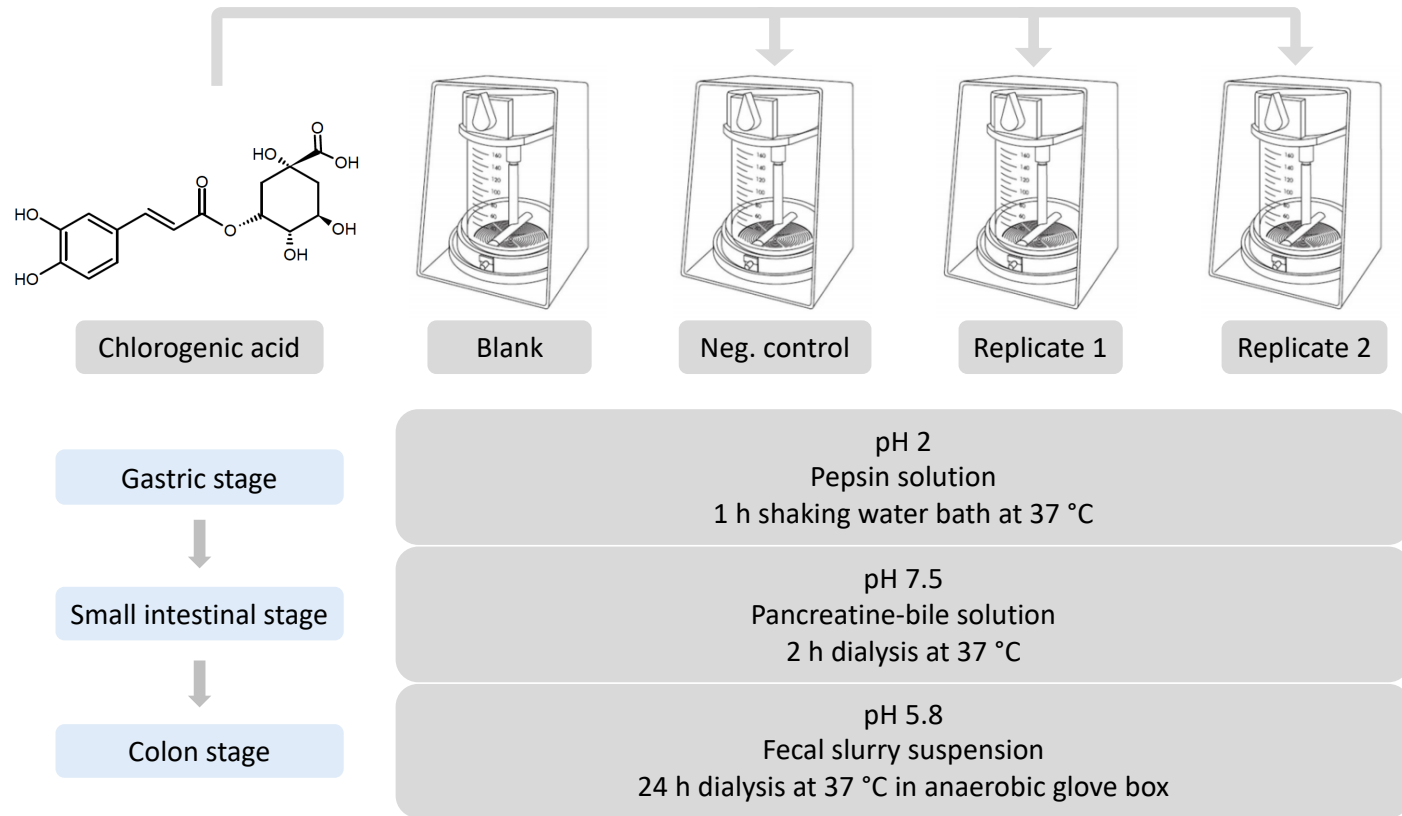
Figure 2-2: Experimental setup during the GIDM-Colon experiment with chlorogenic acid.

2.3.1.5 **Sample preparation procedure**

Four different sample preparation methods were evaluated for the colonic retentate samples to obtain extracts that are compatible with the instrumental detection: (i) centrifugation, (ii) extraction, (iii) sonication, (iv) freeze-drying. With exception of the samples prepared using only the centrifugation step, all colonic retentate samples were immediately frozen at –80 °C after sampling as mentioned above. Centrifugation samples were first centrifuged (4 °C, 14 000 rpm, 8 min) after sampling and 1 mL of supernatant was transferred to an eppendorf tube before storage at –80 °C. Following the sample preparation method, three different dilution factors (1/10, 1/20 and 1/40) were evaluated together with the chosen optimal sample preparation technique. Sample preparation procedure described below refers to the 1/40 dilution. The 1/10 and 1/20 dilutions were prepared by adjustment of the added volume ultrapure water/ACN (1/1, v/v) mixture. The extraction efficiency of the different procedures was visualized as the sum of the peak areas of all biotransformation products identified at a given dialysis-time within one sample preparation procedure. The number of identified biotransformation products was used as a second evaluation-criteria to evaluate the different sample preparation techniques.

2.3.1.5.1   Centrifugation

Before analysis samples were thawed at room temperature (15-25 °C). Samples were spiked with an internal standard (10 µL of 2 mg/mL theophylline solution in ACN) and vortexed during 30 s. 25 µL of the samples was transferred to a new eppendorf and 975 µL of ultrapure water/ACN (1/1, v/v) was added. Samples were transferred to a 0.2 µm nylon centrifugal filter and centrifuged (5 min, 8000 rpm) before analysis with liquid chromatography coupled to quadrupole time-of-flight mass spectrometry (LC-Q-TOF-MS).

2.3.1.5.2   Extraction and sonication

Samples were thawed at room temperature (15–25 °C) and spiked with 10 µL of 2 mg/mL theophylline solution (as internal standard). One mL of ice-cold MeOH (-80 °C) was added to quench remaining ongoing biotransformation reactions. Extraction samples were vortexed for 60 s, and sonication samples were sonicated for 60 min. Samples were further diluted by transferring 25 µL of sample to 475 µL of ultrapure water/ACN (1/1, v/v) and filtered as described above.

2.3.1.5.3   Freeze-drying

Samples were lyophilized using the automatic start-up software of the FreeZone 1 Liter Benchtop Freeze Dry System (Model 7740030, Labconco). This method maintained a temperature of -40 °C with a high vacuum of 0.133 mbar over time to remove the ice via sublimation. After lyophilization, 1 mL of ice-cold MeOH (-80 °C) and 10 µL of 2 mg/mL theophylline solution (as internal standard) were added to the freeze-dried samples. Samples were sonicated for 45 min and additionally vortexed. Finally, the samples were diluted and filtered as described for the centrifugation samples.

2.3.1.5.4   Optimization of injection solvent

A schematic overview of the optimization of the injection solvent procedure is given in Figure 2-3. GIDM-Colon samples which were prepared according to the extraction sample preparation procedure were reinjected after overnight storage at -20 °C, before and after homogenization (vortexing). An additional experiment was carried out with an adjusted sample preparation procedure: after centrifugation, samples were evaporated to dryness followed by reconstitution in the same volume mobile phase A. These samples were analyzed both before and after storage at -20 °C. The samples stored overnight were reinjected the next day before and after homogenization.

Colon-stage
sample

1/20 dilution with
1/1 (v/v) ACN/mQ

500 µL

200 µL to
HPLC vial (*)

200 µL: Evaporate and
reconsitute in MFA (*)

(*)   Store at -20 °C overnight   (*)

(*)   Homogenization   (*)
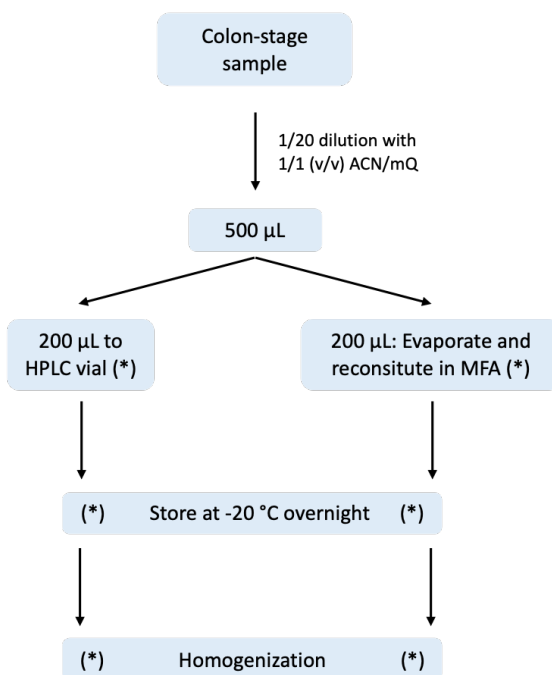
Figure 2-3: Overview of the additional experiment to study the chromatographic peak shape of biotransformation products after LC-MS analysis. Conditions marked with (*) were analyzed by LC-Q-TOF-MS.

2.3.1.6 Analysis of extracts resulting from GIDM-Colon experiment

2.3.1.6.1 Column screening

Three columns, all acquired from Phenomenex (Utrecht, the Netherlands) were selected to optimize the choice of the LC column. A Luna Omega PS C18 (100 x 2.1 mm, 3 µm), Kinetex XB C18 100 Å (150 x 2.1 mm, 1.7 µm) and Luna Omega Polar C18 100 Å (100 x 2.1 mm, 3 µm) were used to analyze a 24 h incubation sample from the colon-stage.

2.3.1.6.2   Instrumental parameters

Extracts resulting from the GIDM-Colon experiment were analyzed using an Agilent 1290 Infinity ultra-high-performance liquid chromatography instrument coupled to an Agilent 6530 Accurate-Mass quadrupole time-of-flight (LC-Q-TOF-MS) (Agilent, Santa Clara, CA, USA). After interpretation of the results of the column screening, chromatographic separation was performed on a Luna Omega PS C18 column (100 x 2.1 mm; 3 μm particle size) from Phenomenex (Utrecht, the Netherlands) using a mobile phase composed of ultrapure water with 0.04% (v/v) formic acid (A) and 80/20 (v/v) ACN/ultrapure water with 0.04% (v/v) formic acid (B) with a constant flow of 0.3 mL/min. The gradient elution was constructed as follows: for 3 min A was used at 99%, after which B increased till 8% at 18 min. B was further increased till 95% at 28 min. Consecutively, the column was rinsed with 95% B for 4 min, and re-equilibrated at 99% A for 4 min before the next injection. The injection volume was 5 μL. The eluent was directed to the waste during the first minute of each run to protect the ion source from extensive contamination as well as during the 4 min of re-equilibration. The column temperature was kept constant at 40 °C.

All samples were analyzed in negative ionization mode using Agilent Jet Stream electrospray ionization (ESI) with following parameters: 300 °C drying gas temperature, 8 L/min drying gas flow, 25 psig nebulizer pressure, 350 °C sheath gas temperature, 11 L/min sheath gas flow, 3500 V sampling capillary voltage and 500 V nozzle voltage.

The Q-TOF mass spectrometer was operated in the 2 GHz (extended dynamic range) mode in a data-dependent acquisition. Calibration of the mass axis was performed in negative ionisation mode with respect to two ions with a mass of charge (m/z)-value of 119.0363 and 966.0007. Data were recorded in a m/z-range from 50 to 1000 with scan rates of 2.5 spectra/s and 6.7 spectra/s for MS and tandem mass spectrometry (MS/MS) respectively. Each cycle, three precursors were selected for MS2. Selection

was based on abundance, a threshold of 1500 was used, of the detected *m/z*-values in MS1. The *m/z*-values of the reference masses were actively excluded for precursor-selection. Fixed collision energies of 5, 10 and 20 V were applied. If needed, reanalysis of extracts in targeted MS/MS mode was applied for interesting features where no MS/MS spectrum was obtained in the data-dependent MS/MS mode. All data were stored in centroid mode. Instrumental variation was evaluated by monitoring the relative standard deviation of the internal standard peak area in the samples throughout the analysis.

2.3.1.6.3 *Data analysis workflows*

Three complementary data processing workflows were applied for the detection and identification of biotransformation products. The workflows were developed in-house and were based on earlier optimized workflows used in *in vitro* human liver biotransformation investigations for xenobiotics (Mortele et al. 2018, Vervliet et al. 2018). Apart from a suspect screening approach based on literature and *in silico* prediction strategies, two non-targeted screening workflows were applied to the data.

A list of possible biotransformation products was received using the *in silico* prediction software tools Biotransformer (Biotransformer.ca, v1.0.0) and Meteor Nexus (v2.1, Lhasa Limited, Leeds, UK). The Biotransformer-tool allowed *in silico* predictions of human gut metabolome biotransformation products. The SMILES string of chlorogenic acid was uploaded and 'Human Gut Microbial Transformation' was selected as metabolic transformation on 'BioTransformer.ca'. The online tool generated a csv file containing molecular formula, InChIKey, synonyms, major isotope mass, type of biotransformation reaction and precursor ID. Meteor software predicted the human phase I and phase II biotransformation products of chlorogenic acid. The molecular formulas and corresponding exact masses of all predicted biotransformation products were stored in a csv database. Microbial biotransformation products of chlorogenic acid described in literature and not predicted by Biotransformer or Meteor were

added to the database (Gonthier MP 2003, Olthof et al. 2003, Konishi and Kobayashi 2004, Rechner et al. 2004, Gonthier et al. 2006, Del Rio et al. 2010, Tomas-Barberan et al. 2014, Breynaert et al. 2015, Pinta et al. 2018).

Identification was based on the accurate mass, isotopic pattern, fragmentation pattern of the product ions and injection of an analytical standard if available. Applied criteria were: (a) maximal mass variation of $\pm$ 10 parts per million (ppm) between theoretical and measured parent ions; (b) product ions may not exceed the maximal mass variation of $\pm$ 25 ppm; (c) the identified biotransformation products were not present in the blank or negative control sample, unless mentioned otherwise in the manuscript and (d) the biotransformation product was present in both replicates at a certain sampling time.

One of the non-targeted screening workflows used the software packages MzMine and R. Raw data files were uploaded in MZmine 2.33 (Pluskal et al. 2010). Molecular features were detected using the centroid algorithm followed by a chromatogram building step. A noise amplitude algorithm was used to deconvolute the chromatograms. Deisotoping was performed by retaining the lowest m/z as the representative isotope. Peaks with a peak width lower than 0.05 min or more than 1 min were discarded. Next, the random sample consensus (RANSAC) alignment algorithm aligned the peaks across samples. Finally, any missing peaks were extracted with the same retention time and m/z gap filler algorithm. The obtained m/z features were exported as a csv file, imported into R and processed using a previously published in-house developed script (Vervliet 2018, Vervliet et al. 2018). Fold changes of each feature were calculated between samples and blank samples, as well as the p-value from a student t-test. Features with a log-10 fold change greater or equal to 1 and a p-value <0.05 were retained. For each m/z value, the log-10 fold change was plotted to the log-10 p-value leading to a volcano plot (supplementary information Figure SI- 2-2). Corresponding molecular formulas to the m/z values were calculated using the Generate Formulas algorithm in the MassHunter Qualitative Analysis software (version

B.07.00, Agilent Technologies, Santa Clara, CA, USA). Identification was based on the same criteria as mentioned for the suspect screening.

Finally, the third data analysis workflow combined the MassHunter Qualitative (version B.07.00, Agilent Technologies, Santa Clara, CA, USA) and MassProfiler Professional (v12.6, Agilent Technologies, Santa Clara, CA, USA) software packages. The Find by Molecular Feature algorithm in MassHunter Qualitative software extracted the features from the data without restrictions concerning retention time or *m/z* value. The data were imported in Mass Profiler Professional. Samples were classified per type (blank, negative control or replicate) and incubation time (0 h, 2 h, 4 h, 6 h or 24 h). Features present in one or more blanks were discarded by filtering the data on frequency. Additional filtering was performed on the features by retainment of the features present in both replicates at a given incubation time. The Generate Formulas algorithm in MassHunter Qualitative software was used to predict the molecular formulas based on the found *m/z* values. Identification was based on the same criteria as mentioned for the suspect screening.

2.3.2   Results and discussion

2.3.2.1   *Optimization of processing and incubation of fecal samples*

2.3.2.1.1   *Evaluation of storage conditions on gut microbiome composition*

Figure 2-4 presents the 16S rDNA gene results of the three fecal samples sequences after varying storage intervals at -80 °C. No clear shifts in bacterial composition were observed over time when stored at -80 °C, which is in agreement with previous studies (Kia et al. 2016, Tap et al. 2019). Tap et al. (2019) investigated the stability of fecal samples over a period of 5 year at -80 °C and reported limited effects on the alpha-diversity, beta-diversity and taxonomic composition. The observed differences were reported to be less than the biological variation (inter- and intrasubject) and inter-sequencing variation (Tap et al. 2019).

2.3.2.1.2   *Optimization of incubation medium*

The principle coordinates analysis (PCoA) plot shown in Figure 2-5 represents the comparison of the microbial composition between the samples of the lean volunteers, the pooled fecal sample and the 17 h incubated pooled fecal suspension in WCB or sterile phosphate buffer based on the 16S rDNA gene sequencing results. Incubation of the fecal pooled sample in WCB led to a clear change in bacterial composition of the pool, while this effect was less pronounced for the sterile phosphate buffer as medium (Figure 2-6). A phosphate buffer was chosen as test incubation medium as it does not contain any nutrients, and thus would be less likely to lead to a shift in bacterial composition. The fecal pooled sample incubated in sterile phosphate buffer for 17 h showed a closer resemblance to the composition of the initial pool (i.e. before incubation) and to the composition of the individual volunteers. These results suggest that the choice of a sterile phosphate buffer as incubation medium led to an incubated fecal pool with a closer resemblance to the *in vivo* situation leading to a more representative *in vitro* model.
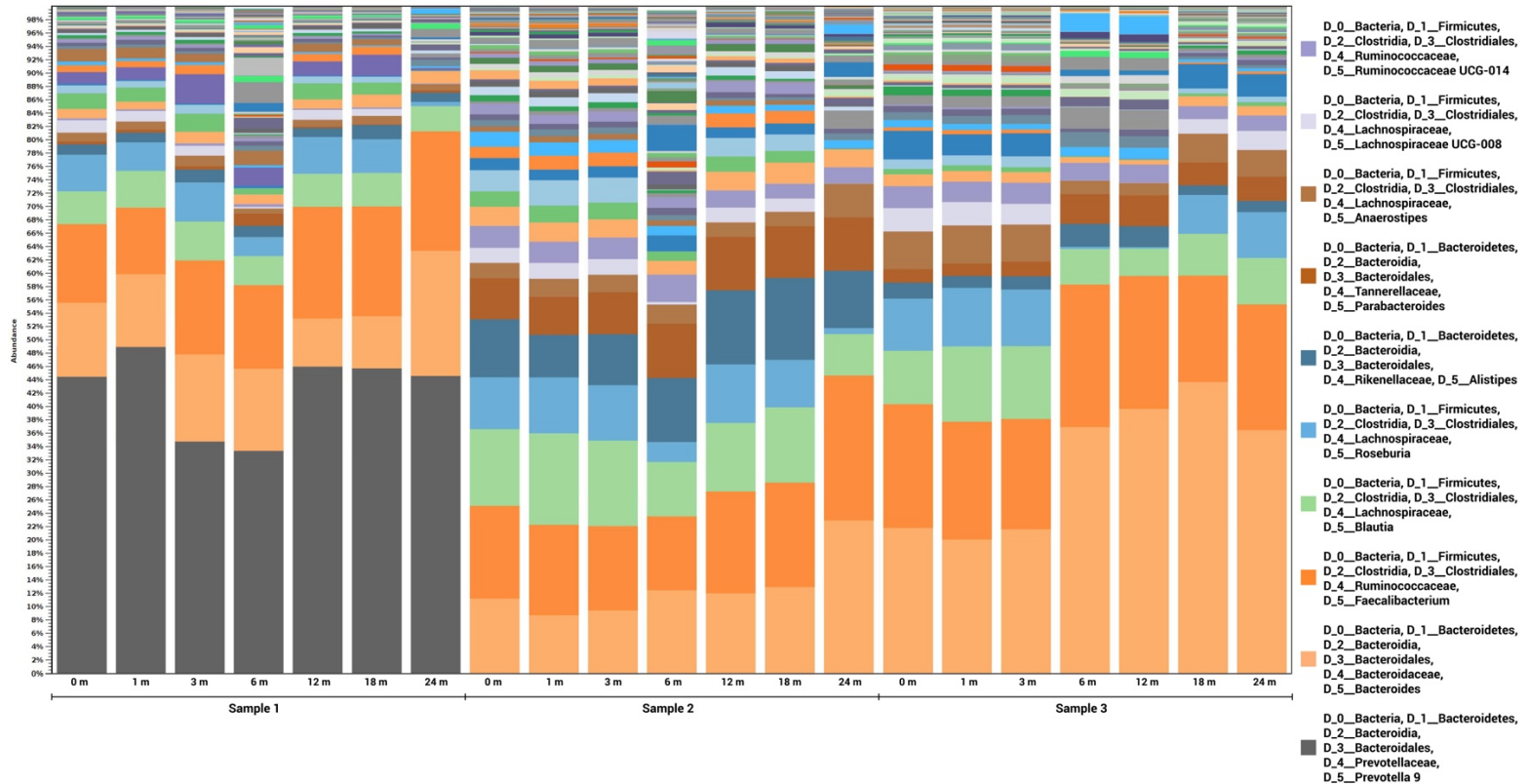
Figure 2-4: The 16s rDNA gene sequencing results (at genera level) of the fecal samples (n=3) sequenced after 1, 3, 6, 12, 18 and 24 months of storage at -80 °C.
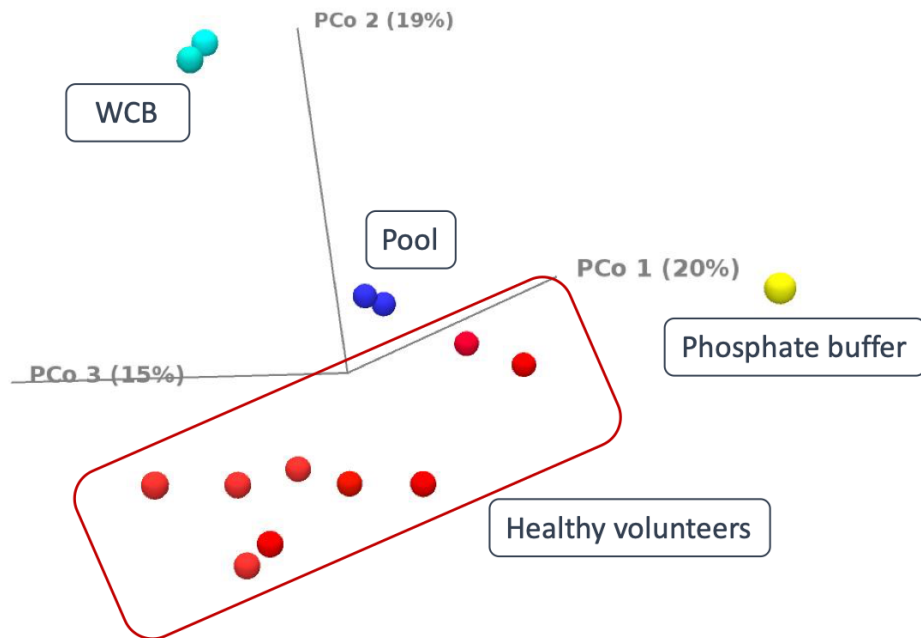
Figure 2-5: Principle coordinates analysis (PCoA) plot showing the comparison between the 16S rDNA gene sequencing results of the samples of the lean volunteers (Control samples, red), the pooled fecal slurry (blue), the pooled fecal slurry suspension after 17 h of incubation in phosphate buffer (yellow) and the pooled fecal slurry suspension after 17 h of incubation in Wilkin-Chalgren Anaerobe Broth (WCB) (turquoise).
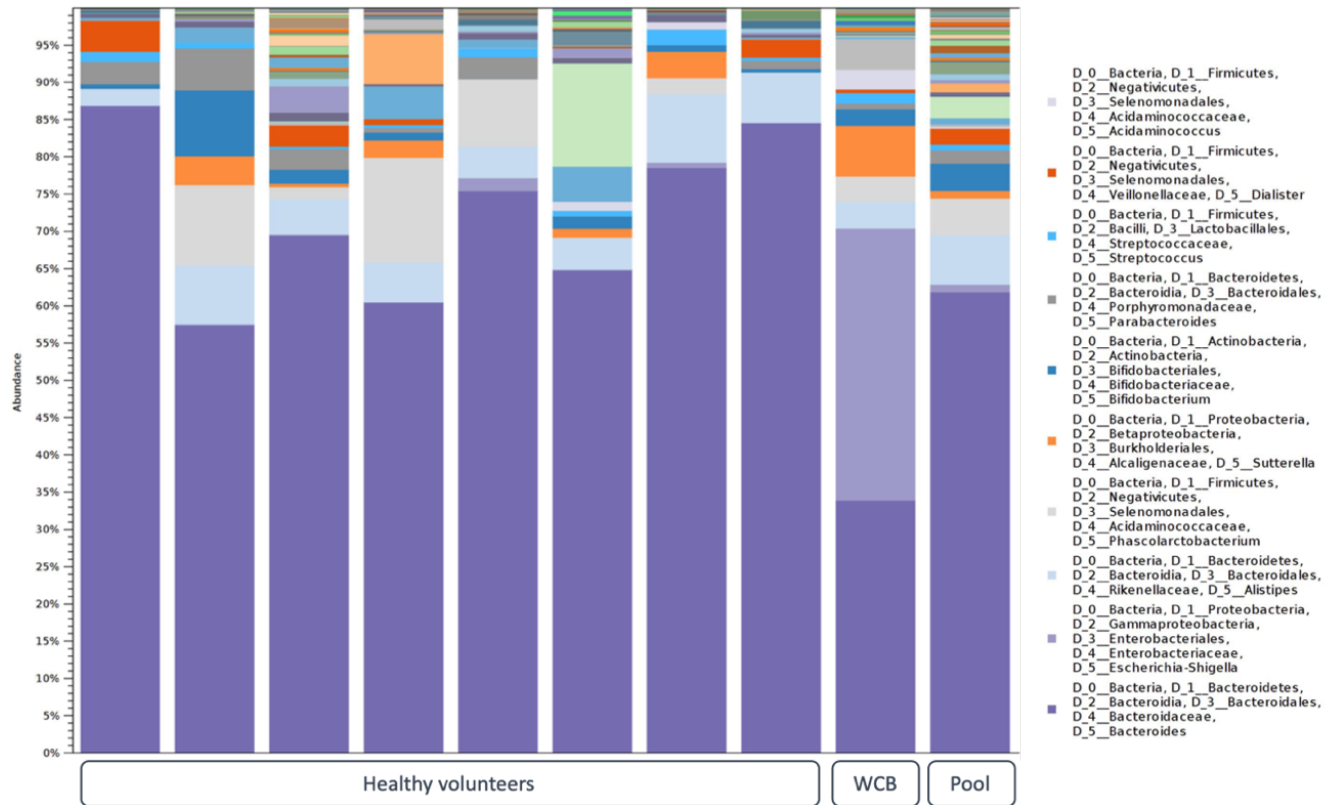
Figure 2-6: The 16s rDNA gene sequencing results (at genera level) of the fecal samples of the lean volunteers, the fecal slurry pool and the pooled fecal slurry suspension after 17 h of incubation in WCB.

2.3.2.1.3 Optimization of incubation time

As the original protocol, described by Breynaert et al. (2015), used WCB as incubation medium instead of a sterile phosphate buffer, additional experiments regarding the effect of the incubation time in the sterile phosphate buffer on the number of bacteria was necessary. A pooled fecal sample incubated for 17 h in WCB, as described in the original protocol, was added as comparison. Incubation of the pooled fecal sample over 24 h in the new medium showed no clear increase or decrease in CFU/g. The number of CFU/g over time is represented in Figure 2-7. A detailed overview of the results can be found in supplementary information (Table SI- 2-3). In comparison to phosphate buffer, a clear effect of incubation in WCB was observed as the sample contained 1.48 x 10^9 CFU/g bacteria after 17 h. However, the disadvantage of this method, with a shift in bacterial composition, was already described above. The minor influence of a sterile phosphate buffer on the bacterial concentration in comparison to WCB was expected as this medium did not contain any growth factors or energy sources. As biotransformation products of chlorogenic acid were identified after incubation of chlorogenic acid with fecal suspensions in phosphate buffer, the colonic biotransformation activity of the bacteria was ensured. With regard to the increased risk of introducing variation during incubation when using WCB and the results discussed above, it was concluded that the 17 h incubation time in WCB, as described by Breynaert et al. (2015), showed no advantage over phosphate buffer. Furthermore, replacing the 17 h incubation step with a one-hour adaptation period of the fecal slurry suspension in the anaerobic glove box will reduce the total time of the GIDM-Colon experiment, thus increasing the throughput of the total platform.
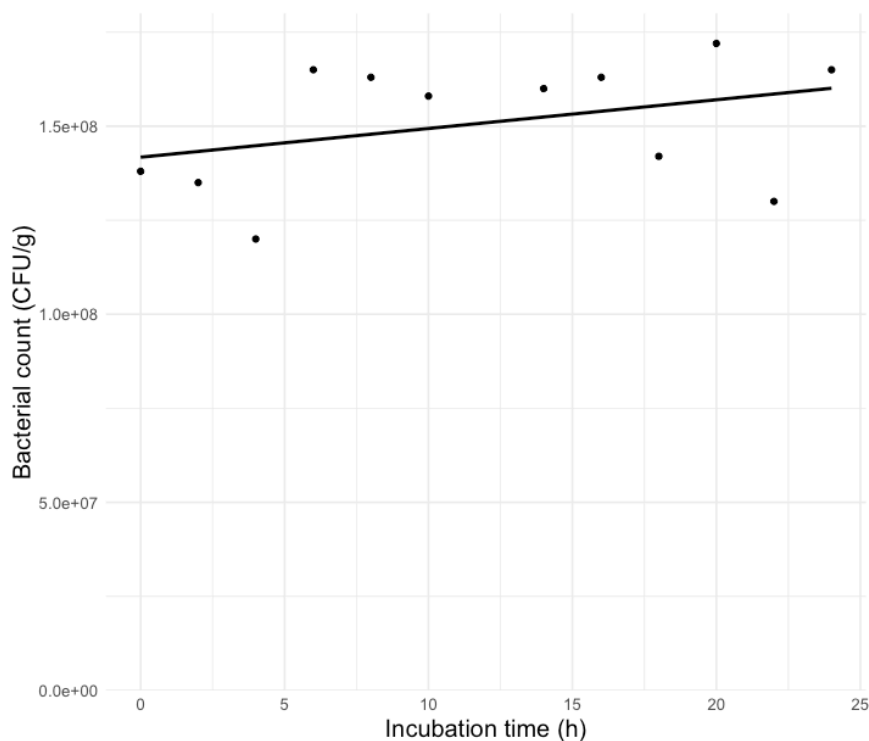
Figure 2-7: The concentration of anaerobic bacteria, expressed as colony forming units per gram, after different incubation times in phosphate buffer (0.1 M, pH 7). The trend line is depicted.

2.3.2.2 Column screening

Three different mixed-mode C18 stationary phase columns were chosen for optimization of the chromatographic separation. The choice for a C18 stationary phase was based on the available literature, as this stationary phase was the most used for separation of chlorogenic acid, it's isomers and/or biotransformation products (Zhao et al. 2014, de Melo and Sawaya 2015, Choi et al. 2018, Wang et al. 2018, Wianowska and Gil 2018, Yang et al. 2020). Mixed-mode stationary phases, a stationary phase characterized by two functional groups of different properties (e.g. C18-chain and a polar group), were chosen as they show some advantages on the separation of

complex samples, a mix of polar and non-polar compounds, in contrast to the traditional C18 stationary phases. This could be useful for the analysis of GIDM-Colon samples of chlorogenic acid as it is a polar compound while reductive and hydrolytic metabolism, the majority of the gut microbiome biotransformation reactions, can lead to more non-polar biotransformation products (Sousa et al. 2008, Spanogiannopoulos et al. 2016). All columns should provide good retention of the more non-polar compounds due to the apolar C18 chains. The polar functional groups of the mixed-mode stationary phase provide enhanced retention for polar compounds such as polar acids (e.g. chlorogenic acid) and polar biotransformation products (e.g. conjugates) (Wang et al. 2015).

The chromatograms of a 24 h retentate colon sample injected by using three different columns are shown in Figure SI- 2-3. Analysis with the Luna Omega PS C18 (Figure SI-2-3-A) resulted in high quality separation and peak shapes. The isomers of chlorogenic acid were almost baseline separated and no co-elution of the biotransformation products occurred. The chromatogram of the Kinetex XB C18 is shown in Figure SI-2-3-B. Using this column, the isomers of chlorogenic acid were not fully separated, peaks showed tailing and more co-elution of the peaks was observed. Finally, the isomers of chlorogenic acid were not separated using the Luna Omega Polar C18 (Figure SI-2-3-C) as only one peak was observed. The Luna Omega PS C18 HPLC column was chosen as optimal choice for the analysis.

2.3.2.3 Optimization of sample preparation procedure

2.3.2.3.1 Extract preparation

Figure 2-8 shows an overview of the extraction efficiency of the different sample preparation procedures. The sum of the peak areas of all biotransformation products identified at a given dialysis time was plotted against the different procedures. Freeze-

drying as a sample preparation method overall resulted in a lower extraction efficiency of colonic biotransformation products in comparison to the three other methods (Figure 2-8, sample preparation procedure F). No clear differences were observed for the three other procedures. Additionally, biotransformation product M11 (Table 2-1) was not detected by freeze-drying in comparison to the other sample preparation procedures.
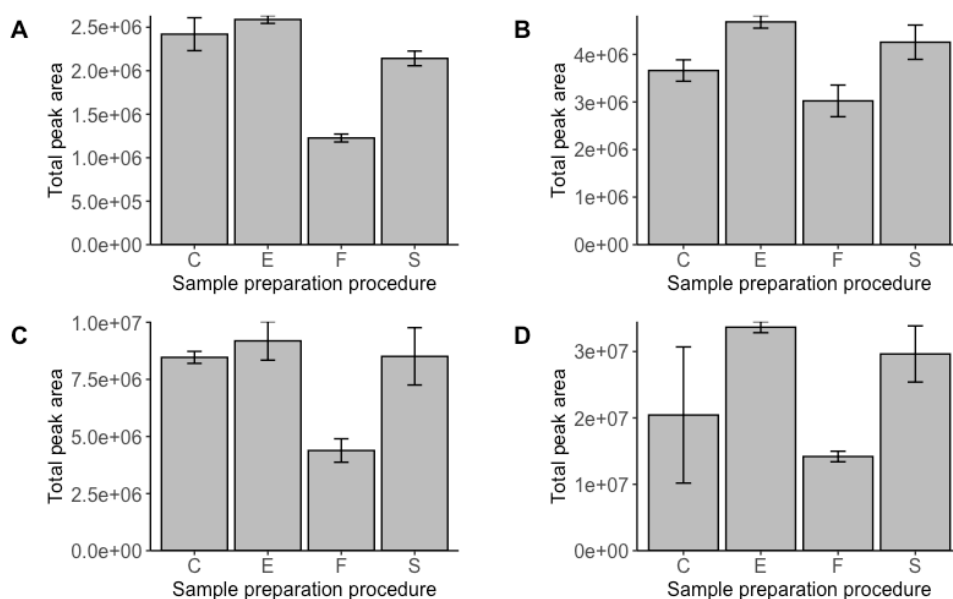
Figure 2-8: Sum of the peak areas of the identified biotransformation products for each sample preparation procedure at different dialysis-times in the GIDM-colon: 2 h (A), 4 h (B), 6 h (C) and 24 h (D). Terminology sample preparation procedures: C: Centrifugation, E: Extraction, F: Freeze-drying, S: Sonication.

Irreversible binding of hydrophilic biotransformation products to matrix components (microbial membranes and/or cell wall macromolecules) and precipitation of these molecules during extraction steps such as centrifugation could explain the inferiority of freeze-drying as a sample preparation procedure (Gromova and Roby 2010, Wu et al. 2010). No big differences in extraction efficiency were detected, suggesting that sonication and extraction by centrifugation did not result in more leakage of intracellular biotransformation products compared to the centrifugation method or all

biotransformation products of chlorogenic acid were excreted in the extracellular environment by the bacteria. The extraction method was selected as optimal method as the latter procedure has the big advantage of the limited time needed to prepare the samples, leading to the ability to perform more experiments in a shorter period.

2.3.2.3.2 Dilution

Biotransformation product M16 was not detected using the 1/40 retentate dilution, as this dilution negatively influenced the sensitivity of the detection of biotransformation products in comparison to the 1/10 and 1/20 dilution. Usage of a 1/20 dilution was selected as most optimal method as this resulted in highly sensitive detection of biotransformation products of chlorogenic acid. Using a 1/10 dilution would introduce a risk of contamination of the LC-MS system and ion suppression, which could lead to a. loss of analysis time due to instrument-cleaning and a loss of sensitivity.

2.3.2.4 Analysis of extract

2.3.2.4.1 Injection solvent

Poor chromatographic peak shapes were observed when analyzing extracts immediately after sample preparation by LC-Q-TOF-MS (Figure 2-9-A). Reinjection of the same samples after storage at -20 °C surprisingly led to an improvement of the peak shape (Figure 2-9-B). These findings could be explained by cold-induced aqueous ACN phase separation, a process that has been described after storage of a 1/1 (v/v) ACN-water mixture at -17 °C for several hours (e.g. overnight) by Gu et al. (1994). Shao et al. (2017) observed that the upper and lower phase contained 71.7% and 13.6% ACN respectively (Gu et al. 1994, Shao et al. 2017). Injection of the samples after overnight storage at -20 °C without homogenization (e.g. vortexing) led to injection of the aqueous phase. The injected part of the sample showed a higher resemblance to the

starting mobile phase, leading to better chromatographic peaks. An additional experiment where samples were homogenized after storage confirmed this hypothesis. Homogenization of the samples by vortex mixing, and removing the ACN-water phase-separation and thus increasing the ACN-percentage in the injected sample, after overnight storage at -20 °C led to poor quality peak shapes (Figure 2-9-C). Based on these results the procedure after the sample preparation extraction method was adjusted. Evaporation of the samples to dryness followed by reconstitution in mobile phase A led to high quality peak shapes (Figure 2-9-D) and no influence of storage at -20 °C or subsequent homogenization was observed (Figure 2-9-E,F). This proves the importance to check the compatibility of the extract with the mobile phase used in the LC set-up.

Table 2-1: Overview of identified biotransformation products and additional information: metabolite ID, compound name, molecular formula, level of confirmation as proposed by Schymanski et al. (Figure SI-2-4) (Schymanski et al. 2014), detected by which workflow, retention time, exact mass, detected parent ion, mass difference. MPP: MassProfiler Professional. NA: Not acquired. A: Confirmed using mzCloud.org, B: Confirmed based on Kang et al. (Kang et al. 2016).

ID	Compound name	Molecular formula	Level of confirmation	Workflow	t_r (min)	Exact mass (g/mol)	Parent ion (m/z)	Δ Mass (ppm)	MS/MS product ions
M1	Trihydroxycyclohexane carboxylic acid	C7H12O5	L3	Suspect, MZmine	1.10	176.0685	175.0613	-0.03	157.0493 [C7H9O4]-; 113.0609 [C6H9O2]-; 95.0493 [C6H7O]-; 73.0297 [C3H5O2]-; 44.9992 [CHO2]-
M2	NA	C10H12O6	L4	MPP	1.10	228.0617	227.056	-7.22	NA
M3	NA	C10H12O7	L3	MZmine	1.10	244.0599	243.0523	6.64	175.0601 [C7H11O5]-; 95.0494 [C6H7O]-; 44.9978 [CHO2]-
M4	Quinic acid	C7H12O6	L1	All	1.12	192.0635	191.0564	0.47	85.0297 [C4H5O2]-; 73.0271 [C3H5O2]-; 59.0157 [C2H3O2]-
M5	Dihydroxycyclohexane carboxylic acid	C7H12O4	L3	Suspect, MPP	1.12	160.0733	159.0662	-1.41	113.0594 [C6H9O2]-
M6	NA	C10H12O8	L4	MZmine	1.12	260.0516	259.0446	-6.08	191.0583 [C7H11O6]-; 172.9757 [C5HO7]-; 127.0425 [C6H7O3]-; 85.0305 [C4H5O2]-
M7	NA	C12H16O9	MS, MS/MS	MZmine	1.13	304.078	303.0713	-4.69	191.0556 [C7H11O6]-; 143.0108 [C9H3O2]-; 135.0848 [C9H11O]-; 111.0449 [C6H7O2]-; 109.0260 [C6H5O2]-; 89.0141 [C3H5O3]-; 85.0311 [C4H5O2]-; 60.9936 [CHO3]-

Table 2-1 (Continued)

ID	Compound name	Molecular formula	Level of confirmation*	Workflow	tr (min)	Exact mass (g/mol)	Parent ion (*m/z*)	Δ Mass (ppm)	MS/MS product ions
M8	NA	C18H20O8	L4	MZmine	10.90	364.115	363.1079	-2.14	181.0496 [C9H9O4]-; 137.0596 [C8H9O2]-
M9	6-(3-(3,4-dihydroxyphenyl)-1-hydroxypropoxy)cyclohexane-1,2,4-triol	C15H22O7	L3	MPP	11.00	314.1352	313.1282	-4.21	203.0314 [C11H7O4]-; 181.0496 [C9H9O4]-; 135.0442 [C8H7O2]-; 131.0704 [C6H11O3]-; 107.0490 [C7H7O]-
M10	Dihydrocaffeic acid	C9H10O4	L1	All	11.42	182.0579	181.0507	-0.01	137.0593 [C8H9O2]-; 121.0286 [C7H5O2]-; 119.0465 [C8H7O]-; 109.0287 [C6H5O2]-; 59.0138 [C2H3O2]-
M11	Hydroxybenzaldehyde	C7H6O2	L2aᴬ	Suspect, MZmine	11.52	122.0367	121.0294	-0.84	93.0310 [C6H5O]-
M12	Caffeic acid	C9H8O4	L1	All	15.21	180.0414	179.0342	-4.63	135.0431 [C8H7O2]-; 117.0353 [C8H5O]-; 91.0000 [C6H3O]-; 44.9992 [CHO2]-
M13	Caffeic acid quinone	C9H6O4	L3	All	15.40	178.0265	177.0191	-0.83	105.0331 [C7H5O]-; 45.0001 [CHO2]-

Table 2-1 (Continued)

ID	Compound name	Molecular formula	Level of confirmation*	Workflow	tr (min)	Exact mass (g/mol)	Parent ion (*m/z*)	Δ Mass (ppm)	MS/MS product ions
M14	Dihydrochlorogenic acid	C16H20O9	L3	Suspect, MPP	16.28	356.1094	355.1022	-3.74	191.0540 [C7H11O6]-; 173.0446 [C7H9O5]-; 137.0630 [C8H9O2]-
M15	Hydroxy-dihydrocaffeoylquinic acid	C16H20O10	L3	Suspect, MPP	16.51	372.1045	371.0983	-0.84	353.0867 [C16H17O9]-; 191.0556 [C7H11O6]-
M16	NA	C10H12O5	L4	All	19.14	212.0674	211.0603	-5.14	165.0551 [C9H9O3]-; 121.0656 [C8H9O]-; 106.0426 [C7H6O]-
M17	3-Phenyllactic acid	C9H10O3	L2a[A]	All	16.79	166.0628	165.0556	-1.26	147.0415 [C9H7O2]-; 119.0472 [C8H7O]-; 103.0533 [C8H7]-; 91.0547 [C7H7]-; 72.9901 [C2HO3]-; 44.9972 [CHO2]-

Table 2-1 (Continued)

ID	Compound name	Molecular formula	Level of confirmation*	Workflow	tr (min)	Exact mass (g/mol)	Parent ion (*m/z*)	Δ Mass (ppm)	MS/MS product ions
M18	1-Caffeoylglycerol	C12H14O6	L2a[B]	All	19.92	254.0791	253.0719	0.11	179.0328 [C9H7O4]-; 161.0236 [C9H5O3]-; 135.0443 [C8H7O2]-; 133.0298 [C8H5O2]-
M19	NA	C10H12O4	L4	Suspect, MPP	21.26	196.0729	195.0658	-3.32	NA
M20	4-ethylcatechol	C8H10O2	L3	All	21.63	138.0679	137.0607	-1.34	NA
M21	NA	C12H14O5	L4	MPP	21.96	238.0838	237.0763	-1.43	161.0231 [C9H5O3]-; 135.0441 [C8H7O2]-; 119.0358 [C4H7O4]-
M22	Ferulic acid	C10H10O4	L1	All	22.52	194.058	193.0507	0.47	178,0270 [C9H6O4]-; 161,0273 [C9H5O3]-; 134,0373 [C8H6O2]-; 133,0292 [C8H5O2]-
Parent	Chlorogenic acid	C16H18O9	L1	Suspect	18.51	354.095	353.0878	-0.27	191.0546 [C7H11O6]-; 173.0451 [C7H9O5]-; 161.0214 [C9H5O3]-; 135.0413 [C8H7O2]-
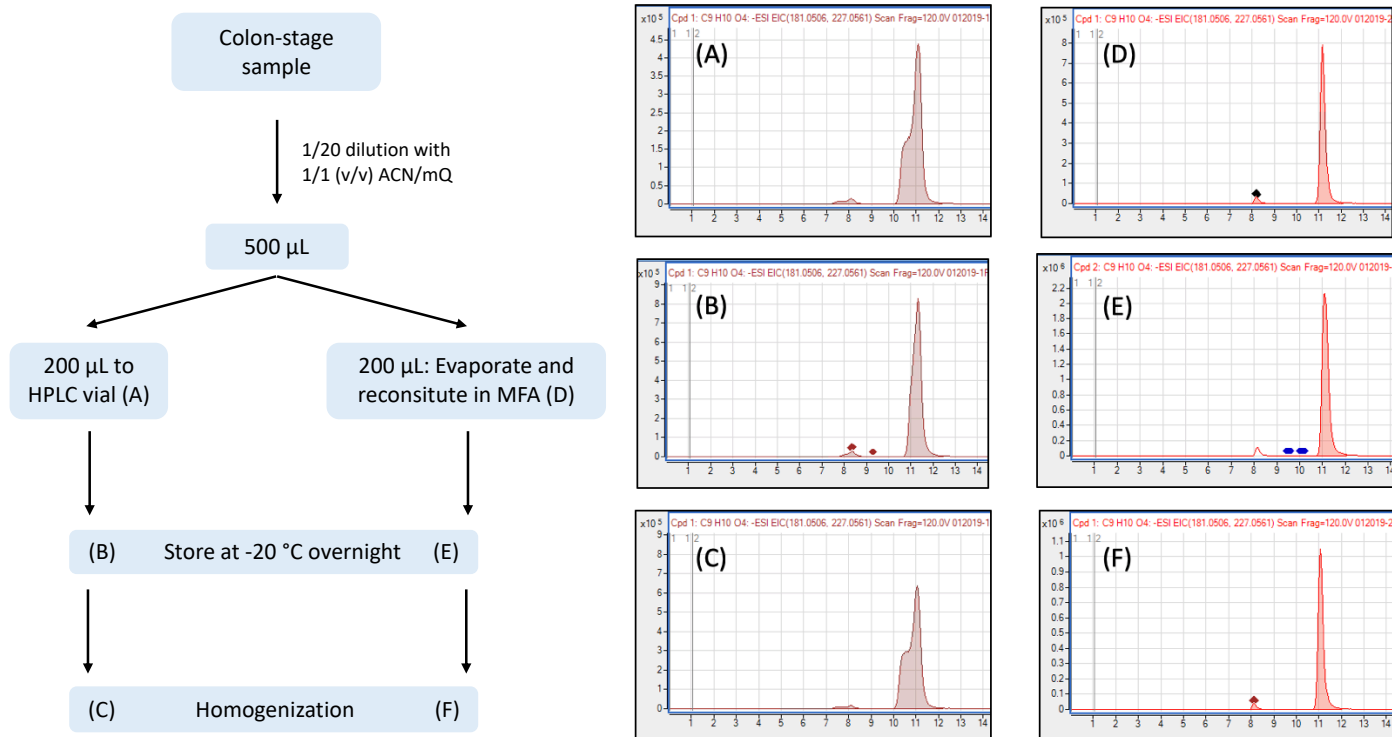
Figure 2-9: Left: Overview of the experiment to study the chromatographic peak shape of biotransformation products after LC-MS analysis. Labels (A), (B), etc. correspond to the labels used on the right-side. Right: Peak shape of biotransformation product M4 after the additional experiments described on the left-side of the figure.

2.3.2.4.2 Evaluation data-analysis workflows

By combining the three data-analysis workflows, a total of 23 colonic biotransformation products of chlorogenic acid were identified (Table 2-1). An overview of the results can be found in Figure 2-10
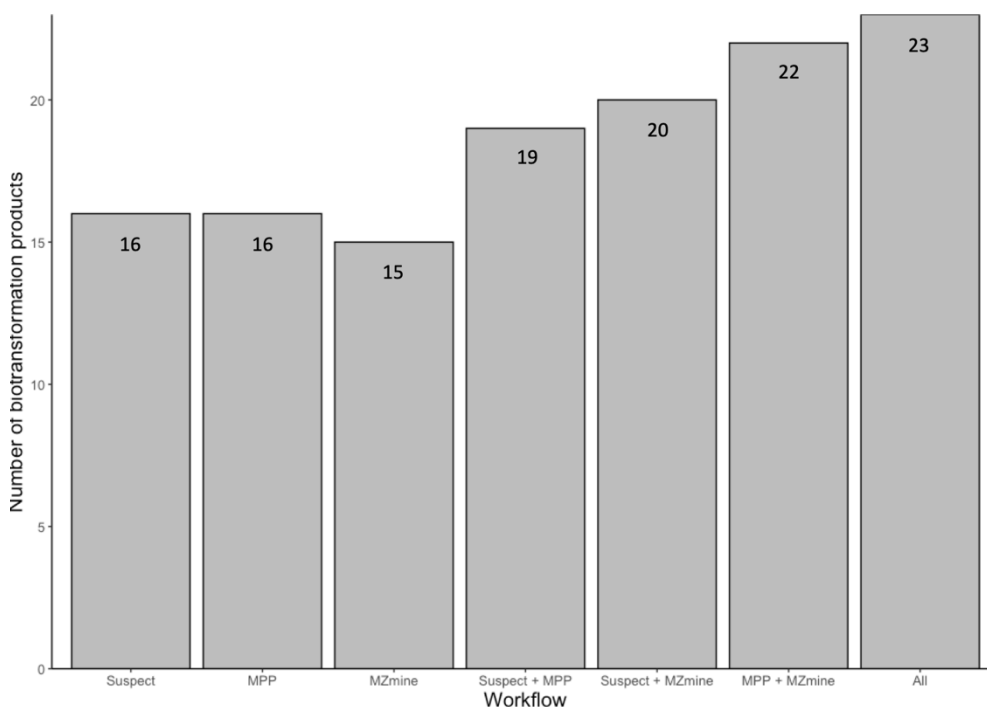
Figure 2-10: Comparison of the different data-analysis workflows based on the number of identified biotransformation products.

Figure 2-10 clearly shows that combining multiple data-analysis workflows leads to an increased number of identified biotransformation products. Processing the data with only one data-analysis workflow would have led to the identification of 16 biotransformation products of chlorogenic acid for the suspect screening and the MPP workflow and 15 biotransformation products for the MZmine workflow. Combining two workflows led to a clear increase in the number of identified biotransformation products: 19, 20 and 22 for the combinations 'suspect + MPP', 'suspect + MZmine' and 'MPP + MZmine' respectively. One, four and five identified biotransformation products

were unique for the suspect screening, MPP and MZmine workflow respectively. These findings confirmed our previous results of *in vitro* human liver microsome biotransformation studies with new psychoactive substances (NPS) (Mortele et al. 2018, Vervliet et al. 2018). Hohrenk et al. compared different non-targeted screening data processing worfklows using the same raw data files. Although all workflows included similar steps (e.g. peak picking, blank subtraction), the resulting feature lists showed dissimilarities which could be explained by differences in the underlying algorithms (Hohrenk et al. 2020). An example of a difference between the two used non-targeted screening workflows in this chapter is the blank subtraction. The MPP workflow removed all features present in the blank sample, while the MZmine workflow only removed features exceeding a certain intensity. Further research is needed to investigate the influence of the different processing steps and parameters on the quality of the outcome (Hohrenk et al. 2020). The observed differences in processing steps and the resulting outcome confirms the added value of combining multiple data-analysis workflows as used in this chapter.

2.4 Evaluation of performing dialysis during the colon-stage on the microbiotic biotransformation of chlorogenic acid

2.4.1 Introduction

The current GIDM-Colon protocol results in a lack of information on the colonic behavior of the studied xenobiotic between 6 h and 24 h dialysis. Expanding the GIDM-Colon protocol with additional timepoints would lead to a more in-depth knowledge on the colonic behavior and the microbiotic biotransformation of the xenobiotic. This study investigated the complementarity of parallel GIDM-Colon experiments, covering different sampling timepoints. However, due to practical reasons (overnight experiments), changing the sampling timepoints also influenced the dialysis timing. Venema et al (2015) reported that performing dialysis during an *in vitro* gut microbiome biotransformation experiment is required to maintain highly active microbiota and representative concentrations of microbial metabolites in the *in vitro* model.

2.4.2 Materials and methods

2.4.2.1 Chemicals, reagents and materials

Same chemicals, reagents and materials as mentioned in 2.3.1.1 and 2.3.1.2 were used during this study.

2.4.2.2 In vitro gastrointestinal biotransformation model

The GIDM-Colon was applied to study the influence of the dialysis on the microbiotic biotransformation of chlorogenic acid. The experiment was carried out for both the lean as obese population (Chapter 3). The experiment set-up is visualized in Figure 2-11.

2.4.2.2.1 *Fecal slurry*

The fecal slurry aliquots from both the lean as obese volunteers (see chapter 3 for inclusion criteria) were used. By using fecal slurry aliquots from the same donors within both population-experiments, a standardized microbial inoculum was ensured, which allowed comparison between the experiments. A pooled fecal slurry suspension (10 % (v/v)) was created in a sterile phosphate buffer and incubated for 1 h in the anaerobic glove box as adaptation period.

2.4.2.2.2 *GIDM-Colon*

The GIDM-Colon experiment was based on the procedure described previously (Figure 2-11, Original protocol) with minor changes to the sampling timepoints and dialysis (Adjusted protocol). Samples were taken at the start of the experiment after which no dialysis was performed overnight. After 14 h incubation, samples were taken for the dialysis cells and dialysis was started for the remaining time of the experiment. Samples were taken after 16 h, 18 h, 20 h and 22 h and immediately stored at -80 °C.
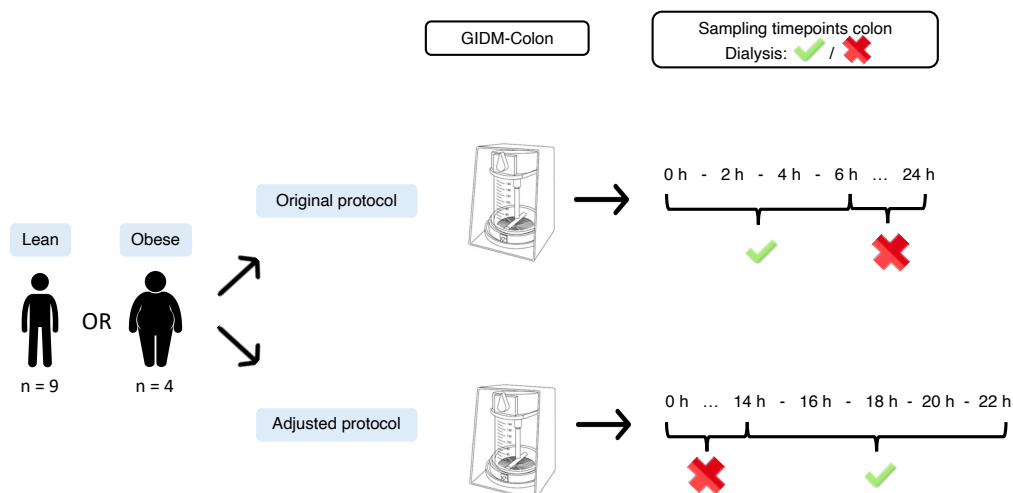
Figure 2-11: Experimental setup of the additional study regarding the influence of dialysis on the detected biotransformation products.

2.4.2.2.3   *Sample preparation, LC-Q-TOF-MS and data-analysis*

The optimized sample preparation procedure was applied to the samples. Samples were thawed at room temperature and one mL of MeOH (-80 °C) was added together with 10 µL of 2 mg/mL theophylline solution (internal standard). Samples were vortexed 60 s and 1/10 diluted in 1/1 (v/v) ACN/water. Samples were filtered using a 0.2 µm centrifugal filter (5 min, 8000 rpm). Samples were evaporated to dryness under a gentle N_2-stream at 37 °C and reconstituted in the starting mobile phase. Samples and resulting data were analyzed according to the procedures described in 2.3.1.6.2 and 2.3.1.6.3.

2.4.3 Results and discussion

2.4.3.1 Lean GIDM-Colon experiments

Dissimilarities were observed between the protocols for biotransformation products M8, M14, M15 and M20 (Table 2-1, Figure 2-12). In the adjusted protocol, an increase in relative area of M8 and M20 was seen over colonic dialysis time. The while the relative area of M8 after 24 h of colonic dialysis with the original protocol was clearly lower while M20 was not longer detected (Figure 2-12-A,B). For both M14 and M15 decreasing signals were observed between 14 h and 22 h of colonic dialysis with the adjusted protocol, however, the relative area after 24 h colonic stage did not match the observed declining trend (Figure 2-12-C,D).
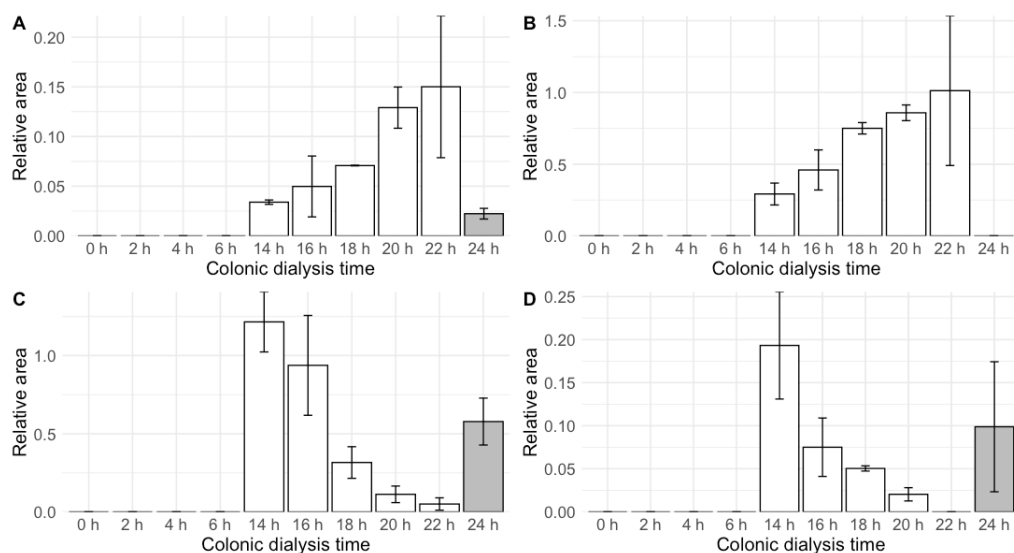
Figure 2-12: Relative area of M8 (A), M20 (B), M14 (C) and M15 (D) in the original (grey) of adjusted (white) lean GIDM-Colon protocol over colonic dialysis time.

2.4.3.2   *Obese GIDM-Colon experiments*

More pronounced differences were observed between the obese GIDM-Colon experiments. Starting from 14 h and 20 h of colonic incubation respectively, chlorogenic acid isomers 5-CQA and 3-CQA were no longer detected in the GIDM-Colon samples using the adjusted protocol. However, applying the original protocol, 3-CQA, 4-CQA and 5-CQA were still detected after 24 h of colonic dialysis.

Both M12 and M22 were not detected in the adjusted protocol 14 h – 22 h of colonic dialysis samples while they were present in the 24 h samples (Figure 2-13-A,B). M10, M20 and M8 were not present in the 24 h colonic samples, while they were detected in the 14 h - 22 h dialysis samples of the adjusted protocol (Figure 2-13-C-E).
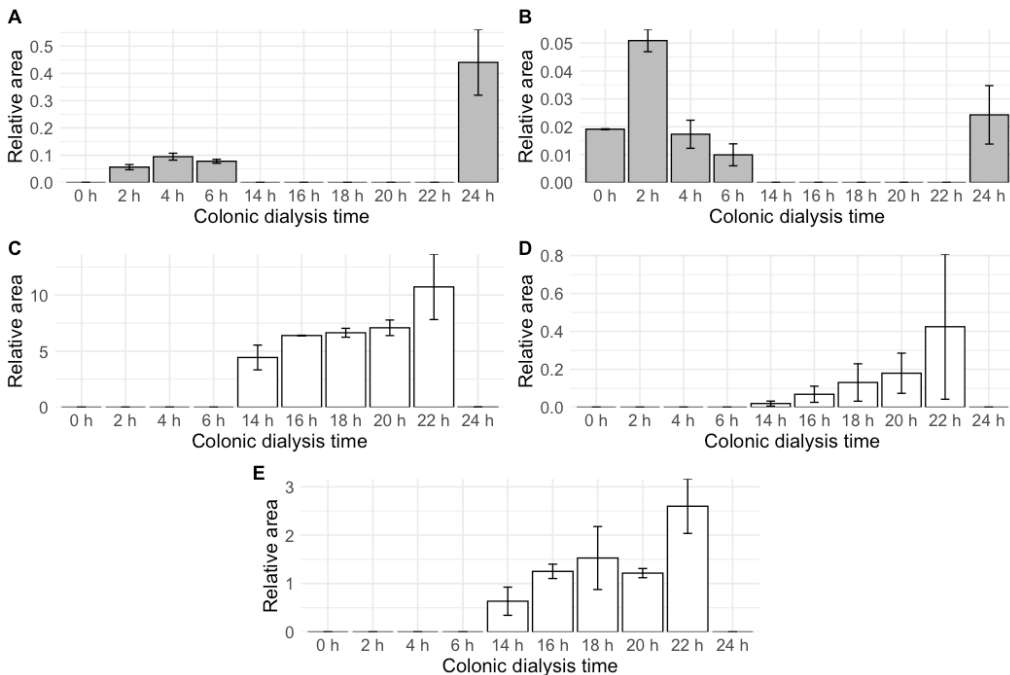
Figure 2-13: Relative area of M12 (A), M22 (B), M10 (C), M20 (D) and M8 (E) in the original (grey) of adjusted (white) obese GIDM-Colon protocol over colonic dialysis time.

As the timing of the dialysis is the only variable between the two protocols, these results clearly show an effect of the dialysis on the detected biotransformation products. Not performing dialysis during the GIDM-Colon experiment could led to an accumulation of microbial metabolites and chlorogenic acid biotransformation products (Venema 2015). Even though the exact underlying mechanism is not known, the hypothesis of saturation of microbial enzymes combined with a different starting timepoint of the dialysis, 0 h vs 14h of colonic stage, is a possible explanation causing the observed differences. Based on these results, the optimal GIDM-Colon performs dialysis to prevent saturation of microbial enzymes and includes continue 2 h interval sampling timepoints over a period of 24 h.

2.5 Conclusions

This chapter presents the optimization of a complete and ready-to-use *in vitro* bioanalytical platform to investigate the gastrointestinal biotransformation of different xenobiotics, starting from the GIDM-Colon developed by Breynaert et al. (2015). The incubation medium WCB showed to introduce variation in the bacterial composition of the pooled fecal slurry suspension. A sterile phosphate buffer guaranteed a closer resemblance to the *in vivo* composition and was chosen as optimal incubation medium for future experiments. Furthermore, incubation of the 10 % (v/v) fecal slurry in a sterile phosphate buffer during 24 h showed no clear increase or decrease in anaerobic bacterial concentration. Future *in vitro* experiments investigating the colonic biotransformation of xenobiotics using the GIDM-Colon, can be performed with a one-hour incubation step instead of the original proposed 17 h, reducing the risk of changes to the *in vivo* fecal bacterial composition. This will guarantee a closer resemblance to the *in vivo* human colonic biotransformation when performing *in vitro* gastrointestinal dialysis experiments.

Four different sample preparation procedures were investigated to evaluate the influence of the procedure on the detection of biotransformation products. The freeze-drying procedure showed to be inferior, while centrifugation, sonication and extraction gave similar results. Considering the shorter time period needed to obtain samples suitable for LC injection, extraction was selected as optimal method. Additionally, a 1/20 dilution of the samples prior to LC-Q-TOF-MS analysis was chosen as most optimal dilution in comparison to a 1/10 and 1/40 dilution. Finally, the injection solvent was optimized. Additional experiments showed that evaporation of the samples to dryness and reconstitution in the starting mobile phase prior to LC-MS analysis improved the quality of the peak shapes and no influence of storage at -20 °C was observed. Combining suspect screening with two non-targeted screening data-analysis workflows (MZmine + R and MPP workflow) showed a clear added value to the number of identified colonic biotransformation products.

CHAPTER 2

Optimization of the GIDM-Colon procedure and the pre-analytical sample preparation phase, as well as the combination of complementary data-analysis workflows for biotransformation product identification resulted in the establishment of a unique ready-to-use platform to investigate colonic biotransformation of different xenobiotics. This platform can be used to investigate inter-individual differences in colonic biotransformation, by using different fecal donors. When using this platform, chlorogenic acid will be implemented as a positive control.

Parallel GIDM-Colon experiments with deviating dialysis- and sampling intervals resulted in deviating results, limiting the complementarity. If the colonic behavior of a xenobiotic is studied over an interval of 24 h, all samples should originate from one GIDM-Colon experiment, with a duration of 24 h and dialysis should be performed continuously to prevent influence on the dialysis timing on the obtained results.

2.6 **Supplementary information**

Table SI- 2-1: Overview of inclusion criteria for fecal donors

Inclusion criteria for fecal donors
Women aged 25 to 45 years
Not pregnant at time of fecal donation, no treatment with high hormonal doses, no treatment with in vitro fertilization (oral contraceptives (low hormonal doses) is not a problem for participation).
No menses at the time of donation
Non-smoker: min. 3 years in advance of the donation
No vegetarian or vegan
No acute condition (e.g. diarrhea, fever or vomiting) at the time of donation
No chronic condition requiring medical attention or medication at time of the donation
No diagnosed infections (including HIV, hepatitis A, hepatitis B, hepatitis C …). Inclusion of statement of recent vaccinations or history of major infections
Normal defecation: no diarrhea, no constipation and no treatment of any of these conditions in the past 3 months in advance of the donation
No history of bowel disorders (Crohn's disease, ulcerative colitis, irritable bowel syndrome, Clostridium difficile colitis, stomach ulcer, Helicobacter pylori infection …).
No history of major gastrointestinal tract operations (e.g. gastric bypass).
No intake of antibiotics or antifungal, antiviral, antiparasitic medication 6 months in advance of the donation.
No chronic intake of pre- and/or probiotics supplements 3 months in advance of the donation.
No history of traveling to geographic areas with high risk of traveler's diarrhea (Africa with exclusion of South Africa, Middle East, Asia with exclusion of Japan and Thailand, Australian continent with exclusion of Australia and New Zealand, Central and South America and the Caribbean with exclusion of Argentina and Chile) in the last 6 months. No residence of a couple of years in these areas.
No history of typhoid fever.
No allergic diseases.
No history of immunosuppressants or chemotherapeutics use.

Table SI- 2-1: Overview of inclusion criteria for fecal donors (Continued)

No vaccinations 3 months in advance of the donation (no flu vaccination 1 month before donation).
Maximum 7 alcoholic drinks per week.
No illegal drug use.
No risky sexual behaviour

Table SI- 2-2: Selection criteria for lean volunteers.

Group	Lean
BMI (kg/m²)	< 25
Waist circumference (cm)	< 80
Fasting glycaemia (mg/dL)	< 126
Glycaemia after oral glucose tolerance test (mg/dL)	< 200
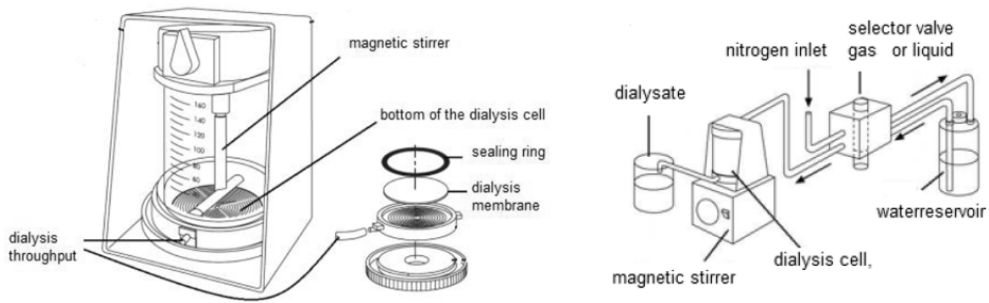
Figure SI- 2-1: Magnification of an ultrafiltration cell, just before connecting to the system (left) and schematic representation of the colonic and small intestinal stage of the GIDM-colon (right). Adapted from Breynaert et al., Planta Medica, 2015;81(12-13):1075-83. (Breynaert et al. 2015)
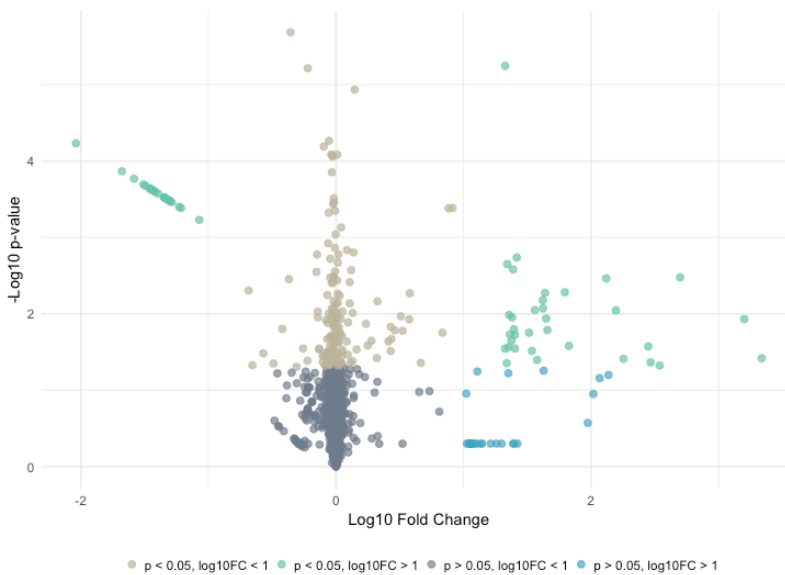
Figure SI- 2-2: *m/z* features, present in a colon-stage sample after 24 h of incubation, are visualized by a volcano plot. Features coloured in green with a log10 fold change > 1 and a p-value <0.05, represent the features of interest.
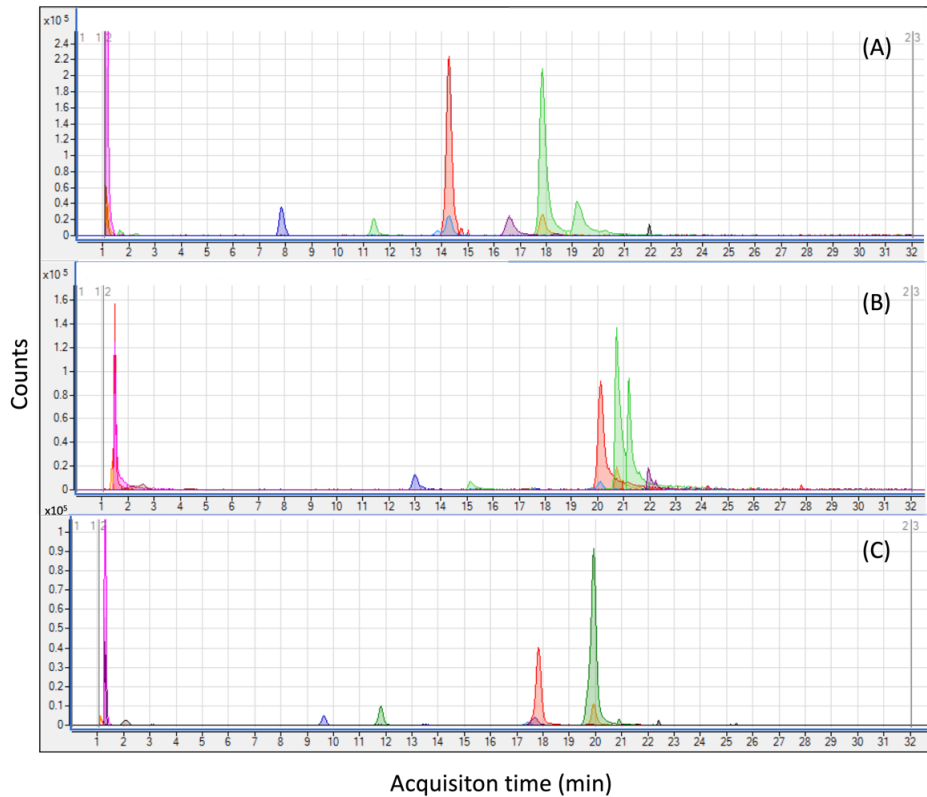
Figure SI- 2-3: Chromatogram of the colonic biotransformation products of chlorogenic acid detected in a 24 h retentate colon sample, analyzed by using three different HPLC columns. (A) Luna Omega PS C18 column. (B) Kinetex XB-C18 column. (C) Luna Omega Polar C18.

Table SI- 2-3: Number of anaerobic bacteria over 24 h of incubation in a sterile phosphate buffer (0.1 M, pH 7). Sample WCB-17 corresponds to a pooled sample incubated in WCB for 17 h.

Pool	Incubation time (h)	Concentration anaerobic bacteria (CFU/g)
	0	1.38×10^8
	2	1.35×10^8
	4	1.20×10^8
Pool 1	6	1.65×10^8
	8	1.63×10^8
	10	1.58×10^8
	24	1.65×10^8
	0	1.48×10^8
	14	1.60×10^8
	16	1.63×10^8
Pool 2	18	1.42×10^8
	20	1.72×10^8
	22	1.30×10^8
	24	1.30×10^8
WCB	17	1.48×10^9

Figure SI- 2-4: Levels of confirmation as proposed by Schymanski et al. (2014).

References

Borody TJ, Paramsothy S and Agrawal G. Fecal microbiota transplantation: indications, methods, evidence, and future directions. *Current gastroenterology reports* 2013, 15(8): 337-337.

Breynaert A, Bosscher D, Kahnt A, Claeys M, Cos P, Pieters L and Hermans N. Development and Validation of an in vitro Experimental GastroIntestinal Dialysis Model with Colon Phase to Study the Availability and Colonic Metabolisation of Polyphenolic Compounds. *Planta Medica* 2015, 81(12-13): 1075-1083.

Carmody RN and Turnbaugh PJ. Host-microbial interactions in the metabolism of therapeutic and diet-derived xenobiotics. *Journal of Clinical Investigation* 2014, 124(10): 4173-4181.

Choi WG, Kim JH, Kim DK, Lee Y, Yoo JS, Shin DH and Lee HS. Simultaneous Determination of Chlorogenic Acid Isomers and Metabolites in Rat Plasma Using LC-MS/MS and Its Application to A Pharmacokinetic Study Following Oral Administration of Stauntonia Hexaphylla Leaf Extract (YRA-1909) to Rats. *Pharmaceutics* 2018, 10(3).

Dawidowicz AL and Typek R. Thermal Stability of 5-o-Caffeoylquinic Acid in Aqueous Solutions at Different Heating Conditions. *Journal of Agricultural and Food Chemistry* 2010, 58(24): 12578-12584.

de Melo LV and Sawaya ACHF. UHPLC–MS quantification of coumarin and chlorogenic acid in extracts of the medicinal plants known as guaco (Mikania glomerata and Mikania laevigata). *Revista Brasileira de Farmacognosia* 2015, 25(2): 105-110.

Del Rio D, Stalmach A, Calani L and Crozier A. Bioavailability of Coffee Chlorogenic Acids and Green Tea Flavan-3-ols. *Nutrients* 2010, 2(8): 820-833.

Gonthier MP, Remesy C, Scalbert A, Cheynier V, Souquet JM, Poutanen K and Aura AM. Microbial metabolism of caffeic acid and its esters chlorogenic and caftaric acids by human faecal microbiota in vitro. *Biomedicine & Pharmacotherapy* 2006, 60(9): 536-540.

Gonthier MP VM, Besson C, Rémésy C, Scalbert A. Chlorogenic acid bioavailability largely depends on its metabolism by the gut microflora in rats. *The Journal of Nutrition* 2003, 133(6): 1853-1859.

Gromova M and Roby C. Toward Arabidopsis thaliana hydrophilic metabolome: assessment of extraction methods and quantitative 1H NMR. *Physiologia Plantarum* 2010, 140(2): 111-127.

Gu T, Gu Y, Zheng Y, Wiehl PE and Kopchick JJ. Phase separation of acetonitrile-water mixture in protein purification. *Separations Technology* 1994, 4(4): 258-260.

Hohrenk LL, Itzel F, Baetz N, Tuerk J, Vosough M and Schmidt TC. Comparison of Software Tools for Liquid Chromatography–High-Resolution Mass Spectrometry Data Processing in Nontarget Screening of Environmental Samples. *Analytical Chemistry* 2020, 92(2): 1898-1907.

Jandhyala SM, Talukdar R, Subramanyam C, Vuyyuru H, Sasikala M and Nageshwar Reddy D. Role of the normal gut microbiota. *World Journal of Gastroenterology* 2015, 21(29): 8787-8803.

Kang J, Price WE, Ashton J, Tapsell LC and Johnson S. Identification and characterization of phenolic compounds in hydromethanolic extracts of sorghum wholegrains by LC-ESI-MSn. *Food Chemistry* 2016, 211: 215-226.

Kia E, Wagner Mackenzie B, Middleton D, Lau A, Waite DW, Lewis G, Chan YK, Silvestre M, Cooper GJ, Poppitt SD and Taylor MW. Integrity of the Human Faecal Microbiota following Long-Term Sample Storage. *PLoS One* 2016, 11(10): e0163666.

Konishi Y and Kobayashi S. Transepithelial transport of chlorogenic acid, caffeic acid, and their colonic metabolites in intestinal Caco-2 cell monolayers. *Journal of Agricultural and Food Chemistry* 2004, 52(9): 2518-2526.

Minekus M, Alminger M, Alvito P, Ballance S, Bohn T, Bourlieu C, Carriere F, Boutrou R, Corredig M, Dupont D, Dufour C, Egger L, Golding M, Karakaya S, Kirkhus B, Le Feunteun S, Lesmes U, Macierzanka A, Mackie A, Marze S, McClements DJ, Menard O, Recio I, Santos CN, Singh RP, Vegarud GE, Wickham MS, Weitschies W and Brodkorb A. A standardised static in vitro digestion method suitable for food - an international consensus. *Food & Function* 2014, 5(6): 1113-1124.

Mortele O, Vervliet P, Gys C, Degreef M, Cuykx M, Maudens K, Covaci A, van Nuijs ALN and Lai FY. In vitro Phase I and Phase II metabolism of the new designer benzodiazepine cloniprazepam using liquid chromatography coupled to quadrupole time-of-flight mass spectrometry. *Journal of Pharmaceutical and Biomedical Analysis* 2018, 153: 158-167.

O'Hara AM and Shanahan F. The gut flora as a forgotten organ. *EMBO reports* 2006, 7(7): 688-693.

Olthof MR, Hollman PCH, Buijsman M, van Amelsvoort JMM and Katan MB. Chlorogenic acid, quercetin-3-rutinoside and black tea phenols are extensively metabolized in humans (vol 133, pg 1806, 2003). *Journal of Nutrition* 2003, 133(8): 2692-2692.

Pinta MN, Montoliu I, Aura AM, Seppanen-Laakso T, Barron D and Moco S. In Vitro Gut Metabolism of U-C-13 -Quinic Acid, The Other Hydrolysis Product of Chlorogenic Acid. *Molecular Nutrition & Food Research* 2018, 62(22): 7.

Pluskal T, Castillo S, Villar-Briones A and Oresic M. MZmine 2: Modular framework for processing, visualizing, and analyzing mass spectrometry-based molecular data. *BMC Bioinformatics* 2010, 11: 395-405.

Pruesse E, Quast C, Knittel K, Fuchs BM, Ludwig W, Peplies J and Glöckner FO. SILVA: a comprehensive online resource for quality checked and aligned ribosomal RNA sequence data compatible with ARB. *Nucleic Acids Research* 2007, 35(21): 7188-7196.

Rechner AR, Smith MA, Kuhnle G, Gibson GR, Debnam ES, Srai SKS, Moore KP and Rice-Evans CA. Colonic metabolism of dietary polyphenols: Influence of structure on microbial fermentation products. *Free Radical Biology and Medicine* 2004, 36(2): 212-225.

Schymanski EL, Jeon J, Gulde R, Fenner K, Ruff M, Singer HP and Hollender J. Identifying small molecules via high resolution mass spectrometry: communicating confidence. *Environmental Science and Technology* 2014, 48(4): 2097-2098.

Shao G, Agar J and Giese RW. Cold-induced aqueous acetonitrile phase separation: A salt-free way to begin quick, easy, cheap, effective, rugged, safe. *Journal of Chromatography A* 2017, 1506: 128-133.

Sousa T, Paterson R, Moore V, Carlsson A, Abrahamsson B and Basit AW. The gastrointestinal microbiota as a site for the biotransformation of drugs. *International Journal of Pharmaceutics* 2008, 363(1-2): 1-25.

Spanogiannopoulos P, Bess EN, Carmody RN and Turnbaugh PJ. The microbial pharmacists within us: a metagenomic view of xenobiotic metabolism. *Nature Reviews Microbiology* 2016, 14(5): 273-287.

Stojancevic M, Bojic G, Al Salami H and Mikov M. The Influence of Intestinal Tract and Probiotics on the Fate of Orally Administered Drugs. *Current Issues in Molecular Biology* 2014, 16: 55-67.

Tap J, Cools-Portier S, Pavan S, Druesne A, Öhman L, Törnblom H, Simren M and Derrien M. Effects of the long-term storage of human fecal microbiota samples collected in RNAlater. *Scientific Reports* 2019, 9(1): 601.

Tomas-Barberan F, Garcia-Villalba R, Quartieri A, Raimondi S, Amaretti A, Leonardi A and Rossi M. In vitro transformation of chlorogenic acid by human gut microbiota. *Molecular Nutrition & Food Research* 2014, 58(5): 1122-1131.

Venema K (2015). The TNO In Vitro Model of the Colon (TIM-2). *The Impact of Food Bioactives on Health: in vitro and ex vivo models*. K. Verhoeckx, P. Cotter, I. López-Expósito et al. Cham, Springer International Publishing**:** 293-304.

Venema K and van den Abbeele P. Experimental models of the gut microbiome. *Best Pract Res Clinical Gastroenterology* 2013, 27(1): 115-126.

Verhoeckx K, Cotter P, Lopez-Exposito I, Kleiveland C, Lea T, Mackie A, Requena T, Swiatecka D and Wichers H. The Impact of Food Bioactives on Health: in vitro and ex vivo models. *Springer* Cham (CH), 2015: 338.

Vervliet P. invitRo - in vitro HLM assay freature prioritization. *Zenodo* 2018.

Vervliet P, Mortele O, Gys C, Degreef M, Lanckmans K, Maudens K, Covaci A, van Nuijs ALN and Lai FY. Suspect and non-target screening workflows to investigate the in vitro and in vivo metabolism of the synthetic cannabinoid 5Cl-THJ-018. *Drug Testing and Analysis* 2018, 11(3): 479-491.

CHAPTER 2

Wang F, Shang Z, Xu L, Wang Z, Zhao W, Mei X, Lu J and Zhang JY. Profiling and identification of chlorogenic acid metabolites in rats by ultra-high-performance liquid chromatography coupled with linear ion trap-Orbitrap mass spectrometer. *Xenobiotica* 2018, 48(6): 605-617.

Wang Q, Ye M, Xu L and Shi ZG. A reversed-phase/hydrophilic interaction mixed-mode C18-Diol stationary phase for multiple applications. *Analytica Chimica Acta* 2015, 888: 182-190.

Wianowska D and Gil M. Recent advances in extraction and analysis procedures of natural chlorogenic acids. *Phytochemistry Reviews* 2018, 18(1): 273-302.

Wilson ID and Nicholson JK. Gut microbiome interactions with drug metabolism, efficacy, and toxicity. *Translational Research* 2017, 179: 204-222.

Wu XH, Yu HL, Ba ZY, Chen JY, Sun HG and Han BZ. Sampling methods for NMR-based metabolomics of Staphylococcus aureus. *Biotechnology Journal* 2010, 5(1): 75-84.

Yang F, Gong JF, Shen L, Zhang C, Kou FR, Gao J, Li Y and Bing Xu G. Development of an LC-MS/MS method for quantitative analysis of Chlorogenic acid in human plasma and its application to a pharmacokinetic study in Chinese patients with advanced solid tumor. *Journal of Pharmaceutical and Biomedical Analysis* 2020, 177: 112809.

Zhao L, Qian X, Li W, Lv L, Zhang H, Chai Y and Zhang G. An LC-MS/MS method for the simultaneous determination and pharmacokinetic studies of bergenin, chlorogenic acid and four flavonoids in rat plasma after oral administration of a QingGanSanJie decotion extract. *Biomedical Chromatography* 2014, 28(12): 1670-1678.

CHAPTER 2

CHAPTER 3: INVESTIGATING INTER-INDIVIDUAL DIFFERENCES IN COLONIC BIOTRANSFORMATION OF XENOBIOTICS BY THE GUT MICROBIOME: OBESE VERSUS LEAN
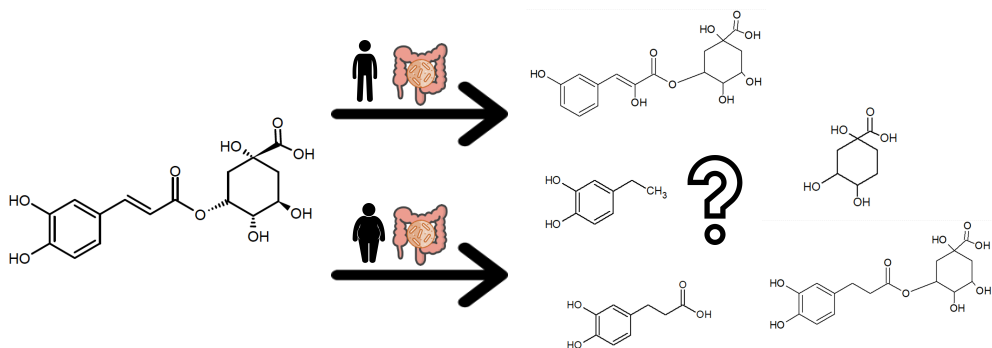
Based on following paper:

Mortelé O, Xavier B B, Lammens C, Malhotra-Kumar S, Jorens P G, van Nuijs A L N and Hermans N. Obesity influences the microbiotic biotransformation of chlorogenic acid by the gut microbiome. *Metabolites* (Submitted)

CHAPTER 3

CHAPTER 3

3.1 Introduction

In 2016, over 650 million adults worldwide were obese and more than 1.9 billion adults had overweight making obesity a major public health problem (WHO 2020). Besides environmental, dietary, genetic and lifestyle factors, the gut microbiome has been identified as an important factor related to obesity. Alterations in gut microbiome composition are believed to be responsible for enhanced energy harvest from the human diet leading to a disruption of the energy homeostasis (Ley et al. 2005, Ley et al. 2006, Turnbaugh et al. 2008, Turnbaugh et al. 2009). The association between obesity and the gut microbiome was initially suggested based on animal studies. A study in germ-free mice observed a 60% increase in body fat within two weeks when the gut microbiota of obese mice was transferred to sterile mice, while germ-free mice receiving the microbiota of lean mice remained lean (Bäckhed et al. 2004). Associations between obesity and the gut microbiome have also been observed in humans (Turnbaugh et al. 2009, Sweeney and Morton 2013). A comparative study with monozygotic and dizygotic twins revealed phylum-level changes, reduced bacterial diversity, altered representation of bacterial genes and metabolic pathways associated with obesity (Turnbaugh et al. 2009). Multiple studies have demonstrated that representatives of the phylum Bacteroidetes were decreased and representatives of the phylum Firmicutes were increased in obese individuals (Ley et al. 2005, Ley et al. 2006, Turnbaugh et al. 2008, Turnbaugh et al. 2009). It has to be mentioned, however, that diverse information is still published (Duncan et al. 2008, Zhang et al. 2009, Murphy et al. 2010) showing the need for further research.

The gut microbiome is considered an additional metabolizing organ as it is able to influence the activity and toxicity of pharmaceuticals and other xenobiotics (O'Hara and Shanahan 2006, Borody et al. 2013, Wilson and Nicholson 2017). Related to the role of the gut microbiome in obesity, it is suggested that the obese gut microbiome features highly efficient metabolic pathways extracting energy from the human diet. Studies related to differences in metabolic capacity of the obese and lean gut

microbiome are limited to *in vitro* fermentation experiments studying the microbiotic biotransformation of dietary fibers, however, the effect of obesity related dysbiosis on the microbial biotransformation of xenobiotics such as pharmaceuticals remains unknown (Turnbaugh et al. 2008, Aguirre et al. 2016). Differences in biotransformation of xenobiotics by the gut microbiome between lean and obese populations could result in differences in activity and toxicity of the ingested compound. This information can have an impact on the dosage and dosing regimen of pharmaceuticals or food-supplements and can aid in the development of a more personalized medical treatment for an obese population. In this chapter, the optimized *in vitro* gastrointestinal platform, including the GIDM-Colon, was used to study inter-individual differences in the microbial biotransformation of the model compound chlorogenic acid. Optimization of the platform ensured a better resemblance of the *in vivo* situation which allows interpopulation comparison of lean and obese populations. The differences in gut microbiome conditions were mimicked using collected fecal samples from both populations (Mortelé et al. 2019).

3.2 Aims and preface

The objective of this chapter was to investigate (i) if differences in gut microbiome composition, bacterial diversity and/or the absolute number of bacteria could be observed between a lean and obese population and (ii) if inter-individual differences on the *in vitro* microbiotic biotransformation of chlorogenic acid by the gut microbiome could be observed between the two populations. The optimized *in vitro* gastrointestinal platform described earlier was applied as this model is suitable to study interindividual differences.

3.3 Materials and methods

3.3.1 Chemicals, reagents and materials

Sodium phosphate dibasic (Na_2HPO_4, ≥ 99%), sodium phosphate monobasic dihydrate ($NaH_2PO_4.2H_2O$, ≥ 99%), thioglycollate broth, pepsin from porcine gastric mucosa, bile extract porcine, pancreatin from porcine pancreas, theophylline (≥ 99%, anhydrous), caffeic acid (> 98%), chlorogenic acid (≥ 95%), dihydrocaffeic acid (98%), ferulic acid (99%) and quinic acid (98%) were purchased from Sigma-Aldrich (St Louis, MO, USA). Deionized water and sodium bicarbonate ($NaHCO_3$, > 99.7%, ACS grade) were acquired from respectively Millipore (Burlington, Massachusetts, USA) and Acros Organics (Pittsburgh, Pennsylvania, USA). Hydrochloric acid (HCl, 32 wt.% for analysis), formic acid (98-100%, Suprapur) and sodium hydroxide pellets (NaOH) were obtained from Merck (Darmstadt, Germany). Acetonitrile (ACN) and methanol (MeOH, ≥ 99.9%, LC-MS grade) were acquired from Fisher Scientific (Hampton, New Hampshire, USA). Ultrapure water (Purelab flex apparatus) was obtained from ELGA Veolia (UK). Nitrogen gas (N_2, AZOTE N28) and a gas mixture of hydrogen, carbon dioxide and nitrogen (5% H_2, 5% CO_2 and 90% N_2, Alphagaz Mix) were purchased from Air Liquide Belge (Liege, Belgium).

Stirred ultrafiltration cells (model 8200, 200 mL, 63.5 mm diameter), the related controller (controller MF2 and reservoir RC800) and ultrafiltration discs (Ultracel, MWCO 1000 Da, 63.5 mm diameter) were purchased from Amicon Ltd (USA). A shaking warm water bath from VWR (Radnor, Pennsylvania, USA) was used during the gastric stage of the gastrointestinal dialysis model with colon phase (GIDM-Colon). An immersion circulator (model 1122S) and dialysis tubing (MWCO 12-14 kDa, Visking size 6 Inf Dia 27/32 – 21.5 mm: 30 M) were acquired respectively from VWR and Medicell Ltd. (London, UK), for use during the small intestinal stage. An anaerobic environment was created during the colonic stage using a Jacomex glove box T3 from TCPS (Belgium).

3.3.2 Fecal samples

3.3.2.1 Collection and processing of the fecal samples

Additionally to the nine fecal samples collected from lean volunteers as described in Chapter 2, four fecal samples from human metabolically healthy obese donors, defined according to the international guidelines of the World Health Organization (WHO), were collected in collaboration with the department of Clinical Pharmacology (Prof. P. Jorens) and Endocrinology-Diabetology and Clinical Nutrition (Prof. L. Van Gaal and Dr. E. Dirinck) of the Antwerp University Hospital. Patients met the same inclusion criteria as mentioned in 2.3.1.3.1 and Table SI-2.1. However, in comparison to the lean volunteers, a body mass index (BMI) and waist circumference of > 30 kg/m^2 and > 88 cm was required as proposed by the WHO guidelines for obesity (Table 3-1) (WHO 2020). Fasting glycaemia and glycaemia after oral glucose tolerance test below 126 mg/dL and 200 mg/dL glucose respectively were mandatory in order to exclude hyperglycemic patients as type I and type II diabetes are also associated with gut microbiome dysbiosis. Ethical approval for the project was acquired from the Ethical Committee of the Antwerp University Hospital (reference number: 16/43/442). The donors collected the fecal sample using Protocult collection containers (Ability Building

Center, Rochester, USA). Samples were held at room temperature in an anaerocult bag (Merck, Darmstadt, Germany). Feces were processed and stored within 3 h as described in 2.3.1.3.1.

Table 3-1: Selection criteria for lean and metabolically healthy obese patients.

Group	Lean	Metabolically healthy obese
BMI (kg/m^2)	< 25	>30
Waist circumference (cm)	< 80	>88
Fasting glycaemia (mg/dL)	< 126	< 126
Glycaemia after oral glucose tolerance test (mg/dL)	< 200	< 200

3.3.2.2 Gut microbiome-comparison between the lean and obese population

The gut microbiota composition of the fecal samples from the obese volunteers (n=4) was characterized according to the procedure described in 2.3.1.3. Differences in relative abundance on all taxonomic levels among samples (lean vs obese) were identified by linear discriminant analysis effect size (LEfSe). The concentration anaerobic colony forming units per gram (CFU/g) was determined for all samples according to the procedure described in 2.3.1.3.5.

3.3.3 Optimized *in vitro* gastrointestinal platform

The optimized *in vitro* platform described in chapter two and previously developed by Breynaert et al. (2015) was applied to evaluate inter-individual differences in microbiotic metabolism of chlorogenic acid between a lean and obese population (Mortelé et al. 2019).

3.3.3.1 *Incubation of fecal slurry suspension*

Fecal slurry aliquots of the lean or obese donors were thawed and pooled with the samples from the same population. A 10% (v/v) pooled fecal slurry suspension was created by addition of a sterile phosphate buffer (0.1 M, pH 7), which was incubated for 1 h in the anaerobic glove box before use in the colonic-stage of the GIDM-Colon experiment.

3.3.3.2 *GIDM-Colon*

The protocol of the GIDM-Colon experiment is described in detail in chapter two (2.3.4). 50 mL of the appropriate 10% (v/v) fecal slurry suspension (lean/obese, Figure 3-1) was added the ultrafiltration cells with exception of the negative control cell, which received 50 mL of sterile phosphate buffer. Samples were collected before and after the gastric stage, after the small intestinal stage and after 0 h, 2 h, 4 h, 6 h and 24 h of colonic dialysis.

3.3.3.3 *Sample preparation*

The optimized sample preparation procedure discussed in chapter two was applied to the samples of the GIDM-Colon. Shortly, samples (one mL volume) were thawed at room temperature and one mL MeOH (-80 °C) was added. 10 μL of 2 mg/mL theophylline solution (as internal standard) was spiked to the sample, followed by 60 s vortex mixing. A subsequent 1/10 dilution of the samples in 1/1 (v/v) ACN/water was carried out, after which the samples were filtered using a 0.2 μm centrifugal filter (5

min, 8000 rpm). Finally, samples were evaporated to dryness under a gentle N_2-stream at 37 °C, reconstituted in the starting mobile phase and transferred to an LC-vial with insert.
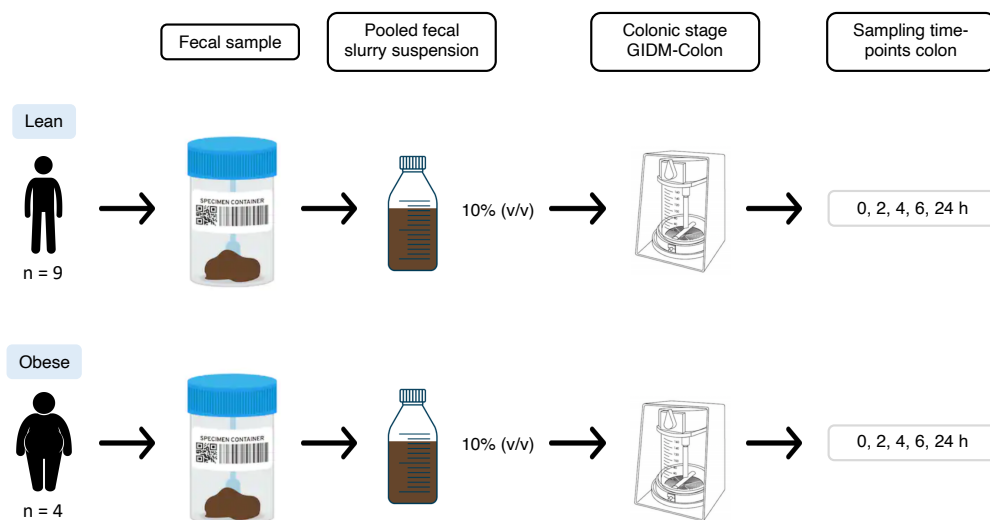
Figure 3-1: Overview of the lean and obese population GIDM-Colon experiments.

3.3.4 Data acquisition and data analysis

Instrumental analysis of the samples by liquid chromatography coupled to quadrupole time-of-flight mass spectrometry (LC-Q-TOF-MS) and application of three complementary data analysis workflows for biotransformation products identification was performed as described in 2.3.1.6.2 and 2.3.1.6.3. All biotransformation products of chlorogenic acid mentioned in chapter two (Table 2-1) were added to the suspect list together with the results of available literature and *in silico* prediction tools Biotransformer (Biotransformer.ca, v1.0.0) and Meteor Nexus (Lhasa Limited, v2.1). Identification was based on injection of an analytical standard if available, fragmentation pattern of the products ions, accurate mass and isotopic pattern. Parent ions may not exceed $\pm$ 10 ppm mass variation between the theoretical and measured parent ion. A maximal mass variation of $\pm$ 25 ppm for the product ions was

allowed. Identified biotransformation products had to be present in both replicates at a certain sampling time and were not present in blank or negative control samples unless otherwise mentioned in the chapter.

3.4   Results and discussion

3.4.1   The gut microbiome: lean versus obese population

3.4.1.1   CFU determination

Table 3-2 summarizes the concentration anaerobic CFU in all samples. The concentration of anaerobic bacteria was lower for all obese samples in comparison to the samples of the lean volunteers, with exception of sample C3. A mean of 3.45×10^8 CFU/mL and 0.133×10^8 CFU/mL anaerobic bacteria were determined in the lean and obese samples respectively.

Table 3-2: Overview of the concentration colony forming units (CFU) in the individual lean (C) and obese (O) samples and the mean concentration within the population.

Sample	Concentration (x 10^8 CFU/mL)	Mean (x 10^8 CFU/mL)
C2	4.47	
C3	0.45	
C4	12.9	
C5	2.76	
C6	1.06	3.45
C7	2.68	
C8	2.44	
C9	0.81	
C10	3.50	
O1	0.006	
O3	0.45	0.13
O6	0.027	
O7	0.05	

3.4.1.2   Alpha diversity

Figure 3-2 visualizes the number of observed species in the lean and obese samples. The data suggest a lower alfa diversity of the obese gut microbiota as previously reported in the literature (Turnbaugh et al. 2009). However, no conclusions can be

made due to the limited number of samples. The outlier observed in the obese population corresponds with sample O7.
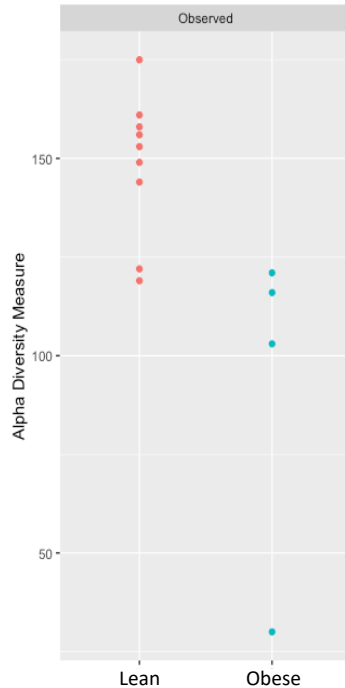
Figure 3-2: Overview of the number of observed species in the lean (red) and obese (blue) samples.

3.4.1.3 Beta diversity

The following bacterial operational taxonomic units (OTUs) were uniquely present in the lean volunteers; Bacteriodales (order), Tenericutes (phylum), *Mogibacteriaceae* (family) and genus *Oscillospira, Odoribacter, Lactobacillus, Enterococcus and Lactococcus*. OTUs uniquely represented by the obese population were genus *Megamonas, Blautia, Collinsella, Eggerthella* and *Acetobacter* (Table SI- 3-1). Interestingly, based on the principal coordinates analysis (PCoA), samples O1, O2, O6 clustered separately from lean volunteers but among the obese volunteers, O7 showed a deviating composition and clustered far away from other obese patients

(Figure 3-3). Additionally, to the low alpha diversity, a high relative abundance of genus *Faecalibacterium* in comparison to the other volunteers was observed.

Genus *Lactococcus* was previously reported to be enriched in lean volunteers in comparison to obese individuals (Chavez-Carbajal et al. 2019). Furthermore, Clarke et al. (2012) reported a positive correlation between genera *Enterococcus* and *Lactobacillus* with decreasing BMI. Genus *Megamonas* and *Blautia* have been previously reported to be enriched in obese patients in comparison to lean individuals (Chavez-Carbajal et al. 2019, Chen et al. 2020, Maya-Lucas et al. 2019). Furthermore, Ozato et al. (2019) reported an association of genus *Blautia* with visceral fat accumulation in adults. Finally, Kang et al. (2014) reported a decrease of phylum Tenericutes in mice when administered a high fat diet.

With mean Firmicutes/Bacteroidetes ratios of 2.4 ($\pm$ 0.7) and 2.0 ($\pm$ 1.2) for the obese and lean population respectively, no increased ratio as reported by literature was observed (Ley et al. 2005, Ley et al. 2006, Turnbaugh et al. 2008, Turnbaugh et al. 2009). The limiting statistical power due to low number of replicates may be a possible explanation for the deviating results.
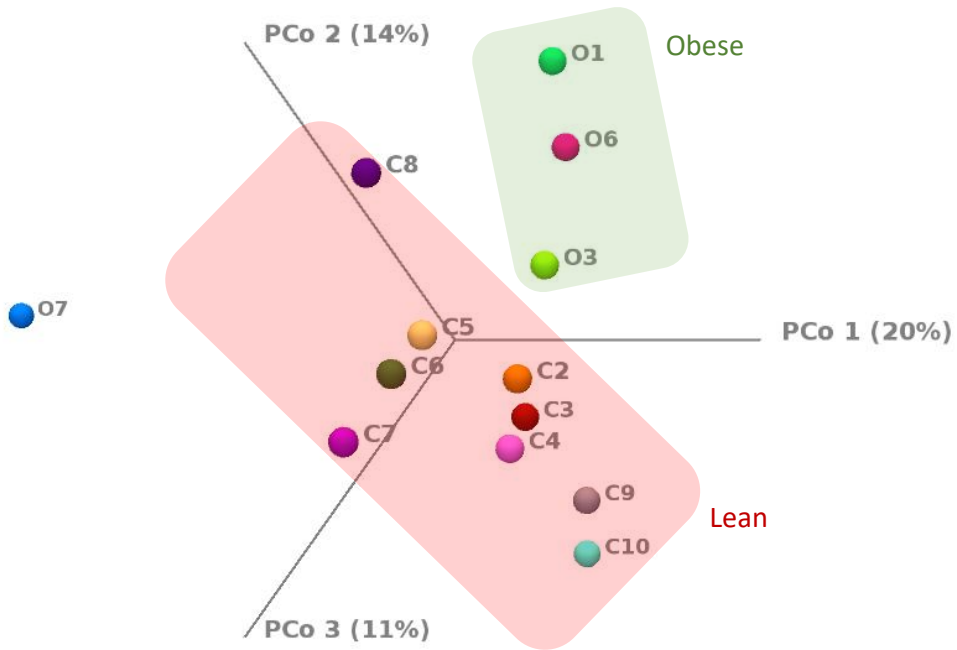
Figure 3-3: Principal coordinates analysis (PCoA) of all fecal slurry samples based on the calculated Bray-Curtis score. Red square includes the healthy volunteers. Green square includes the obese patients with exception of O7.

3.4.2 The microbiotic biotransformation of chlorogenic acid: lean versus obese population

3.4.2.1 Differences in number of identified biotransformation products

A total of 24 biotransformation products were identified in both experiments (Table 3-3). Table 3-4 summarizes the presence or absence of the different biotransformation products at the different time points in the GIDM-Colon for the lean and obese populations. 23 biotransformation products were detected in the lean population, while 13 biotransformation products were detected in the obese GIDM-Colon experiments. Dihydrocyclohexane carboxylic acid was the unique biotransformation product detected in the obese population. The 11 unique biotransformation products identified in the lean population were 1-caffeoylglycerol, 4-ethylcatechol, dihydrochlorogenic acid, hydroxycoumaroylquinic acid, hydroxydihydrocaffeoylquinic acid, M7, M8, M9, M18, M20 and M23 (full names can be found in Table 3-3).

3.4.2.2 Differences in biotransformation rate

3.4.2.2.1 Faster formation of biotransformation product in lean population

Figure 3-6 presents the number of identified biotransformation products at the different dialysis time points for the lean and obese population respectively. From 4 h dialysis on, differences in number of identified biotransformation products were observed between the populations that increased over time (Figure 3-6). The microbial biotransformation pathways for the lean and obese population from 0 h to 6 h colonic dialysis are represented in Figure SI- 3-3 and Figure SI- 3-4 respectively. The divergent results at 4 h colonic dialysis were caused by the presence of 1-caffeoylglycerol in the lean population, which is one of the unique biotransformation products for this population. Both M2 and trihydroxycyclohexane carboxylic acid were detected starting from 6 h dialysis in the lean GIDM-Colon samples, while they were only present after 24 h in the obese replicate (Table 3-4, Figure SI- 3-5, Figure SI- 3-6).

Figure 3-4: Biotransformation pathway of chlorogenic acid in the lean population at 24 h of colonic dialysis. Biotransformation products for which no structure was found could not be included. Structures highlighted in green represent unique biotransformation products for the lean population samples. The red cross indicates biotransformation products no longer present in the 24 h lean replicates. Dotted line indicates the presence of intermediate steps. [A] Quinic acid may be formed by multiple precursor structures containing the quinic acid moiety. For reasons of clarity, only the pathway from chlorogenic acid is shown. [B] Proposed structure of M7 based on the structural formula and presence of M5 and M2. [C] M20 could correspond to dihydroferulic acid, however, identification was not conclusive based on the MS/MS spectra.

Figure 3-5: Biotransformation pathway of chlorogenic acid in the obese population at 24 h of colonic dialysis. Structure highlighted in green represents the unique biotransformation products for the obese population samples. Dotted line indicates the presence of intermediate steps.
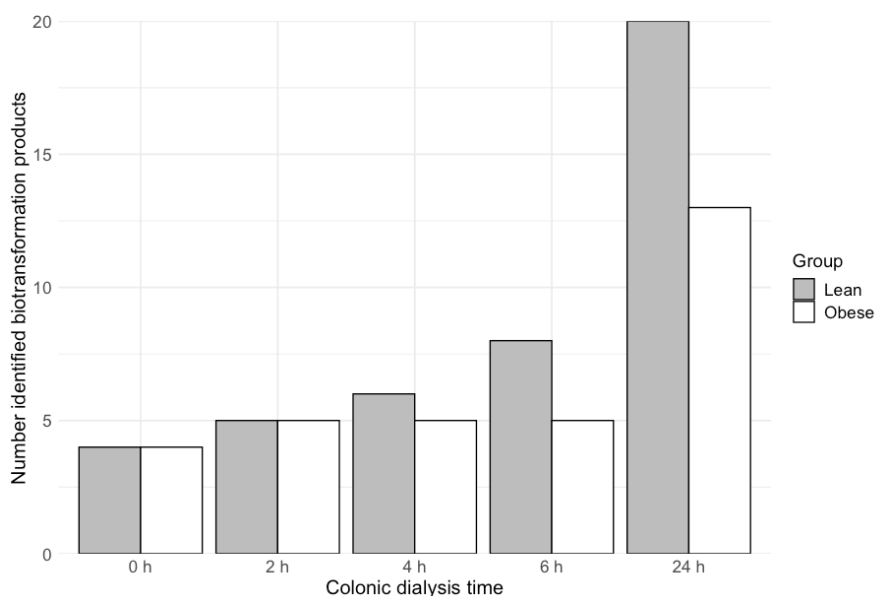
Figure 3-6: Comparison of the number of identified biotransformation products over colonic dialysis time between the lean (grey) and obese (white) GIDM-Colon experiment.

3.4.2.2.2   Chlorogenic acid

Isomerization of 5-CQA to isomers 3-CQA and 4-CQA ([M - H]⁻, *m/z* 353.0863), occurred in the small intestinal phase. Identification of the isomers was based on the injection of an analytical reference standard (5-CQA) and MS/MS spectra as described by Wianowska and Gil (2018) (Figure SI- 3-1). The chlorogenic acid isomers were no longer detected after 24 h dialysis in the lean population experiment, while all 3 isomers were still present in the obese 24 h replicates confirming less microbiotic biotransformation of chlorogenic acid in the obese population (Figure SI- 3-2-B,C).

The proposed biotransformation pathways of chlorogenic acid in the lean and obese population are presented in Figure 3-4 and Figure 3-5 respectively.

3.4.2.2.3 Caffeic acid pathway

Caffeic acid showed an increase in relative area over the first 6 h of dialysis in the lean population samples (Figure 3-7-A). The increase in signal of caffeic acid in the obese samples was not clear and remained stable after 2 h of dialysis. Caffeic acid was further metabolized into 1-caffeoylglycerol and dihydrocaffeic acid, which in turn gave rise to the formation of 3-phenyllactic acid and 4-ethylcatechol for the lean population. The biotransformation rate observed for the obese population appeared to be lower as caffeic acid was still detected in the obese 24 h samples. The signal of dihydrocaffeic acid in the obese samples (0.012 ± 0.001) was negligible in comparison to the signal in the lean 24 h replicates (4.7 ± 1.4) and a similar result was observed for 3-phenyllactic acid (Figure 3-8-A,C). Furthermore, 1-caffeoylglycerol and 4-ethylcatechol were not detected in the obese replicates.

3.4.2.2.4 Feruoylquinic acid pathway

Feruoylquinic acid was the precursor of ferulic acid. Similar to caffeic acid, an increase in relative area over the first 6 h of dialysis was observed in the lean population samples, while the same trend was not observed for the obese samples (Figure 3-7-B). The relative area of feruoylquinic acid (Figure 3-7-E) was stable over 6 h of dialysis in the obese population, with a slight drop in signal after 24 h dialysis. Lower relative areas of feruoylquinic acid were detected in the lean population samples starting from 2 h dialysis in comparison to the obese population. Given the higher relative areas of ferulic acid in the lean samples, a more pronounced formation of ferulic acid could lead to the lower signals of feruoylquinic acid.

Both feruoylquinic acid and ferulic acid were no longer detected in the lean 24 h samples. Successive biotransformation of ferulic acid to M20 is reasonable explanation, but for which no definite proof has been found. Biotransformation product M20, with structural formula $C_{10}H_{12}O_4$, could correspond to dihydroferulic acid. The identification was not conclusively based on the MS/MS spectra. The

detected product ion *m/z* 121.0291 [$C_7H_5O_2$]⁻ corresponded to the hydroxy-methoxyphenyl moiety. However, the major product ion according to the spectra of the MassBank of North America (MoNA), *m/z* 136.0452 [$C_8H_8O_2$]⁻ was not present in the acquired MS/MS spectra.

3.4.2.2.5 Quinic acid pathway

For both quinic acid and M5, an increase in relative area over colonic dialysis time was observed in the obese population while the signal declined after 4 h of dialysis in the lean GIDM-Colon samples (Figure 3-7-C,D). This decline in signal of quinic acid and M5 can be explained by the formation of trihydroxycyclohexane carboxylic acid and M2 respectively at 6 h of colonic dialysis (Figure SI- 3-3) in the lean population. The lower biotransformation rate of the obese gut microbiome was once more confirmed by the pathway resulting from quinic acid as precursor: (i) relative areas of M2, trihydroxycyclohexane carboxylic acid and hydroxybenzaldehyde were clearly higher in the lean replicates (Figure 3-8-B,D,E), (ii) in comparison to the obese 24 h samples, M5 was no longer detected in the lean replicates (Figure 3-4) and (iii) M7 was only detected in the lean replicates (Figure 3-4).
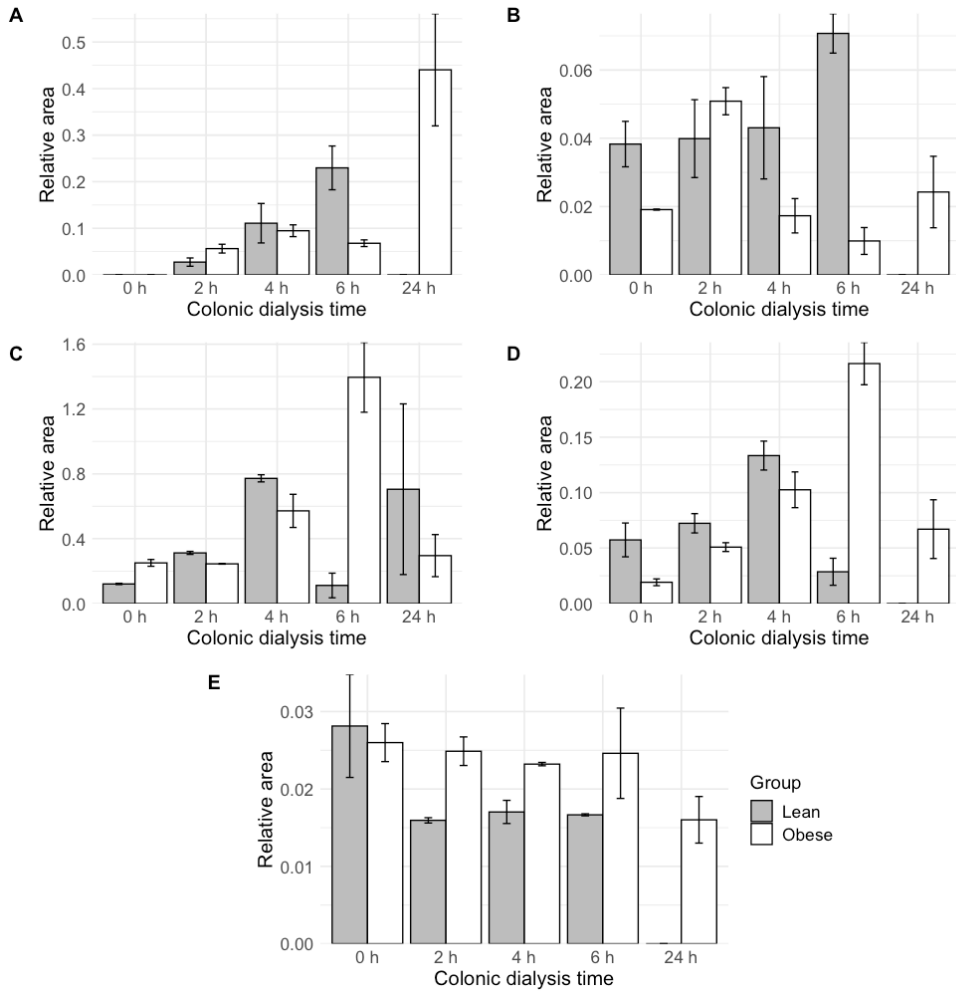
Figure 3-7: The relative area of biotransformation products caffeic acid (A), ferulic acid (B), quinic acid (C), M5 (D) and feruoylquinic acid (E), in the lean (grey) and obese (white) population, plotted against colonic dialysis time.
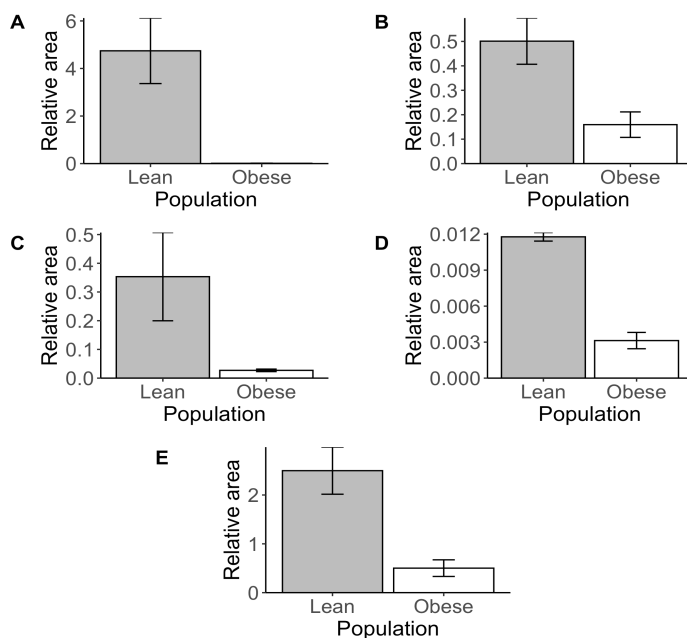
Figure 3-8: Relative areas of dihydrocaffeic acid (A), M2 (B), 3-phenyllactic acid (C), hydroxybenzaldehyde (D) and trihydroxycylcohexane carboxylic acid (E) in the 24 h replicates of the lean (grey) and obese (white) GIDM-Colon experiment respectively.

3.4.2.2.6   M17

Although M17 was detected in the 24 h replicates of both the lean and obese population samples, differences were observed between the two groups. Concerning M17, two peaks were present in the EIC of $C_{16}H_{18}O_8$ (*m/z* 337.0923) for both populations. The peak at 18.6 min corresponded to M17, while the peak at 20.9 min was identified as coumaroylquinic acid based on the MS/MS spectrum (Figure SI- 3-7-A,B,E). Coumaroylquinic acid was however present in the negative control sample meaning it may not be interpretated as a microbial biotransformation product (Figure SI- 3-7-C). The signal of coumaroylquinic acid in the obese 24 h samples was similar to the negative control sample. The signal in the lean 24 h replicates was clearly lower in comparison to the negative control, suggesting further biotransformation of coumaroylquinic acid (Figure SI- 3-7-A,B,C). The peak at 18.6 min (M17) was not identified as coumaroylquinic acid based on the absence of product ion *m/z* 191.0567

and the presence of *m/z* 179.0336. Product ion *m/z* 179.0336 corresponds to the caffeic acid fragment suggesting the loss of a hydroxylgroup on the quinic acid moiety in comparison to chlorogenic acid (Figure 3-4, Figure SI- 3-7-D).

3.4.2.3   Association with health-promoting effects of chlorogenic acid in lean and obese patients

Multiple studies have proposed possible mode of actions for the health-promoting effects of chlorogenic acid such as scavenging of reactive oxygen species (ROS) and inhibition of hepatic peroxisome proliferators'-activated receptor γ (PPARγ), causing a lower expression of inflammation and reduced uptake of fatty acids in the liver respectively (Naveed et al. 2018). As chlorogenic acid is less subjected to microbiotic biotransformation by the obese gut microbiome, a larger fraction of the parent compound is available for absorption resulting in increased systemic chlorogenic acid concentrations in the obese in comparison to the lean population. This could possible lead to enhanced health-promoting effects in the obese patients, however, further research is needed as microbial biotransformation products of chlorogenic acid, enhanced in the lean population, may also possess biological effects. Our findings however present a promising basis for further research on personalized medicine.

3.4.2.4   Comparison to the literature

Based on the results discussed above, a clearly lower biotransformation rate of chlorogenic acid by the obese gut microbiome was observed in comparison to a lean population. This is in disagreement with the proposed highly efficient metabolic pathways of the obese microbiota in extracting energy from food (Ley et al. 2005, Ley et al. 2006, Turnbaugh et al. 2008, Turnbaugh et al. 2009). Aguirre et al (2016) observed deviating fermentation kinetics of arabinogalactan and inulin in terms of short chain fatty acid (SCFA) production between an obese and lean population suggesting the metabolic activity of the gut microbiome may be substrate-dependent, which may explain the results obtained for chlorogenic acid.

A similar study has been conducted by Zhou et al. (2017) on the microbiotic biotransformation of saponins present in *Siraitia fructus* by the gut microbiome of type 2 diabetic (T2D) and non-diabetic patients. This study reported a higher number of identified biotransformation products for the T2D population in comparison to the non-diabetic population. Furthermore, oxidation and isomerization biotransformation reactions were more pronounced in the T2D population (Zhou et al. 2017). This study confirmed interpopulation differences in microbiotic biotransformation of xenobiotics which is in agreement with the reported findings in this chapter.

3.4.2.5   *Limitations of the study*

There are some limitations to the presented study that have to be pointed out. Firstly, this study included a limited number of lean (n=9) and obese patients (n=4). Including a higher number of donors in the fecal suspension pools of both populations will result in a more representative microbiota for the whole lean or obese population (Aguirre et al. 2014). Secondly, GIDM-Colon samples were analyzed by LC-Q-TOF-MS. The high resolution of the applied analysis aids in the identification, however, it does not provide quantitative data on the detected biotransformation products. Analyzing the samples by liquid chromatography coupled to triple quadrupole mass spectrometry (LC-MS/MS) would provide absolute concentrations of the identified biotransformation products which could supply additional information on biotransformation trends and timing differences and aid in improving the knowledge on the microbiotic biotransformation pathway of chlorogenic acid. The conclusions on differences in biotransformation trends based on relative areas should be interpretated with caution as the LC-Q-TOF-MS dynamic linear range, the range over which the ion signal has a linear trend with analyte concentration, is reported to be less compared to LC-MS/MS (Allen and McWhinney 2019).

Table 3-3: Overview of identified biotransformation products and additional information: metabolite ID, compound name, molecular formula, level of confirmation as proposed by Schymanski et al. (Figure SI-2-4) (Schymanski et al. 2014), retention time, exact mass, detected parent ion, mass difference. Level 1 (L1): Structure confirmed by analytical reference standard; level 2a (L2a): Probable structure by library spectrum match; level 3 (L3): tentative candidates based on experimental data; level 4 (L4): Unequivocal molecular formula based on MS1 and isotope ratios. NA: not acquired. A: Confirmed using mzCloud.org. B: Confirmed based on Kang et al. (Kang et al. 2016)

ID	Compound name	Molecular formula	Level of confirmation	t_r (min)	Exact mass (g/mol)	Parent ion (m/z)	Δ Mass (ppm)	MS/MS product ions
M1	Trihydroxycyclohexane carboxylic acid	C7H12O5	L3	1.1	176.0685	175.0611	-0.71	157.0493 [C7H9O4]-; 113.0609 [C6H9O2]-; 95.0493 [C6H7O]-; 73.0297 [C3H5O2]-; 44.9992 [CHO2]-
M2	3-[(carboxyethynyl)oxy]-1,4-dihydroxycyclohexane-1-carboxylic acid	C10H12O7	L3	1.1	244.0599	243.0474	6.45	175.0601 [C7H11O5]-; 95.0494 [C6H7O]-; 44.9978 [CHO2]-
M3	Quinic acid	C7H12O6	L1	1.1	192.0635	191.0560	-0.94	85.0297 [C4H5O2]-; 73.0271 [C3H5O2]-; 59.0157 [C2H3O2]-
M4	Dihydroxycyclohexane carboxylic acid	C7H12O4	L3	1.6	160.0733	159.0661	-6.16	113.0594 [C6H9O2]-
M5	3-[(carboxyethynyl)oxy]-1,4,5-trihydroxycyclohexane-1-carboxylic acid	C10H12O8	L3	1.1	260.0516	259.0456	-1.46	191.0583 [C7H11O6]-; 173.0427 [C7H9O5]-; 127.0424 [C6H7O3]-; 111.0222 [C6H7O2]-

Table 3-3 (continued)

ID	Compound name	Molecular formula	Level of confirmation*	t_r (min)	Exact mass (g/mol)	Parent ion (m/z)	Δ Mass (ppm)	MS/MS product ions
M6	NA	C12H16O9	L4	1.1	304.078	303.0752	-1.84	191.0556 [C7H11O6]-; 135.0848 [C9H11O]-; 111.0449 [C6H7O2]-; 109.0260 [C6H5O2]-; 89.0141 [C3H5O3]-; 85.0311 [C4H5O2]-; 60.9936 [CHO3]-
M7	NA	C10H12O6	L4	9.6	228.0617	227.0564	0.5	NA
M8	Methyl 3-((3-(3,4-dihydroxyphenyl)propanoyl)oxy}-4-hydroxy-5-methoxycyclohexa-1,5-diene-1-carboxylate	C18H20O8	L3	9.6	364.115	363.1082	-0.85	181.0496 [C9H9O4]-; 137.0596 [C8H9O2]-; 121.0289 [C7H5O2]-; 59.0151 [C2H3O2]-
M9	6-(3-(3,4-dihydroxyphenyl)-1-hydroxypropoxy)cyclohexane-1,2,4-triol	C15H22O7	L3	9.6	314.1352	313.1299	2.13	181.0496 [C9H9O4]-; 135.0442 [C8H7O2]-; 131.0704 [C6H11O3]-; 107.0490 [C7H7O]-
M10	Dihydrocaffeic acid	C9H10O4	L1	9.6	182.0579	181.0508	0.48	137.0593 [C8H9O2]-; 121.0286 [C7H5O2]-; 119.0465 [C8H7O]-; 109.0287 [C6H5O2]-; 59.0138 [C2H3O2]-

Table 3-3 (continued)

ID	Compound name	Molecular formula	Level of confirmation*	t_r (min)	Exact mass (g/mol)	Parent ion (*m/z*)	Δ Mass (ppm)	MS/MS product ions
M11	Hydroxybenzaldehyde	C7H6O2	L2aᴬ	11	122.0367	121.0304	8.94	93.0310 [C6H5O]-
M12	Caffeic acid	C9H8O4	L1	13.5	180.0414	179.035	-0.55	135.0431 [C8H7O2]-; 117.0353 [C8H5O]-; 91.0000 [C6H3O]-; 44.9992 [CHO2]-
M13	Hydroxycoumaroylquinic acid	C16H18O9	L3	14.6	354.095	353.0866	7.38	191.0561 [C7H11O6]-; 173.0455 [C7H9O5]-; 93.0351 [C6H5O]-
M14	Dihydrochlorogenic acid	C16H20O9	L3	14.6	356.1094	355.1019	-4.19	191.0540 [C7H11O6]-; 173.0446 [C7H9O5]-; 137.0630 [C8H9O2]-
M15	Hydroxydihydrocaffeoylquinic acid	C16H20O10	L3	14.6	372.1045	371.098	-0.91	353.0867 [C16H17O9]-; 191.0556 [C7H11O6]-
M16	3-Phenyllactic acid	C9H10O3	L2aᴬ	14.9	166.0628	165.0554	-1.68	147.0415 [C9H7O2]-; 119.0472 [C8H7O]-; 103.0533 [C8H7]-; 91.0547 [C7H7]-; 72.9901 [C2HO3]-; 44.9972 [CHO2]-
M17	methyl 3-((3-(3,4-dihydroxyphenyl)propanoy))oxy}-4-hydroxy-5-methoxycyclohexa-1,5-diene-1-carboxylate	C16H18O8	L3	18.6	338.1002	337.0923	-1.85	179.0336 [C9H7O4]-; 161.0267 [C9HO3]-; 135.0435 [C8H7O2]-

Table 3-3 (continued)

ID	Compound name	Molecular formula	Level of confirmation*	t_r (min)	Exact mass (g/mol)	Parent ion (*m/z*)	Δ Mass (ppm)	MS/MS product ions
M18	3-((3-(3,4-dihydroxyphenyl)propanoyl)oxy}-1,4-dihydroxycyclohexane-1-carboxylic acid	C16H20O8	L3	18.6	340.1158	339.1077	-3.57	181.0490 [C9H9O4]-; 157.0487 [C7H9O4]-; 137.0602 [C8H9O2]-
M19	1-Caffeoylglycerol	C12H14O6	L2a[B]	18.7	254.0791	253.0717	-0.08	179.0328 [C9H7O4]-; 161.0236 [C9H5O3]-; 135.0443 [C8H7O2]-; 133.0298 [C8H5O2]-
M20	NA	C10H12O4	L4	20.7	196.0729	195.0658	-3.15	160.8407; 121.0291 [C7H5O2]-
M21	4-ethyl-catechol	C8H10O2	L3	20.5	138.0679	137.0600	-5.4	122.0374 [C7H6O2]-
M22	Feruoylquinic acid	C17H20O9	L3	21.7	368.1107	367.102	-2.84	191.0585 [C7H11O6]-; 179.0344 [C9H7O4]-; 161.0276 [C9H5O3]-; 135.0458 [C8H7O2]-
M23	NA	C12H14O5	L4	22	238.0838	237.0765	-0.47	179.0340 [C9H7O4]-; 161.0231 [C9H5O3]-; 135.0441 [C8H7O2]-
M24	Ferulic acid	C10H10O4	L1	22.3	194.058	193.0505	-0.19	178,0270 [C9H6O4]-; 161,0273 [C9H5O3]-; 134,0373 [C8H6O2]-; 133,0292 [C8H5O2]-
Parent	Chlorogenic acid	C16H18O9	L1	17.1	354.095	353.0863	-4.38	191.0546 [C7H11O6]-; 173.0451 [C7H9O5]-; 161.0214 [C9H5O3]-; 135.0413 [C8H7O2]-

Table 3-4: Overview of the presence (green) or absence (orange) of the identified biotransformation products in the lean (L) or obese (O) GIDM-Colon experiments at the different sampling time-points.

Biotransformation product	Population	Stomach	Small int.	Colon 0 h	Colon 2 h	Colon 4 h	Colon 6 h	Colon 24 h
3-phenyllactic acid	L	orange	orange	orange	orange	orange	orange	green
	O	orange	orange	orange	orange	orange	orange	green
4-ethylcatechol	L	orange	orange	orange	orange	orange	orange	green
	O	orange	orange	orange	orange	orange	orange	orange
Chlorogenic acid	L	green	green	green	green	green	green	orange
	O	green	green	green	green	green	green	green
Caffeic acid	L	orange	orange	orange	green	green	green	orange
	O	orange	orange	orange	green	green	green	green
Caffeoylglycerol	L	orange	orange	orange	orange	green	green	green
	O	orange	orange	orange	orange	green	green	green
Dihydrocaffeic acid	L	orange	orange	orange	orange	orange	orange	green
	O	orange	orange	orange	orange	orange	orange	green
Dihydrochlorogenic acid	L	orange	orange	orange	orange	orange	orange	green
	O	orange	orange	orange	orange	orange	orange	green
Dihydrocyclohexane carboxylic acid	L	orange	orange	orange	orange	orange	orange	orange
	O	orange	orange	orange	orange	orange	orange	green

Table-3-4 (continued)

Biotransformation product	Population	Stomach	Small int.	Colon 0 h	Colon 2 h	Colon 4 h	Colon 6 h	Colon 24 h
Feruoylquinic acid	L							
	O							
Ferulic acid	L							
	O							
Hydroxybenzaldehyde	L							
	O							
Hydroxycoumaroylquinic acid	L							
	O							
Hydroxydihydrocaffeoylquinic acid	L							
	O							
M2	L							
	O							
M5	L							
	O							
M6	L							
	O							

Table-3-4 (continued)

Biotransformation product	Population	Stomach	Small int.	Colon 0 h	Colon 2 h	Colon 4 h	Colon 6 h	Colon 24 h
M7	L							
	O							
M8	L							
	O							
M9	L							
	O							
M18	L							
	O							
M19	L							
	O							
M20	L							
	O							
M23	L							
	O							
Quinic acid	L							
	O							
Trihydroxycyclo carboxylic acid	L							
	O							

3.5 Conclusions

Differences in gut microbiome composition, bacterial diversity and bacterial concentration were observed between the obese and lean samples. Unique OTUs were identified for both populations. The previously reported increased Firmicutes/Bacteroidetes ratio was not observed. Lower bacterial concentrations were observed for the obese population in comparison to the lean population samples.

Clear differences in microbial biotransformation of chlorogenic acid between a lean and obese population were observed. 23 and 13 biotransformation products were identified in the samples of the lean and obese GIDM-Colon experiment respectively. 11 biotransformation products were unique for the lean population, while only 1 biotransformation product was unique for the obese samples. Furthermore, a clearly higher metabolic activity of the lean gut microbiome was observed. The reported differences in biotransformation between the populations provide new research opportunities for other scientific fields and perspectives such as drug development and pharmacokinetic studies.

3.6   Supplementary information

Table SI- 3-1:Unique operational taxonomic units (OTUs) in the lean (n=9) and obese (n=4) population. LDA: Linear discriminant analysis.

Population	Taxonomy	LDA-score	p-value
Lean	*Lactococcus* (Genus)	2.2	0.043
	Lactobacillus (Genus)	3.0	0.024
	Enterococcus (Genus)	2.7	0.012
	Odoribacter (Genus)	3.3	0.021
	Oschillospira (Genus)	3.5	0.021
	Mogibacteriaceae (Family)	2.9	0.013
	Bacteroidales (Order)	3.3	0.044
	Tenericutes (Phylum)	3.0	0.024
Obese	*Blautia* (Genus)	4.4	0.013
	Megamonas (Genus)	3.0	0.011
	Collinsella (Genus)	3.4	0.034
	Acetobacter (Genus)	2.9	0.001
	Eggerthella (Genus)	2.3	0.032
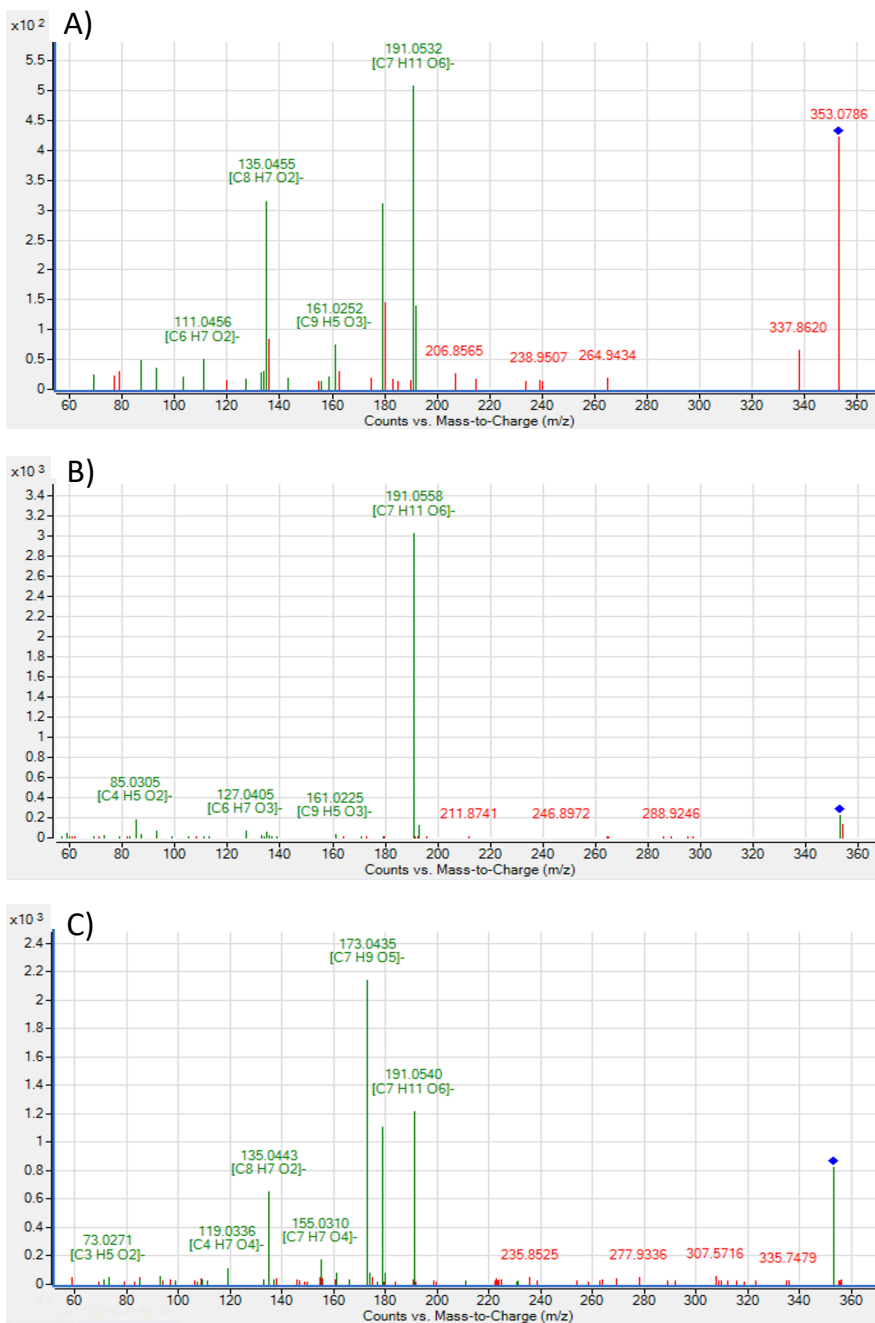
Figure SI- 3-1: MS/MS spectra of 3-caffeoylquinic acid (A), 5-caffeoylquinic acid (B) and 4-caffeoylquinic acid (C) in accordance with Wianowska and Gil. (Wianowska and Gil 2018)

Identification of chlorogenic acid isomers

Identification of the individual caffeoylquinic acid isomers was confirmed based on the identification scheme proposed by Wianowska and Gil (2018). Confirmation of 3-CQA was based on the main product ion m/z 191.0582 and m/z 179.0336 as secondary product ion (relative abundance $\pm$ 50 %). 4-CQA was identified based on the primary product ion m/z 173.0345. The presence of product ion m/z 191.0558 and the absence of product ion m/z 179.0336 is confirmative for the identification of 5-CQA.

Hydroxycoumaroylquinic acid

An additional isomer, hydroxycoumaroylquinic acid ([M - H]$^-$, m/z 353.0866), was only detected in the lean population samples after 24 h dialysis (Figure SI- 3-2-B). The main product ion was m/z 191.0561 which corresponded to the quinic acid moiety. Product ion m/z 173.0455 corresponded to the quinic acid moiety with loss of H_2O. Finally, product ion m/z 93.0351 corresponded to a hydroxylated benzene ring.
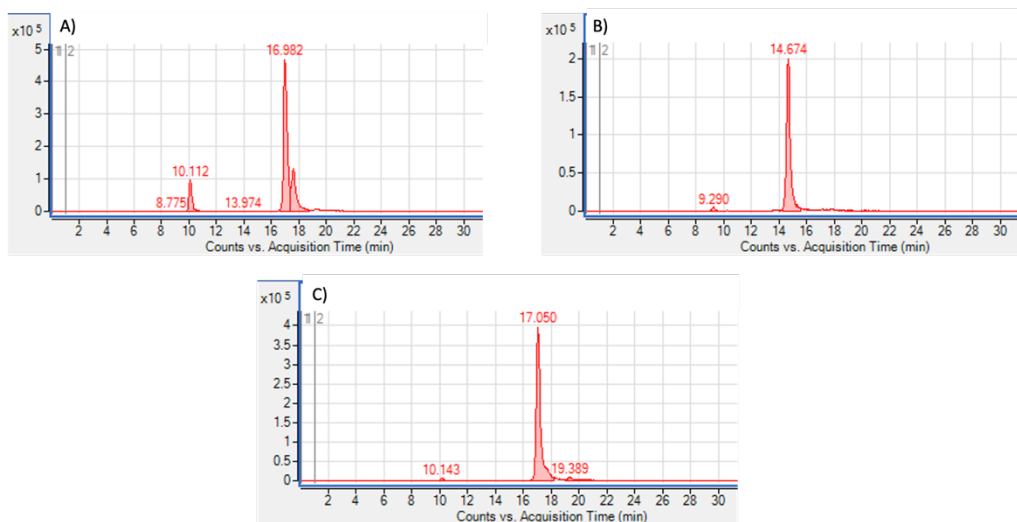
Figure SI- 3-2: Extracted ion chromatogram (EIC) of m/z 353.0878 ($C_{16}H_{17}O_9^-$, [M - H]$^-$) which presents the number of counts of the extracted ion over acquisition time (min). The three chlorogenic acid isomers (3-CQA, 4-CQA and 5-CQA) were identified in the negative control sample (A) and the 24 h obese replicates (C). 3-CQA, 4-CQA and 5-CQA were no longer detected in the 24 h lean population replicate (B). Hydroxycoumaroylquinic acid (RT = 14.7 min) was only detected in the 24h lean samples.
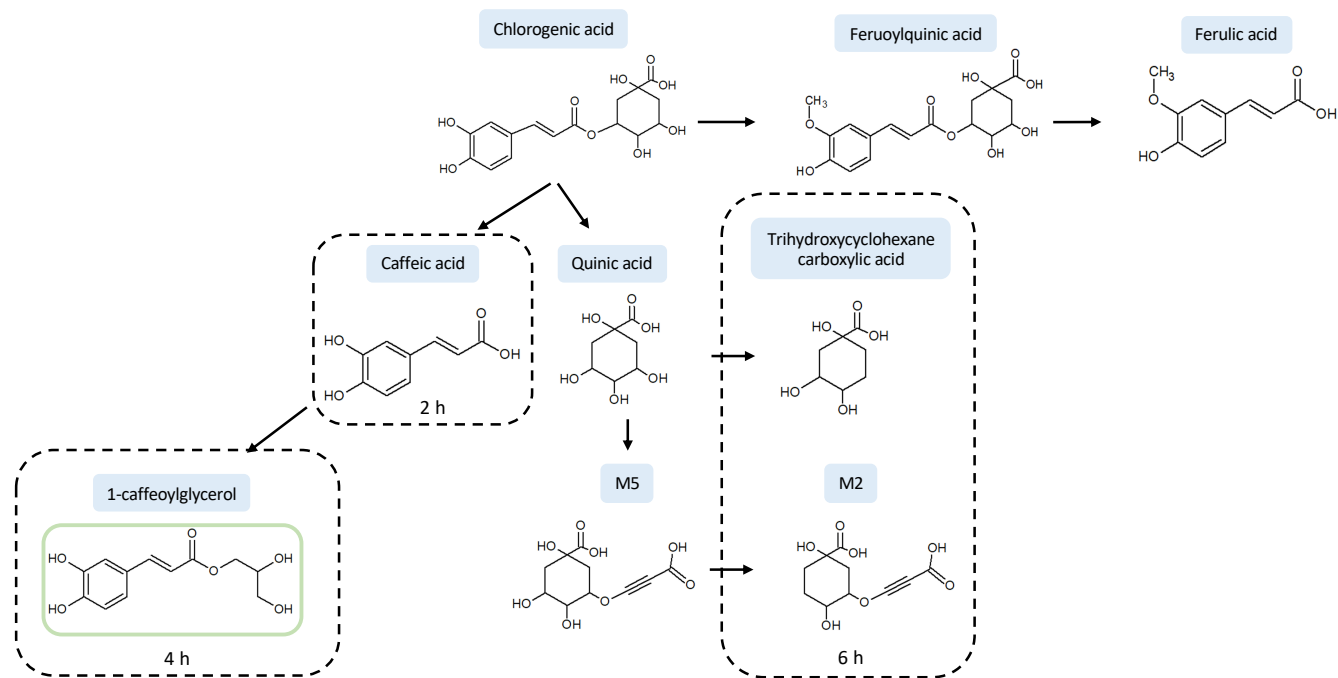
Figure SI- 3-3:Microbial biotransformation pathway of chlorogenic acid in the **lean** population samples from 0 h to 6 h colonic dialysis. Structures highlighted in green represent unique biotransformation products for the lean population samples. The dotted line indicates the time of formation of the biotransformation products. Structures not marked were present at the start of colonic dialysis.
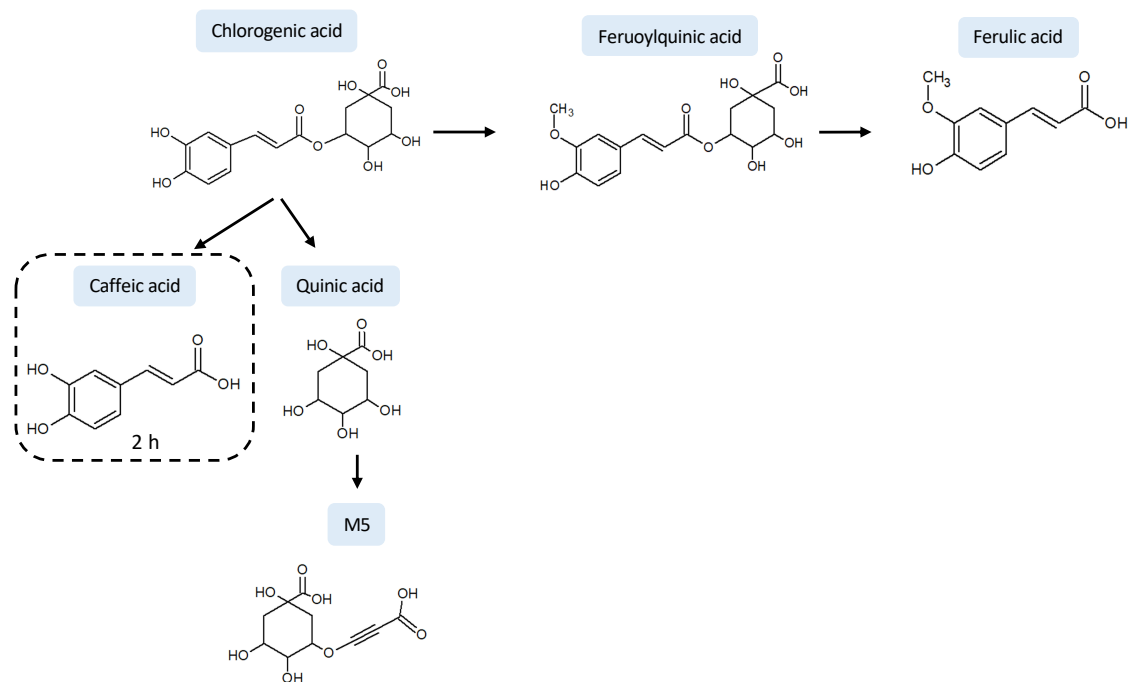
Figure SI- 3-4: Microbial biotransformation pathway of chlorogenic acid in the **obese** population samples from 0 h to 6 h of colonic dialysis. The dotted line indicates the time of formation of the biotransformation products. Structures not marked were present at the start of colonic dialysis.
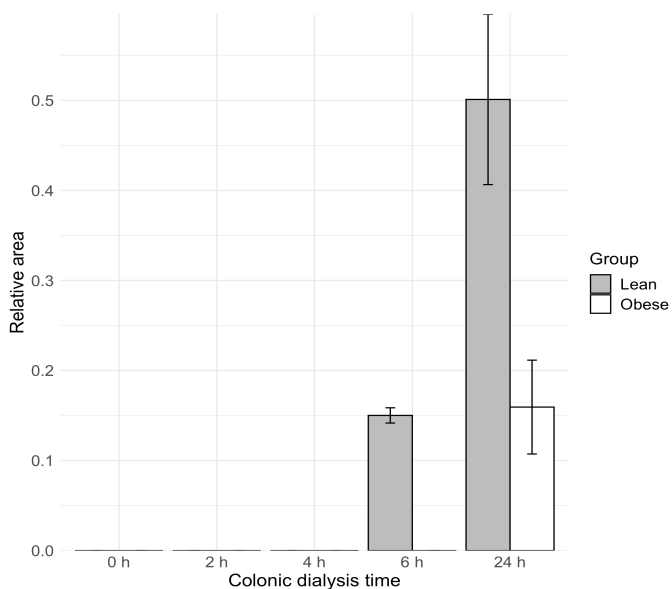
Figure SI- 3-5: Relative area of M2 over colonic dialysis time in the lean (grey) or obese (white) GIDM-Colon samples
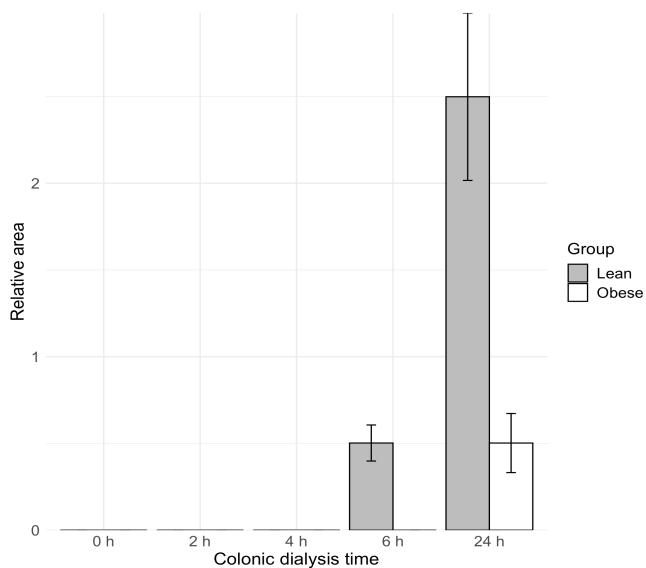
Figure SI- 3-6: Relative area of trihydroxycyclohexane carboxylic acid over colonic dialysis time in the lean (grey) or obese (white) GIDM-Colon samples
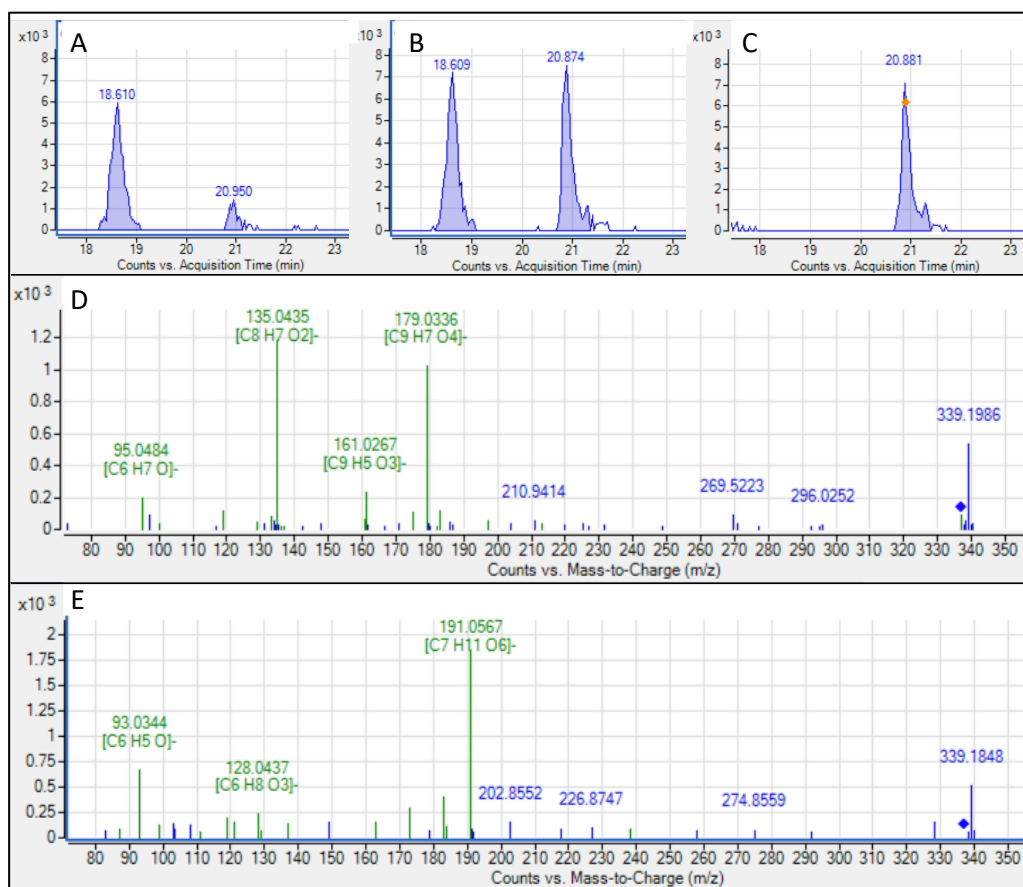
Figure SI- 3-7: The extracted ion chromatogram (EIC) of $C_{16}H_{18}O_9$ in the 24 h retentate replicates of the lean (A) and obese (B) GIDM-Colon experiment. C: EIC of $C_{16}H_{18}O_9$ in the negative control 24 h retentate sample. D and E correspond to the MS/MS spectra of the peak at 18.6 and 20.9 min respectively.

CHAPTER 3

References

Aguirre M, Bussolo de Souza C and Venema K. The Gut Microbiota from Lean and Obese Subjects Contribute Differently to the Fermentation of Arabinogalactan and Inulin. *PLoS One* 2016, 11(7): e0159236.

Aguirre M, Ramiro-Garcia J, Koenen ME and Venema K. To pool or not to pool? Impact of the use of individual and pooled fecal samples for in vitro fermentation studies. *Journal of Microbiological Methods* 2014, 107: 1-7.

Allen DR and McWhinney BC. Quadrupole Time-of-Flight Mass Spectrometry: A Paradigm Shift in Toxicology Screening Applications. *The Clinical biochemist. Reviews* 2019, 40(3): 135-146.

Bäckhed F, Ding H, Wang T, Hooper LV, Koh GY, Nagy A, Semenkovich CF and Gordon JI. The gut microbiota as an environmental factor that regulates fat storage. *Proceedings of the National Academy of Sciences of the United States of America* 2004, 101(44): 15718.

Borody TJ, Paramsothy S and Agrawal G. Fecal microbiota transplantation: indications, methods, evidence, and future directions. *Current gastroenterology reports* 2013, 15(8): 337-337.

Chavez-Carbajal A, Nirmalkar K, Perez-Lizaur A, Hernandez-Quiroz F, Ramirez-Del-Alto S, Garcia-Mena J and Hernandez-Guerrero C. Gut Microbiota and Predicted Metabolic Pathways in a Sample of Mexican Women Affected by Obesity and Obesity Plus Metabolic Syndrome. *International Journal of Molecular Sciences* 2019, 20(2).

Chen X, Sun H, Jiang F, Shen Y, Li X, Hu X, Shen X and Wei P. Alteration of the gut microbiota associated with childhood obesity by 16S rRNA gene sequencing. *PeerJ* 2020, 8: e8317.

Clarke SF, Murphy EF, Nilaweera K, Ross PR, Shanahan F, O'Toole PW and Cotter PD. The gut microbiota and its relationship to diet and obesity: new insights. *Gut Microbes* 2012, 3(3): 186-202.

Duncan SH, Lobley GE, Holtrop G, Ince J, Johnstone AM, Louis P and Flint HJ. Human colonic microbiota associated with diet, obesity and weight loss. *International Journal of Obesity* 2008, 32(11): 1720-1724.

Kang SS, Jeraldo PR, Kurti A, Miller MEB, Cook MD, Whitlock K, Goldenfeld N, Woods JA, White BA, Chia N and Fryer JD. Diet and exercise orthogonally alter the gut microbiome and reveal independent associations with anxiety and cognition. *Molecular Neurodegeneration* 2014, 9(1): 36.

Kang J, Price WE, Ashton J, Tapsell LC and Johnson S. Identification and characterization of phenolic compounds in hydromethanolic extracts of sorghum wholegrains by LC-ESI-MSn. *Food Chemistry* 2016, 211: 215-226.

Ley RE, Bäckhed F, Turnbaugh P, Lozupone CA, Knight RD and Gordon JI. Obesity alters gut microbial ecology. *Proceedings of the National Academy of Sciences of the United States of America* 2005, 102(31): 11070.

Ley RE, Turnbaugh PJ, Klein S and Gordon JI. Human gut microbes associated with obesity. *Nature* 2006, 444(7122): 1022-1023.

Maya-Lucas O, Murugesan S, Nirmalkar K, Alcaraz LD, Hoyo-Vadillo C, Pizano-Zárate ML and García-Mena J. The gut microbiome of Mexican children affected by obesity. *Anaerobe* 2019, 55: 11-23.

Mortelé O, Iturrospe E, Breynaert A, Verdickt E, Xavier BB, Lammens C, Malhotra-Kumar S, Jorens PG, Pieters L, van Nuijs ALN and Hermans N. Optimization of an in vitro gut microbiome biotransformation platform with chlorogenic acid as model compound: From fecal sample to biotransformation product identification. *Journal of Pharmaceutical and Biomedical Analysis* 2019, 175: 112768.

Murphy EF, Cotter PD, Healy S, Marques TM, Sullivan O, Fouhy F, Clarke SF, Toole PW, Quigley EM, Stanton C, Ross PR, Doherty RM and Shanahan F. Composition and energy harvesting capacity of the gut microbiota: relationship to diet, obesity and time in mouse models. *Gut* 2010, 59(12): 1635.

Naveed M, Hejazi V, Abbas M, Kamboh AA, Khan GJ, Shumzaid M, Ahmad F, Babazadeh D, FangFang X, Modarresi-Ghazani F, WenHua L and XiaoHui Z. Chlorogenic acid (CGA): A pharmacological review and call for further research. *Biomedicine & Pharmacotherapy* 2018, 97: 67-74.

O'Hara AM and Shanahan F. The gut flora as a forgotten organ. *EMBO reports* 2006, 7(7): 688-693.

Ozato N, Saito S, Yamaguchi T, Katashima M, Tokuda I, Sawada K, Katsuragi Y, Kakuta M, Imoto S, Ihara K and Nakaji S. Blautia genus associated with visceral fat accumulation in adults 20-76 years of age. *NPJ Biofilms Microbiomes* 2019, 5(1): 28.

Schymanski EL, Jeon J, Gulde R, Fenner K, Ruff M, Singer HP and Hollender J. Identifying small molecules via high resolution mass spectrometry: communicating confidence. *Environmental Science and Technology* 2014, 48(4): 2097-2098.

Sweeney TE and Morton JM. The human gut microbiome: a review of the effect of obesity and surgically induced weight loss. *JAMA Surgery* 2013, 148(6): 563-569.

Turnbaugh PJ, Backhed F, Fulton L and Gordon JI. Diet-induced obesity is linked to marked but reversible alterations in the mouse distal gut microbiome. *Cell Host Microbe* 2008, 3(4): 213-223.

Turnbaugh PJ, Hamady M, Yatsunenko T, Cantarel BL, Duncan A, Ley RE, Sogin ML, Jones WJ, Roe BA, Affourtit JP, Egholm M, Henrissat B, Heath AC, Knight R and Gordon JI. A core gut microbiome in obese and lean twins. *Nature* 2009, 457(7228): 480-484.

WHO. (2020). "Obesity and overweight."   Retrieved August 2020, 2020, from https://www.who.int/en/news-room/fact-sheets/detail/obesity-and-overweight.

Wianowska D and Gil M. Recent advances in extraction and analysis procedures of natural chlorogenic acids. *Phytochemistry Reviews* 2018, 18(1): 273-302.

Wilson ID and Nicholson JK. Gut microbiome interactions with drug metabolism, efficacy, and toxicity. *Translational Research* 2017, 179: 204-222.

Zhang H, DiBaise JK, Zuccolo A, Kudrna D, Braidotti M, Yu Y, Parameswaran P, Crowell MD, Wing R, Rittmann BE and Krajmalnik-Brown R. Human gut microbiota in obesity and after gastric bypass. *Proceedings of the National Academy of Sciences* 2009, 106(7): 2365.

Zhou G, Peng Y, Zhao L, Wang M and Li X. Biotransformation of Total Saponins in Siraitia Fructus by Human Intestinal Microbiota of Normal and Type 2 Diabetic Patients: Comprehensive Metabolite Identification and Metabolic Profile Elucidation Using LC-Q-TOF/MS. *Journal of Agricultural and Food Chemistry* 2017, 65(8): 1518-1524.

CHAPTER 4: INVESTIGATING THE INTESTINAL ABSORPTION OF CHLOROGENIC ACID AND ONE OF ITS MAJOR MICROBIAL BIOTRANSFORMATION PRODUCTS, QUINIC ACID, USING A CACO-2 BIDIRECTIONAL PERMEABILITY ASSAY
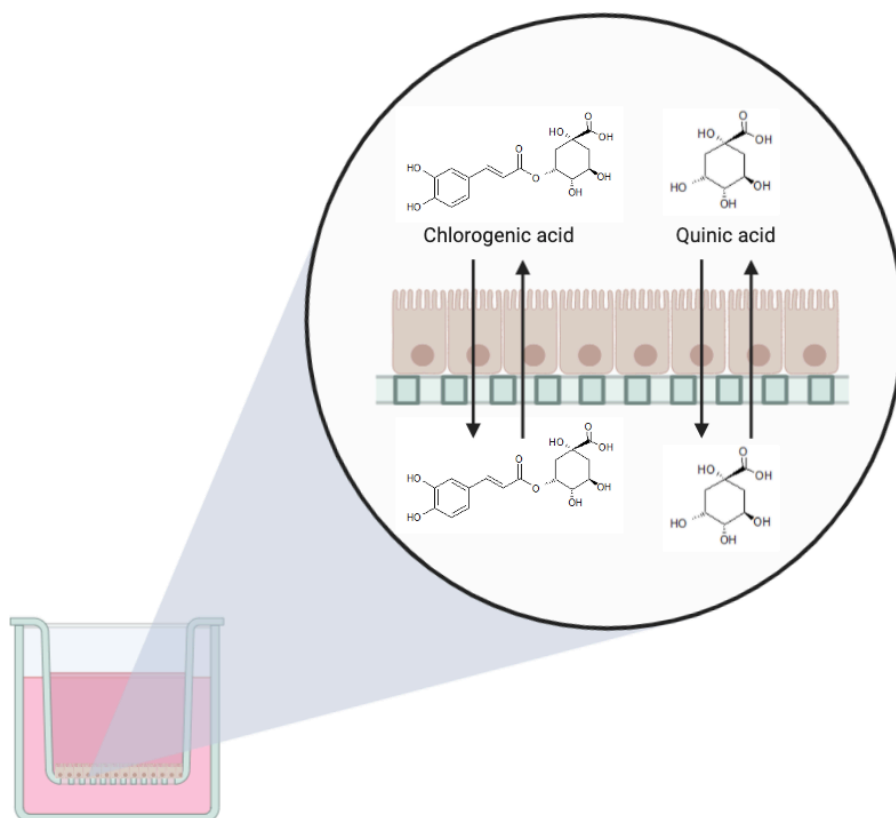
Based on following paper:

CHAPTER 4

CHAPTER 4

4.1   Introduction

Multiple *in vivo* animal studies and human clinical trials have attributed chlorogenic acid, the target compound of chapter two and three, health-promoting properties such as anti-inflammatory (dos Santos et al. 2006, Liang and Kitts 2018), antioxidative (Agudelo-Ochoa et al. 2016), antidiabetic (Hunyadi et al. 2012) and antihypertensive effects (Mubarak et al. 2012). These beneficial effects are dependent on its bioavailability, which is determined by the pharmacokinetic properties: absorption, distribution, metabolism and excretion (ADME). Our earlier results, and multiple other studies have shown that chlorogenic acid is subjected to microbiotic biotransformation in the colon, meaning that the biological properties of chlorogenic acid could be influenced by the ADME properties of the microbiotic biotransformation products (Gonthier MP 2003, Tomas-Barberan et al. 2014, Breynaert et al. 2015, Pinta et al. 2018). Quinic acid, one of the most prominent microbiotic biotransformation products of chlorogenic acid, is attributed indirect antioxidative effects as it is able to induce the antioxidant metabolism by enhancing the synthesis of tryptophan and nicotinamide in the gastrointestinal tract. Increased production of these compounds will lead to DNA repair enhancement and NF-kB inhibition (Pero et al. 2009, Pero and Lund 2011). Furthermore, neuroprotective effects on aluminum chloride-induced dementia have been described for quinic acid when administered to rats (Liu et al. 2020).

In order to have a more profound understanding of the biological properties of chlorogenic acid and to optimize formulation and dosing strategies of chlorogenic acid-containing food supplements, detailed information on the absorption of chlorogenic acid and its microbial biotransformation products is imperative. Multiple studies have investigated the *in vivo* bioavailability in humans and rats after coffee consumption (Dupas et al. 2006, Stalmach et al. 2009, Stalmach et al. 2010), oral ingestion of a green coffee extract (Farah et al. 2008) or a chlorogenic acid supplemented diet (Gonthier et al. 2003). *In vivo* bioavailability studies, however, do not provide the necessary information to make statements on the intestinal absorption of chlorogenic acid and

its microbial biotransformation products. Firstly, chlorogenic acid is susceptible to microbial biotransformation by the gut microflora leading to multiple phenolic biotransformation products and quinic acid derivatives, meaning that a low recovery of chlorogenic acid in plasma or urine cannot be necessarily linked to a low intestinal absorption. Furthermore, the measured analytes in plasma can also result from hepatic biotransformation (Gonthier et al. 2006). Secondly, instant/brewing coffee and coffee extracts, frequently used in *in vivo* studies, contain multiple chlorogenic acids including caffeoylquinic acids, dicaffeoylquinic acids, feruloylquinic acids and p-coumaroylquinic acids (Farah et al. 2008, Stalmach et al. 2009, Stalmach et al. 2010). Biotransformation of these chlorogenic acids could lead to common microbial biotransformation products and therefore to misleading conclusions on the intestinal absorption of chlorogenic acid and/or its microbial biotransformation products.

In vitro permeability studies can provide information on the absorption of chlorogenic acid and microbial biotransformation products without influence of the other pharmacokinetic ADME properties. The human intestinal epithelial Caco-2 cell-line, derived from a colorectal adenocarcinoma, is widely used to mimic the intestinal barrier *in vitro* (Lea 2015). Caco-2 cells have the ability to spontaneously differentiate towards a cell monolayer with the characteristic apical brush border with microvilli and adjacent cells with tight junctions (Lea 2015) (Figure 4-1).
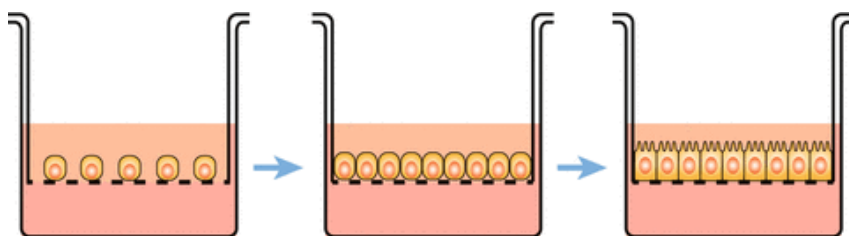
Figure 4-1: Differentiation of the Caco-2 cells on a cell culture insert. *Middle*: Caco-2 cells reach confluence after which they will start to spontaneously differentiate. *Right:* After 21 days culture period, the Caco-2 cells will appear as a cell monolayer with the characteristic apical brush border with microvilli and tight junctions with adjacent cells. From Lea (2015).

Multiple studies have shown a high correlation between Caco-2 permeability results and *in vivo* small intestinal and colonic absorption of orally ingested compounds, which makes them a suitable tool for evaluation and estimation of colonic absorption of chlorogenic acid and its microbial biotransformation products (Rubas et al. 1996, Foger et al. 2008, Tannergren et al. 2009, Obringer et al. 2016). Additionally, Caco-2 cells lack the expression of cytochrome P450 enzymes, which should prevent further biotransformation of the tested compounds during the permeability assay (Küblbeck et al. 2016). Positive control compounds should be included in the experimental setup of bidirectional Caco-2 permeability studies as between-experiments variations in P_{app} values have been reported. These variations could result from differences in cell characteristics (age, passage number, etc.), cell culture conditions and/or varying experimental conditions (Grès et al. 1998, Volpe 2008, Lea 2015, Stockdale et al. 2019).

4.2   Aims and preface

This chapter aims to expand our *in vitro* gastrointestinal platform with an *in vitro* permeability assay to study the intestinal absorption of chlorogenic acid and microbial biotransformation products. The intestinal absorption of chlorogenic acid in its native form and quinic acid, one of its most prominent intestinal biotransformation products, was investigated by an *in vitro* permeability assay using the Caco-2 cell line. Investigating the absorption of chlorogenic acid and quinic acid can aid in a more comprehensive evaluation of the health-promoting effects of chlorogenic acid and eventually a better formulation and/or dosage of chlorogenic acid-containing food supplements.

4.3   Material and methods

4.3.1   Chemicals and reagents

Chlorogenic acid (96.63 % (w/w)) was acquired from LGC standards (Teddington, United Kingdom). Ferulic acid-D$_3$, digoxin (98% (w/w) and digoxin-D$_3$ (97%) were acquired from Toronto Research Chemicals (Ontario, Canada). Quinic acid (98%), propranolol-D$_7$ (100 µg/mL in MeOH with 5% 1 M HCl), propranolol HCl (1.0 mg/mL in MeOH), ammonium acetate ($\geq$ 98%), Hank's balanced salt solution (HBSS) and MEM (Eagle's minimum essential medium) non-essential amino acid solution (100x) were obtained from Sigma-Aldrich (St Louis, MO, USA). DMEM (Dulbecco's Modified Eagle Medium; high glucose, no glutamine, no phenol red), heat-inactivated foetal calf serum (FCS), GlutaMAX^{TM} and Trypsin-EDTA (0.05%, with phenol red) were acquired from Gibco (Thermo Scientific, Massachusetts, US). PenStrep (10 000 U/mL penicillin and 10 000 µg/mL streptomycin mix) was obtained from Life Technologies (California, US). Caco-2 cells (HTB-37^{TM}) were obtained from ATCC (Rockville, MD, USA). Formic acid (98-100%, Suprapur) was purchased from Merck (Darmstadt, Germany).

Acetonitrile (ACN) and methanol (MeOH, ≥ 99.9%, LC-MS grade) were obtained from Fisher Scientific (Hampton, New Hampshire, USA). Ultrapure water (Purelab flex apparat) was acquired from ELGA Veolia (UK).

4.3.2　　　Materials

Cellstar® 12-well plates, ThinCert^{TM} Cell Culture Inserts for 12-well plates, and 75 cm^2 cell culture flasks were acquired from Greiner (Vilvoorde, Belgium). The EVE^{TM} Automatic Cell Counter was purchased from NanoEnTek (South-Korea). The centrifuge used during handling of the Caco-2 cells was acquired from Eppendorf (Type 5702, Hamburg, Germany). A Sigma 1-15PK centrifuge (sample preparation) and centrifugal filters (modified nylon membrane, 0.2 μm, 500 μL sample capacity) were obtained respectively from Sigma Laborzentrifugen GmbH (Germany) and VWR (Radnor, Pennsylvania, USA). Trans epithelial resistance (TEER) values were measured with the Voltmètre-Ohmmètre Millicell-ERS from Merck (New Jersey, US). Cells were maintained in a C150 E2 CO_2 incubator from Binder and a MaxQ Mini 4450 incubator from Thermo Scientific was used during the permeability experiment.

4.3.3　　　Cultivation of the cells

Caco-2 cells were cultured in 75 cm^2 cell culture flasks containing 20 mL DMEM supplemented with 10% FCS and 1x nonessential amino acids (hereafter referred to as supplemented DMEM medium) and maintained in a humidified 5% CO_2 incubator at 37 °C. The medium was changed every 3 days and the cells were passaged every 5-7 days at a 1:4 to 1:6 split ratio (depending on growth) using 0.05% trypsin-EDTA for detachment.

The cultivated Caco-2 cells were seeded on the ThinCerts when 70-90% confluent, between 21 and 29 days before the bidirectional transport experiment. First, the cells were rinsed with a 0.05% trypsin solution followed by an incubation of maximal 15 min (5% CO_2, 37 °C) in fresh trypsin solution to detach the cells from the cell culture flask. The reaction was stopped by the addition of 10 mL supplemented DMEM medium. The content of the flask was transferred to a Falcon tube and cells were pelleted by centrifugation (7 min, 300 relative centrifugal force (rcf)). The pellet was resuspended in 6.5 mL supplemented DMEM medium with PenStrep and cell density and viability were calculated with the EVE cell counter after addition of 0.2% Trypan Blue. Cell suspensions were diluted to 0.6 x 10^6 viable cells/mL in supplemented DMEM medium with PenStrep. ThinCerts were pre-wetted with 100 µL supplemented DMEM medium with PenStrep at least two minutes before addition of 500 µL cell suspension and basolateral chambers were filled with 1.5 mL of the same medium. After six hours incubation at 37 °C, 5% CO_2, the apical medium was replaced with 500 µL fresh supplemented DMEM medium with PenStrep to remove the non-adherent cells in order to reduce the risk of multilayer formation. Apical and basolateral media were replaced every second day and between 12 and 24 h before the permeability experiment.

4.3.4   Tested compounds

Chlorogenic acid, as parent compound, and quinic acid, one of the most prominent intestinal biotransformation products were selected as test compounds during the permeability experiment. The chlorogenic acid (10 µM and 50 µM) and quinic acid (10 µM) concentrations were chosen based on the work of Hubatsch et al. (2007) which states that concentrations of 10 µM or less should be used when studying possible active transport to prevent transport protein saturation. The 50 µM concentration-level of chlorogenic acid was included in the experimental setup to evaluate, (i) if active

transport was involved, (ii) if the transport was concentration-dependent and/or (iii) saturated (Hubatsch et al. 2007). Furthermore, two positive control compounds were included in the experimental setup: (i) digoxin (10 µM) was used as positive control for the active P-glycoprotein (P-gp, MDR1) efflux mechanism and (ii) propranolol (50 µM) as a positive control for high passive permeability. Used concentrations were based on the available literature (Zheng et al. 2015, Obringer et al. 2016). Test solutions were prepared starting from standard solutions in MeOH using HBSS as dilution medium. The total volume of organic solvent did not exceed 1% to ensure the integrity of the cell monolayer (Hubatsch et al. 2007). Chemical structures of all compounds included in the permeability assay are shown in Figure 4-2. Previous experiments were performed investigating (i) possible adverse effects of chlorogenic acid and quinic acid on the Caco-2 cell monolayer integrity and (ii) degradation or biotransformation of chlorogenic acid and quinic acid during the permeability assay (4.6 Supplementary information).

4.3.5 Permeability experiment

The following protocol was based on the procedure described by Hubatsch et al. (2007). Before the experiment, the cell monolayer was washed with prewarmed HBSS to remove the residual medium. The medium was decanted from the ThinCerts and the filter supports were placed in a new 12 well plate containing fresh prewarmed HBSS (37 °C, 1.5 mL per well). 500 µL fresh HBSS was added to the apical side. The cells were incubated with gentle shaking (70 rpm) for 15 min at 37 °C in a humidified atmosphere.

The transportation experiments were carried out in both directions; from the apical to basolateral (A-B) and from basolateral to apical side (B-A), including three replicates for each compound and/or concentration level. An overview of the experimental setup is shown in Figure 4-2. The preincubation medium was removed and replaced with test

solutions. 400 µL prewarmed donor solutions was added to the apical side of the A-B ThinCerts, while the basolateral compartment contained 1200 µL prewarmed HBSS containing the same percentage of methanol as the donor solutions to prevent precipitation during the experiment. For the B-A wells, 1200 µL donor solution was added to the basolateral side while 400 µL HBSS with an equal methanol-percentage was added to the apical compartment. Well plates were incubated under gentle shaking (70 rpm), to minimize the effect of an unstirred water layer, at 37 °C in a humidified atmosphere. Inadequate stirring will result in a lower permeability of highly permeable compounds. However, too high rpm settings can affect the cell monolayer integrity. A preliminary experiment demonstrated that the applied shaking-intensity in this study had no adverse effect on the Caco-2 cell monolayer integrity (4.6 Supplementary information). Samples, 600 µL for the A-B experiment and 200 µL for B-A experiment, were taken after 30, 60, 90 and 120 min from the receiving compartment and replaced with the same volume of fresh HBSS medium containing the same percentage of methanol as the donor solutions. Samples were immediately stored at -80 °C until analysis. Cell monolayer integrity of all wells was confirmed before and after the permeability experiment using the transepithelial electrical resistance (TEER) values.
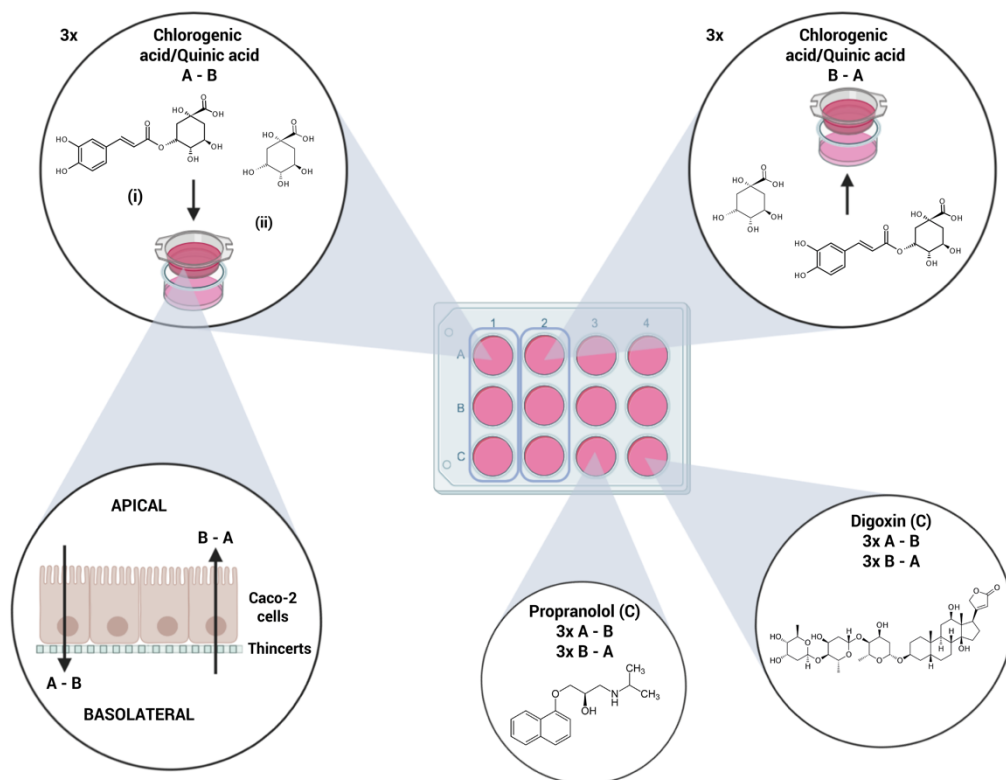
Figure 4-2: Overview of the experimental setup during the permeability assay with (i) chlorogenic acid and (ii) quinic acid in Caco-2 monolayers. Propranolol and digoxin were included as positive control (C) compounds. A-B: Apical to basolateral side transport. B-A: Basolateral to apical side transport.

4.3.6 Sample preparation

20 µL internal standard solution (1 µg/mL) was added to 200 µL sample aliquots followed by addition of 180 µL MeOH. Samples were vortexed for 30 s, transferred to a 0.2 µm nylon centrifugal filter and centrifuged for 5 min at 8000 rpm. The filtrates were transferred to an LC vial before analysis with liquid chromatography coupled to triple quadrupole mass spectrometry (LC-MS/MS).

4.3.7   LC-MS/MS analysis

Samples were analyzed using an Agilent 1290 Infinity II liquid chromatography instrument coupled to an Agilent 6495 triple quadrupole mass spectrometer (Agilent Technologies) with electrospray ionization (ESI) source. Chromatographic separation was performed on a Luna Omega PS C18 column (100 x 2.1 mm; 3 µm) from Phenomenex (Utrecht, the Netherlands). A multiple reaction monitoring (MRM) method was applied for all analytes. An overview of the ionization mode parameters and MRM transitions of the analytes are shown in Table 4-1. Details on mobile phase composition, gradient elution and source parameters for the different analytes are described further.

Table 4-1: Overview of the used internal standard (IS), polarity and MRM transitions for the compounds included in the *in vitro* permeability assay (CE= collision energy). Precursor ion, MRM transitions of the IS are mentioned between brackets. [Q]:quantifier, [q]:qualifier.

Compound	IS	Polarity	Precursor ion (*m/z*)	Product ions (*m/z*)	CE (V)
Chlorogenic acid	Ferulic acid-D$_3$	Negative	353.1 (196.0)	191.0[Q]; 85.0[q] (178.0[q]; 151.9[q]; 133.9[Q])	17; 52 (10; 10; 15)
Quinic acid	Ferulic acid-D$_3$	Negative	191.0 (196.0)	93.0[q]; 85.0[Q]; 43.2[q] (178.0[q]; 151.9[q]; 133.9[Q])	25; 25; 40 (10; 10; 15)
Propranolol	Propranolol-D$_7$	Positive	260.1 (267.2)	183.0[q]; 116.1[Q]; 56.2[q] (116.1[q]; 72.1[q]; 56.1[Q])	20; 20; 35 (20; 25;35)
Digoxin	Digoxin-D$_3$	Positive	798.3 (801.3)	651.2[q]; 112.9[q]; 96.8[Q] (654.3[q]; 96.8[Q])	10; 40; 33 (10; 30)

4.3.7.1   *Chlorogenic acid and ferulic acid-D₃*

The used mobile phase compositions were ultrapure water with 0.1 % (v/v) formic acid (A) and MeOH (B) with a constant flow of 0.3 mL/min. The gradient was constructed as follows: for 1 min B was used at 2%, followed by an increase to 98% B over 3.5 min. The column was rinsed for 6 min with 98% B and re-equilibrated at 2% B for 6 min. The LC-stream was directed to the waste after 6 min to limit source contamination.

Chlorogenic acid, and ferulic acid-D₃ as internal standard, were measured in negative MRM mode (Table 4-1). Gas temperature and flow were set at 200 °C and 14 L/min respectively. A nebulizer pressure of 20 psi was chosen, while sheath gas temperature and flow were optimized to 400 °C and 11 L/min. A capillary and nozzle voltage of 4000 V and 2000 V respectively were chosen.

4.3.7.2   *Quinic acid*

The mobile phase compositions were ultrapure water with 0.04% (v/v) formic acid (A) and MeOH (B) with a constant flow of 0.3 mL/min. Mobile phase B started at 1% for 2 min, followed by an increase to 98% B over 8 min. The column was rinsed for 6 min before 4 min re-equilibration at 1% B. The LC-stream was directed to the waste after 6 min.

Quinic acid was analyzed in negative MRM mode. Ferulic acid-D₃ was used as the internal standard (Table 4-1). Optimized source parameters were as follows: gas temperature of 200 °C, gas flow of 14 L/min, nebulizer pressure of 50 psi, sheath gas temperature of 400 °C, sheath gas flow of 12 L/min, capillary voltage of 2500 V and a nozzle voltage of 2000 V.

4.3.7.3   *Propranolol and digoxin*

Mobile phase A consisted of 20 mM ammoniumacetate in ultrapure water. Acetonitrile was used as mobile phase B. The chromatographic run started at 10% B for 1 min,

followed by an increase to 95% B over 9 min. The column was rinsed for 5 min at 95 % B before 5 min re-equilibration at 10% B. The LC-stream was directed to the waste after 8 min to limit source contamination.

Propranolol, propranolol-D_7 (internal standard), digoxin and digoxin-D_3 (internal standard) were analyzed in positive mode (Table 4-1). Gas temperature, flow and nebulizer pressure were identical to the parameters described for chlorogenic acid. Sheath gas temperature was set to 200 °C with a flow of 11 L/min. Capillary and nozzle voltages were 3500 V and 1500 V.

4.3.8   *P_{app}* and efflux ratio calculations

The apparent permeability coefficient (P_{app}, cm/s) was calculated using Equation 1. A is the area of the used ThinCerts (1.131 cm^2), C_0 is the dosing concentration of the tested compound expressed as µmol/mL and dQ/dt is the steady-state-flux (µmol/sec) which is the slope of the regression curve when plotting the cumulative amount of detected compound (mol) over time (s). The P_{app} (A-B) values of the tested compounds were divided by the P_{app} (A-B) value of propranolol obtained in the same permeability assay. The following P_{app}(A-B)$_{target}$/P_{app}(A-B)$_{PROP}$ ratios relate to the fraction test compound absorbed, as propranolol is almost completely absorbed *in vivo* (Obringer et al. 2016).

Equation 1: Formula used to calculate P_{app}

$$P_{app} = \left(\frac{dQ}{dt}\right) x \; \frac{1}{A \; x \; C_0}$$

The efflux ratio was calculated by dividing the P_{app} of the B-A direction by the P_{app} of the A-B direction (Equation 2). An efflux ratio greater or equal to two indicates the involvement of an active efflux transport mechanism (Hubatsch et al. 2007).

Equation 2: Efflux ratio formula

$$Efflux\ ratio = \frac{P_{app}(B-A)}{P_{app}(A-B)}$$

4.3.9   Validation of analytical methods

Validation of the LC-MS/MS methods was carried out over three days based on the guidelines provided by the European Medicines Agency (EMA 2011). Performance parameters such as intra-day and inter-day precision and accuracy, linearity, calibration range, selectivity and carry-over were evaluated.

A nine-point multi-component calibration curve, with a concentration range from 5 ng/mL to 1000 ng/mL, was prepared in HBSS. A broad calibration range was chosen since the expected concentrations of the assay samples were unknown. The linearity-range was evaluated for each compound. Calibration curves were $1/x$ or $1/x^2$ weighted. The concentration of the lowest calibration curve was referred to as the lowest limit of quantification (LLOQ). The area of the LLOQ sample should be at least five times higher than the signal of the blank. Accuracy of all calibration levels had to be within 20% of the nominal value.

Four concentration levels of quality control (QC) samples were prepared in HBSS following the sample preparation procedure described in section 4.3.6: LLOQ (5 ng/mL), low QC (QCL, 15 ng/mL), mid QC (QCM, 400 ng/mL) and high QC (QCH, 900 ng/mL).

Carry-over was evaluated by injection of a solvent blank (HBSS without addition of standards or internal standards) after the highest calibration point. The peak area of the blank sample should not exceed 20% of the peak area of the LLOQ sample and 5% of the internal standard peak. Selectivity was evaluated by injection of a solvent blank

(HBSS, without addition of standards or internal standard). Peak areas in the solvent blank should not be more than 20% of the peak area at LLOQ level and < 5% of the internal standard peak area.

The within- and between-day accuracy and precision were evaluated by analysis of 5 replicates of the 4 QC-levels over a 3-day period. Accuracy was evaluated as the deviation from the nominal spiked value (% bias). Precision was calculated as the relative standard deviation (RSD) of the mean quantified concentration. Acceptance criteria for both precision and accuracy were set at 20% for the LLOQ-level and 15% for low, mid and high QC-levels.

4.4   Results and discussion

4.4.1   Validation of analytical methods

A linear calibration curve was obtained for all compounds with a concentration range from 5 to 1000 ng/mL (Table 4-2, Figure SI- 4-4). Table 4-2 summarizes the within-run and between-run accuracy and precision results. The results at LLOQ-level were within the range of <20% bias and <20% RSD for all compounds. Chlorogenic acid, quinic acid and propranolol met the criteria of < 15% bias and < 15% RSD respectively at QCL, QCM and QCH. Digoxin did not meet the accuracy criteria at the QC high level, with an intra- and inter-day accuracy of 20% and 18% respectively. However, concentrations of all digoxin permeability assay samples were below 200 ng/mL, which made the method suitable for analysis of the permeability samples.

All compounds met the required carry-over EMA guidelines criteria as peak areas of blanks analyzed after the highest calibration level did not exceed 20% of the LLOQ standard peak area and 5% of the internal standard. Furthermore, the chromatographic methods of all compounds were in compliance with the EMA selectivity guidelines as no peaks with a peak area above 20% of the LLOQ and 5% of the peak area of the internal standard were detected in the blank samples.

Table 4-2: Overview of the method validation data for all compounds: Linear range, R^2, intra- and interday accuracy and precision. Lower limit of quantification, LLOQ; Quality control low, QCL; Quality control mid, QCM and Quality control high, QCH.

| Compound | Linear range (ng/mL) | R^2 | Accuracy (in % bias) | | | | | | | | Precision (%RSD) | | | | | | | |
| | | | Intraday (n=5) | | | | Interday (n=15) | | | | Intraday (n=5) | | | | Interday (n=15) | | | |
			LLOQ	QCL	QCM	QCH	LLOQ	QCL	QCM	QCH	LLOQ	QCL	QCM	QCH	LLOQ	QCL	QCM	QCH
Chlorogenic acid	5-1000	0.995	12.2	14.5	7.8	12.4	12.2	14.5	7.0	12.4	4.6	3.0	4.8	3.9	5.3	4.8	7.2	4.7
Quinic acid	5-1000	0.992	4.4	9.3	9.0	6.9	5.4	9.0	8.3	5.6	9.8	7.6	4.9	2.7	9.8	8.0	7.8	6.5
Propranolol	5-1000	0.995	5.2	2.5	7.5	4.3	5.2	2.5	7.5	3.8	4.0	4.2	6.6	4.7	4.8	4.9	6.7	6.3
Digoxin	5-1000	0.991	7.3	7.9	2.8	19.8	7.3	4.4	2.8	17.7	7.8	7.4	5.9	6.2	8.3	9.7	6.1	7.5

4.4.2   Chlorogenic acid permeability experiment

4.4.2.1   Positive control compounds

Positive control compounds were included in the experimental setup as between-experiments variations in P_{app} values can be observed using a Caco-2 cell experimental setup. These variations could result from differences in cell characteristics (age, passage number, etc.), cell culture conditions and/or varying experimental conditions (Grès et al. 1998, Volpe 2008, Lea 2015, Stockdale et al. 2019). As suggested by Stockdale et al. (2019), the acquired P_{app} values of the tested compounds should be compared with the permeability values of the positive control compounds included in the same permeability assay. This methodology was also previously used by Obringer et al. (2016), who divided the P_{app} (A-B) of the tested compounds by the measured P_{app} (A-B) of propranolol in the same assay. As propranolol is completely absorbed *in vivo*, the absorption rate of compounds with a ratio greater than 1 was equal to 100%. In this study, propranolol and digoxin were included as reference compounds for a high passive permeability and P-gp mediated efflux, respectively (Obringer et al. 2016, Stockdale et al. 2019).

Permeability coefficients of 5.45×10^{-6} cm/s (A-B) and 8.40×10^{-6} cm/s (B-A) were calculated for propranolol. These values can be used as reference values for high passive permeability as propranolol is almost completely absorbed *in vivo* (Grès et al. 1998). As depicted in Figure 4-3 and Table SI- 4-2, no clear differences were observed for propranolol permeability in the A-B and B-A direction. This led to an efflux ratio of 1.5, which does not indicate the involvement of an active transport mechanism. This is in agreement with the findings of Zheng et al. (2015).

A clear difference in permeability between the A-B and B-A direction was observed for digoxin. In the A-B direction, a P_{app} of 0.36×10^{-6} cm/s was calculated, which is a factor 15 lower in comparison to propranolol, while the P_{app} in B-A direction was 7.91×10^{-6} cm/s. As digoxin is known to be a substrate of the active efflux P-gp protein, a higher

permeability coefficient from the basolateral to apical side was expected. Accordingly, the calculated efflux ratio of digoxin was 22. The results obtained for both propranolol and digoxin confirm the reliability of the assay.

4.4.2.2   Chlorogenic acid

P_{app} (A-B) values of 2.42 x 10^{-6} cm/s and 2.61 x 10^{-6} cm/s were calculated for the 10 µM and 50 µM concentrations respectively, with corresponding P_{app}(A-B)$_{CHL}$/P_{app}(A-B)$_{PROP}$ ratios of 44% and 48% which suggests a moderate intestinal absorption of chlorogenic acid. However, the data clearly show a higher apparent permeability coefficient in the basolateral to apical direction in comparison to the A-B direction (Figure 4-3-A, Table SI- 4-2). In the B-A direction, permeability coefficients of 8.01 x 10^{-6} cm/s (10 µM) and 8.41 x 10^{-6} cm/s (50 µM) were measured for chlorogenic acid which results in respective efflux ratios of 3.3 and 3.2 (Table SI- 4-2). The results, consistent for both applied concentrations, suggest the involvement of active transport from the basolateral to apical side, leading to an overall poor absorption of chlorogenic acid. However, the effect is less pronounced than for the positive control digoxin. Furthermore, no effect of the applied concentrations on the bidirectional permeability was observed which shows that the active transport proteins involved in the transport of chlorogenic acid were not saturated.
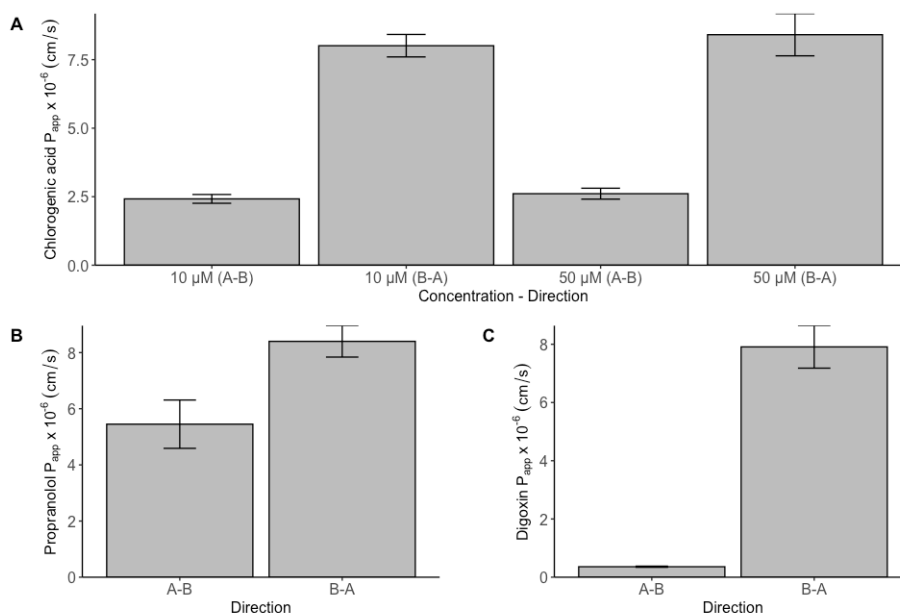
Figure 4-3: Overview of the mean P_{app} values (n=3) $\pm$ standard deviation (SD), both in the apical to basolateral side (A-B) and basolateral to apical side direction (B-A), of chlorogenic acid (A), propranolol (B) and digoxin (C) obtained after the permeability experiment evaluating chlorogenic acid.

The reported involvement of an active efflux in the absorption mechanism of chlorogenic acid in this study is in agreement with the findings of Erk et al. (Erk et al. 2014) who reported an active efflux for chlorogenic acid using a pig jejunal mucosa in an Ussing chamber model. A 3.8-fold higher transport rate from basolateral to apical side was reported which corresponds to the presented efflux ratios in this work. Erk et al. proposed P-gp as the responsible protein for the active efflux as the secretion of chlorogenic acid was affected by the P-gp inhibitor sodiumazide (NaN$_3$) (Erk et al. 2014). Dupas et al. (2006) and Monente et al. (2015) studied the *in vitro* absorption of chlorogenic acid in Caco-2 cells in the apical to basolateral direction and reported a 0.14% and 0.3% recovery of the initial quantity respectively (Dupas et al. 2006, Monente et al. 2015). The basolateral to apical transport was neglected in these studies and the involvement of an active efflux mechanism as observed in our

CHAPTER 4

experiments was not studied. Konishi et al. (2004) and Farrell et al. (2012) investigated the bidirectional *in vitro* transepithelial transport of chlorogenic acid using Caco-2 cells and did not report a higher permeation in the B-A direction. However, Konishi et al. used a concentration of 5 mM which is a factor 500 above the threshold of 10 µM described by Hubatsch et al. for active transport studies. Saturation of the active transport proteins could occur and explain the deviating results (Konishi and Kobayashi 2004, Hubatsch et al. 2007). A possible explanation of the deviating results reported by Farrell et al. may be varying expression of efflux proteins due to variations of Caco-2 cell age, passage number or culture conditions (Grès et al. 1998, Volpe 2008, Farrell et al. 2012, Lea 2015, Stockdale et al. 2019).

4.4.3 Quinic acid permeability experiment

4.4.3.1 Positive control compounds

An overview of the results of the positive control compounds can be found in Table SI-4-3 and Figure 4-4. For propranolol, permeability values of 5.14×10^{-6} cm/s (A-B) and 5.22×10^{-6} cm/s (B-A) were obtained. The calculated P_{app} values of digoxin in A-B and B-A direction were 0.7×10^{-6} cm/s and 6.17×10^{-6} cm/s respectively, leading to an efflux ratio of 9.01. As mentioned in section 3.2.1, variations in permeability values could be observed between different experiments. Digoxin showed a lower efflux ratio in comparison to the chlorogenic acid experiment. This shows the importance of including positive control compounds in each experiment to ensure correct interpretation of the acquired results.

4.4.3.2 Quinic acid

The mean P_{app} values of quinic acid are summarized in Table SI- 4-3. Quinic acid presented a $P_{app}(A-B)$ of 3.8×10^{-6} cm/s with a corresponding $P_{app}(A-B)_{QA}/ P_{app}(A-B)_{PROP}$

ratio of 74%. An apparent permeability coefficient of 22.6 x 10^{-6} cm/s was detected for the basolateral to apical direction, resulting in an efflux ratio of 5.9 (Figure 4-4-A, Table SI- 4-3). Given the obtained efflux ratio for quinic acid is above the cut-off value of two and the comparison with digoxin (efflux ratio of 9.01), the involvement of an active efflux mechanism for quinic acid is demonstrated. Although quinic acid demonstrated a high permeability (74% of the propranolol permeability coefficient), the overall intestinal absorption will be moderately low due to the involved active efflux mechanism.

High concentrations of quinic acid in human plasma and urine following coffee consumption have been described (Erk et al. 2012). However, no statements on the absorption of quinic acid can be made based on these data as (i) *in vivo* studies represent the bioavailability of a certain compound including all ADME aspects and (ii) coffee contains multiple quinic acid containing hydroxycinnamic esters. Thus, high concentrations of quinic acid in plasma and/or urine are not necessarily linked to a high absorption of the compound. To our knowledge this is the first study to investigate the *in vitro* gastrointestinal absorption of quinic acid using a Caco-2 permeability assay and reporting the involvement of an active efflux transporter. The major efflux transporters located in the intestine are the ATP binding cassette (ABC)-transporters like P-gp, BCRP (breast cancer resistance protein) and MRP2 (multidrug resistance-associated protein 2) (Schinkel and Jonker 2003). In order to identify the protein responsible for the active-efflux, additional experiments with suitable transport-inhibitors or Caco-2 Efflux Transporter Knockout Cells should be carried out.
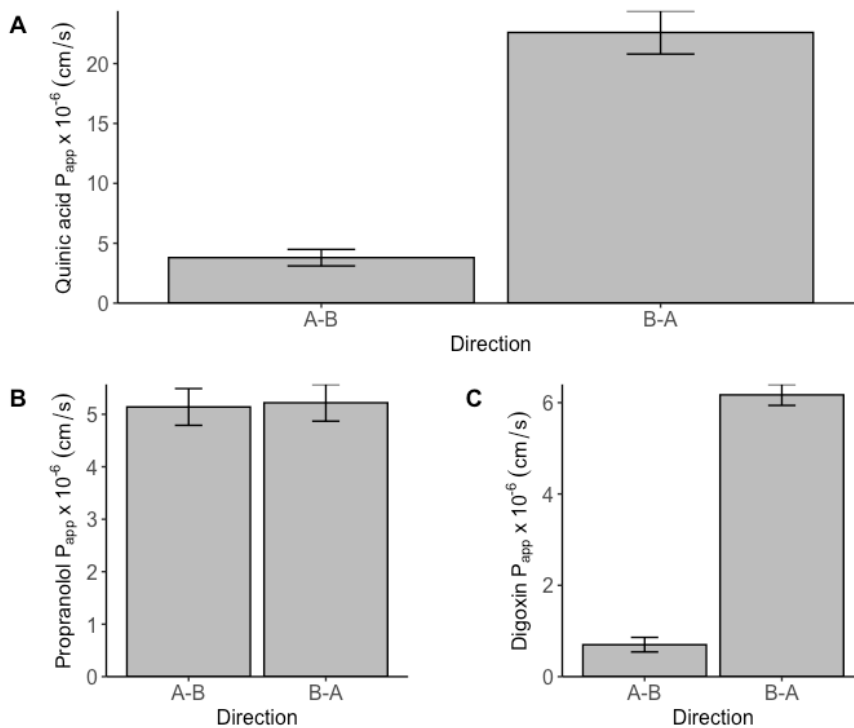
Figure 4-4: Overview of the mean P_{app} values (n=3) $\pm$ SD, both in the apical to basolateral side (A-B) and basolateral to apical side direction (B-A), of quinic acid (A), propranolol (B) and digoxin (C) obtained after the permeability experiment evaluating quinic acid.

4.5   Conclusions

In this chapter, the intestinal absorption of chlorogenic acid and one of its most prominent intestinal biotransformation products, quinic acid, was investigated using a bidirectional Caco-2 permeability assay. The data demonstrate the presence of an active efflux transport for both chlorogenic acid and quinic acid leading to an overall low intestinal absorption of both compounds. This could be of interest for (i) studies investigating the health-promoting effects of chlorogenic acid and its biotransformation products and (ii) the optimal formulation and dosing of chlorogenic acid in food supplements in order to obtain beneficial health effects.

4.6   Supplementary information

Investigating the effects of chlorogenic acid and quinic acid on the Caco-2 cell monolayer-integrity

Methodology

Caco-2 cells were cultivated as previously described and seeded in a Cellstar® 12-well plate. The cell monolayers were exposed to 1 mL of a 1 mM, 5 mM, 10 mM or 20 mM concentration level of chlorogenic acid or quinic acid, which were prepared in HBSS. Final methanol-concentrations were 0.1%, 0.5%, 1% and 2% respectively for the chlorogenic acid solutions, while no methanol was present in the quinic acid solutions. The 12-well plate was placed in a CO_2 incubator (C150 E2, Binder) for 7 h with a visual check of the cell monolayer by microscopy after 2 h, 4 h and 7 h.

Results and discussion

No adverse effects on the Caco-2 cell monolayer were observed after 2 h incubation for all concentration-levels for both chlorogenic acid and quinic acid with exception of the 5 mM quinic acid well. However, the disruption was caused during the change of medium when maintaining the cells and thus was already present at the start of the exposure-experiment. Therefore, it should not be included in the interpretation of the results. Starting from 4 h exposure, disruption of the cell monolayer was observed for the 20 mM chlorogenic acid well (Figure SI- 4-1). Similar disruptions in the monolayer were observed for the 10 mM chlorogenic acid concentration after 7 h exposure. No adverse effects were observed for the 1 mM and 5 mM chlorogenic acid concentration levels (Figure SI- 4-2). No loss of cell monolayer-integrity was observed for the 1 mM, 10 mM and 20 mM quinic acid concentration-levels after 7 h exposure (Figure SI- 4-2).

As no loss of cell monolayer-integrity was observed after 2 h exposure for all wells, which corresponds to the duration of the *in vitro* permeability assay, adverse effects

due to chlorogenic acid or quinic acid during the *in vitro* assay are ruled out. Furthermore, the used concentration-levels during the assay will be a factor 2000 (10 µM) and 400 (50 µM) lower than the highest concentration-level included in this exposure-experiment. This study evaluated the toxicity visually. Future experiments should aim to include viability parameters as markers of toxicity (e.g. specific endogenous Caco-2 metabolites using metabolomics approaches).

Conclusions

Based on the acquired results it can be concluded that the use of 10 and 50 µM chlorogenic acid and 10 µM quinic acid concentration-levels during the permeability assay will not lead to disruptions of the Caco-2 cell monolayer integrity.
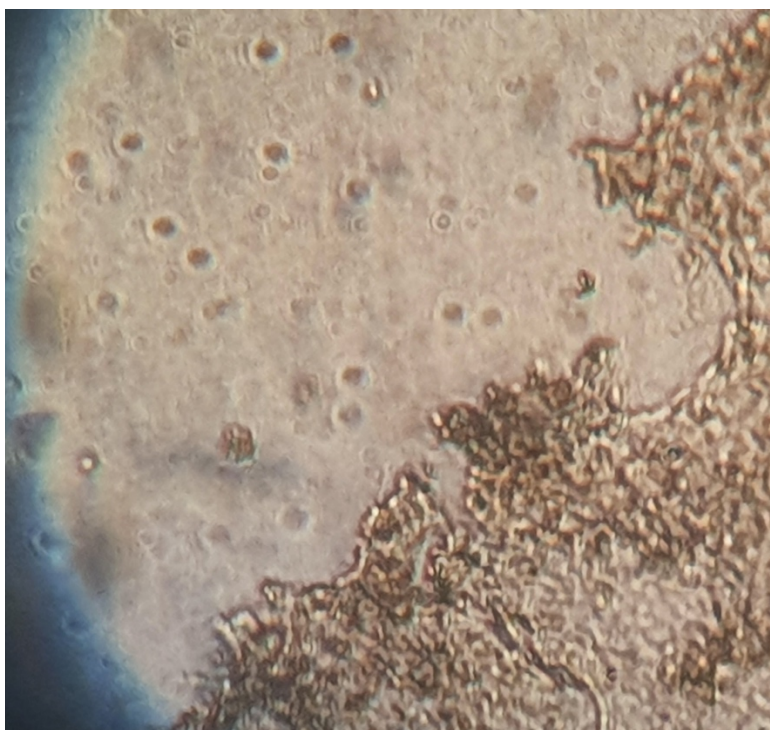
Figure SI- 4-1: Microscopic image of the 20 mM chlorogenic acid well after 7 h exposure. A loss of Caco-2 cell monolayer integrity was observed for this well.
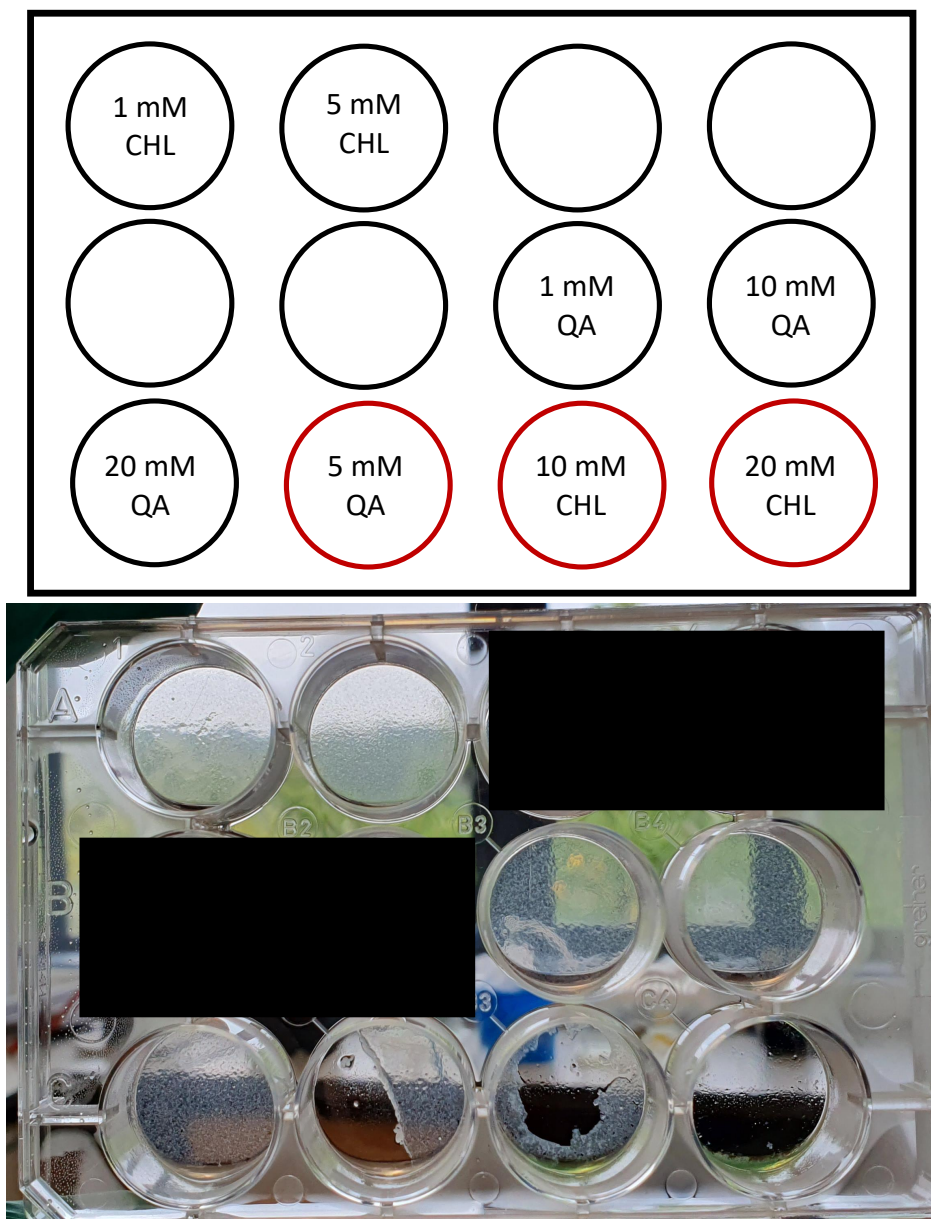
Figure SI- 4-2: *Top:* Overview of the exposed concentration-level and compound (chlorogenic acid (CHL)/quinic acid (QA)) to the specific well. Wells highlighted in red showed disruptions in the Caco-2 cell monolayer after 7 h in the CO_2 incubator. *Bottom:* Picture of the 12-well plate after 7 h exposure to the test solutions. Damages to the Caco-2 cell monolayer are clear for the 5 mM QA, 10 mM and 20 mM CHL wells.

CHAPTER 4

No degradation or biotransformation of chlorogenic acid and quinic acid

Methodology

After the 7 h exposure-experiment described above, the supernatants of the 5 mM exposed chlorogenic acid well and the 1 mM quinic acid well were collected. The 12-well plate was flash frozen in liquid nitrogen and transferred to the lab on dry ice.

Detachment and extraction of the Caco-2 cells from the well

The Caco-2 cell monolayers were detached from the well based on the protocol of Cuykx et al. (2017). The cells were quenched using a -80 °C methanol solution: 400 µL of the cooled methanol was added to the well and cells were detached using a cell scraper (Corning Inc., NY, USA), after which the supernatant was collected (Cuykx et al. 2017). This step was repeated once more an both fractions were pooled followed by vortexing for 30 s and centrifugation (0.2 µm centrifugal filter, 5 min, 8000 rpm).

Sample preparation

20 µL of the 5 mM chlorogenic acid supernatants was diluted in 480 µL mQ containing 0.04% formic acid. 100 µL of the 1 mM quinic acid sample was diluted in 400 µL mQ containing 0.04% formic acid. The samples were vortexed (30 s) and transferred to a 0.2 µm centrifugal filter and centrifuged 5 min at 8000 rpm. 150 µL of the filtered sample was transferred to a LC-vial.

The 200 µL supernatants of the centrifuged cell-extracts was transferred to a new Eppendorf and evaporated to dryness followed by reconstitution in 100 µL mQ containing 0.04% formic acid.

Instrumental and data-analysis

Samples were analyzed according to the LC-Q-TOF-MS method described in chapter two on an Agilent 1290 Infinity ultra-high-performance liquid chromatography

instrument coupled to an Agilent 6530 Accurate-Mass Q-TOF. Suspect screening, with a database based on biotransformation products described in literature, Meteor Nexus (Lhasa Limited, v2.1) and Biotransformer (Biotransformer.ca, v1.0.0) for chlorogenic acid and quinic acid respectively, was performed to identify the presence of degradation or biotransformation products.

Results and discussion

No degradation or biotransformation products were identified for both chlorogenic acid and quinic acid after applying the suspect screening to the data. Dawidowicz et al. (2010) described 9 possible degradation products of chlorogenic acid (5-caffeoylquinic acid) when dissolved in aqueous solution and heated. Apart from isomerization to 3- and 4-caffeoylquinic acid, no other degradation products of chlorogenic acid were observed. (Dawidowicz and Typek 2010). Furthermore, the chlorogenic acid-isomers were measured as a whole as they co-eluted as 1 peak with the LC-MS/MS method applied to the Caco-2 samples, given the different gradient in comparison to the LC-Q-TOF-MS method described in chapter two, minimizing the effect of the isomerization on the outcome.

Conclusion

No biotransformation or extensive degradation of the tested compounds occurred when exposing chlorogenic acid and quinic acid for a duration of 7 h to the Caco-2 cell monolayer in a CO_2 incubator at 37 °C.

Evaluation of shaking-intensity and sampling procedure on Caco-2 cell monolayer integrity

Methodology

Caco-2 cells were cultured and seeded on ThinCerts as previously described. The cell monolayers grown on ThinCerts were divided over two Cellstar® 12-well plates (Figure SI- 4-3). The first well plate was placed in the shaking MaxQ Mini 4450 incubator from Thermo Scientific while the second plate was not exposed to shaking. The shaking intensity was set at 70 rpm which was the maximal setting possible without the risk of medium loss from the wells. The procedure of sampling with a 30 min interval (according to the procedure in 4.3.5) was performed on three replicates from each well plate while the remaining three replicates were not handled during incubation. The 2 h duration of the experiment was in correspondence with the duration of the permeability assay. TEER of each well was measured at the beginning and end the experiment using the Voltmètre-Ohmmètre Millicell-ERS from Merck.

Results and discussion

Table SI- 4-1 summarizes the TEER values for the tested conditions before and after the 2 h incubation. The wells exposed to 70 rpm shaking and sampling had a mean TEER value of 640 Ωcm^2 after 2 h incubation while the wells not exposed to shaking and sampling featured a mean TEER of 678 Ωcm^2. No clear effects of the used shaking intensity and the sampling procedure could be observed based on the TEER measurements. As TEER values are dependent of multiple factors such as culture conditions, passage number of the cells, temperature, etc., establishing a clear cut-off for the TEER is difficult (Lea 2015).
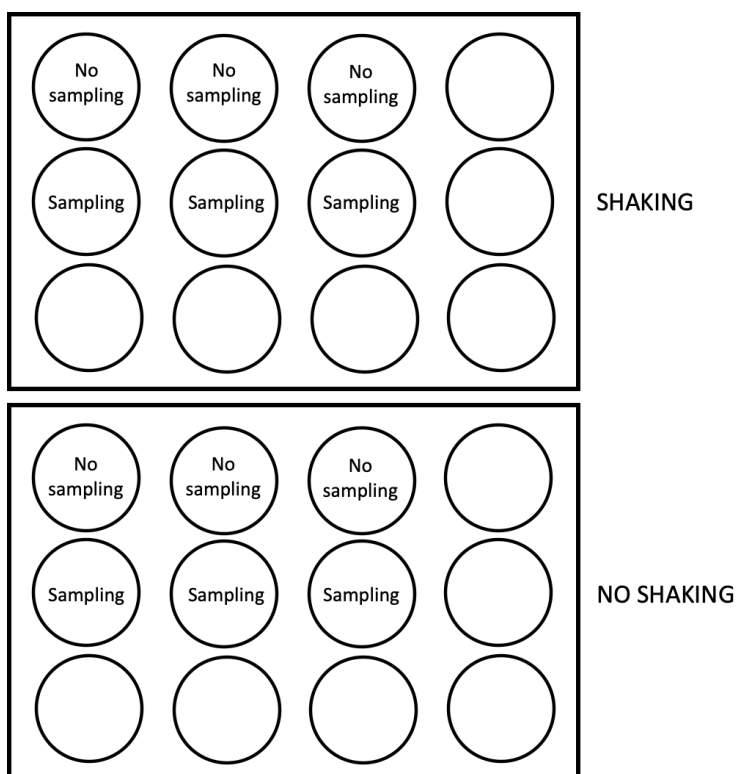
Figure SI- 4-3: Overview of the experimental set-up and the test conditions: shaking or no shaking and simulation of sampling or no sampling.

Table SI- 4-1: Mean transepithelial electrical resistance (TEER) values (n=3) for the tested conditions before (TEER$_{start}$) and after (TEER$_{end}$) 2 h incubation.

Test condition	Mean TEER$_{start}$ (Ωcm^2) ($\pm$ SD) (n=3)	Mean TEER$_{end}$ (Ωcm^2) ($\pm$ SD) (n=3)
No shaking + no sampling	806 ($\pm$ 24)	678 ($\pm$ 45)
Shaking + no sampling	832 ($\pm$ 24)	603 ($\pm$ 47)
No shaking + sampling	836 ($\pm$ 85)	648 ($\pm$ 43)
Shaking + sampling	825 ($\pm$ 81)	640 ($\pm$ 107)

Conclusion

The sampling procedure and shaking of the well plates at 70 rpm did not affect the cell monolayer integrity.
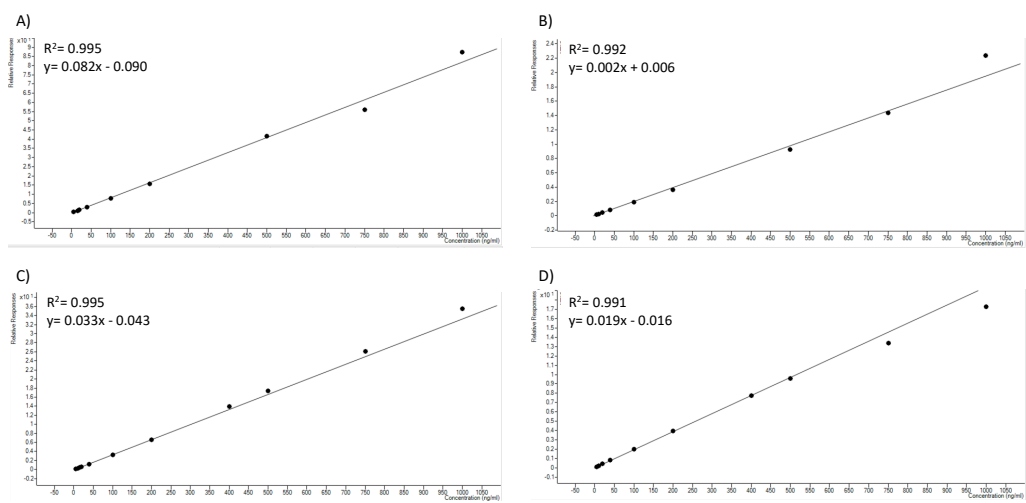
Figure SI- 4-4: Overview of the calibration curves of chlorogenic acid (A), quinic acid (B), propranolol (C) and digoxin (D).

Table SI- 4-2: Overview of the calculated P_{app} values and efflux ratios for chlorogenic acid and the positive control compounds.

Compound	P_{app}(A-B) (cm/s) ($\pm$ SD) x 10^{-6} (n=3)	P_{app}(B-A) (cm/s) ($\pm$ SD) x 10^{-6} (n=3)	Efflux ratio
Chlorogenic acid 10 µM	2.42 ($\pm$ 0.16)	8.01 ($\pm$ 0.41)	3.3 ($\pm$ 0.2)
Chlorogenic acid 50 µM	2.61 ($\pm$ 0.20)	8.41 ($\pm$ 0.77)	3.2 ($\pm$ 0.4)
Propranolol	5.45 ($\pm$ 0.86)	8.40 ($\pm$ 0.56)	1.5 ($\pm$ 0.3)
Digoxin	0.36 ($\pm$ 0.02)	7.91 ($\pm$ 0.73)	22.0 ($\pm$ 2.4)

Table SI- 4-3: Overview of the calculated Papp values and efflux ratios for quinic acid and the positive control compounds.

Compound	P_{app}(A-B) (cm/s) ($\pm$ SD) x 10^{-6} (n=3)	P_{app}(B-A) (cm/s) ($\pm$ SD) x 10^{-6} (n=3)	Efflux ratio
Quinic acid	3.8 ($\pm$ 0.69)	22.6 ($\pm$ 1.8)	5.9 ($\pm$ 1.2)
Propranolol	5.14 ($\pm$ 0.35)	5.22 ($\pm$ 0.35)	1.0 ($\pm$ 0.1)
Digoxin	0.70 ($\pm$ 0.16)	6.17 ($\pm$ 0.23)	8.7 ($\pm$ 2.1)

References

Agudelo-Ochoa GM, Pulgarín-Zapata IC, Velásquez-Rodriguez CM, Duque-Ramírez M, Naranjo-Cano M, Quintero-Ortiz MM, Lara-Guzmán OJ and Muñoz-Durango K. Coffee Consumption Increases the Antioxidant Capacity of Plasma and Has No Effect on the Lipid Profile or Vascular Function in Healthy Adults in a Randomized Controlled Trial. *The Journal of Nutrition* 2016, 146(3): 524-531.

Breynaert A, Bosscher D, Kahnt A, Claeys M, Cos P, Pieters L and Hermans N. Development and Validation of an in vitro Experimental GastroIntestinal Dialysis Model with Colon Phase to Study the Availability and Colonic Metabolisation of Polyphenolic Compounds. *Planta Medica* 2015, 81(12-13): 1075-1083.

Cuykx M, Mortelé O, Rodrigues RM, Vanhaecke T and Covaci A. Optimisation of in vitro sample preparation for LC-MS metabolomics applications on HepaRG cell cultures. *Analytical Methods* 2017, 9(24): 3704-3712.

Dawidowicz AL and Typek R. Thermal Stability of 5-o-Caffeoylquinic Acid in Aqueous Solutions at Different Heating Conditions. *Journal of Agricultural and Food Chemistry* 2010, 58(24): 12578-12584.

dos Santos MD, Almeida MC, Lopes NP, de Souza G, oacute, ria E, iacute and lia P. Evaluation of the Anti-inflammatory, Analgesic and Antipyretic Activities of the Natural Polyphenol Chlorogenic Acid. *Biological and Pharmaceutical Bulletin* 2006, 29(11): 2236-2240.

Dupas C, Marsset Baglieri A, Ordonaud C, Tome D and Maillard MN. Chlorogenic acid is poorly absorbed, independently of the food matrix: A Caco-2 cells and rat chronic absorption study. *Molecular Nutrition & Food Research* 2006, 50(11): 1053-1060.

EMA. Guideline on bioanalytical method validation. *Londen: European Medicines Agency* 2011.

Erk T, Hauser J, Williamson G, Renouf M, Steiling H, Dionisi F and Richling E. Structure- and dose-absorption relationships of coffee polyphenols. *Biofactors* 2014, 40(1): 103-112.

Erk T, Williamson G, Renouf M, Marmet C, Steiling H, Dionisi F, Barron D, Melcher R and Richling E. Dose-dependent absorption of chlorogenic acids in the small intestine assessed by coffee consumption in ileostomists. *Molecular Nutrition & Food Research* 2012, 56(10): 1488-1500.

Farah A, Monteiro M, Donangelo CM and Lafay S. Chlorogenic Acids from Green Coffee Extract are Highly Bioavailable in Humans. *The Journal of Nutrition* 2008, 138(12): 2309-2315.

Farrell TL, Poquet L, Dew TP, Barber S and Williamson G. Predicting phenolic acid absorption in Caco-2 cells: a theoretical permeability model and mechanistic study. *Drug Metabolism and Disposition* 2012, 40(2): 397-406.

Foger F, Kopf A, Loretz B, Albrecht K and Bernkop-Schnurch A. Correlation of in vitro and in vivo models for the oral absorption of peptide drugs. *Amino Acids* 2008, 35(1): 233-241.

Gonthier MP, Remesy C, Scalbert A, Cheynier V, Souquet JM, Poutanen K and Aura AM. Microbial metabolism of caffeic acid and its esters chlorogenic and caftaric acids by human faecal microbiota in vitro. *Biomedicine & Pharmacotherapy* 2006, 60(9): 536-540.

Gonthier MP, Verny MA, Besson C, Rémésy C and Scalbert A. Chlorogenic Acid Bioavailability Largely Depends on Its Metabolism by the Gut Microflora in Rats. *The Journal of Nutrition* 2003, 133(6): 1853-1859.

Gonthier MP VM, Besson C, Rémésy C, Scalbert A. Chlorogenic acid bioavailability largely depends on its metabolism by the gut microflora in rats. *The Journal of Nutrition* 2003, 133(6): 1853-1859.

Grès MC, Julian B, Bourrié M, Meunier V, Roques C, Berger M, Boulenc X, Berger Y and Fabre G. Correlation between oral drug absorption in humans, and apparent drug permeability in TC-7 cells, a human epithelial intestinal cell line: comparison with the parental Caco-2 cell line. *Pharmaceutical research* 1998, 15(5): 726-733.

Hubatsch I, Ragnarsson EG and Artursson P. Determination of drug permeability and prediction of drug absorption in Caco-2 monolayers. *Nature Protocols* 2007, 2(9): 2111-2119.

Hunyadi A, Martins A, Hsieh T-J, Seres A and Zupkó I. Chlorogenic Acid and Rutin Play a Major Role in the In Vivo Anti-Diabetic Activity of Morus alba Leaf Extract on Type II Diabetic Rats. *PLoS One* 2012, 7(11): e50619.

Konishi Y and Kobayashi S. Transepithelial Transport of Chlorogenic Acid, Caffeic Acid, and Their Colonic Metabolites in Intestinal Caco-2 Cell Monolayers. *Journal of Agricultural and Food Chemistry* 2004, 52(9): 2518-2526.

Küblbeck J, Hakkarainen JJ, Petsalo A, Vellonen K-S, Tolonen A, Reponen P, Forsberg MM and Honkakoski P. Genetically Modified Caco-2 Cells With Improved Cytochrome P450 Metabolic Capacity. *Journal of Pharmaceutical Sciences* 2016, 105(2): 941-949.

Lea T (2015). Caco-2 Cell Line. *The Impact of Food Bioactives on Health: in vitro and ex vivo models*. K. Verhoeckx, P. Cotter, I. Lopez-Exposito et al. Cham (CH)**:** 103-111.

Liang N and Kitts DD. Amelioration of Oxidative Stress in Caco-2 Cells Treated with Pro-inflammatory Proteins by Chlorogenic Acid Isomers via Activation of the Nrf2–Keap1–ARE-Signaling Pathway. *Journal of Agricultural and Food Chemistry* 2018, 66(42): 11008-11017.

Liu L, Liu Y, Zhao J, Xing X, Zhang C and Meng H. Neuroprotective Effects of D-(-)-Quinic Acid on Aluminum Chloride-Induced Dementia in Rats. *Evidence-based complementary and alternative medicine : eCAM* 2020, 2020: 5602597-5602597.

Monente C, Ludwig IA, Stalmach A, de Pena MP, Cid C and Crozier A. In vitro studies on the stability in the proximal gastrointestinal tract and bioaccessibility in Caco-2 cells of chlorogenic acids from spent coffee grounds. *International Journal of Food Sciences and Nutrition* 2015, 66(6): 657-664.

Mubarak A, Bondonno CP, Liu AH, Considine MJ, Rich L, Mas E, Croft KD and Hodgson JM. Acute Effects of Chlorogenic Acid on Nitric Oxide Status, Endothelial Function, and Blood Pressure in Healthy Volunteers: A Randomized Trial. *Journal of Agricultural and Food Chemistry* 2012, 60(36): 9130-9136.

Obringer C, Manwaring J, Goebel C, Hewitt NJ and Rothe H. Suitability of the in vitro Caco-2 assay to predict the oral absorption of aromatic amine hair dyes. *Toxicology In Vitro* 2016, 32: 1-7.

Pero RW and Lund H. Dietary quinic acid supplied as the nutritional supplement AIO + AC-11(R) leads to induction of micromolar levels of nicotinamide and tryptophan in the urine. *Phytotherapy Research* 2011, 25(6): 851-857.

Pero RW, Lund H and Leanderson T. Antioxidant metabolism induced by quinic acid. Increased urinary excretion of tryptophan and nicotinamide. *Phytotherapy Research* 2009, 23(3): 335-346.

Pinta MN, Montoliu I, Aura AM, Seppanen-Laakso T, Barron D and Moco S. In Vitro Gut Metabolism of U-C-13 -Quinic Acid, The Other Hydrolysis Product of Chlorogenic Acid. *Molecular Nutrition & Food Research* 2018, 62(22): 7.

Rubas W, Cromwell MEM, Shahrokh Z, Villagran J, Nguyen TN, Wellton M, Nguyen TH and Mrsny RJ. Flux Measurements across Caco-2 Monolayers May Predict Transport in Human Large Intestinal Tissue. *Journal of Pharmaceutical Sciences* 1996, 85(2): 165-169.

Schinkel AH and Jonker JW. Mammalian drug efflux transporters of the ATP binding cassette (ABC) family: an overview. *Advanced Drug Delivery Reviews* 2003, 55(1): 3-29.

Stalmach A, Mullen W, Barron D, Uchida K, Yokota T, Cavin C, Steiling H, Williamson G and Crozier A. Metabolite profiling of hydroxycinnamate derivatives in plasma and urine after the ingestion of coffee by humans: identification of biomarkers of coffee consumption. *Drug Metabolism and Disposition* 2009, 37(8): 1749-1758.

Stalmach A, Steiling H, Williamson G and Crozier A. Bioavailability of chlorogenic acids following acute ingestion of coffee by humans with an ileostomy. *Archives of Biochemistry and Biophysics* 2010, 501(1): 98-105.

Stockdale TP, Challinor VL, Lehmann RP, De Voss JJ and Blanchfield JT. Caco-2 Monolayer Permeability and Stability of Chamaelirium luteum (False Unicorn) Open-Chain Steroidal Saponins. *ACS Omega* 2019, 4(4): 7658-7666.

Tannergren C, Bergendal A, Lennernäs H and Abrahamsson B. Toward an Increased Understanding of the Barriers to Colonic Drug Absorption in Humans: Implications for Early Controlled Release Candidate Assessment. *Molecular Pharmaceutics* 2009, 6(1): 60-73.

Tomas-Barberan F, Garcia-Villalba R, Quartieri A, Raimondi S, Amaretti A, Leonardi A and Rossi M. In vitro transformation of chlorogenic acid by human gut microbiota. *Molecular Nutrition & Food Research* 2014, 58(5): 1122-1131.

Volpe DA. Variability in Caco-2 and MDCK cell-based intestinal permeability assays. *J Pharm Sci* 2008, 97(2): 712-725.

Zheng Y, Benet LZ, Okochi H and Chen X. pH Dependent but not P-gp Dependent Bidirectional Transport Study of S-propranolol: The Importance of Passive Diffusion. *Pharmaceutical research* 2015, 32(8): 2516-2526.

CHAPTER 4

CHAPTER 5: OPTIMIZATION AND APPLICATION OF AN *IN VITRO* INTESTINAL FIRST-PASS ASSAY INVESTIGATING CHLOROGENIC ACID AND ITS MICROBIAL BIOTRANSFORMATION PRODUCTS
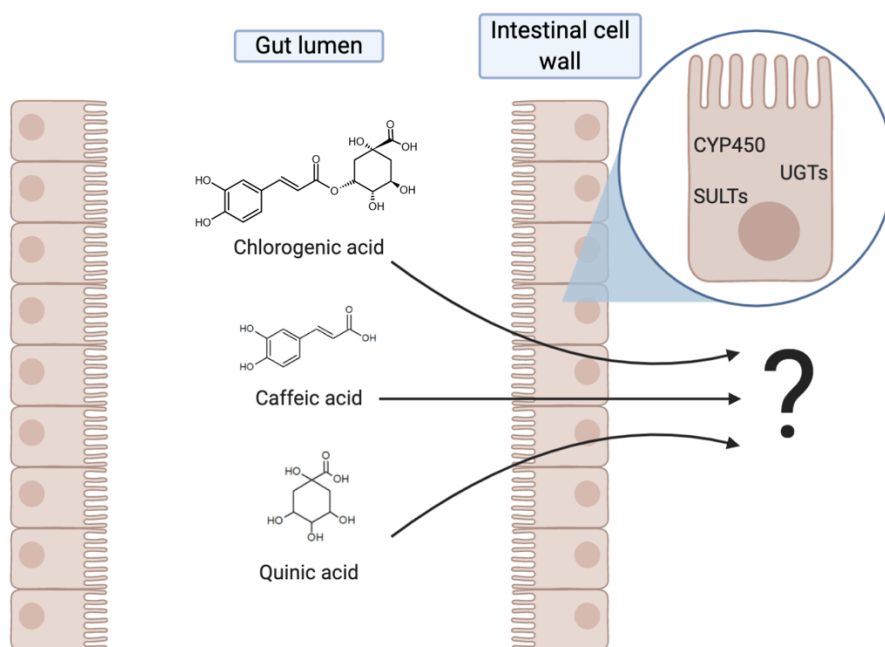
Based on following paper:

Mortelé O, van Nuijs A L N and Hermans N. Optimization and application of an in vitro intestinal first-pass assay investigating chlorogenic acid and its microbial biotransformation products. Journal of Food and Drug Metabolism (Under Review)

CHAPTER 5

CHAPTER 5

5.1   Introduction

The intestinal first-pass effect refers to the intestinal biotransformation reactions expressed in the intestinal cell wall, able to transform xenobiotics before they reach the systemic circulation. The intestinal first-pass biotransformation can be cytochrome P450 enzymes (CYP450)-mediated, but uridine 5'-diphospho(UDP)-glucuronosyltransferases (UGTs)- and sulfotransferases (SULTs)-mediated glucuronidation and sulfation have also been reported (Peters et al. 2016). Xenobiotics susceptible to extensive intestinal biotransformation will be characterized by a low oral bioavailability and will be subjected to drug-drug interactions in combination with CYP450 inducers and inhibitors (Xie et al. 2016). Furthermore, first-pass biotransformation could influence the bio efficacy of the xenobiotics. Related to the model compound chlorogenic acid, the antioxidant capacity of hydroxycinnamic microbial biotransformation products such as caffeic acid, is reported to be linked to the presence of free hydroxyl groups, which are also the primary sites of glucuronidation and sulfation biotransformation reactions (Giacomelli et al. 2004, Wong et al. 2010).

Several studies have reported on the differences in intestinal and hepatic biotransformation. Methylation, hydrogenation, glucuronidation and sulfation have been reported for both intestinal and hepatic biotransformation, however, glycine conjugation has been solely described in the liver (Clifford et al. 2020). CYP3A4 and CYP2C9 are the most prominent expressed CYP450 isotypes in the intestinal epithelia cells, accounting for 80% and 14% of the present CYP450 enzymes, respectively. Minor expressed CYP450 isoforms are CYP2C19, CYP2J2 and CYP2D6 (Xie et al. 2016). In general, more isoforms are expressed in the liver including CYP3A4, CYP2C9, CYP2C8, CYP2E1 and CYP1A2 as major isoenzymes. CYP2J2 is mainly present extrahepatically (Zanger and Schwab 2013). Human intestinal microsomes (HIM) and human intestinal cytosol (HICYT) are suitable sources of enzymes for examination of the in vitro human intestinal first-pass effect of xenobiotics. The HIM fraction contains the CYP450

isoenzymes and the UGTs, while the HICYT contains SULTs responsible for sulfation conjugation reactions (Hatley et al. 2017). In comparison to human liver microsomes (HLM), lower enzymatic activity has been reported for the HIM fractions linked to the isolation method of the subcellular fractions. The development of new isolation methods and the use of protease inhibitors during the isolation process has resulted in enhanced stability and activity of the drug biotransforming enzymes (Wong et al. 2010, Hatley et al. 2017).

5.2 Aims and preface

This chapter aims to study the first-pass biotransformation of chlorogenic acid and two of its most prominent microbial biotransformation products, caffeic acid and quinic acid, in the intestinal cell wall using an *in vitro* assay based on HIM and HICYT. The intestinal biotransformation of xenobiotics in the intestinal cell wall is essential information to completely unravel the gastrointestinal behavior of chlorogenic acid and have more detailed information on its bioavailability.

5.3 Material and methods

5.3.1 Chemicals and reagents

HIMs (10 mg/mL, mixed gender, n = 15) and HICYT (4 mg/mL, mixed gender, n = 15) were acquired from Tebu-Bio (Boechout, Belgium). Caffeic acid (≥98%), chlorogenic acid (≥ 95%), quinic acid (98%) theophylline (anhydrous, > 99%), 2,5-uridinediphosphate glucuronic acid (UDPGA), adenosine-3'-phosphate 5'-phosphosulfate (PAPS, > 60%) lithium salt hydrate, alamethicin (neat, > 98%), dimethyl sulfoxide (DMSO), and 4-nitrophenol (4-NP) were obtained from Sigma-Aldrich (St Louis, MO, USA). Nicotinamide adenine dinucleotide phosphate (NADPH) tetrasodium salt hydrate (> 96%) was purchased from Acros (Geel, Belgium). Acetonitrile (ACN, HPLC-grade) and methanol (MeOH, ≥ 99.9 % LC–MS grade) were acquired from Fisher Chemical (Loughborough, UK), formic acid (> 98 %) and hydrochloric acid (HCl, 37 %) from Merck KGaA (Darmstadt, Germany). Fentanyl (> 99%) was acquired from LGC standards (Teddington, United Kingdom). Valsartan was purchased from Novartis (Basel, Switserland). A 100 mM TRIS-buffer was prepared by dissolving 12.11 g Trizma base (Janssen Chimica, Beerse, Belgium) and 1.02 g $MgCl_2$ (Merck KGaA, Darmstadt, Germany) in 1 L ultrapure water. The pH was adjusted to 7.4 by adding 1 M HCl solution. Ultra-pure water was produced in-house with a PURELAB-purifier system of Elga Labwater (Tienen, Belgium).

5.3.2   *In vitro* biotransformation assay

5.3.2.1   *Optimization of HIM and HICYT concentrations*

The applied *in vitro* assay was adapted from an in-house developed and validated protocol of *in vitro* liver metabolism assays using HLM and cytosol (HLCYT) (Mortele et al. 2018, Vervliet et al. 2018). The HIM and HICYT concentrations used during phase I and phase II incubation protocols were previously optimized using the positive control compounds phenacetin and 4-NP.

5.3.2.1.1   Phase I incubations

Five µL of a 5 µg/mL phenacetin solution was incubated with 250, 500 and 1000 µg/mL HIM (10 mg/mL) in TRIS buffer (total volume reaction mixture: 500 µL). Both 500 and 1000 µg/mL concentration levels were incubated for 3h and 8 h. Five µL of nicotinamide adenine dinucleotide phosphate (NADPH, 100 mM in TRIS buffer) was added after 5, 60 and 120 min incubation for the 3 h samples. The 8 h incubation samples used NADPH regenerating system. Phase I reactions were stopped after 3 h and 8 h by addition of 125 µL ACN containing 1% (v/v) FA and 5 µg/mL valsartan and theophylline (stop solution). A negative control sample without HIM was included. The formation of phase I biotransformation products N-(4-hydroxyphenyl)-acetamide and N-(4-ethoxy-2-hydroxyphenyl)-acetamide was monitored.

5.3.2.1.2   Glucuronidation incubations

The optimal concentration of HIM in the reaction mixture was determined by incubation of 4-NP with 250, 500 and 1000 µg/mL HIM (10 mg/mL). Five µL of a 1 mM 4-NP and 5 µL alamethicin (1 mg/mL in DMSO) were added to the reaction mixture. 5 µL of uridinediphosphate glucuronic acid (UDPGA, 100 mM in TRIS buffer) was added after 5, 60 and 120 min incubation in a warm water bath (37 °C). Glucuronidation was stopped after 180 min by addition of 125 µL ACN containing 1% (v/v) FA and 5 µg/mL

valsartan and theophylline (stop solution). A negative control sample without HIM and a positive control sample using HLM (end concentration: 1000 µg/mL) instead of HIM were included.

5.3.2.1.3   Sulfation incubations

The optimal concentration of HICYT in the reaction mixture was determined by incubation of 4-NP with 500, 750 and 1000 µg/mL HICYT (4 mg/mL). Five µL of a 1 mM 4-NP was added to the reaction mixture. Five µL of adenosine-3'-phosphate 5'-phosphosulfate (PAPs) (10 mM in TRIS buffer) was added after 5, 60 and 120 min incubation in a warm water bath (37 °C). Sulfation was stopped after 180 min by addition of 125 µL ACN containing 1% (v/v) FA and 5 µg/mL valsartan and theophylline (stop solution). A negative control sample without HICYT and positive control samples using HLCYT at the same concentration-levels as HICYT were included.

5.3.2.2   **Optimized in vitro biotransformation assay**

5.3.2.2.1   Phase I incubations

An overview of the experimental setup can be found in Figure 5-1. A reaction mixture containing 440 µL (1 h incubation) or 430 µL (3 h incubation) TRIS-buffer (pH 7.4, 100 mM), 50 µL of HIMs (10 mg/mL in 250 mM sucrose in water) and 5 µL of a 0.5 mM stock solution of chlorogenic acid, caffeic acid or quinic acid was incubated in an Eppendorf tube at 37 °C. Three replicates were included for each sample set (Figure 5-1). Five µL of the cofactor NADPH (100 mM in TRIS-buffer) was added after 5, 60 and 120 minutes. During incubation the total volume of organic solvent did not exceed 1% in order to avoid any effects on microsomal activity (Jia and Liu 2007). Three different negative control samples (i.e. without substrate, HIMs or NADPH) were prepared in parallel. The reaction was stopped after 1 h or 3 hours by the addition of 125 µL ice-cold ACN containing 1% formic acid and 5 µg/mL of the internal standards theophylline and valsartan (phase I experiments) or by putting the samples on ice for 3 minutes

(samples for further phase II experiments, see further). Fentanyl (0.3 mM in MeOH), a substrate of CYP3A4, was included in the experimental setup as a positive control for phase I enzymatic activity. The formation of norfentanyl and β-hydroxyfentanyl was monitored.

5.3.2.2.2   *Phase II incubations*

Following the phase I experiments, samples were exposed to phase II conjugation through glucuronidation and sulfation. Three replicates were included for each sample set (Figure 5-1). For glucuronidation experiments, 430 μL of the supernatant originating from phase I samples was incubated with 50 μL of HIMs and 5 μL of alamethicin (1 mg/mL in DMSO). Five μL of UDPGA (100 mM in TRIS-buffer) was added as cofactor after 5, 60, and 120 minutes. Sulfation samples consisted of a mixture of 422.5 μL supernatant and 62.5 μL HICYT (4 mg/mL in buffer containing 150 mM potassium chloride and 50 mM TRIS, pH 7.5, with 2 mM EDTA), with addition of 5 μL PAPs (10 mM in TRIS-buffer) as cofactor after 5, 60, and 120 minutes of incubation. Negative control samples were prepared by omitting substrate, intestinal microsomes/cytosol or the cofactor (UDPGA and PAPs) in order to exclude false-positive results. A positive control was included by incubating 4-NP (5 μL of 10 mM in TRIS-buffer) and monitoring the formation of 4-NP glucuronide (4-NP-Gluc) and 4-NP sulfate (4-NP-Sulf). For both glucuronidation and sulfation, one replicate was included without previous phase I incubation (gluc-direct and sulf-direct). Reactions were stopped as described earlier for the phase I incubations.

Samples from both phase I and phase II incubations were centrifuged for 5 minutes at 8000 rpm (5900 g). 500 μL of the supernatant was transferred to a clean glass tube, evaporated under nitrogen at 38 °C, and reconstituted in 100 μL of the starting mobile phase for liquid chromatography coupled to quadrupole time-of-flight mass spectrometry (LC–Q-TOF–MS) analysis.
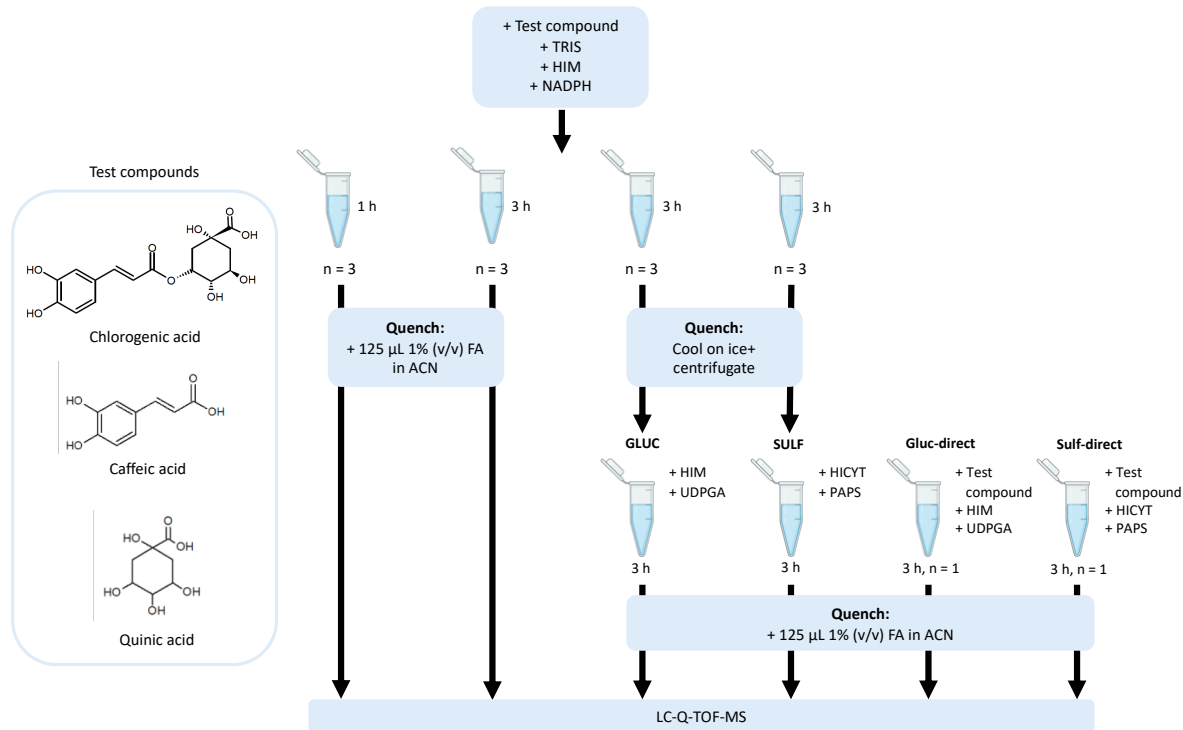
Figure 5-1: Overview of the experimental setup of the in vitro biotransformation assay. HIM: Human intestinal microsomes, FA: formic acid, ACN: acetonitrile, NADPH: nicotinamide adenine dinucleotide phosphate, UDPGA: 2,5-uridinediphosphate glucuronic acid, PAPS: adenosine-3'-phosphate 5'-phosphosulfate, GLUC: glucuronidation, SULF: sulfation. Gluc-direct and sulf-direct: GLUC and SULF replicate without previous phase I incubation.

5.3.3   LC-Q-TOF-MS

Extracts form the chlorogenic acid and caffeic acid incubations were analyzed by LC-Q-TOF-MS as earlier described in 2.3.1.6.2.

The applied chromatographic method for quinic acid samples was based on the untargeted LC-MS platform developed by Iturrospe and Da Silva et al. (in preparation) to investigate hydrophilic metabolites in biological matrices. Quinic acid eluted at retention time 1.1 min using the chromatographic method applied for chlorogenic acid and caffeic acid, due to its polar structure, which is not desirable when aiming to separate and analyze polar biotransformation products. Chromatographic separation was performed on an iHILIC®-Fusion(+) (100 x 2.1 mm, 1.8 µm) from Hilicon AB (Umeå, Sweden) using a mobile phase consisting of ultrapure water with 0.1% formic acid (A) and acetonitrile (B) at a flow rate of 0.2 mL/min. The first minute starts with 1 min isocratic at 5% A, after which A increased until 80% at 10 min. The percentage of A was held constant during 4 min after which A returned to 5% over 1 min. Finally, the column was re-equilibrated at 95% B for 5 min before the next injection. The column temperature was set at 30 °C and the injection volume was 3 µL. The eluent was directed to the waste during the first 0.5 min and from 18 min analysis (Iturrospe et al. In preparation).

Samples were analyzed in negative ionization mode with following parameters: 250 °C drying gas temperature, 10 L/min drying gas flow, 45 psig nebulizer pressure, 250 °C sheat gas temperature, 10 L/min sheat gas flow, 3500 V capillary voltage and 500 V nozzle voltage. Operation mode, calibration, acquisition parameters and collision energies of the QTOF mass spectrometer-method were identical to the procedure described in 2.3.1.6.2.

5.3.4   Data-analysis workflows

Raw data were analyzed as previously described in 2.3.1.6.3 using the three complementary data-analysis workflows. The suspect lists of chlorogenic acid, caffeic acid and quinic acid were constructed based on available literature and *in silico* prediction tools Biotransformer (Biotransformer.ca, v1.0.0) and Meteor Nexus (Lhasa Limited, v2.1).

5.4 Results and discussion

5.4.1 Optimization of the *in vitro* intestinal biotransformation assay

5.4.1.1 Phase I assay

N-(4-hydroxyphenyl)-acetamide and N-(4-ethoxy-2-hydroxyphenyl)-acetamide were not detected in all HIM concentration and incubation-duration samples suggesting no biotransformation of phenacetin. A slight decrease in relative area of phenacetin over increasing HIM concentrations and incubation duration was observed, as well as a difference in phenacetin intensity with the negative control sample, however, interpretation of the results is limited as only one replicate is included in the assay Figure 5-2.

CYP3A4 and CYP2C9 account for 80% and 14% respectively of the total intestinal expressed CYP450 enzymes. CYP1A2, the CYP450 enzyme responsible for phenacetin biotransformation, is not present in the intestinal cells which explains the lack of phase I biotransformation products (Huang et al. 2012, Xie et al. 2016). Future *in vitro* intestinal biotransformation assays should include a CYP3A4 or CYP2C9 substrate as positive control compound for phase I. Optimization of the HIM concentration using a CYP3A4 substrate (e.g. fentanyl) was no longer feasible within the timeframe of this thesis and should be performed in the future. In accordance with the HLM experiments, the same microsome concentration was used for the glucuronidation and phase I incubations.
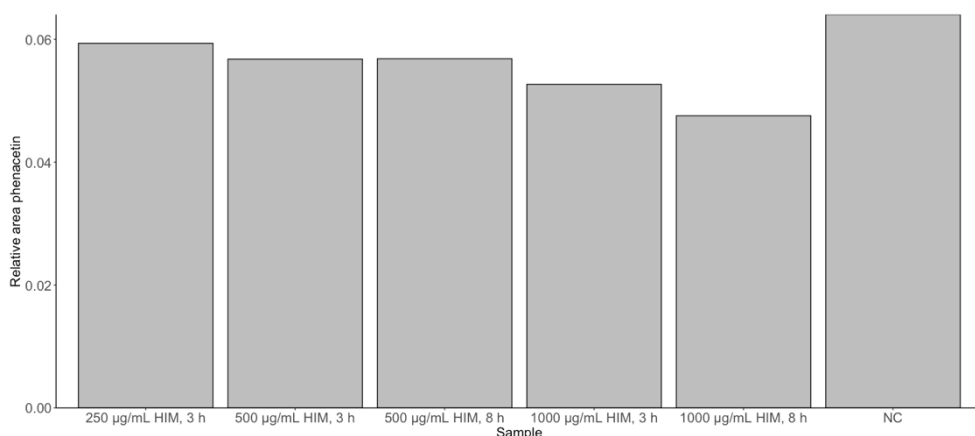
Figure 5-2: Relative area of phase I positive control compound phenacetin in the different test conditions. HIM: human intestinal microsomes, NC: negative control sample.

5.4.1.2   Glucuronidation assay

Although only one replicate per sample composition was included, a clear effect of HIM-concentration on the biotransformation rate of 4-NP were observed. Increasing HIM-concentrations gave rise to higher 4-NP-Gluc relative areas. A lower glucuronidation activity was observed for the HIM in comparison to the HLM as (i) 4-NP was no longer detected after 3 h incubation when using 1000 µg/mL HLM, while it was still detected at the same HIM concentration (Figure 5-3-A) and (ii) clearly lower relative area of the biotransformation product 4-NP-Gluc were detected in the HIM samples (Figure 5-3-B). No 4-NP-Gluc was detected in the negative control sample. Based on these results, 1000 µg/mL was chosen as optimal HIM concentration for the phase II glucuronidation incubations. The glucuronidation rate of intestinal S9 homogenates was previously reported to be comparatively lower to liver S9 homogenates (Wong et al. 2010).
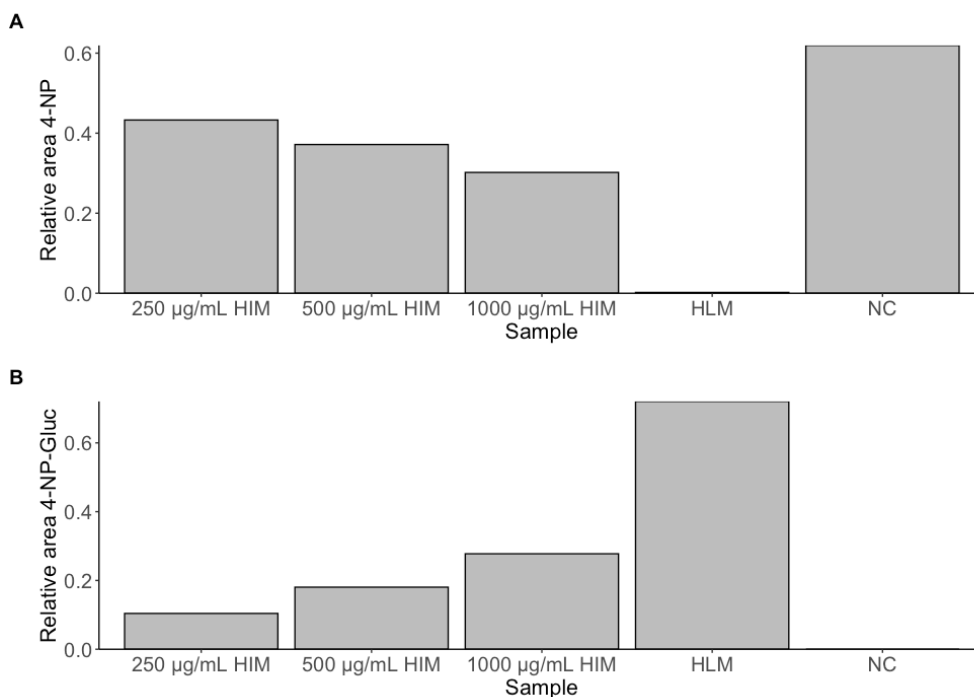
Figure 5-3: Relative areas of 4-nitrophenol (4-NP, **A**) and 4-NP-glucuronide (4-NP-Gluc, **B**) in the samples with varying human intestinal microsome (HIM) concentrations, the sample containing 1000 µg/mL human liver microsomes (HLM) and the negative control (NC) sample.

5.4.1.3   *Sulfation assay*

No clear differences in enzymatic activity between HICYT and HLCYT were observed (Figure 5-4). Increasing concentrations of HICYT and HLCYT gave rise to in decreasing relative areas of 4-NP. Based on these results, 500 µg/mL was chosen as optimal HICYT concentration as 500 µg/mL corresponds to the concentration of HLCYT previously used in *in vitro* liver biotransformation assays and the observed sulfation-rate of the HICYT is comparable.
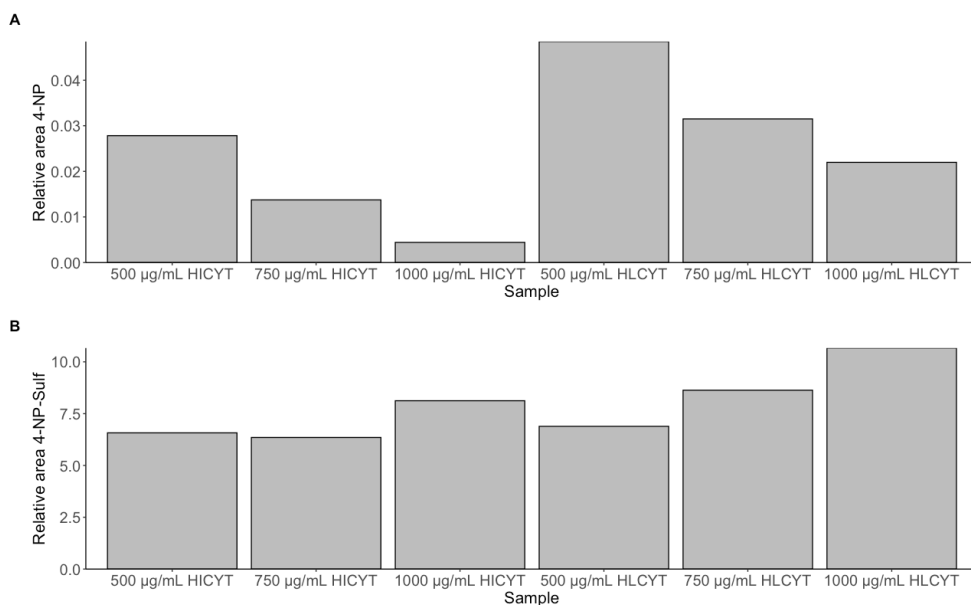
Figure 5-4: Relative areas of 4-nitrophenol (4-NP, **A**) and 4-NP-sulfate (4-NP-Sulf, **B**) in the samples with varying human intestinal cytosol (HICYT) and human liver cytosol (HLCYT) concentrations.

5.4.2 Phase I biotransformation

5.4.2.1 *Positive control*

Phase I biotransformation products norfentanyl and β-hydroxyfentanyl were monitored as positive control for the phase I assay. Fentanyl, substrate of CYP3A4, was still present after 3 h phase I incubation, however, both norfentanyl and β-hydroxyfentanyl were detected confirming the phase I enzymatic activity (Figure 5-5). Identification of fentanyl and its biotransformation products was based on the MS/MS spectra and comparison with the online spectra database mzCloud. (mzcloud.org). These results have confirmed the activity of isoenzyme CYP3A4 in the phase I assay.
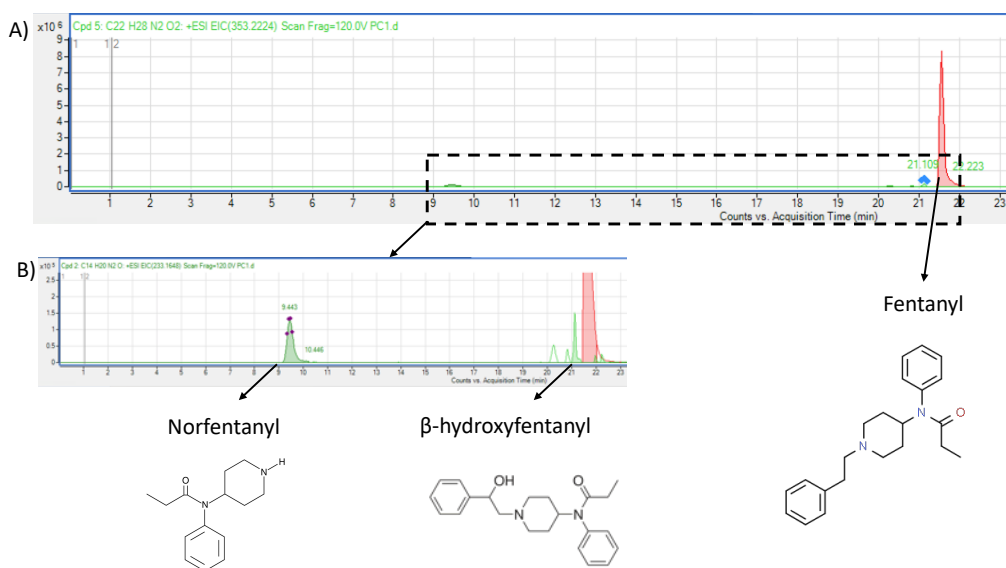
Figure 5-5: A) Chromatogram of fentanyl (red) and biotransformation products norfentanyl and β-hydroxyfentanyl (green) with corresponding structural formulas. A more detailed chromatogram is shown in (B).

5.4.2.2 *Chlorogenic acid, caffeic acid and quinic acid*

No phase I biotransformation products were detected for the three tested xenobiotics suggesting no phase I biotransformation of these compounds in the intestinal cell wall. Figure 5-6 presents the relative areas of chlorogenic acid, caffeic acid and quinic acid in the negative control samples and 1 h (n=3) and 3 h (n=3) phase I replicates. For all three tested xenobiotics, no differences in relative area were observed between 1 h and 3 h incubation, suggesting no further biotransformation. Higher relative abundances were observed for chlorogenic acid and caffeic acid negative control samples without cofactor (NO COF), however differences in relative area between the negative control without HIM (NO HIM) and the replicates were negligible, suggesting a negative influence of the cofactor on the relative area of the xenobiotics. The signal in the quinic acid NC COF sample was clearly lower in comparison to the replicates due to high signal of internal standard valsartan. The same trend was observed for internal

standard theofyllin and thus the deviating results may be caused by an error during addition of the internal standard-containing stop-solution.

Lafay et al. (2006) reported the recovery of caffeic acid due to esterase activity of the gut mucosa when chlorogenic acid was perfused in an *in situ* rat perfusion model. The applied HIM in this assay were eluted using the esterase inhibitor phenylmethylsulfonyl-fluoride (PMSF), necessary to protect CYP450 enzymatic activity during the isolation of the microsomes. PMSF-free HIM fractions should be used to study esterase biotransformation-pathways. Furthermore, the reported intestinal biotransformation of caffeic acid into ferulic acid was not observed in this study.

As no phase I biotransformation products were detected, the results suggest that the CYP450 isotypes responsible for chlorogenic acid, caffeic acid and quinic acid biotransformation are not expressed in the HIM. CYP3A4 and CYP2C9 are the most prominent expressed isotypes in the intestinal epithelia cells, accounting for 80% and 14% of the present CYP450 enzymes. Minor CYP450 isoforms are CYP2C19, CYP2J2 and CYP2D6 (Xie et al. 2016). Furthermore, caffeic acid has been reported to feature inhibitory effects on CYP1A2, CYP2C9, CYP2C19 and CYP3A4 isotypes in HLM which could interfere with the enzymatic activity of the CYP450 isotypes expressed in the HIM and thus may explain the lack of biotransformation products (Rastogi and Jana 2014).
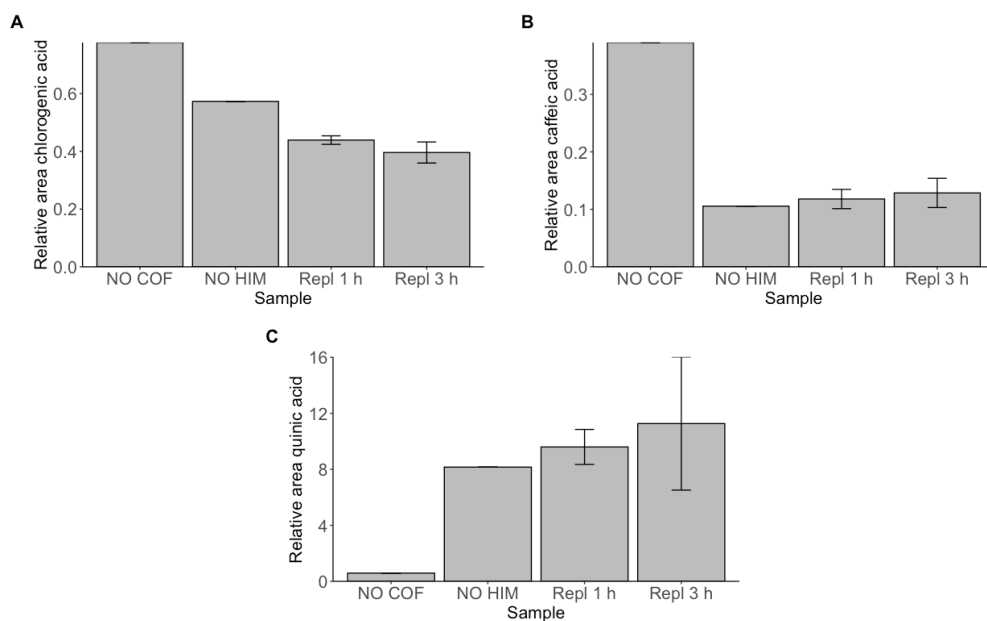
Figure 5-6: Relative area of chlorogenic acid (A), caffeic acid (B) and quinic acid (C) in the negative control samples without cofactor (NO COF) and human intestinal microsomes (NO HIM) and in the 1 h (n=3) and 3 h (n=3) phase I replicates (Repl 1 h,Repl 3 h).

5.4.3   Phase II biotransformation

5.4.3.1   Positive control

4-NP-Gluc and 4-NP-Sulf were monitored as positive control compounds for the phase II enzymatic activity. 4-NP-Gluc and 4-NP-Sulf were both detected in the positive control samples. 4-NP was no longer detected in the sulfate positive control sample, while 4-NP was still detected in the glucuronide positive control sample. These results confirm the reliability of both the glucuronidation and sulfation assay.
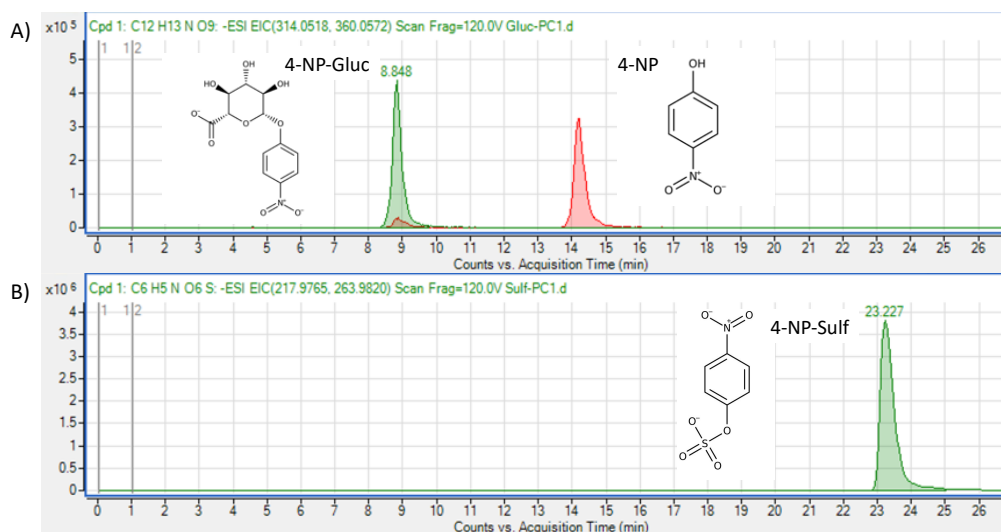
Figure 5-7: A) Chromatogram of the glucuronide positive control sample with 4-nitrophenol (4-NP) and 4-NP-glucuronide (4-NP-Gluc). B) Chromatogram of the sulfate positive control sample with 4-NP-sulfate (4-NP-Sulf).

5.4.3.2 Chlorogenic acid

Two features with molecular formula $C_{22}H_{26}O_{15}$ ([M - H]$^-$, *m/z* 433.0432), corresponding to chlorogenic acid-glucuronide were detected at 19.3 and 21.0 min in all three replicates and the gluc-direct sample. However, the abundance was low in all replicates and thus no MS/MS spectra could be recorded (Table 5-1, Figure SI- 5-1-A). Identification corresponds to confirmation level 4 as proposed by Schimansky et al. (2014) (Figure SI-2-4). Two isomers of chlorogenic acid-sulfate ([M - H]$^-$, *m/z* 433.0432, Figure 5-9) were mainly detected in the sulf-direct sample (Figure 5-8-A, Table 5-1). The relative areas in the replicates including phase I incubation (relative area of 0.021 $\pm$ 0.005) were negligible in comparison to the sulf-direct sample (relative area of 0.12). These results suggest that prior phase I incubations influence the amount of chlorogenic acid-sulfate formation. However, the underlying mechanism remains unclear. Identification was based on the acquired MS/MS spectra. Product ion *m/z* 353.0878 corresponded to the loss of the sulfate-group, *m/z* 191.0549 corresponded to the quinic acid moiety (Figure 5-8-B).

The reported data are in agreement with the findings of an *in vivo* study in ileostomy patients, which detected both chlorogenic acid-glucuronide and -sulfate in the ileal fluid after coffee consumption (Stalmach et al. 2010).
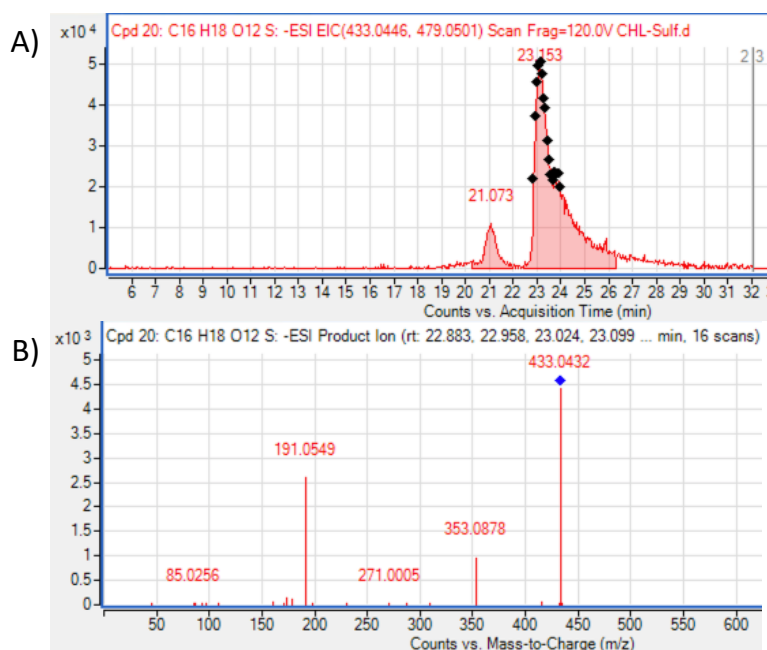
Figure 5-8: A) Extracted ion chromatogram (EIC) of chlorogenic acid-sulfate (m/z 433.0432, $C_{16}H_{17}O_{12}S^-$, $[M - H]^-$) which presents the number of counts of the extracted ion over acquisition time (min). B) The acquired MS/MS spectrum of chlorogenic acid-sulfate.

5.4.3.3   Caffeic acid

Similar results as reported for chlorogenic acid were observed for caffeic acid. Two features ($[M - H]^-$, *m/z* 355.0694) with molecular formula $C_{15}H_{16}O_{10}$, corresponding to the glucuronidation of caffeic acid, were detected in the caffeic acid-glucuronide replicates. However, detected abundances were low and no MS/MS spectra were recorded (L4-confirmation, Table 5-1, Figure SI- 5-1). Two caffeic acid-sulfate isomers, corresponding to caffeic acid-3- and 4-O-sulfate ($[M - H]^-$, *m/z* 258.9918, Figure 5-9) were detected in the sulfate samples and identification was confirmed based on the acquired MS/MS spectra (L3-confirmation, Figure 5-10). Product ion *m/z* 179.038

corresponded to the loss of the sulfate group and product ion *m/z* was a mutual product ion with caffeic acid. The relative areas of caffeic acid-sulfate were lower in the replicates in comparison to the sulf-direct sample, however, the difference was less pronounced as observed for chlorogenic acid: relative area of 0.6 ± 0.2 (replicates) vs. 1.0 (sulf-direct). Caffeic acid-3'- and 4'-O-sulfate were detected by Stalmach et al. (2010) with caffeic acid-3'-O-sulfate as the major isomer.

The findings reported for chlorogenic acid and caffeic acid are in correspondence with the study of Wong et al. (2010) who studied the phase II conjugation biotransformation pathways of hydroxycinnamic acids using intestinal S9 homogenates and recombinant UGTs and SULTs. The study reported sulfate-conjugates accounted for 95% of the detected phase II conjugation biotransformation products. Furthermore, sulfation was favored on the 3'-hydroxyl over the 4'-hydroxyl position, suggesting chlorogenic acid-3'-sulfate and caffeic acid-3'-sulfate corresponded to the features with retention times 23.2 and 22.3 min respectively. Caffeic acid-glucuronide isomers were detected however at low levels (Wong et al. 2010). *In vivo* studies investigating the caffeic acid biotransformation products in urine and ileal fluid of human volunteers after coffee consumption identified caffeic acid-sulfate isomers. Free caffeic acid and caffeic acid-glucuronides were not detected (Stalmach et al. 2010, Wong et al. 2010).

R = H
A) Caffeic acid-3'-sulfate
B) Caffeic acid-4'-sulfate

R =

A) Chlorogenic acid-3'-sulfate
B) Chlorogenic acid-4'-sulfate
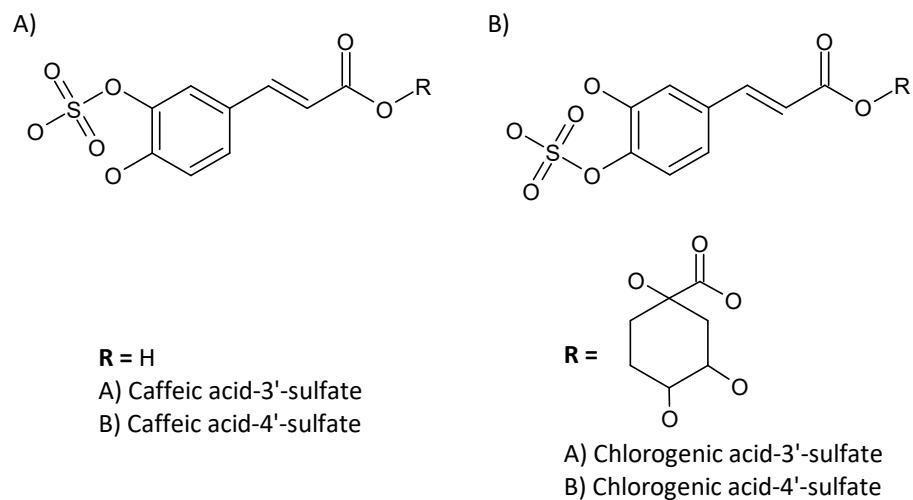
Figure 5-9: Chemical structures of the identified sulfate-conjugation biotransformation products of caffeic acid and chlorogenic acid.
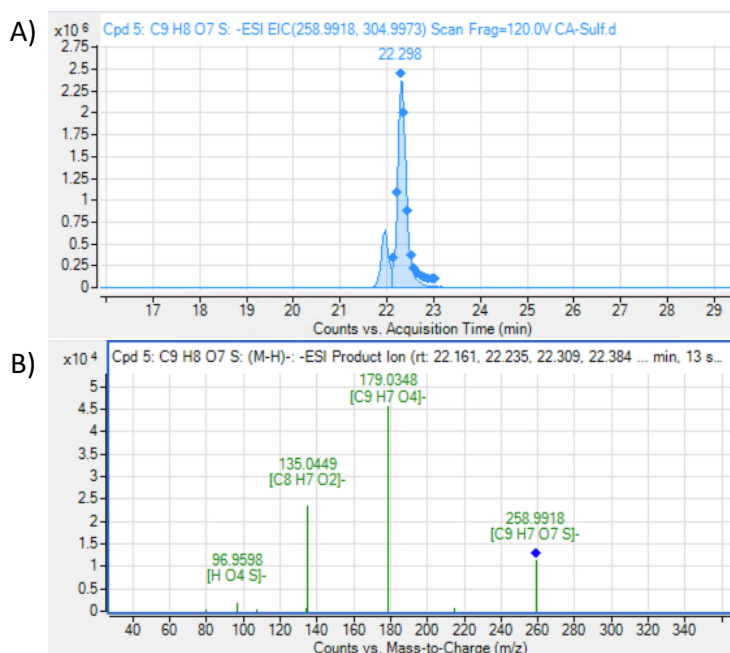
Figure 5-10: A) Extracted ion chromatogram (EIC) of caffeic acid-sulfate (*m/z* 258.9918, $C_9H_7O_7S^-$, [M - H]$^-$) which presents the number of counts of the extracted ion over acquisition time (min). B) The acquired MS/MS spectrum of caffeic acid-sulfate.

Table 5-1: Overview of identified biotransformation products and additional information: compound name, molecular formula, level of confirmation as proposed by Schymanski et al.(Figure SI- 2-4) (Schymanski et al. 2014), retention time (t_r), exact mass, detected parent ion, mass difference. Level 3 (L3): tentative candidates based on experimental data; level 4 (L4): Unequivocal molecular formula based on MS1 and isotope ratios. NA: not acquired.

Compound name	Molecular formula	Level of confirmation	t_r (min)	Exact mass (g/mol)	Parent ion (*m/z*)	Δ Mass (ppm)	MS/MS product ions
Chlorogenic acid-glucuronide isomer 1	$C_{22}H_{26}O_{15}$	L4	19.3	530.1272	529.1202	1.65	NA
Chlorogenic acid-glucuronide isomer 2	$C_{22}H_{26}O_{15}$	L4	21.0	530.1272	529.1196	3.2	NA
Chlorogenic acid-3'-sulfate	$C_{16}H_{18}O_{12}S$	L3	23.2	434.0519	433.0447	0.26	353.0878 $[C_{16}H_{17}O_9]^-$; 191.0549 $[C_7H_{11}O_6]^-$
Chlorogenic acid-4'-sulfate	$C_{16}H_{18}O_{12}S$	L3	21.1	434.0519	433.0444	-0.23	353.0878 $[C_{16}H_{17}O_9]^-$; 191.0549 $[C_7H_{11}O_6]^-$
Caffeic acid-glucuronide isomer 1	$C_{15}H_{16}O_{10}$	L4	12.8	356.0743	355.0694	1.26	NA
Caffeic acid-glucuronide isomer 2	$C_{15}H_{16}O_{10}$	L4	16.1	356.0743	355.0660	-3.25	NA
Caffeic acid-3'-sulfate	$C_9H_8O_7S$	L3	22.3	259.9991	258.9925	2.61	179.0348 $[C_9H_7O_4]^-$; 135.0449 $[C_8H_7O_2]^-$; 96.9598 $[SO_4H]^-$
Caffeic acid-4'-sulfate	$C_9H_8O_7S$	L3	21.9	259.9991	258.9918	-0.15	179.0346 $[C_9H_7O_4]^-$; 135.0450 $[C_8H_7O_2]^-$; 96.9598 $[SO_4H]^-$

5.4.3.4 *Quinic acid*

No phase II biotransformation products of quinic acid were detected. Although a decrease in relative area of quinic acid was observed in the sulfate replicates in comparison to the negative control, no sulfate-conjugates were detected using the complementary data-analysis workflows. No clear difference in relative area of quinic acid was observed for the glucuronide replicates and negative control (Figure 5-11). Quinic acid and phase II biotransformation products were not reported by Stalmach et al. (2010) and Wong et al. (2010). However, it is not clear if quinic acid and related biotransformation products were not detected or not investigated by the authors. To the best of our knowledge, no glucuronide or sulfate-conjugates of quinic acid have been reported in the literature.
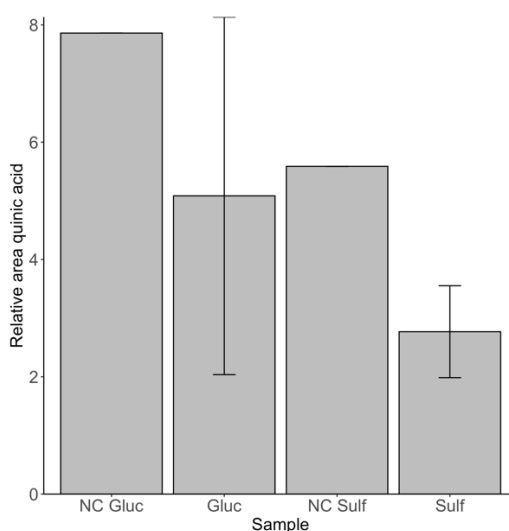
Figure 5-11: Relative area of quinic acid in the glucuronide negative control (NC Gluc) sample, glucuronide replicates (Gluc, n=3), sulfate negative control sample (NC Sulf) and sulfate replicates (Sulf, n=3)

5.4.3.5 *Regional differences in expression of drug biotransforming enzymes*

The reported results present the first-pass biotransformation of chlorogenic acid, caffeic acid and quinic acid in the small intestinal gut wall as HIM are isolated from enterocytes. However, although regional differences across the gastrointestinal tract on the expression of some drug biotransforming enzymes have been reported (Bergheim et al. 2005, Teubner et al. 2007), results can be correlated to the colonic first-pass biotransformation. It has been shown that the total CYP450 content decreases in the ileum and colon in comparison to the proximal parts of the gastrointestinal tract limiting the importance of the phase I biotransformation pathways in this regions (Bergheim et al. 2005). Regarding the phase II enzymes, expression of UGTs isoforms have been reported to be constant over the small intestine and the colon (Wu et al. 2011, Peters et al. 2016), while differences in SULTs have been described (Teubner et al. 2007). However, SULT1A1 and SULT1A3, present in both small intestine and colon, have been reported to be the major isoforms responsible for sulfation of caffeic acid (Teubner et al. 2007, Wong et al. 2010).

5.5 Conclusions

No phase I biotransformation products of chlorogenic acid, caffeic acid or quinic acid were detected in the intestinal *in vitro* biotransformation assay incubations. For both chlorogenic acid and caffeic acid (i) two isomers of the sulfate-conjugates were identified and (ii) low-abundance features corresponding to chlorogenic acid-glucuronide and caffeic acid-glucuronide were detected. No phase II biotransformation products of quinic acid were identified. These first-pass results can aid in a better understanding of the oral bioavailability of chlorogenic acid and its biotransformation products together with other variables such as fraction absorbed and fraction subjected to hepatic biotransformation.

5.6   Supplementary information
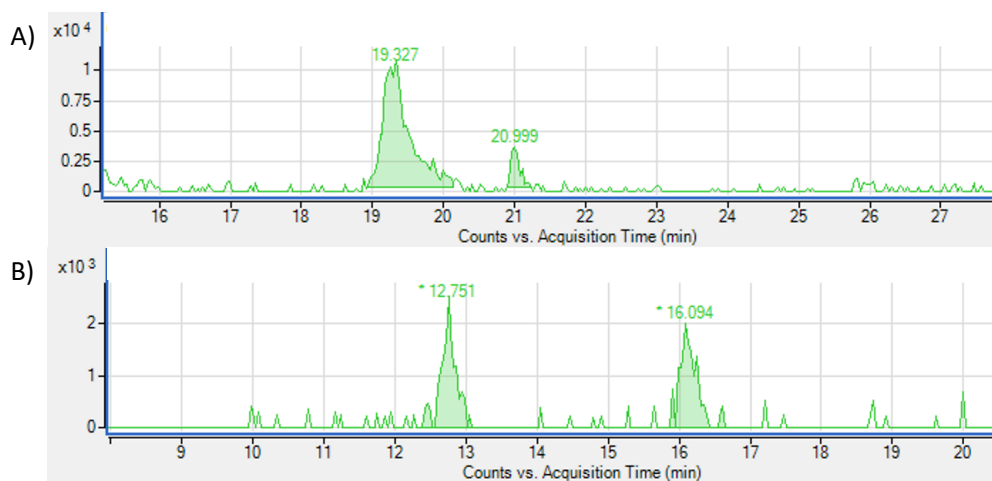
Figure SI- 5-1: Extracted ion chromatogram (EIC) of features *m/z* 529.1196 (A) and *m/z* 355.0694 (B) corresponding to glucuronide-conjugates of chlorogenic acid and caffeic acid respectively.

References

Bergheim I, Bode C and Parlesak A. Distribution of cytochrome P450 2C, 2E1, 3A4, and 3A5 in human colon mucosa. *BMC clinical pharmacology* 2005, 5: 4-4.

Clifford MN, Kerimi A and Williamson G. Bioavailability and metabolism of chlorogenic acids (acyl-quinic acids) in humans. *Comprehensive Reviews in Food Science and Food Safety* 2020, 19(4): 1299-1352.

Giacomelli C, Miranda FdS, Gonçalves NS and Spinelli A. Antioxidant activity of phenolic and related compounds: a density functional theory study on the O–H bond dissociation enthalpy. *Redox Report* 2004, 9(5): 263-269.

Hatley OJD, Jones CR, Galetin A and Rostami-Hodjegan A. Quantifying gut wall metabolism: methodology matters. *Biopharmaceutics & Drug Disposition* 2017, 38(2): 155-160.

Huang Q, Deshmukh RS, Ericksen SS, Tu Y and Szklarz GD. Preferred binding orientations of phenacetin in CYP1A1 and CYP1A2 are associated with isoform-selective metabolism. *Drug metabolism and disposition: the biological fate of chemicals* 2012, 40(12): 2324-2331.

Iturrospe E, Da Silva KM, Andujar BT, Cuykx M, Vanhaecke T, Covaci A and van Nuijs ALN. An exploratory approach for an oriented development of an untargeted multi-purpose LC-MS platform to investigate hydrophilic metabolites in different biological matrices. In preparation.

Jia L and Liu X. The conduct of drug metabolism studies considered good practice (II): in vitro experiments. *Current Drug Metabolism* 2007, 8(8): 822-829.

Mortele O, Vervliet P, Gys C, Degreef M, Cuykx M, Maudens K, Covaci A, van Nuijs ALN and Lai FY. In vitro Phase I and Phase II metabolism of the new designer benzodiazepine cloniprazepam using liquid chromatography coupled to quadrupole time-of-flight mass spectrometry. *Journal of Pharmaceutical and Biomedical Analysis* 2018, 153: 158-167.

Peters SA, Jones CR, Ungell A-L and Hatley OJD. Predicting Drug Extraction in the Human Gut Wall: Assessing Contributions from Drug Metabolizing Enzymes and Transporter Proteins using Preclinical Models. *Clinical Pharmacokinetics* 2016, 55: 673-696.

Rastogi H and Jana S. Evaluation of inhibitory effects of caffeic acid and quercetin on human liver cytochrome p450 activities. *Phytotherarphy Research* 2014, 28(12): 1873-1878.

Schymanski EL, Jeon J, Gulde R, Fenner K, Ruff M, Singer HP and Hollender J. Identifying small molecules via high resolution mass spectrometry: communicating confidence. *Environmental Sciences and Technology* 2014, 48(4): 2097-2098.

Stalmach A, Steiling H, Williamson G and Crozier A. Bioavailability of chlorogenic acids following acute ingestion of coffee by humans with an ileostomy. *Archives of Biochemistry and Biophysics* 2010, 501(1): 98-105.

Teubner W, Meinl W, Florian S, Kretzschmar M and Glatt H. Identification and localization of soluble sulfotransferases in the human gastrointestinal tract. *The Biochemical journal* 2007, 404(2): 207-215.

Vervliet P, Mortele O, Gys C, Degreef M, Lanckmans K, Maudens K, Covaci A, van Nuijs ALN and Lai FY. Suspect and non-target screening workflows to investigate the in vitro and in vivo metabolism of the synthetic cannabinoid 5Cl-THJ-018. *Drug Testing and Analysis* 2018, 11(3): 479-491.

Wong CC, Meinl W, Glatt H-R, Barron D, Stalmach A, Steiling H, Crozier A and Williamson G. In vitro and in vivo conjugation of dietary hydroxycinnamic acids by UDP-glucuronosyltransferases and sulfotransferases in humans. *The Journal of Nutritional Biochemistry* 2010, 21(11): 1060-1068.

Wu B, Kulkarni K, Basu S, Zhang S and Hu M. First-pass metabolism via UDP-glucuronosyltransferase: a barrier to oral bioavailability of phenolics. *Journal of Pharmaceutical Sciences* 2011, 100(9): 3655-3681.

Xie F, Ding X and Zhang Q-Y. An update on the role of intestinal cytochrome P450 enzymes in drug disposition. *Acta pharmaceutica Sinica. B* 2016, 6(5): 374-383.

Zanger UM and Schwab M. Cytochrome P450 enzymes in drug metabolism: Regulation of gene expression, enzyme activities, and impact of genetic variation. *Pharmacology & Therapeutics* 2013, 138(1): 103-141.

CHAPTER 6: GENERAL DISCUSSION, CONCLUSIONS AND FUTURE PERSPECTIVES

CHAPTER 6

CHAPTER 6

6.1 General discussion

The main objective of this PhD project was to gain a more in-depth understanding on the role of the gut microbiome on the gastrointestinal fate of orally ingested xenobiotics. Three sub-objectives were defined (Table 6-1): (i) optimize a ready-to-use *in vitro* gastrointestinal platform including the gastrointestinal dialysis model with colon phase (GIDM-Colon) and bioanalytical strategies to investigate and elucidate the gastrointestinal biotransformation of xenobiotics, (ii) application of the *in vitro* gastrointestinal platform to investigate inter-population differences in microbiotic biotransformation of xenobiotics between a lean and obese population and (iii) expand the *in vitro* gastrointestinal platform with an *in vitro* intestinal absorption and *in vitro* intestinal first-pass assay using a Caco-2 cell line and human intestinal microsomes (HIM)/human intestinal cytosol (HICYT) respectively.

6.1.1 *In vitro* gastrointestinal biotransformation platform

In order to obtain a high level of physiological significance, *in vitro* platforms should be optimized to be representative for the *in vivo* conditions. Chapter 2 illustrated the optimization of a ready-to-use *in vitro* gastrointestinal platform including the GIDM-Colon to study the microbiotic biotransformation of xenobiotics. Incubation medium and incubation time of the pooled fecal slurry suspension, a bioanalytical platform to elucidate microbiotic biotransformation products and dialysis-timing were optimized.

6.1.1.1 Incubation medium

The GIDM-Colon, previously developed and validated by Breynaert et al. (2010), was applied throughout the PhD project as *in vitro* gastrointestinal model. This model included a 17 h incubation step of the pooled fecal slurry suspension in Wilkin-Chalgren Anaerobe broth (WCB) before use as inoculum in the colon stage. The results illustrated in chapter 2 showed that 17 h incubation of the pooled fecal slurry suspension in WCB led to a change in bacterial composition which compromised

comparability with the *in vivo* situation. Incubation of the pooled fecal slurry suspension in sterile phosphate buffer as medium guaranteed a closer resemblance to the *in vivo* situation. Sterile phosphate buffer was chosen as alternative medium as a shift in bacterial composition would be less likely as it does not contain any nutrients and as it was previously applied in other gut microbiome biotransformation studies (Tomas-Barberan et al. 2014, Amaretti et al. 2015). Other available *in vitro* gastrointestinal models such as the SHIME include the use of growth medium. The use of growth medium throughout SHIME is justified as these experiments last a few weeks (2 weeks stabilization, 2 weeks basal period and 2-4 weeks treatment period) and thus nutrients are required to ensure the viability of the bacteria, while the colon stage of the GIDM-Colon only lasts 24 h (Breynaert et al. 2015, Van de Wiele et al. 2015). Viability of the bacteria in phosphate buffer over the duration for the GIDM-Colon experiment was confirmed as presented in chapter 2. Furthermore, biotransformation activity of the bacteria using the optimized protocol was ensured by application of model compound chlorogenic acid, which should be included as positive control compound in future experiments (Mortelé et al. 2019).

6.1.1.2   Bioanalytical platform

Multiple bioanalytical aspects of the *in vitro* gastrointestinal biotransformation platform were optimized. The presented liquid chromatography column screening is compound-dependent and should be performed for each tested xenobiotic based on available literature and physicochemical properties of the compound. The effect of 4 sample preparation procedures on the biotransformation product extraction efficiency was evaluated. The centrifugation sample preparation procedure immediately removed the bacteria from the sample thus neglecting possible intracellular biotransformation products. No significant differences were observed when applying the extraction and sonication sample preparation procedures suggesting the procedures did not result in additional leakage of intracellular biotransformation products. The freeze-drying procedure could clearly be considered

the minor option. The inferiority of the latter could be explained by irreversible binding of hydrophilic biotransformation products to matrix components during the process of lyophilization (Gromova and Roby 2010, Wu et al. 2010). The extraction method was chosen as optimal procedure due to the limited time needed for sample preparation, leading to an increased throughput of samples.

Combining suspect and non-targeted data-analysis workflows has proven to have an added value on the elucidation and identification of biotransformation products. None of the data-analysis workflows was able to identify all reported biotransformation products and thus combination of workflows is advisable to obtain an increased output. The reported findings are in agreement with previous *in vitro* human liver microsome (HLM) biotransformation studies (Mortele et al. 2018, Vervliet et al. 2018). Elucidating the origin of the observed differences in number of identified biotransformation products between the different data-analysis workflows remains a challenge as the underlying algorithms of data-analysis software are not fully known. Hohrenk et al. (2020) applied multiple non-targeted screening data-analysis workflows to the same raw data files and observed dissimilarities in the final feature list, although all workflows include similar steps (e.g. peak picking, blank subtraction). Further research is necessary to unravel the influence of different processing steps and parameters on the outcome (Hohrenk et al. 2020).

6.1.1.3   *Dialysis*

The GIDM-Colon protocol includes dialysis of small intestinal and colonic fluids. Dialysis have been reported to be an essential tool to maintain highly active microbiota and representative microbial metabolite-concentrations during gut microbiota biotransformation experiments (Venema 2015). However, dialysis was not performed overnight (between 6 h and 24 h colonic stage) in the original GIDM-Colon protocol due to the risk of too much fluid loss from the dialysis cells. Not performing dialysis could lead to accumulation of xenobiotic biotransformation products or bacterial

metabolites (Venema 2015). Chapter 2.4 illustrated that parallel GIDM-Colon experiments covering different sampling timepoints and dialysis-timing were not complementary. As the timing of the dialysis was the only variable, it was concluded that performing dialysis influences the microbial biotransformation activity and thus the detected biotransformation products. The exact cause of the observed differences is not known, however, (i) saturation of microbial enzymes due to accumulation of chlorogenic acid biotransformation products and (ii) a different starting point of the dialysis are possible hypotheses. Future GIDM-Colon experiments should include continuous dialysis as this will ensure a stable biotransformation activity of the gut microbiota during the colonic stage and will allow analysis of biotransformation reactions over the timeframe of 0 h and 24 h incubation. The instrumental adaptations necessary to allow 24 h dialysis throughout the GIDM-Colon are available and can be implemented and optimized for future experiments.

6.1.2 Gut microbiome dysbiosis is associated with differences in microbiotic biotransformation of xenobiotics

6.1.2.1 *Gut microbiome dysbiosis in obesity*

The number of fecal samples included in this thesis was limited and thus hampering the evaluation of gut microbiome dysbiosis between an obese and lean population. A study by Falony et al. (2016) reported 865 lean and obese volunteers would be necessary to evaluate obesity-related microbiota compositional changes with 5% significance level and statistical power of 80%. Sample size could be reduced to 535 individuals of both populations when gender and age were taken into account (Falony et al. 2016). Very stringent inclusion criteria were included in the recruitment process of this study to exclude variables, other than obesity, possibly influencing the gut microbiome. Downside of this procedure was the difficulty of finding suitable volunteers willing to donate a fecal sample. Despite the limited number of samples,

differences in gut microbiota composition and bacterial concentration were observed between the obese and lean population. Reduced bacterial diversity has been previously associated with obesity (Turnbaugh et al. 2009, Davis 2016). The illustrated data in this thesis showed a similar trend. Less diversity of bacterial species was observed in the obese samples (Figure 6-1), as well as a lower concentration of anaerobic bacteria. Furthermore, unique operational taxonomic units (OTUs) were reported for both the lean and obese population. The increased Firmicutes/Bacteroidetes ratio repeatedly associated with obesity was not detected in the samples, but again, this may be explained by the low number of samples (Ley et al. 2005, Ley et al. 2006, Turnbaugh et al. 2008, Turnbaugh et al. 2009). Future experiments should include metagenomic shotgun sequencing as it provides information on the potential functions of the gut microbiome (Davis 2016).
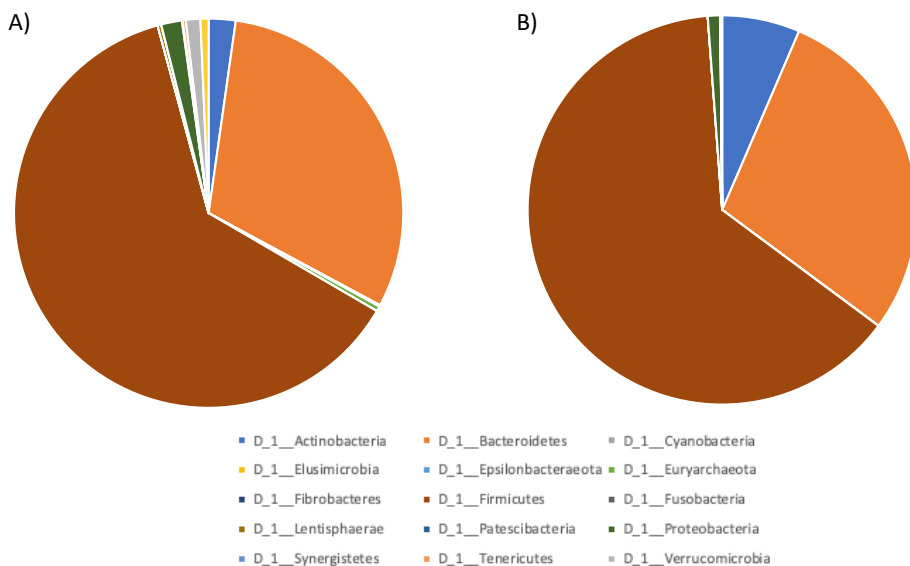
Figure 6-1: Mean gut microbiota composition of the lean (A, n=9) and obese (B, n=4) population on phylum-level.

6.1.2.2   *Differences in microbiotic biotransformation*

Using the optimized *in vitro* gastrointestinal platform, interindividual differences in number of biotransformation products and biotransformation rate between a lean and obese population were detected. The reported lower biotransformation rate of chlorogenic acid by the obese population is in disagreement with the proposed highly efficient energy extracting metabolic pathways of the obese gut microbiome (Ley et al. 2005, Ley et al. 2006, Turnbaugh et al. 2008, Turnbaugh et al. 2009). However, as reported for CYP450 enzymes, the microbiotic biotransformation reactions are substrate-dependent (Aguirre et al. 2016b). This may explain the observed results and emphasizes the importance of investigating the differences in microbiotic biotransformation between populations for each xenobiotic individually. Further research should reveal if the observed differences are due to the differences in number of bacteria, diversity and/or the presence or absence of specific bacterial strains. No conclusions on the cause of the observed differences could be drawn based on the data presented in this thesis. Knowledge on the underlying cause will aid in a better understanding and future development of the research field of personalized medicine.

One of the limitations of the study is the limited number of included lean (n=9) and obese donors (n=4). Aguirre et al. (2014) previously stated that the use of pooled fecal samples as inoculum brings important advantages for *in vitro* fermentation studies, as pooling will increase the biodiversity and will lead to a more representative microbiota for the tested population. Thus, suggesting that increasing the number of obese and lean donors would improve the representation of both populations. Until now, no general guideline on the number of donors needed for a representative fecal pool has been published, and varying protocols are reported in literature. A study on the fermentation differences of arabinogalactan and inulin between lean and obese subjects included 8 and 7 donors respectively (Aguirre et al. 2016a). Studies reporting protocols for standardized fecal inocula included 4 (Aguirre et al. 2015) and 6 (O'Donnell et al. 2016) donors.

The presented results in this thesis confirmed that changes in gut microbiota related to obesity are associated with differences in microbiotic biotransformation of xenobiotics and thus possibly influencing the activity, bioavailability and toxicity of orally administered xenobiotics. This was, to the best of our knowledge, the first study investigating differences in microbiotic biotransformation of xenobiotics between obese and lean volunteers. Differences in microbiotic biotransformation of saponins between T2D and non-diabetic patients have previously been reported, suggesting differences could also be observed for other diseases (Zhou et al. 2017). Multiple human diseases, including type 2 diabetes (T2D) (Larsen et al. 2010, Qin et al. 2012, Sedighi et al. 2017), inflammatory bowel disease (Machiels et al. 2014, Schirmer et al. 2018) and colorectal cancer (Wang et al. 2012, Wu et al. 2013) are associated with gut microbiome-dysbiosis and should be included in future research.

6.1.3 Expansion of the *in vitro* gastrointestinal platform

The *in vitro* gastrointestinal platform was expanded using model compound chlorogenic acid and two of its most abundant gastrointestinal biotransformation products caffeic acid and quinic acid.

6.1.3.1 *In vitro intestinal absorption*

Intestinal absorption of chlorogenic acid and quinic acid was studied using the human intestinal epithelial Caco-2 cell line derived form a colorectal adenocarcinoma (Lea 2015). Although the cell line differentiates towards a cell monolayer with characteristic apical brush border with microvilli, studies have shown that Caco-2 cells are a suitable tool for the estimation of colonic absorption of xenobiotics (Rubas et al. 1996, Tannergren et al. 2009). The absorption of lipophilic compounds, which is not applicable for chlorogenic acid and its microbial biotransformation products, may be underestimated in the current setup due to the absence of bile acids (Lea 2015,

Pavlović et al. 2018). This should be kept in mind for future experiments and may be solved by the use of samples resulting from the GIDM-Colon experiments as donor solutions in the Caco-2 permeability assay. The use of GIDM-Colon samples would enhance the representation to the *in vivo* situation in comparison to the use of standard-solutions as currently applied in the assay: (i) the composition of the donor solution, including bile acids and pH will be more representative for the *in vivo* composition, and (ii) the donor solution will contain the test xenobiotic and/or multiple microbiotic biotransformation products which will result in competition for protein binding sites. The use of extracts resulting from the SHIME as donor solutions in Caco-2 assays have been previously reported and should be included in future experiments for the GIDM-Colon (Garcia-Villalba et al. 2017, Réquilé et al. 2018). Difficulties and challenges related to the utilization of GIDM-Colon samples in the Caco-2 assay are further addressed in the future perspectives (6.3).Including positive control compounds in the experimental setup are essential for reliability of the assay and proper interpretation of the data as variability between Caco-2 permeability experiments have been described (Grès et al. 1998, Volpe 2008, Lea 2015, Stockdale et al. 2019). The use of propranolol and digoxin as reference compounds for a high passive permeability and P-glycoprotein (P-gp) mediated efflux confirmed the reliability of the *in vitro* permeability assay and the acquired results.

6.1.3.2   *In vitro intestinal first-pass metabolism*

Poor reproducibility and low abundances of CYP450 enzymes and low enzymatic activity have been reported for human intestinal microsomes (HIM). Factors causing these difficulties include degradation of enzymes during the isolation process and greater heterogeneity of the intestine in comparison to the liver. Past few years, improvements have been made due to the use of protease inhibitors, limiting the degradation of enzymes, and new isolation methodologies. However, a wide range of different HIM-preparation protocols are still applied and further standardization, which will enhance inter-experiment comparability, is needed (Hatley et al. 2017).

The HIM and HICYT concentrations of the applied *in vitro* biotransformation assay, based on an in-house developed protocol using human liver microsomes (HLM) and cytosol (HLCYT), were optimized using positive control compounds for phase I and II biotransformation (Mortele et al. 2018, Vervliet et al. 2018). The absence of phase I biotransformation products of phenacetin confirmed the differences in CYP450 isotypes expression between HLM and HIM. CYP1A2, mainly responsible for phenacetin biotransformation and expressed in the liver, is not expressed in the intestinal cell wall (Zanger and Schwab 2013, Xie et al. 2016). Fentanyl was successfully included in the experimental setup as positive control for CYP3A4 enzymatic activity to check the reliability of the assay. The experimental assay should be further expanded with a CYP2C9 substrate (e.g. diclofenac) as positive control. The lower reported glucuronidation rate observed for 4-nitrophenol (4-NP), in comparison to HLM, was in agreement with previous experiments using intestinal and liver S9 fractions (Wong et al. 2010). The expression of sulfotransferases (SULTs) was reported to be slightly higher in the enterocytes in comparison to hepatocytes (Riches et al. 2009). Subsequently no differences in 4-NP sulfation were observed. As HIM and HICYT are isolated from the small intestinal enterocytes, extrapolation of the assay results to the colonic first-pass should take differences in enzymatic expression, as described for CYP450 and SULTs, into consideration as demonstrated for chlorogenic acid, caffeic acid and quinic acid in chapter 5 (Bergheim et al. 2005, Teubner et al. 2007).

6.1.4   The gastrointestinal behavior of chlorogenic acid and microbial biotransformation products

The oral bioavailability (F) of a xenobiotic is calculated according to equation 1, where F_a corresponds to the fraction absorbed and F_G and F_H correspond to the fractions escaping gastrointestinal and hepatic biotransformation respectively (Peters et al. 2016).

Equation 1: Formula defining the oral bioavailability (F) of a xenobiotic

$$F = F_a \text{ x } F_G \text{ x } F_H$$

This thesis aimed to evaluate the influence of the gut microbiome on the oral bioavailability and thus absorption and biotransformation using chlorogenic acid as a model compound. Factors F_a and F_G of chlorogenic acid were investigated using the GIDM-Colon, *in vitro* intestinal biotransformation and first-pass assays. The fraction chlorogenic acid available for intestinal absorption (F_a) will mainly be determined by the microbiotic biotransformation, together with other factors such as solubility, stability and formulation dissolution if applicable. As seen for the lean population, chlorogenic acid will be biotransformed in numerous biotransformation products, all of which will be subjected to absorption and intestinal first-pass enzymes.

6.1.4.1   *In vitro intestinal absorption*

The absorption experiments included in the thesis were restricted to chlorogenic acid and quinic acid, however, all microbiotic biotransformation products should be investigated to characterize the gastrointestinal behavior of chlorogenic acid. Due to time constraints, the *in vitro* intestinal absorption of only two compounds could be tested. Quinic acid was chosen over caffeic acid as the intestinal absorption of the latter has been previously investigated using a Caco-2 permeability assay (Konishi and Kobayashi 2004, Farrell et al. 2012, Monente et al. 2015). The illustrated results in chapter 4 suggest an active efflux mechanism involved in the intestinal absorption of chlorogenic acid and quinic acid. The involvement of an active efflux mechanism is of importance for the oral bioavailability as it will influence the fraction absorbed and will result in reduced intracellular xenobiotic concentrations, thus influencing the intestinal first-pass biotransformation (Peters et al. 2016). The involvement of the active efflux protein P-gp in the intestinal absorption of chlorogenic acid was previously reported by Erk et al. (2014) using a pig jejunal mucosa in an Ussing chamber model. However, previous studies investigating the absorption of chlorogenic acid

using a Caco-2 permeability assay did not report the involvement of an active efflux protein (Konishi and Kobayashi 2004, Farrell et al. 2012). Deviating results of Konishi et al. (2004) could be explained by high chlorogenic acid concentrations leading to saturation of the efflux protein (Hubatsch et al. 2007). Deviating results reported by Farrell et al. (2012) may be explained by variations in protein-expression related to Caco-2 cell characteristics (age, passage number) or cell culture conditions (Grès et al. 1998, Volpe 2008, Lea 2015, Stockdale et al. 2019). Dupas et al. (2006) and Monente et al. (2015) both neglected the basolateral to apical transport and thus the presence of an active efflux mechanism was not studied, however, both studies reported a poor apical to basolateral transport of chlorogenic acid which is in agreement with the reported results in this thesis.

The intestinal absorption of quinic acid was studied for the first time. Although high quinic acid concentrations were reported in human plasma after coffee consumption (Erk et al. 2012), these data do not provide information on the intestinal absorption of quinic acid. Additional experiments should be carried out to unravel the efflux protein involved in the transport of quinic acid.

Farrell et al. (2011) studied the intestinal absorption of chlorogenic acid microbial biotransformation products caffeic acid and ferulic acid across a Caco-2 cell monolayer. Ferulic acid showed higher basolateral recoveries in comparison to caffeic acid suggesting methylation positively correlates with enhanced intestinal absorption. These results were confirmed by Monente et al. (2015) who reported similar results including for dihydrocaffeic acid and dihydroferulic acid. No efflux mechanisms were reported for caffeic acid and ferulic acid (Farrell et al. 2012). Since, unlike chlorogenic acid and quinic acid, no active efflux was reported for caffeic acid and ferulic acid, the quinic acid moiety may be the determining factor for active efflux. This hypothesis presents a basis for further research.

6.1.4.2   *In vitro intestinal first-pass*

The lack of identified phase I biotransformation products suggests CYP450 isoenzymes responsible for biotransformation of chlorogenic acid, caffeic acid or quinic acid are not expressed in the human intestinal microsomes. CYP3A4 (80%) and CYP2C9 (14%) are the major expressed isoenzymes in the intestinal epithelial cells. Minor CYP450 expressed isoforms are CYP2C19, CYP2J2 and CYP2D6 (Xie et al. 2016). Phase I CYP450 mediated biotransformation in the intestinal cell wall will be limited to substrates of the expressed isoforms as illustrated with lack and presence of biotransformation products of phenacetin (CYP1A2 substrate) and fentanyl (CYP3A4 substrate) respectively.

The reported phase II biotransformation results of chlorogenic acid and caffeic acid were in agreement with previous *in vitro* and *in vivo* studies (Stalmach et al. 2010, Wong et al. 2010). Sulfation was the major observed conjugation reaction by Wong et al. (2010) when investigating the phase II biotransformation of caffeic acid. Only low levels of caffeic acid-glucuronide were detected *in vitro*. Stalmach et al. (2010) only reported sulfate conjugation products in the ileal fluid and urine of human volunteers after coffee consumption. Apart from conjugates of the parent compounds, no other phase II biotransformation products were identified for chlorogenic acid and caffeic acid. This can be explained by the absence of any phase I biotransformation products. No phase II conjugates of quinic acid were identified. No previous data on quinic acid conjugation biotransformation products could be retrieved from the literature. Furthermore, the *in vitro* and *in vivo* studies by Wong et al. (2010) and Stalmach et al. (2010) did not report quinic acid or biotransformation products.

Our results show that both chlorogenic acid and microbial biotransformation product quinic acid exhibit a low intestinal absorption due to the involvement of an active efflux mechanism (Figure 6-2). Low absorption has also been reported for caffeic acid in the literature (Farrell et al. 2012). The fraction absorbed of chlorogenic acid and

caffeic acid, however, will be exposed to intestinal phase II conjugation reactions, while no intestinal first-pass has been detected for quinic acid.

Table 6-1: Overview of the predefined objectives, the main findings resulting from this PhD thesis and the related future perspectives. CA: caffeic acid, CHL: chlorogenic acid, GIDM-Colon: gastrointestinal dialysis model with colon-stage, OTUs: operational taxonomic units, QA: quinic acid, WCB: Wilkin-Chalgren Anaerobe Broth.

Objectives	Main findings	Future perspectives
1. Optimize a ready-to-use *in vitro* platform including the GIDM-Colon and bioanalytical strategies to investigate the gastrointestinal biotransformation of xenobiotics. **Chapter 2**	• Incubation medium WCB was replaced by **sterile phosphate buffer**: closer resemblance to the *in vivo* situation. • 17 h incubation step: no advantages over a **1 h adaptation period**. • Optimization of sample preparation procedure of GIDM-Colon extracts • Confirming the added value of combining suspect and non-targeted screening **data-analysis workflows** • GIDM-Colon experiments with deviating dialysis- and sampling intervals were not complementary.	• Optimize protocol for 24 h continuous dialysis GIDM-Colon experiments
2. Application of the optimized *in vitro* platform to study interindividual differences in microbiotic biotransformation of xenobiotics between lean and obese populations, using CHL as model compound. **Chapter 3**	• **Differences in alfa- and beta-diversity** between the lean and obese gut microbiome. • **Lower concentration** of bacteria in the obese samples • **Lower biotransformation rate of the obese** gut microbiome in comparison to the lean gut microbiome.	• Unravel cause of the observed differences between the lean and obese population: number of bacteria or unique OTUs. • Obese/lean experiment with 24 h continuous dialysis experiment. • Study interpopulation differences in microbiotic biotransformation of other human diseases associated with gut microbiome dysbiosis

Table 6-1 (continued)

Objectives	Main findings	Future perspectives
3. Expansion of the *in vitro* gastrointestinal platform with an *in vitro* intestinal absorption and *in vitro* intestinal first pass assay using CHL as model compound. **Chapter 4 and Chapter 5**	• Presence of an **active efflux transport** for CHL and QA intestinal absorption. • **No intestinal phase I** biotransformation products of CHL, CA and QA. • CHL and CA: **glucuronidation and sulfation**	• Study the *in vitro* intestinal absorption and first-pass effect of all microbiotic biotransformation products of CHL • Identify the protein responsible for QA active efflux. • Optimize the *in vitro* permeability assay to allow the use of GIDM-Colon extracts as donor solutions
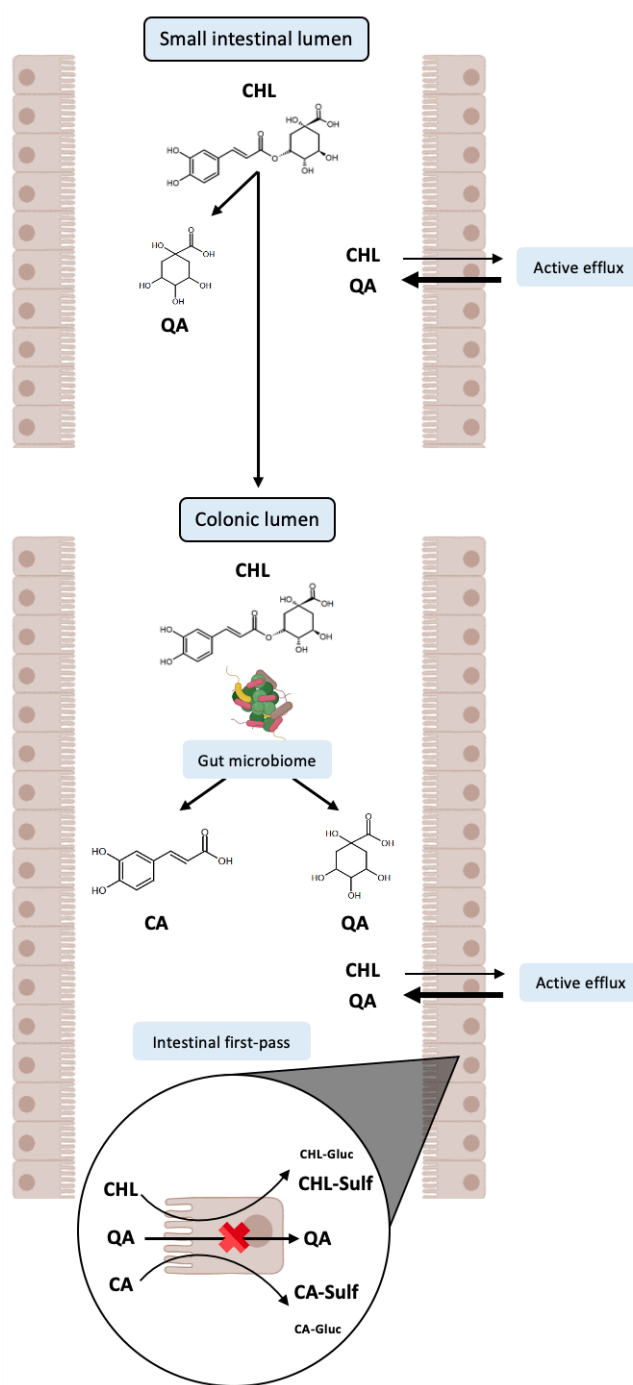
Figure 6-2: Overview of the gastrointestinal behavior of chlorogenic acid and two of its microbiotic biotransformation products including microbiotic biotransformation, intestinal absorption and intestinal first-pass effect.

6.2 Conclusions

This thesis reports the optimization of a complete and ready-to-use *in vitro* bioanalytical platform to study the gastrointestinal biotransformation of xenobiotics starting from the GIDM-Colon using chlorogenic acid as model compound. *In vivo* representation of the pooled fecal slurry suspension was enhanced by changing the incubation medium from Wilkin-Chalgren Anaerobe Broth (WCB) to a sterile phosphate buffer. Incubation time of the pooled fecal slurry before use in the GIDM-Colon was limited to one hour as longer incubation times did not prove to be of added value. Optimization of the GIDM-Colon procedure, sample preparation procedures and the addition of complementary data-analysis workflows resulted in a ready-to-use *in vitro* platform to elucidate colonic biotransformation of xenobiotics. The platform can be used to study the influence of the physiological conditions of the gastrointestinal tract and the gut microbiome on orally administered xenobiotics.

The platform has been successfully applied on investigating interpopulation differences in microbiotic biotransformation of chlorogenic acid between a lean and obese population. 16S rDNA analysis and CFU/g-determination observed differences in gut microbiome-diversity and composition between the two populations. Differences in microbiotic biotransformation were observed on the number of identified biotransformation products and biotransformation rate. A clearly higher microbiotic biotransformation activity was observed for the healthy population. The observed differences confirmed that changes in gut microbiota related to obesity are associated to differences in microbiotic biotransformation of xenobiotics and thus possibly influencing the activity, bioavailability and toxicity of orally administered xenobiotics.

Finally, the *in vitro* gastrointestinal platform was expanded with *in vitro* absorption and first-pass assays by using chlorogenic acid and microbial biotransformation products quinic acid and caffeic acid. The involvement of an active efflux mechanism in the

absorption of chlorogenic acid and quinic acid was established resulting in an overall low intestinal absorption. Quinic acid was not subjected to intestinal first-pass biotransformation, while for both chlorogenic acid and caffeic acid sulfation and glucuronidation, with the first representing the major pathway, were observed.

6.3 Future perspectives

Several recommendations for future research, mentioned throughout the thesis and within the general discussion have been summarized below and in Table 6-1.

Future GIDM-Colon experiments aiming to study the colonic behavior of ingested xenobiotics over a timeframe of 24 h should perform dialysis throughout the whole colonic phase. This adjusted protocol will allow a representative 24 h overview of the microbiotic biotransformation of the xenobiotic. This optimized workflow should be applied to the obese and lean population with 2 h sampling intervals between 0 h and 24 h in order to obtain a more in-depth understanding of differences in microbiotic biotransformation of chlorogenic acid. Furthermore, the obese/lean GIDM-Colon experiments should be repeated including more donors of both populations to verify if the obtained results can be reproduced or additional differences could be observed. Guidelines on the number of donors needed to provide a population-representative gut microbiome should be formulated as they will increase the comparability between experiments.

Future research should be conducted to unravel the cause of the observed differences in microbiotic biotransformation between the lean and obese population. Two variables have been observed between the lean and obese population: unique OTUs for both populations and less anaerobic bacteria for the obese. Performing the GIDM-Colon experiment using a diluted lean pooled fecal slurry suspension with a bacterial concentration similar to the obese pooled fecal slurry suspension could provide additional information. If differences are observed resulting from latter experiment, these will rather originate from the OTUs-differences. This experiment has been conducted and the diluted lean pooled fecal slurry suspension barely showed biotransformation activity. There are, however, a few points of attention that need to be taken into account: (i) additional dilution of the lean pooled fecal slurry suspension will lead to changes in matrix-composition between the experiments which could

influence the ionization efficiency of biotransformation products in the source of the mass spectrometer and (ii) viability of the bacteria in the diluted lean pooled fecal slurry suspension is unknown and should be investigated.

This PhD project limited the study on interpopulation differences in microbiotic biotransformation of xenobiotics to obese and lean individuals, however, multiple human diseases, including T2D, inflammatory bowel disease and colorectal cancer, are associated with gut microbiota dysbiosis and provide an opportunity for further research. In order to include a large number of donors in the experimental setup, and provide a representative fecal pool, collection of fecal samples should start well in advance as this appeared to be a bottleneck in the presented study. Furthermore, multiple studies have shown that systemic diseases can influence the physiology of the GIT and thus alter the pharmacokinetic properties of xenobiotics leading to significant differences in comparison to the healthy population (Stillhart et al. 2020). Delayed gastric emptying (diabetic gastroparesis), increased gastric pH and increased permeability of the mucosal barrier (leaky gut) have been reported with T2D patients. Future GIDM-Colon experiments should be carried out with the gastrointestinal physiological conditions of the tested population if applicable.

The intestinal absorption of chlorogenic acid and its microbial biotransformation quinic acid has been investigated and reported in chapter 4. Additional experiments with transport-inhibitors or Caco-2 Efflux Transporter Knockout Cells should be carried out to identify the protein responsible for the quinic acid active efflux. The use of extracts resulting from the GIDM-Colon as donor solutions in the *in vitro* permeability assay would improve the comparability to the *in vivo* conditions. Firstly, the presence of bile acids could positively influence the absorption of lipophilic compounds. Secondly, the GIDM-Colon samples will contain multiple biotransformation products which is representative to the *in vivo* situation in the colonic lumen. This will require optimization of the assay concerning viability of the Caco-2 cells in combination of extracts resulting from the GIDM-Colon. The use of extracts resulting from the SHIME

as donor solutions in Caco-2 assays have been previously reported, however, the authors experienced a loss of monolayer integrity. Suggested future experiments to enhance the viability and cell monolayer integrity were (i) centrifugation, (ii) filtration through a 0.2 μm pore membrane and/or dilution of the samples in medium before addition to the Caco-2 cells (Réquilé et al. 2018). The *in vitro* intestinal absorption and first-pass biotransformation assays should be performed for the remaining biotransformation products of chlorogenic acid for a more comprehensive knowledge on the gastrointestinal fate of chlorogenic acid.

This thesis provided insights on the impact of the gastrointestinal tract and in specific the gut microbiome on the bioavailability of orally ingested xenobiotics. *In vitro* gastrointestinal platforms including the gut microbiome should be included in future drug/food supplement development strategies. Inter-populational differences in the gastrointestinal behavior of oral administered xenobiotics should be further investigated and can aid in the development of the personalized medicine research field.

References

Aguirre M, Bussolo de Souza C and Venema K. The Gut Microbiota from Lean and Obese Subjects Contribute Differently to the Fermentation of Arabinogalactan and Inulin. *PLoS One* 2016a, 11(7): e0159236.

Aguirre M, Eck A, Koenen ME, Savelkoul PH, Budding AE and Venema K. Evaluation of an optimal preparation of human standardized fecal inocula for in vitro fermentation studies. *Journal of Microbiological Methods* 2015, 117: 78-84.

Aguirre M, Eck A, Koenen ME, Savelkoul PH, Budding AE and Venema K. Diet drives quick changes in the metabolic activity and composition of human gut microbiota in a validated in vitro gut model. *Research in Microbiology* 2016b, 167(2): 114-125.

Amaretti A, Raimondi S, Leonardi A, Quartieri A and Rossi M. Hydrolysis of the rutinose-conjugates flavonoids rutin and hesperidin by the gut microbiota and bifidobacteria. *Nutrients* 2015, 7(4): 2788-2800.

Bergheim I, Bode C and Parlesak A. Distribution of cytochrome P450 2C, 2E1, 3A4, and 3A5 in human colon mucosa. *BMC clinical pharmacology* 2005, 5: 4-4.

Breynaert A, Bosscher D, Kahnt A, Claeys M, Cos P, Pieters L and Hermans N. Development and Validation of an in vitro Experimental GastroIntestinal Dialysis Model with Colon Phase to Study the Availability and Colonic Metabolisation of Polyphenolic Compounds. *Planta Medica* 2015, 81(12-13): 1075-1083.

Davis CD. The Gut Microbiome and Its Role in Obesity. *Nutrition today* 2016, 51(4): 167-174.

Erk T, Williamson G, Renouf M, Marmet C, Steiling H, Dionisi F, Barron D, Melcher R and Richling E. Dose-dependent absorption of chlorogenic acids in the small intestine assessed by coffee consumption in ileostomists. *Molecular Nutrition & Food Research* 2012, 56(10): 1488-1500.

Falony G, Joossens M, Vieira-Silva S, Wang J, Darzi Y, Faust K, Kurilshikov A, Bonder MJ, Valles-Colomer M, Vandeputte D, Tito RY, Chaffron S, Rymenans L, Verspecht C, De Sutter L, Lima-Mendez G, D'Hoe K, Jonckheere K, Homola D, Garcia R, Tigchelaar EF, Eeckhaudt L, Fu J, Henckaerts L, Zhernakova A, Wijmenga C and Raes J. Population-level analysis of gut microbiome variation. *Science* 2016, 352(6285): 560-564.

Farrell TL, Poquet L, Dew TP, Barber S and Williamson G. Predicting phenolic acid absorption in Caco-2 cells: a theoretical permeability model and mechanistic study. *Drug Metabolism and Disposition* 2012, 40(2): 397-406.

Garcia-Villalba R, Vissenaekens H, Pitart J, Romo-Vaquero M, Espin JC, Grootaert C, Selma MV, Raes K, Smagghe G, Possemiers S, Van Camp J and Tomas-Barberan FA. Gastrointestinal Simulation Model TWIN-SHIME Shows Differences between Human Urolithin-Metabotypes in Gut Microbiota Composition, Pomegranate Polyphenol Metabolism, and Transport along the Intestinal Tract. *Journal of Agricultural and Food Chemistry* 2017, 65(27): 5480-5493.

Grès MC, Julian B, Bourrié M, Meunier V, Roques C, Berger M, Boulenc X, Berger Y and Fabre G. Correlation between oral drug absorption in humans, and apparent drug permeability in TC-7 cells, a human epithelial intestinal cell line: comparison with the parental Caco-2 cell line. *Pharmaceutical research* 1998, 15(5): 726-733.

Gromova M and Roby C. Toward Arabidopsis thaliana hydrophilic metabolome: assessment of extraction methods and quantitative 1H NMR. *Physiologia Plantarum* 2010, 140(2): 111-127.

Hatley OJD, Jones CR, Galetin A and Rostami-Hodjegan A. Quantifying gut wall metabolism: methodology matters. *Biopharmaceutics & Drug Disposition* 2017, 38(2): 155-160.

Hohrenk LL, Itzel F, Baetz N, Tuerk J, Vosough M and Schmidt TC. Comparison of Software Tools for Liquid Chromatography–High-Resolution Mass Spectrometry Data Processing in Nontarget Screening of Environmental Samples. *Analytical Chemistry* 2020, 92(2): 1898-1907.

Hubatsch I, Ragnarsson EG and Artursson P. Determination of drug permeability and prediction of drug absorption in Caco-2 monolayers. *Nature Protocols* 2007, 2(9): 2111-2119.

Konishi Y and Kobayashi S. Transepithelial transport of chlorogenic acid, caffeic acid, and their colonic metabolites in intestinal Caco-2 cell monolayers. *Journal of Agricultural and Food Chemistry* 2004, 52(9): 2518-2526.

Larsen N, Vogensen FK, van den Berg FW, Nielsen DS, Andreasen AS, Pedersen BK, Al-Soud WA, Sorensen SJ, Hansen LH and Jakobsen M. Gut microbiota in human adults with type 2 diabetes differs from non-diabetic adults. *PLoS One* 2010, 5(2): e9085.

Lea T (2015). Caco-2 Cell Line. *The Impact of Food Bioactives on Health: in vitro and ex vivo models*. K. Verhoeckx, P. Cotter, I. Lopez-Exposito et al. Cham (CH)**:** 103-111.

Ley RE, Bäckhed F, Turnbaugh P, Lozupone CA, Knight RD and Gordon JI. Obesity alters gut microbial ecology. *Proceedings of the National Academy of Sciences of the United States of America* 2005, 102(31): 11070.

Ley RE, Turnbaugh PJ, Klein S and Gordon JI. Human gut microbes associated with obesity. *Nature* 2006, 444(7122): 1022-1023.

Machiels K, Joossens M, Sabino J, De Preter V, Arijs I, Eeckhaut V, Ballet V, Claes K, Van Immerseel F, Verbeke K, Ferrante M, Verhaegen J, Rutgeerts P and Vermeire S. A decrease of the butyrate-producing species Roseburia hominis and Faecalibacterium prausnitzii defines dysbiosis in patients with ulcerative colitis. *Gut* 2014, 63(8): 1275-1283.

Monente C, Ludwig IA, Stalmach A, de Pena MP, Cid C and Crozier A. In vitro studies on the stability in the proximal gastrointestinal tract and bioaccessibility in Caco-2 cells of chlorogenic acids from spent coffee grounds. *International Journal of Food Sciences and Nutrition* 2015, 66(6): 657-664.

Mortelé O, Iturrospe E, Breynaert A, Verdickt E, Xavier BB, Lammens C, Malhotra-Kumar S, Jorens PG, Pieters L, van Nuijs ALN and Hermans N. Optimization of an in vitro gut microbiome biotransformation platform with chlorogenic acid as model compound: From fecal sample to biotransformation product identification. *Journal of Pharmaceutical and Biomedical Analysis* 2019, 175: 112768.

Mortele O, Vervliet P, Gys C, Degreef M, Cuykx M, Maudens K, Covaci A, van Nuijs ALN and Lai FY. In vitro Phase I and Phase II metabolism of the new designer benzodiazepine cloniprazepam using liquid chromatography coupled to quadrupole time-of-flight mass spectrometry. *Journal of Pharmaceutical and Biomedical Analysis* 2018, 153: 158-167.

O'Donnell MM, Rea MC, O'Sullivan Ó, Flynn C, Jones B, McQuaid A, Shanahan F and Ross RP. Preparation of a standardised faecal slurry for ex-vivo microbiota studies which reduces inter-individual donor bias. *Journal of Microbiological Methods* 2016, 129: 109-116.

Pavlović N, Goločorbin-Kon S, Đanić M, Stanimirov B, Al-Salami H, Stankov K and Mikov M. Bile Acids and Their Derivatives as Potential Modifiers of Drug Release and Pharmacokinetic Profiles. *Frontiers in pharmacology* 2018, 9: 1283-1283.

Peters SA, Jones CR, Ungell A-L and Hatley OJD. Predicting Drug Extraction in the Human Gut Wall: Assessing Contributions from Drug Metabolizing Enzymes and Transporter Proteins using Preclinical Models. *Clinical Pharmacokinetics* 2016, 55: 673-696.

Qin J, Li Y, Cai Z, Li S, Zhu J, Zhang F, Liang S, Zhang W, Guan Y, Shen D, Peng Y, Zhang D, Jie Z, Wu W, Qin Y, Xue W, Li J, Han L, Lu D, Wu P, Dai Y, Sun X, Li Z, Tang A, Zhong S, Li X, Chen W, Xu R, Wang M, Feng Q, Gong M, Yu J, Zhang Y, Zhang M, Hansen T, Sanchez G, Raes J, Falony G, Okuda S, Almeida M, LeChatelier E, Renault P, Pons N, Batto JM, Zhang Z, Chen H, Yang R, Zheng W, Li S, Yang H, Wang J, Ehrlich SD, Nielsen R, Pedersen O, Kristiansen K and Wang J. A metagenome-wide association study of gut microbiota in type 2 diabetes. *Nature* 2012, 490(7418): 55-60.

Réquilé M, Gonzàlez Alvarez DO, Delanaud S, Rhazi L, Bach V, Depeint F and Khorsi-Cauet H. Use of a combination of in vitro models to investigate the impact of chlorpyrifos and inulin on the intestinal microbiota and the permeability of the intestinal mucosa. *Environmental Science and Pollution Research* 2018, 25(23): 22529-22540.

Riches Z, Stanley EL, Bloomer JC and Coughtrie MWH. Quantitative evaluation of the expression and activity of five major sulfotransferases (SULTs) in human tissues: the SULT "pie". *Drug metabolism and disposition: the biological fate of chemicals* 2009, 37(11): 2255-2261.

Rubas W, Cromwell MEM, Shahrokh Z, Villagran J, Nguyen TN, Wellton M, Nguyen TH and Mrsny RJ. Flux Measurements across Caco-2 Monolayers May Predict Transport in Human Large Intestinal Tissue. *Journal of Pharmaceutical Sciences* 1996, 85(2): 165-169.

Schirmer M, Franzosa EA, Lloyd-Price J, McIver LJ, Schwager R, Poon TW, Ananthakrishnan AN, Andrews E, Barron G, Lake K, Prasad M, Sauk J, Stevens B, Wilson RG, Braun J, Denson LA, Kugathasan S, McGovern DPB, Vlamakis H, Xavier RJ and Huttenhower C. Dynamics of metatranscription in the inflammatory bowel disease gut microbiome. *Nature Microbiology* 2018, 3(3): 337-346.

Sedighi M, Razavi S, Navab-Moghadam F, Khamseh ME, Alaei-Shahmiri F, Mehrtash A and Amirmozafari N. Comparison of gut microbiota in adult patients with type 2 diabetes and healthy individuals. *Microbial Pathogenesis* 2017, 111: 362-369.

Stalmach A, Steiling H, Williamson G and Crozier A. Bioavailability of chlorogenic acids following acute ingestion of coffee by humans with an ileostomy. *Archives of Biochemistry and Biophysics* 2010, 501(1): 98-105.

Stillhart C, Vučićević K, Augustijns P, Basit AW, Batchelor H, Flanagan TR, Gesquiere I, Greupink R, Keszthelyi D, Koskinen M, Madla CM, Matthys C, Miljuš G, Mooij MG, Parrott N, Ungell A-L, de Wildt SN, Orlu M, Klein S and Müllertz A. Impact of gastrointestinal physiology on drug absorption in special populations—An UNGAP review. *European Journal of Pharmaceutical Sciences* 2020, 147: 105280.

Stockdale TP, Challinor VL, Lehmann RP, De Voss JJ and Blanchfield JT. Caco-2 Monolayer Permeability and Stability of Chamaelirium luteum (False Unicorn) Open-Chain Steroidal Saponins. *ACS Omega* 2019, 4(4): 7658-7666.

Tannergren C, Bergendal A, Lennernäs H and Abrahamsson B. Toward an Increased Understanding of the Barriers to Colonic Drug Absorption in Humans: Implications for Early Controlled Release Candidate Assessment. *Molecular Pharmaceutics* 2009, 6(1): 60-73.

Teubner W, Meinl W, Florian S, Kretzschmar M and Glatt H. Identification and localization of soluble sulfotransferases in the human gastrointestinal tract. *The Biochemical journal* 2007, 404(2): 207-215.

Tomas-Barberan F, Garcia-Villalba R, Quartieri A, Raimondi S, Amaretti A, Leonardi A and Rossi M. In vitro transformation of chlorogenic acid by human gut microbiota. *Molecular Nutrition & Food Research* 2014, 58(5): 1122-1131.

Turnbaugh PJ, Backhed F, Fulton L and Gordon JI. Diet-induced obesity is linked to marked but reversible alterations in the mouse distal gut microbiome. *Cell Host Microbe* 2008, 3(4): 213-223.

Turnbaugh PJ, Hamady M, Yatsunenko T, Cantarel BL, Duncan A, Ley RE, Sogin ML, Jones WJ, Roe BA, Affourtit JP, Egholm M, Henrissat B, Heath AC, Knight R and Gordon JI. A core gut microbiome in obese and lean twins. *Nature* 2009, 457(7228): 480-484.

Van de Wiele T, Van den Abbeele P, Ossieur W, Possemiers S and Marzorati M (2015). The Simulator of the Human Intestinal Microbial Ecosystem (SHIME((R))). *The Impact of Food Bioactives on Health: in vitro and ex vivo models*. K. Verhoeckx, P. Cotter, I. Lopez-Exposito et al. Cham (CH)**:** 305-317.

Venema K (2015). The TNO In Vitro Model of the Colon (TIM-2). *The Impact of Food Bioactives on Health: in vitro and ex vivo models*. K. Verhoeckx, P. Cotter, I. López-Expósito et al. Cham, Springer International Publishing**:** 293-304.

Vervliet P, Mortele O, Gys C, Degreef M, Lanckmans K, Maudens K, Covaci A, van Nuijs ALN and Lai FY. Suspect and non-target screening workflows to investigate the in vitro and in vivo metabolism of the synthetic cannabinoid 5Cl-THJ-018. *Drug Testing and Analysis* 2018, 11(3): 479-491.

Volpe DA. Variability in Caco-2 and MDCK cell-based intestinal permeability assays. *Journal of Pharmaceutical Sciences* 2008, 97(2): 712-725.

Wang T, Cai G, Qiu Y, Fei N, Zhang M, Pang X, Jia W, Cai S and Zhao L. Structural segregation of gut microbiota between colorectal cancer patients and healthy volunteers. *ISME J* 2012, 6(2): 320-329.

Wong CC, Meinl W, Glatt H-R, Barron D, Stalmach A, Steiling H, Crozier A and Williamson G. In vitro and in vivo conjugation of dietary hydroxycinnamic acids by UDP-glucuronosyltransferases and sulfotransferases in humans. *The Journal of Nutritional Biochemistry* 2010, 21(11): 1060-1068.

Wu N, Yang X, Zhang R, Li J, Xiao X, Hu Y, Chen Y, Yang F, Lu N, Wang Z, Luan C, Liu Y, Wang B, Xiang C, Wang Y, Zhao F, Gao GF, Wang S, Li L, Zhang H and Zhu B. Dysbiosis signature of fecal microbiota in colorectal cancer patients. *Microbial Ecology* 2013, 66(2): 462-470.

Wu XH, Yu HL, Ba ZY, Chen JY, Sun HG and Han BZ. Sampling methods for NMR-based metabolomics of Staphylococcus aureus. *Biotechnology Journal* 2010, 5(1): 75-84.

Xie F, Ding X and Zhang Q-Y. An update on the role of intestinal cytochrome P450 enzymes in drug disposition. *Acta pharmaceutica Sinica. B* 2016, 6(5): 374-383.

Zanger UM and Schwab M. Cytochrome P450 enzymes in drug metabolism: Regulation of gene expression, enzyme activities, and impact of genetic variation. *Pharmacology & Therapeutics* 2013, 138(1): 103-141.

Zhou G, Peng Y, Zhao L, Wang M and Li X. Biotransformation of Total Saponins in Siraitia Fructus by Human Intestinal Microbiota of Normal and Type 2 Diabetic Patients: Comprehensive Metabolite Identification and Metabolic Profile Elucidation Using LC-Q-TOF/MS. *Journal of Agricultural and Food Chemistry* 2017, 65(8): 1518-1524.

SUMMARY

SUMMARY

SUMMARY

The gastrointestinal tract accommodates between 10^{12}-10^{13} microorganisms with species diversity increasing longitudinally from mouth to colon, the latter harboring the most bacteria of the whole gastrointestinal tract also known as the gut microbiota. Until recently, it was believed that the biotransformation of xenobiotics occurs mainly by the cytochrome P450 enzyme system (CYP450) in the liver. Recent data clearly show that also the gut microbiota play a significant role in the biotransformation of oral administered xenobiotics, leading to a potential influence of this microbiotic biotransformation on activation, inactivation and possible toxicity of these compounds. Most new pharmaceutical drug candidates experience biopharmaceutical problems like low solubility and/or low permeability leading to longer contact with the gut microbiome. Furthermore, there is currently a lack of knowledge on how the microbiotic biotransformation varies between individuals and different disease-states. This shows the need for more biotransformation studies including the role of the gut microbiome.

The main objective of this PhD project was to gain a more in-depth understanding on the role of the gut microbiome on the gastrointestinal fate of orally ingested xenobiotics using chlorogenic acid as model compound. *In vitro* models are often used to study the colonic biotransformation of xenobiotics by the gut microbiome, as they allow dynamic and multiple sampling overtime. However, the pre-analytical phase should be carefully optimized to enable biotransformation product identification representative for the *in vivo* situation. **Chapter 2** presents the optimization of a ready-to-use *in vitro* gastrointestinal platform including the gastrointestinal dialysis model with colon phase (GIDM-Colon) and bioanalytical strategies to investigate and elucidate the gastrointestinal biotransformation of xenobiotics. Firstly, the effect of storage conditions (-80 °C) over time on the bacterial composition was evaluated over a period of 24 months. Bacterial composition remained stable over a period of 24 months, confirming the *in vivo* representation of the fecal samples after 24 months of storage. Secondly, the influence of different incubation media, Wilkins-Chalgren

SUMMARY

Anaerobic Broth (WCB) and a sterile phosphate buffer, and different incubation times on fecal bacterial composition and concentration were evaluated. A substantial variation in bacterial composition of the pooled fecal slurry suspension was observed with WCB, while the phosphate buffer ensured a closer resemblance to the *in vivo* composition. Incubation time was limited to one-hour as longer incubation times did not prove to be of added value. Furthermore, 4 different sample preparation procedures were evaluated. No significant differences were observed when applying the centrifugation, extraction or sonication sample preparation procedures. The freeze-drying procedure could clearly be considered as the minor procedure. The extraction procedure was selected as optimal sample preparation method given the quick execution together with a good instrumental sensitivity. Next, combining suspect and non-targeted screening workflows (MZmine + R and MassProfiler Professional (Agilent Technologies)) has proven to have an added value on the elucidation and identification of microbial biotransformation products. Based on these results combination of workflows is advisable to obtain an increased output. Finally, the dialysis procedure of the GIDM-Colon was optimized. Dialysis have been reported to be an essential tool to maintain highly active microbiota and representative microbial metabolite-concentrations during gut microbiota biotransformation experiments. Parallel GIDM-Colon experiments with varying dialysis- and sampling intervals resulted in deviating results, limiting the complementarity. Future GIDM-Colon experiments aiming to study the colonic behavior of ingested xenobiotics over a timeframe of 24 h should perform dialysis throughout the whole colonic phase. This adjusted protocol will allow a representative 24 h overview of the microbiotic biotransformation of the xenobiotic.

The *in vitro* gastrointestinal platform was successfully applied to investigate inter-population differences in microbiotic biotransformation of xenobiotics between a lean and obese population (**Chapter 3**). Gut microbiome dysbiosis has been associated with obesity, however, little was known on the effect of the dysbiosis on the microbiotic

biotransformation of xenobiotics. Fecal samples of lean (n=9) and obese (n=4) volunteers were collected and characterized by 16S rDNA sequencing. Differences in gut microbiome composition, bacterial diversity and bacterial concentration were observed between the two populations. The lean and obese microbiotic biotransformation of chlorogenic acid was studied using the collected fecal samples in the colon stage of the GIDM-Colon. The obese gut microbiome presented a lower metabolic activity in comparison to the lean population. Chlorogenic acid was completely biotransformed after 24 h colonic dialysis in the lean population while it was still present in the obese population. Furthermore, 23 and 13 biotransformation products were identified in the lean and obese population respectively. The presented results in this thesis confirmed that changes in gut microbiota related to obesity are associated with differences in microbiotic biotransformation of xenobiotics and thus possibly influencing the activity, bioavailability and toxicity of orally administered xenobiotics. This was, to the best of our knowledge, the first study investigating differences in microbiotic biotransformation of xenobiotics between obese and lean volunteers.

Chapter 4 and **Chapter 5** present the expansion of the *in vitro* gastrointestinal platform with an *in vitro* intestinal permeability assay and an *in vitro* first-pass biotransformation assay. Model compound chlorogenic acid and two of its most abundant gastrointestinal biotransformation products caffeic acid and quinic acid were included in the assays in order to obtain an in-depth understanding of the gastrointestinal behavior of chlorogenic acid. Intestinal absorption of chlorogenic acid and quinic acid was studied using the human intestinal epithelial Caco-2 cell line derived form a colorectal adenocarcinoma (**Chapter 4**). Analytical assays based on liquid chromatography coupled to tandem mass spectrometry (LC-MS/MS) for the quantification of chlorogenic acid, quinic acid, propranolol and digoxin were optimized and validated according to the European Medicines Agency (EMA) guidelines. Propranolol and digoxin were included in the *in vitro* permeability assay as positive

control compounds for high passive permeability and active efflux respectively and confirmed the reliability of the assay and acquired results. The involvement of an active efflux mechanism was observed for the intestinal absorption of both chlorogenic acid and quinic acid. The involvement of active efflux protein P-glycoprotein (P-gp) in the intestinal absorption of chlorogenic acid was previously reported in the literature. The intestinal absorption of quinic acid was studied for the first time.

Finally, the intestinal first-pass effect of chlorogenic acid, caffeic acid and quinic acid was investigated using an *in vitro* intestinal biotransformation assay using human intestinal microsomes (HIM) and human intestinal cytosol (HICYT) (**Chapter 5**). The *in vitro* assay, based on an in-house developed protocol using human liver microsomes (HLM) and cytosol (HLCYT), was optimized using positive control compounds for phase I and II biotransformation. HIM and HICYT concentrations of 1000 μg/mL and 500 μg/mL were applied in the optimized assay. Furthermore, fentanyl was included as positive control compound for enzymatic activity of CYP450 isotype CYP3A4. No phase I biotransformation products of chlorogenic acid, caffeic acid and quinic acid were observed. For both chlorogenic acid and caffeic acid two sulfate-conjugate isomers and low-abundance features corresponding to the glucuronide-conjugates were identified. No phase II biotransformation products of quinic acid were detected.

This thesis provided insights on the impact of the gastrointestinal tract and in specific the gut microbiome on the bioavailability of orally ingested xenobiotics. Future drug/food supplement development strategies should include *In vitro* gastrointestinal platforms including the gut microbiome. Inter-populational differences in the gastrointestinal behavior of oral administered xenobiotics should be further investigated and can aid in the development of the personalized medicine research field.

SAMENVATTING

SAMENVATTING

SAMENVATTING

Het gastro-intestinaal stelsel herbergt tussen de 10^{12}-10^{13} micro-organismen met een toenemede diversiteit in species van de mond tot de dikke darm, waarbij de laatst genoemde de meeste bacteriën van het hele gastro-intestinaal stelsel herbergt, ook wel bekend als het darmmicrobioom. Tot voor kort werd aangenomen dat de biotransformatie van xenobiotica voornamelijk plaatsvond in de lever door het cytochroom P450 enzymsysteem (CYP450). Recente studies tonen echter duidelijk aan dat ook het darmmicrobioom een belangrijke rol spelen in de biotransformatie van oraal toegediende xenobiotica, wat leidt tot een potentiële invloed van de microbiotische biotransformatie op de activiteit, inactiviteit en mogelijke toxiciteit van deze verbindingen. Een merendeel nieuwe farmaceutische kandidaat-geneesmiddelen ervaren biofarmaceutische problemen zoals lage oplosbaarheid en/of lage permeabiliteit wat leidt tot een toegenomen contactduur met het darmmicrobioom. Bovendien is er momenteel een gebrek aan kennis over hoe de microbiotische biotransformatie varieert tussen individuen en verschillende ziektebeelden. Dit benadrukt de behoefte voor meer biotransformatie studies naar de rol van het darmmicrobioom.

Het hoofddoel van dit doctoraatsproject was het verkrijgen van een toegenomen kennis inzake de rol van het darmmicrobioom op het gastro-intestinale lot van xenobiotica na orale toediening met behulp van chlorogeenzuur als modelverbinding. *In vitro* modellen worden vaak toegepast om de colonische biotransformatie van xenobiotica door het darmmicrobioom te bestuderen aangezien ze een dynamische en meervoudige staalname van over tijd mogelijk maken. De pre-analytische fase moet echter zorgvuldig geoptimaliseerd worden zodoende biotransformatie productidentificatie, representatief voor de *in vivo* situatie, mogelijk te maken. **Hoofdstuk 2** presenteert de optimalisatie van een *ready-to-use in vitro* gastro-intestinaal platform inclusief het gastro-intestinale dialyse model met colonfase (GIDM-Colon) en bio-analytische strategieën om de gastro-intestinale biotransformatie van xenobiotica te bestuderen. Eerst werd het effect van de

SAMENVATTING

bewaringscondities (-80 °C) over een periode van 24 maanden op de bacteriële samenstelling geëvalueerd. De bacteriële samenstelling bleef stabiel over een periode van 24 maanden, wat de *in vivo* representatie van de fecale monsters na 24 maanden opslag bevestigde. Vervolgens, werd de invloed van verschillende incubatiemedia, Wilkins-Chalgren Anaerobic Broth (WCB) en een steriele fosfaatbuffer, en verschillende incubatietijden op de fecale bacteriële samenstelling en concentratie geëvalueerd. Een aanzienlijke variatie in de bacteriële samenstelling van de gepoolde fecale suspensie werd waargenomen met WCB, terwijl de fosfaatbuffer zorgde voor een nauwere gelijkenis met de *in vivo* samenstelling. De incubatietijd werd beperkt tot één uur aangezien langere incubatietijden niet over een toegevoegde waarde bleken te beschikken. Bovendien werden 4 verschillende staalvoorbereidingsprocedures geëvalueerd. Er werden geen significante verschillen waargenomen bij het toepassen van de centrifugatie, extractie of sonicatie staalvoorbereidingprocedures. De vriesdroogprocedure gaf duidelijk aanleiding tot de minst kwalitatieve resultaten. De extractieprocedure werd geselecteerd als optimale staalvoorbereidingsprocedure gezien de kortere proceduretijd in combinatie met een goede instrumentele gevoeligheid. Vervolgens heeft het combineren van *suspect* en niet-gerichte *screeningsworkflows* (*non-targeted screening workflows,* MZmine + R en MassProfiler Professional (Agilent Technologies)) bewezen een toegevoegde waarde te hebben voor de opheldering en identificatie van microbiële biotransformatieproducten. Op basis van deze resultaten is een combinatie van *workflows* aangeraden voor toekomstige experimenten om een verhoogde output te verkrijgen. Tot slot is de dialyseprocedure van het GIDM-Colon geoptimaliseerd. Het utvoeren van dialyse is essentieel om zeer actieve microbiota en representatieve microbiële metabolietconcentraties te behouden tijdens darmbiotransformatie-experimenten. Parallelle GIDM-Colon experimenten met variërende dialyse- en staalafname-intervallen resulteerden in afwijkende resultaten, waardoor geconcludeerd kon worden dat parallelle experiment niet compatibel waren. Toekomstige GIDM-Colon experimenten, met als doel het gedrag van oraal toegediende xenobiotica in het colon

te bestuderen over een tijdsbestek van 24 uur, dienen dialyse gedurende de gehele colon fase uit te voeren. Dit aangepaste protocol zal een representatief 24 uurs overzicht van de microbiotische biotransformatie van het xenobioticum mogelijk maken.

Het *in vitro* gastro-intestinale platform werd met succes toegepast om verschillen in microbiotische biotransformatie van xenobiotica tussen een slanke en obese populatie te onderzoeken (**Hoofdstuk 3**). Darmmicrobioom dysbiose is in verband gebracht met obesitas, maar tot op heden was er weinig geweten over het effect van de dysbiose op de microbiotische biotransformatie van xenobiotica. Fecale stalen van slanke (n=9) en obese (n=4) vrijwilligers werden verzameld en gekarakteriseerd door middel van 16S rDNA sequencing. Verschillen in darm-microbiële samenstelling, bacteriële diversiteit en bacteriële concentratie werden waargenomen tussen de twee populaties. De microbiotische biotransformatie van chlorogeenzuur door de slanke en obese populatie werd bestudeerd door middel van inoculatie van de colon fase van het GIDM-Colon met de verzamelde fecale monsters van beide populaties. Het darmmicrobiotoom van de obese populatie presenteerde een lagere metabolische activiteit in vergelijking met de slanke populatie. Chlorogeenzuur werd na 24 uur dialyse volledig gebiotransformeerd in de slanke populatie terwijl het wel nog steeds aanwezig was in de obese populatie. Bovendien werden 23 en 13 biotransformatieproducten geïdentificeerd in respectievelijk de slanke en de obese populatie. De gepresenteerde resultaten in dit proefschrift bevestigen dat veranderingen in darmmicrobioom geassocieerd met obesitas geassocieerd zijn met verschillen in microbiotische biotransformatie van xenobiotica en dus mogelijk de activiteit, biologische beschikbaarheid en toxiciteit van oraal toegediende xenobiotica beïnvloeden. Dit was de eerste studie die de verschillen in microbiotische biotransformatie van xenobiotica tussen zwaarlijvige en magere vrijwilligers onderzocht.

SAMENVATTING

In **Hoofdstuk 4** en **Hoofdstuk 5** wordt de uitbreiding van het *in vitro* gastro-intestinaal platform met een *in vitro* intestinale absorptie *assay* en een *first-pass* biotransformatie *assay* beschreven. Modelverbinding chlorogeenzuur en zijn twee voornaamste gastro-intestinale biotransformatieproducten koffiezuur en kininezuur werden opgenomen in de *assays* om de kennis omtrent het gastro-intestinale gedrag van chlorogeenzuur te verbeteren. De intestinale absorptie van chlorogeenzuur en kininezuur werd bestudeerd met behulp van de humane intestinale epitheliale Caco-2 cellijn afgeleid van een colorectaal adenocarcinoom (**Hoofdstuk 4**). Analyses op basis van vloeistofchromatografie gekoppeld aan tandem-massaspectrometrie (LC-MS/MS) voor de kwantificatie van chlorogeenzuur, kininezuur, propranolol en digoxine werden geoptimaliseerd en gevalideerd volgens de richtlijnen van het *European Medicines Agency* (EMA). Propranolol en digoxine werden geïncludeerd in de *in vitro* permeabiliteitstest als positieve controleverbindingen voor een hoge passieve permeabiliteit en actieve efflux respectievelijk. De resultatenv van de positieve controles bevestigden de betrouwbaarheid van de test en de verkregen resultaten. De betrokkenheid van een actief effluxmechanisme werd waargenomen voor de intestinale absorptie van zowel chlorogeenzuur als kininezuur. De betrokkenheid van het actieve efflux-eiwit P-glycoproteïne (P-gp) bij de intestinale absorptie van chlorogeenzuur werd eerder in de literatuur gerapporteerd. De darmabsorptie van kininezuur werd voor het eerst bestudeerd en gerapporteerd.

Tenslotte werd het intestinale *first-pass*-effect van chlorogeenzuur, koffiezuur en kininezuur onderzocht met behulp van een *in vitro* darmbiotransformatietest met behulp van humane intestinale microsomen (HIM) en humaan intestinaal cytosol (HICYT) (**Hoofdstuk 5**). Het *in vitro assay*, gebaseerd op een intern ontwikkeld protocol met humane levermicrosomen (HLM) en cytosol (HLCYT), werd geoptimaliseerd met behulp van positieve controle verbindingen voor fase I en II biotransformatie. HIM en HICYT concentraties van 1000 µg/mL en 500 µg/mL werden toegepast in de geoptimaliseerde test. Fentanyl werd geïncludeerd als positieve controleverbinding

voor enzymatische activiteit van CYP450-isotype CYP3A4. Er werden geen fase I-biotransformatieproducten van chlorogeenzuur, koffiezuur en kininezuur gedetecteerd. Voor zowel chlorogeenzuur als koffiezuur werden twee sulfaat-conjugaat-isomeren en twee lage-abundantie *features,* die overeenkomen met de glucuronide-conjugaten, geïdentificeerd. Er werden geen fase II-biotransformatieproducten van kininezuur gedetecteerd.

Dit proefschrift gaf additioneel inzicht in de invloed van het gastro-intestinaal stelsel en in het bijzonder het darmmicrobioom op de biologische beschikbaarheid van oraal toegediende xenobiotica. Toekomstige geneesmiddelen/voedingssupplementen ontwikkelingsstrategieën dienen *in vitro* gastro-intestinale platformen, inclusief het darmmicrobioom, te includeren in hun preklinisch onderzoek. Verschillen in het gastro-intestinale gedrag van oraal toegediende xenobiotica tussen verschillende populaties dient verder onderzocht te worden. Dit kan op termijn bijbrengen tot de ontwikkeling van meer gepersonaliseerde theraptie-strategieën.

CURRICULUM VITAE

CURRICULUM VITAE

Personalia

Name:	Olivier Mortelé
Date of birth:	August 18, 1992
Place of birth	Vilvoorde, Belgium
E-mail:	oliviermortele1@hotmail.com

Education

2017 - present	Student Master of Sciences in laboratory Medicine
	University of Antwerp, Belgium
2016 – present	PhD in Pharmaceutical Sciences
	Natural Products and Food – Research & Analysis (NatuRA) and
	Toxicological Centre, University of Antwerp, Belgium
	Title: Understanding the role of the gastrointestinal tract and
	the gut microbiome on the biotransformation, absorption and
	bioavailability of xenobiotics: chlorogenic acid as model
	compound
	Promotors: prof. dr. Nina Hermans, prof. dr. Alexander L.N. van
	Nuijs
2014-2016	Master of Sciences in Drug Development: Pharmacist (great
	distinction)
	University of Antwerp, Belgium
	Thesis title: Optimization of *in vitro* sample preparation for LC-
	MS metabolomics applications on HepaRG cell cultures
	Promotor: prof. dr. Adrian Covaci
2011-2014	Bachelor of Sciences in Pharmaceutical Sciences (distinction)
	University of Antwerp, Belgium
2010-2011	Student Bachelor of Sciences in Biomedical Sciences
	University of Antwerp, Belgium
2004-2010	High School degree: Sciences-mathematics
	Sint-Ritacollege, Kontich, Belgium

Work experience and internships

2016 – present	PhD student at the Natural Products and Food – Research & Analysis (NatuRA) and Toxicological Centre, Faculty of Pharmaceutical, Biomedical and Veterinary Sciences, University of Antwerp (Belgium)
November 2017	Visiting Researcher at RECETOX Masaryk University, Brno (Czech Republic) Topic: Combining suspect and untargeted screening workflows to identify organic contaminants in paired urine and serum samples from US firefighters using LC- and GC-Orbitrap.
February – June 2016	Master thesis at Toxicological Centre University of Antwerp (Belgium) Topic: Optimization of *in vitro* sample preparation for LC-MS metabolomics applications on HepaRG cell cultures.
September 2015 – January 2016	Pharmacy internship, Apotheek Broeckx, Antwerp (Belgium)

Guidance practical sessions

2017-2018	Practical sessions Botany 1st Bachelor Pharmaceutical Sciences University of Antwerp (Belgium)
2017-2018	Practical sessions Pharmaceutical Analysis II 2nd Bachelor Pharmaceutical Sciences University of Antwerp (Belgium)
2018-2019	Practical sessions Pharmaceutical Analysis II 2nd Bachelor Pharmaceutical Sciences University of Antwerp (Belgium)

Scientific curriculum

Peer-reviewed publications (6)

1. Cuykx M, **Mortelé O***, Rodrigues R M, Vanhaecke T, Covaci A, Optimisation of in vitro sample preparation for LC-MS metabolomics applications on HepaRG cell cultures. Analytical Methods, 2017; 9: 3704-3712. (* joint first author)

2. **Mortelé O***, Vervliet P, Gys C, Degreef M, Cuykx M, Maudens K, Covaci A, van Nuijs A L N and Lai F Y. In vitro Phase I and Phase II metabolism of the new designer benzodiazepine cloniprazepam using liquid chromatography coupled to quadrupole time-of-flight mass spectrometry. *Journal of Pharmaceutical and Biomedical Analysis* 2018, 153: 158-167. (* joint first author)

3. Vervliet P, **Mortelé O***, Gys C, Degreef M, Lanckmans K, Maudens K, Covaci A, van Nuijs A L N and Lai F Y. Suspect and non-target screening workflows to investigate the in vitro and in vivo metabolism of the synthetic cannabinoid 5Cl-THJ-018*. Drug Testing and Analysis* 2018, 11(3): 479-491. (* joint first author)

4. **Mortelé O**, Iturrospe E, Breynaert A, Verdickt E, Xavier B B, Lammens C, Malhotra-Kumar S, Jorens P G, Pieters L, van Nuijs A L N and Hermans N. Optimization of an in vitro gut microbiome biotransformation platform with chlorogenic acid as model compound: From fecal sample to biotransformation product identification. *Journal of Pharmaceutical and Biomedical Analysis* 2019, 175: 112768.

5. **Mortelé O**, Iturrospe E, Breynaert A, Lammens C, Britto XB, Malhotra-Kumar S, Jorens P, Pieters L, van Nuijs A L N and Hermans N. Chlorogenic Acid as a Model Compound for Optimization of an In Vitro Gut Microbiome-Metabolism Model. *Proceedings* 2019, 11(1).

6. **Mortelé O**, Jörissen J, Spacova I, Lebeer S, van Nuijs A L N, Hermans N. Demonstrating the involvement of an active efflux mechanism in the intestinal absorption of chlorogenic acid and quinic acid using a Caco-2 bidirectional permeability assay. *Food & Function 2021, DOI: 10.1039/D0FO02629H.*

Oral presentations (8)

1. **Mortelé O**, Vervliet P, Gys C, Degreef M, Cuykx M, Maudens K, Covaci A, van Nuijs A L N and Lai F Y. Identification of *in vitro* metabolites of the designer benzodiazepine cloniprazepam by liquid chromatography coupled to quadrupole time-of-flight mass spectrometry. Oral presentation delivered at the Journées Internationales de Toxicologie, Liège, Belgium, 19-20 October 2017.

2. **Mortelé O**, Vervliet P, Gys C, Degreef M, Lanckmans K,Maudens K, Covaci A, van Nuijs A L N and Lai F Y. Suspect and non-target screening workflows to investigate the *in vitro* and *in vivo* metabolism of the synthetic cannabinoid 5Cl-THJ-018. Flash presentation delivered at The International Association of Forensic Toxicologists (TIAFT) meeting, Ghent, Belgium, 26-30 August 2018.

3. **Mortelé O**, Iturrospe E, Breynaert A, Verdickt E, Xavier B B, Lammens C, Malhotra-Kumar S, Jorens P G, Pieters L, van Nuijs A L N and Hermans N. Chlorogenic acid as a model compound for optimization of an *in vitro* gut

microbiome-metabolism platform. Oral presentation delivered at the NutRedOx COST Action 16112 at Luxemburg, 25-27 March 2019.

4. **Mortelé O**, Vervliet P, Gys C, Degreef M, Lanckmans K,Maudens K, Covaci A, van Nuijs A L N and Lai F Y. Suspect and non-target screening workflows to investigate the *in vitro* and *in vivo* metabolism of the synthetic cannabinoid 5Cl-THJ-018. Oral presentation delivered at the Flanders 2019 meeting, Lille, France, 21-24 May 2019.

5. **Mortelé O**, Iturrospe E, Breynaert A, Verdickt E, Xavier B B, Lammens C, Malhotra-Kumar S, Jorens P G, Pieters L, van Nuijs A L N and Hermans N. Optimization of an *in vitro* gut microbiome biotransformation platform with chlorogenic acid as model compound. Oral presentation delivered at the Human and environmental (bio)monitoring: the Belgian and South Korean perspectives workshop, Wilrijk, Belgium, 1st of July of 2019.

6. **Mortelé O**, Iturrospe E, Breynaert A, Verdickt E, Xavier B B, Lammens C, Malhotra-Kumar S, Jorens P G, Pieters L, van Nuijs A L N and Hermans N. Optimization of an *in vitro* gut microbiome biotransformation platform with chlorogenic acid as model compound: From fecal sample to biotransformation product identification. Oral presentation delivered at Euroanalysis 2019, Istanbul, Turkey, 1-5 September 2019.

7. **Mortelé O,** van Nuijs A L N and Hermans N. *In vitro* gut microbiome biotransformation models. Presented at the NutRedOx training school in Molecular Nutrition, Lisbon, Portugal, 30th September-2nd October 2019. (Invited speaker)

8. **Mortelé O**, Xavier B B, Lammens C, Malhotra-Kumar S, Jorens P G, van Nuijs A L N and Hermans N. Optimization of an *in vitro* gut microbiome biotransformation platform with chlorogenic acid as model compound: From fecal sample to biotransformation product identification. Oral presentation delivered at the Departmental Research Day of the Department Pharmaceutical Sciences, University of Antwerp, Belgium, 20th May 2020.

Poster presentations: first author (2)

1. **Mortelé O**, Vervliet P, Gys C, Degreef M, Lanckmans K, Maudens K, Covaci A, van Nuijs A L N and Lai F Y, Suspect and non-target screening workflows to investigate the *in vitro* and *in vivo* metabolism of the synthetic cannabinoid 5-Cl-THJ-018. Poster presented at the Masstwin Exploratory workshop, Antwerp, Belgium, 18-20 April 2018.

2. **Mortelé O**, Vervliet P, Gys C, Degreef M, Lanckmans K, Maudens K, Covaci A, van Nuijs A L N and Lai F Y, Suspect and non-target screening workflows to investigate the *in vitro* and *in vivo* metabolism of the synthetic cannabinoid 5Cl-THJ-018. Poster presented at The International Association of Forensic Toxicologists (TIAFT) meeting, Ghent, Belgium, 26-30 August 2018.

Poster presentations: co-author (1)

1. Vervliet P, **Mortelé O**, Gys C, Degreef M, Lanckmans K, Maudens K, Covaci A, van Nuijs A L N and Lai F Y, Suspect and non-target screening workflows to investigate the *in vitro* and *in vivo* metabolism of the synthetic cannabinoid 5Cl-THJ-018. Poster presented at the 11th International Symposium on Drug Analysis and the 29th International Symposium on Pharmaceutical and Biomedical Analysis 2018, Leuven, Belgium, 9-12 September 2018.

Organized workshop

1. **Mortelé O***, Vervliet P*, van Nuijs A L N and Hermans N. Colonic metabolite identification by non-targeted screening. Workshop given at the NutRedOx training school in Molecular Nutrition, Lisbon, Portugal, 30th September – 2nd October 2019. (*Invited trainers)

Awards

Euroanalysis 2019: 3th place best oral presentation young scientist session
Departmental Research Day 2020: public award best presentation

Supervised master theses (5)

1. **Stephanie Verheyden:** Onderzoek van xenobiotica in een *in vitro* gastro-intestinaal simulatiemodel: 'GIDM colon' (Translation: Investigating xenobiotica in an *in vitro* gastrointestinal model: 'GIDM-Colon'). Biomedical Sciences, Msc. Thesis 2017 at University of Antwerp

2. **Lisse Broes:** Methylfenidaat: Veiligheid op lange termijn en problematiek in de praktijk (Translation: Methylphenidate: Long-term safety and problems in practice). Pharmaceutical Sciences, Msc. Thesis 2018 at University of Antwerp

3. **Elias Iturrospe:** Identification of colonic metabolites of chlorogenic acid by LC-QTOF-MS: Optimisation of sample preperation and development of suspect and nog-targeted screening workflows. Pharmaceutical Sciences, Msc. Thesis 2019 at University of Antwerp

4. **Roxanne Van De Steene:** De bijdrage van de apotheker inzake de beoordeling van de invloed van geneesmiddelen bij het behalen van een rijgeschiktheidsattest (Translation: The pharmacist's contribution to the assessment of the influence of drugs in obtaining a driving suitability certificate). Pharmaceutical Sciences, Msc. Thesis 2019 at University of Antwerp

5. **Melodi Kilic:** Methode-optimalisatie van *in vitro* fase I en fase II biotransformatie gebruik makend van humane intestinale microsomen (Translation: Method optimisation of *in vitro* phase I and phase II biotransformation using human intestinal microsomes). Pharmaceutical Sciences, Msc. Thesis 2020 at University of Antwerp

ACKNOWLEDGEMENTS - DANKWOORD

Acknowledgements – Dankwoord

This thesis would not have been possible without the support, help and input of a lot of people. I would like to thank all of you for the incredible support during the four past years.

Deze thesis zou niet mogelijk geweest zijn zonder de steun, hulp en inbreng van meerdere mensen. Ik wil jullie allemaal bedanken voor de geweldige steun de afgelopen vier jaar.

Eerst en vooral wil ik mijn twee promotoren bedanken! **Nina en Alexander,** bedankt om mij de kans te geven een doctoraat te starten bij NatuRA en het Toxicologisch Centrum. Bedankt voor de begeleiding en alle kansen die jullie mij de afgelopen vier jaar gegeven hebben. Jullie stonden steeds voor mij klaar wanneer ik advies, tips of hulp nodig had. **Nina,** ik zal me de fijne gesprekken en leuke momenten op de labo uitstappen en congressen in Luxemburg en Lissabon steeds herinneren. Bedankt om me de afgelopen vier jaar alle kansen te geven en voor je hulp en vertrouwen! **Alexander,** bedankt voor de vele leuke gesprekken over wetenschap, voetbal en zaken ver daarbuiten. Ik hoop dat onze jaarlijkse voetbalmatchen blijven doorgaan en dat ik in de toekomst nog een paar keer mag scoren tegen u! **Nina en Alexander,** bedankt voor alles wat jullie gedaan hebben voor mij!

I would like to express my gratitude to the members of the doctoral committee **Prof. Paul Cos, Prof. Philippe Jorens, Prof. Cláudia Nunes dos Santos and Dr. Lubertus Bijlsma**. Thank you for reading and revising the thesis. Your suggestions definitely improved the quality of the thesis.

Ik wil ook iedereen van het **Universitair Ziekenhuis Antwerpen** bedanken die mij geholpen heeft met de inclusie van vrijwilligers en patiënten. **Prof. Philippe Jorens**, bedankt voor alles wat u gedaan heeft om de inclusie van patiënten vlot te laten verlopen. Ik heb dit ten zeerste geappreciëerd! Verder wil ik ook het hele team van het

departement Endocrinologie, Diabetes en Metabole aandoeningen bedanken voor hun hulp de afgelopen jaren, in bijzonder **Prof. Eveline Dirinck** en **Dr. Ilke Mariën** die een groot aandeel hadden in de rekrutering van patiënten. Thank you **Jennifer, Irina, Eline and Prof. Sarah Lebeer** for all the help regarding the Caco-2 experiments.

Verder wil ik ook **Prof. Adrian Covaci** uitvoerig bedanken. **Adrian**, bedankt voor alle hulp en steun tijdens de afgelopen jaren. Tijdens mijn masterthesis had ik de eer om u als promotor te hebben. Tijdens mijn doctoraat was je ondanks je enorm druk schema steeds oprecht geïnteresseerd in mijn werk en kon ik voor vragen steeds bij u terecht. **Prof. Hugo Neels**, bedankt voor de interessante gesprekken over klinische biologie en (forensische) toxicologie.

I want to thank all my colleagues at the research department of the Toxicological Centre for making the past 4 years unforgettable. There were a lot of wonderful moments like the lab retreats, Christmas parties, the TML-sampling and lab dinners. Thank you **Catalina, Christina, Delphine, Elias, Elvio, Foon, Frederic, Giuilia, Jasper, Lidia, Maarten, Malar, Manuela, Matthias C., Matthias O., Tim, Tom, Yunsun and Yukiko** for the scientific discussions and interesting conversations during lunch. **Matthias C**, bedankt voor mij te introduceren tot de wereld van de Q-TOF en je begeleiding tijdens mijn masterthesis. **Foon and Fred,** thank you for all the wonderful moments in the lab, your help and knowledge transfer during the first year(s) of my PhD. I learned a lot thanks to you guys! Ik wil ook **Elias** bedanken**,** uw werk tijdens je masterthesis heeft enorm bijgedragen tot deze thesis waarvoor dank! **Steven**, bedankt om steeds beschikbaar te zijn voor een leuke babbel en al het trouble-shooting met de instrumenten. Verder wil ik ook heel het forensisch team van het Toxicologisch Centrum bedanken voor de leuke tijd: **Carine, Ellie, Evi, Glenn, Kelly, Kristof, Matthias, Machteld, Sofie, Stephanie en Vera**.

Celine, Michiel en Philippe, jullie waren de beste collega's die iemand zich kon inbeelden. Samen hebben we de afgelopen jaren fantastische momenten

meegemaakt: kerstfeestjes, weekendjes in Butchenbach, Praag, Pukkelpop,de Breweries marathon… . Het einde van onze doctoraten mag dan het einde zijn van een periode als collega's, maar de start van een periode als vrienden voor het leven.

I would also like to thank my colleagues from NatuRA. Thank you **Annelies B., Annelies V., Anne-Sophie, Anastasia, Emmy, Laura, Kenn**, **Mamadou, Mart, Maxime, Stefaniya, Tania, Tess and Yunita** for the past years**. Prof. Luc Pieters**, bedankt om me de kans te geven om een doctoraat bij NatuRA uit te voeren. **Annelies B**., bedankt om mij het GIDM-Colon vanbinnen en vanbuiten aan te leren en alle hulp tijdens de afgelopen jaren!

Ik wel verder ook mijn **familie en vrienden** bedanken. Bedankt voor jullie onvoorwaardelijke steun en vriendschap tijdens de afgelopen jaren. Bedankt aan alle vrienden van '**den BET'** voor alle top momenten van de afgelopen jaren! **Joost en Sten**, ik hoop dat jullie na het bestuderen van deze thesis eindelijk begrijpen wat ik de afgelopen vier jaar heb gedaan zodat ik het op een volgende reis niet opnieuw moet uitleggen.
Ik wil ook graag **Frank, Murielle,Nicholas en Tine** bedanken voor alles wat jullie al voor mij gedaan hebben de afgelopen jaren! Bedankt om er steeds voor mij te zijn!

Ik wil mijn **mama, papa en broer** bedanken! Bedankt om mij gedurende heel mijn leven alle kansen te geven en onvoorwaardelijk te steunen in mijn plannen en dromen. Bedankt om er steeds voor mij te zijn! **Mama**, je bent de sterkste vrouw die ik ken en samen kunnen we alles aan!

Ten slotte wil ik mijn **Daphne** bedanken, de liefde van mijn leven, zonder wie ik dit niet had gekund! Bedankt voor al je liefde en steun tijdens de afgelopen jaren. Ik ben enorm dankbaar dat ik jou de afgelopen jaren aan mijn zijde had en dat we de rest van ons leven samen zullen ontdekken.